Regulation of prion protein expression and cellular activity

Haigh, Cathryn Louise

Award date:
2006

Awarding institution:
University of Bath

Regulation of Prion Protein Expression and Cellular Activity

Cathryn Louise Haigh

Submitted in fulfilment for the degree of Doctor of Philosophy

University of Bath
Department of Biology and Biochemistry

April 2006

ProQuest LLC
789 East Eisenhower Parkway
P.O. Box 1346
Ann Arbor, MI 48106-1346

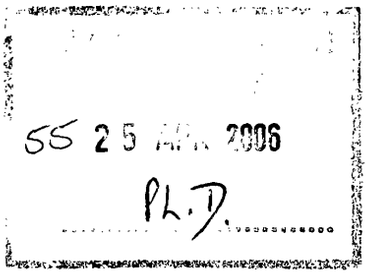
55 25 APR 2006
Ph.D.

Abstract

The transmissible spongiform encephalopathies (TSEs) are a group of neurological disorders caused by the conversion of the cellular prion protein (PrP^{c}) into a structurally distinct isoform (PrP^{Sc}). PrP^{c} is a cell surface glycoprotein, which binds copper via a sequence of highly conserved repeats within its N-terminus. Data on the genetic regulation of PrP^{c} expression is sparse, and its function has been the topic of much unresolved debate. This study aimed to determine the normal cellular methods regulating PrP^{c} expression and metabolism, and to advance current understanding of its function.

The importance of copper is clearly demonstrated both at the gene level, with transcription significantly increased in PrP null cells in response to increased exogenous copper concentrations, and at the protein level. Copper has previously been shown to induce PrP^{c} internalisation. Here it is shown that concentrations of copper, clearly within physiological parameters, showed a significant and rapid internalisation response, and that the octameric repeat domain and palindromic region are essential for this reaction. PrP^{c} protects against copper toxicity induced both by the copper ion itself and the oxidative stress that Fenton reaction of the copper ion can induce. Oxidative stress also stimulates both the prion promoter, with up regulation induced by DMSO, and a PrP^{c} mediated cellular protective reaction in response to DMSO and xanthine oxidase insults. The octameric repeat domain and the hydrophobic region are necessary for protection against both copper and oxidative stress insults, suggesting that they are highly important for PrP^{c} function. The results support the central role of the octameric repeat region and copper binding in the metabolism and function of PrP^{c}, and also provide insight into the importance of other regions in both copper and oxidative stress response.

Acknowledgments

My warmest thanks goes to my supervisor Professor David R Brown for the intellectual guidance during the preparation and undertaking of this research. Also I would like to express my appreciation for the provision of facilities, the exceptional availability and speed in the proof reading of this document, and encouragement, particularly in the final stages of preparation.

I would also like to thank every member of Professor Brown's lab at the University of Bath for their continued support and kindness. Specifically, thank you to Dr Sarah Webb for her superb proof reading abilities and amazing support, Dr Andrew Thompsett for unlimited patience and access to the incredible database that is his brain, and Dr Claire Bowring who provided the much needed technical support and guidance during the early stages of my studies.

I would like to thank Dr Ian Jones for his expertise and time that helped tremendously with the production of the confocal images, and Dr Angus Buckling for assistance with statistics.

Thank you mum, Jen and Tom. It's been a difficult few months all round and your support has meant everything to me. Last but not least, thank you to the wonderful group of friends that have supported me, put up with me at my worst, and made my time at the University of Bath so special – I can't name you all because that would be a thesis in itself but I hope you know who you are.

This work was funded by a studentship from the BBSRC.

Dedicated to the memory of Pete Lonsdale, and Tabbitha and Gordon Haigh. To Tabbitha and Gordon, it was hard loosing you both during this time but the happy times you gave me will never be forgotten. Also Pete Lonsdale, please don't think you've been forgotten – you'll be in my heart always, I hope I've made you proud.

Publications

The research presented within this thesis has produced the following publications.

Papers

Haigh, CL. Edwards, KE, Brown, DR. (2005) Copper binding is the governing determinant of prion protein turnover. *Molecular and Cellular Neuroscience* **30**, 186-96.

Haigh, CL. Brown, DR. (2005) Cellular prion protein protects against both oxidative and non-oxidative copper insult. *Journal of Neurochemistry. In Press.*

Cheng, F. Lindqvist, J. Haigh, CL. Brown, DR. Mani, K. Copper-Dependent Co-Internalisation of the Prion Protein and Glypican-1. *In Press.*

Abstracts

Haigh, CL. Brown, DR. New insights into copper-induced internalisation of the cellular prion protein. Program No. 666.5, *2005 Abstract Viewer / Itinerary Planner*. Washington, DC: Society for Neuroscience.

Haigh, CL. Brown, DR. The Cellular Prion Protein and Metal Ion Trafficking. BNA Postgraduate and Early Career Symposium, September 2005.

Haigh, CL. Edwards, KE. Brown, DR. The Effect of Copper on the Intracellular Trafficking of the Cellular Prion Protein. Joint Funders' TSE Conference, September 2004.

Brown, DR. Haigh, CL. Factors Affecting the Genetic Regulation of Prion Protein Expression. Joint Funders' TSE Conference, September 2004.

Abbreviations

ADAM10	A disintegrin and metalloprotease 10
ATRA	All-trans retinoic acid
BSE	Bovine Spongiform Encephalopathy
cAMP	cyclic adenosine mono-phosphate
CJD	Creutzfeldt-Jakob Disease
CMV	Cytomegalovirus
Cu-4xGly	Copper premixed with a four molar excess of glycine
CWD	Chronic Wasting Disease
DMSO	Di-methyl sulphoxide
EPD	Eukaryotic promoter database
ER	Endoplasmic reticulum
ERAD	ER associated destruction
FFI	Fatal Familial Insomnia
GFP	Green fluorescent protein
GPI	Glycophosphatidylinositol
GSS	Gerstmann-Sträussler-Scheinker
hsp70	Heat shock protein 70
JNK	c-Jun N-terminal kinase
MAPK	Mitogen activated protein kinase
MEF2	Myocyte enhancer factor-2
MMP	Matrix metalloproteases
MRE	Metal response elements
MTF-1	MRE-binding transcription factor-1
MTT	3-(4,5-Dimethyl-2-thiazolyl)-2,5-diphenyl-2H-tetrazolium bromide
MZF-1	Myeloid zinc finger-1
Myt1	Myelin transcription factor 1
NFAT	Nuclear factor of activated T-cells
NGF	Nerve growth factor
NMR	Nuclear magnetic resonance
NO	Nitric oxide
ORF	Open reading frame
PIC	Pre-initiation complex

prnp	Prion gene
PrP^{c}	Cellular prion
PrP^{res}	Proteinase K resistant prion
PrP^{sc}	Scrapie prion
RAR	Retinoic acid receptor
RARE	Retinoic acid response element
RLM-RACE	RNA ligase mediated - rapid amplification of cDNA ends
ROS	Reactive oxygen species
RXR	Retinoic X receptor
SOD	Superoxide Dismutase
TACE	Tumour necrosis factor α-converting enzyme
TESS	Transcription element search system
TF	Transcription factor
TSE	Transmissible Spongiform Encephalopathy
TSS	Transcription start site
vCJD	Variant Creutzfeldt-Jakob Disease

Contents

Contents – Figures

Chapter 1 - Introduction

Chapter 2 - Materials and Methods

Chapter 3 - Genetic Modulation of PrP Expression

Chapter 4 - Copper and PrP^c Internalisation

Chapter 5 - Cellular protection and PrP^c

Chapter 6 - Discussion

Contents – Tables

Contents – Tables

Chapter 2 – Materials and Methods

Chapter 3 - Genetic Modulation of PrP Expression

1 Introduction

The Transmissible Spongiform Encephalopathies (TSEs; also known as prion diseases) are a group of diseases characterised by spongiform changes in the brain tissue. Disease onset manifests as dementia and loss of motor function, leading ultimately to death. The TSEs have received much attention in recent years due to publicity surrounding the increase in cases of Bovine Spongiform Encephalopathy (BSE) in cattle and the emergence of variant Creutzfeldt Jakob disease (vCJD) in humans. A possible link between the two has caused much concern.

BSE and vCJD are the most widely known of the TSEs. Other members of the TSE family include scrapie in sheep and goats; chronic wasting disease in elk and deer; and Gerstmann-Sträussler-Scheinker syndrome (GSS), fatal familial insomnia (FFI), and Kuru in humans. In humans, hereditary and sporadic CJD onsets in later life, usually over the age of 60, with patients displaying the symptoms of dementia and loss of motor function. In these cases death is rapid, usually within 3 months of the onset of symptoms. Post mortem examination of these patients reveals the spongiform changes in the brain from which these diseases derived their name, sometimes accompanied by plaques of insoluble amyloid-like protein. vCJD, the form linked to BSE, differs from this in that onset usually occurs in much younger patients (of age 15-30 years) and progression is slower with death 12-15 months after the onset of symptoms (Will & Ward, 2004).

Despite the transmissible nature of the agent the majority of cases (around 85%) in humans are sporadic or hereditary, thought to be caused by somatic or autosomal dominant inherited mutation in the prion gene (Tabrizi *et al.*, 2003). Following the onset of symptoms, disease progression is rapid and the effect of dominant inheritance on affected families has made the search for prevention and treatment for those affected vital.

The emergence of these diseases is not a recent event. Cases of scrapie in sheep were being reported in the eighteenth century, although the disease may have been present before this time (Brown & Bradley, 1998). Even the early reports show appreciation of the infectious nature of the disease. The transmissible nature was further corroborated in 1936, due to accidental inoculation of flocks of sheep with scrapie from a vaccine against

louping-ill virus. A suspension of brain, spinal cord and spleen tissues from sheep with the louping ill virus was used to make the vaccine. The tissues had been appropriately treated to be used as a killed vaccine (Gordon, 1946). The scrapie agent was in one or more of the tissues used for the vaccine, it was resistant to the denaturing conditions used to prepare the louping-ill virus inoculum, and had an incubation period of at least two years. At this time the agent responsible was thought to be a slow virus. However, it was appreciated that the nature of the virus was unusual, it was very small, resistant to inactivation by chemicals and heat, and had an indefinite life in storage (Gajdusek, 1967).

Early investigations into the scrapie agent indicated that it was resistant to methods usually able to deactivate viruses, such as nucleases, UV irradiation and heat, but unstable in protein denaturing agents such as protease K, trypsin and urea (Prusiner, 1982). From this information the 'protein only' hypothesis of the scrapie agent was proposed. This was the first report of a protein able to cause infection independently of a viral or other foreign agent, and is now widely accepted as the correct theory of prion diseases. The term prion protein (PrP) was first proposed by Stanley Prusiner, who used it to define the agent as an infectious protein. The term is short for proteinacious infectious particle. Later it was determined that this disease isoform (PrP^{Sc}) was a conformationally altered isoform of a normal cellular protein (PrP^{c}). Early studies much overlooked this normal isoform in favour of the disease isoform. However, more recently an appreciation of the need to understand the role of the protein in health to understand how it malfunctions in disease has resulted in considerable investigation into PrP^{c}.

Before the start of the BSE epidemic in 1985, the existence of the TSEs was virtually unknown. The BSE epidemic brought TSEs into the public consciousness, not only because of their detrimental affect on farming and agriculture, but also due to a potential link to vCJD. The BSE epidemic was thought to be caused by the feeding of meat and bone meal (derived from sheep and cattle) to cattle (Wilesmith *et al.*, 1992; Collee & Bradley, 1997a; Pattison, 1998). Some of this meat and bone meal was thought to have come from infected animals so the disease may be passed on by ingestion of the infective agent. Since this linked the consumption of infected foodstuffs and disease, when the new phenotypic variant of CJD (vCJD) emerged for the first time in 1996, this caused a nervous public to place the cause firmly with eating infected beef.

The cost to farming of the BSE epidemic was devastating. Not only did beef sales fall, but also new and strict restrictions on the quality of beef for consumption were enforced. The Feed Ban prohibited the use of animal protein in animal feed to prevent this route of transmission. Only certain parts of the animal could be used for consumption and meat had be prepared in such a way that there was no risk of brain or spinal cord contaminating it. This was known as the Specified Risk Material Control and banned the use of mechanically recovered meat, since mechanical preparation stripped meat from the bone by high pressure and there was a high risk of infected material contaminating the final product. The Over Thirty Months Rule required that cattle for meat had to be sent to the abattoir when still under 30 months in age (Food Standards Agency, 2005). To make matters worse for Britain's farmers, the EU imposed a ban on exports of British beef, effectively destroying the overseas market and causing further financial problems for the UK agricultural industry. Another cause for concern was that several cases of vCJD had been reported in farmers implying an increased risk may arise from working with infected animals. However, whilst this is a consideration for farmers, veterinary surgeons, abattoir workers, and butchers, the link between working with infected animals and developing vCJD is still unproven, and providing precautions are taken workers should not be at unacceptable risk (Collee & Bradley, 1997b).

Some of the restrictions imposed are still currently in place (The Feed Ban and the Specified Risk Material Control) and are deemed to have made the quality of British beef much safer, others have been relaxed (The Over Thirty Months Rule) since the number of cases has declined steadily to almost negligible levels (Pattison, 1998). Instead a BSE screening programme for cattle over the age of 30 months has been implemented to reduce the risk of infected meat entering the food chain (Food Standards Agency, 2005).

The spread of chronic wasting disease (CWD) amongst deer and elk in the wild has also become a cause for some concern. It was originally thought that outbreaks of CWD were localised and self-limiting. However recently it has become evident that this disease is now widespread and still spreading. Since this is happening in wild populations the spread cannot be attributed to farming practises. Links have been demonstrated between deer grazing on land where CWD infected deer have previously grazed or have decomposed and the development of CWD. Also uninfected deer grazing with infected deer are at increased risk of developing CWD. This has lead to the hypothesis that the infective agent can persist for considerable periods in soil after an infected animal has died and

decomposed, and can be transmitted from the saliva and faeces of infected animals to those grazing around them (Miller & Williams, 2004; Miller *et al.*, 2004). In addition the potential for transmission from infected sewage sludge on agricultural land has also been a matter of concern. Since it is unknown if CWD or other TSEs such as BSE can transmit to humans this way, such potential transmission is of concern. Potentially farm produce grown on land where infection has been present previously or where infected animals may have grazed could pose a threat to human health. However, although cattle could potentially be infected this way, infection rates would not be high enough to sustain the epidemic and human contact with soil and vegetable crops is considered acceptably low risk (Gale & Stanfield, 2001).

Whilst public perception of the risks associated with eating infectious meat has not diminished, the general public are widely influenced by media attention, and since cases of BSE and vCJD are in decline, interest has turned to more current threats, such as MRSA and bird flu. There are, however, still important issues that need to be resolved, including how to deal with infected sheep and cattle, especially since the scrapie agent appears so resistant to heat and denaturing agents. As discussed above, the worry that prions may remain in the soil for prolonged periods of time after the animal has decayed, or may enter the water supply is a matter of some concern. Also the potential for spread from milk from contaminated animals has caused worry. However the World Health Organisation (WHO) has found no evidence of infectivity from milk of infected animals, and on this basis milk is deemed to be safe. Finally, despite the reduction in both the number of BSE and vCJD cases, the incubation period of the disease is prolonged, in some reports up to forty years (Croes *et al.*, 2002), and there is no way of knowing how many humans could be incubating a disease that takes so long to present symptoms.

Diagnosis is a problem for the TSEs in both humans and animals. By the time of symptomatic presentation the disease is advanced, and once the brain tissue has been destroyed there is currently no way to reverse the damage. Therefore early diagnosis is essential to maintain the quality of life of the patient. Much research has focused on this problem with many hopeful avenues proving ineffective. Many current diagnostic methods require using techniques such as immunohistochemical analysis of tissue sections and western immunoblotting for the PrP^{sc} agent in brain tissue post mortem, which certainly does not allow for early diagnosis (Kovacs *et al.*, 2004; Gavier-Widen *et al.*, 2005). Attempts have been made to find PrP^{sc} in blood samples or, alternatively, to screen

for changes in blood chemistry that occur during the early stages of the disease with little success. However recently an amplification reaction of PrP^{sc} has been proposed as a possible mechanism for detecting very low levels of PrP^{sc}. The technique is called protein-misfolding cyclic amplification (PMCA) and has been shown to be sensitive enough to detect PrP^{sc} in blood with 100% specificity (Saborio *et al.*, 2001; Castilla *et al.*, 2005). However, despite being a promising early diagnostic test, this is still highly experimental and would not yield rapid results. Accordingly, it might not be appropriate for use as an on site test for farmyard animals but may have a place in human diagnostics.

In addition to the problem of diagnosis there is currently no cure for prion diseases. Treatment focuses on managing the symptoms and making patients comfortable. A great deal of research has focused, ineffectually, on finding a cure. Pentosan sulphate/polysulphate is known to cure PrP^{sc} infected cells *in vitro* and so has been suggested as a potential treatment. Recently pentosan polysulphate was use to treat a eighteen year old (at the start of treatment) male with advanced vCJD (Todd *et al.*, 2005). Drug delivery had to be by daily cerebrovascular infusion and some evidence of improvement in awareness and sleep cycles was detected in the patient. However, despite improvement, brain atrophy continued to progress, and, given the unpleasant administration process of the drug, investigations still continue into finding a better agent for treatment of these diseases.

The problem of the long incubation period coupled with the difficulties in detecting the scrapie agent impacts on other areas of health care. The potential transmission of CJD by use of human pituitary derived hormones was recognised even before the start of the BSE epidemic (Koch *et al.*, 1985), and by 2006 it was documented that at least 160 cases of CJD had been transmitted to patients in this way (Lewis *et al.*, 2006). CJD is also known to have been transmitted to patients by cadaveric dural grafts. Patients that developed iatrogenic CJD as a result of receiving such grafts presented symptoms anywhere between 16 months and 23 years (Thadani *et al.*, 1988; Martinez-Lage *et al.*, 1994; Kobayashi *et al.*, 2003), therefore the onset of the disease can be prolonged. As a result it is difficult to estimate how many patients could have been infected and allow physicians to provide the appropriate follow up support.

Blood and blood product transmitted TSE infection has become a cause of concern. Blood may be collected from a person incubating the disease and distributed unknowingly to

many other people. Several cases of CJD transmission this way have been confirmed and, due to the strict criteria for diagnosis of transfusion acquired infection, more may have occurred but been overlooked (Llewelyn *et al.*, 2004; The vCJD Working Party of the Standard Advisory Committee on Transfusion Transmitted Infections, 2005). Blood products in Europe must comply with specific guidelines concerning the quantity of white blood cells in the final product, since leucocytes are known to express PrP. However, it is not possible to remove the leukocyte population altogether without great excessive cost to the NHS and additionally, it has not been determined if the scrapie agent can exist free in the blood plasma. If it can be transmitted free in plasma the risk cannot be eradicated since even packed cells contain plasma. The risks are compounded for neonatal care where blood and blood products are split into several smaller bags, and so blood from one infected donor may potentially reach several recipients. In light of current knowledge on the transmission of the TSEs, new restrictions on blood donors have been introduced. These exclude people who have received human pituitary derived hormones, patients who have received human dura matter grafts or corneal grafts, people identified as being members of a family at risk of inherited prion disease, and people who have received blood or blood products since 1980 (UK Blood Transfusion Services, 2005). The potential for transmission has been a cause of much distress to patients requiring blood products on a regular basis, such as haemophiliac patients who have already lived through the risk of HIV and hepatitis B from the blood products they have received only to find out that they may now be at risk of vCJD also.

The NHS is further affected by the lack of knowledge on how vCJD can be transmitted. Studies have shown that the disease protein can become attached to surgical instruments so firmly that normal decontamination procedures are rendered useless. If these instruments are then used on further patients, the disease could be passed on through contact. Consequently surgical instruments used for procedures where there is contact with high or medium risk tissues in patients with a potential risk of incubating CJD should be destroyed after use or kept only for research purposes (World Health Organisation, 2003). This has been of considerable concern with tonsillectomies, where the tissue removed contains high numbers of leucocytes and shows positive immunohistochemistry for PrP^{sc} during disease (Frosh *et al.*, 2001). Further disciplines such as endoscopy (Bramble & Ironside, 2002), dentistry (Azarpazhooh & Leake, 2006) and opthalmics (Hogen & Cavanagh, 1995) are also affected by the need to take extra measures to reduce the risk of CJD transmission between patients.

Healthcare professionals are also themselves affected by the potential risks of working with infected patients. Although there has been no evidence to date of transmission from person to person by contact such as that seen in the care environment, there are risks to health workers in terms of contaminated blood and bodily fluids, however as long as standard infection control practises are applied (for example gloves, waste bags, and sharps bins) the risk to healthcare workers is minimal. Other settings where risk may be heightened include post mortem examination of tissue and surgery (ACDP/SEAC Joint Working Group, 2003).

The TSEs still have wide reaching effects both on farming and public health. This is area of so many unknowns and uncertainties that much still needs to be done to establish exact dangers to the public. More needs to be understood about the disease agent to best determine how to treat and manage or prevent prion disease. Elucidating the role of the normal isoform of the prion protein (PrP^c) may provide important information on disease pathogenesis and potential pathways of treatment.

PrP^c is a cell surface glycoprotein, located on the exterior leaflet of the plasma membrane. It is also a metalloprotein with a high affinity for copper (Section 1.3). Its suggested functions have included copper transport and metabolism, cellular protection possibly as an antioxidant itself, and signal transduction (Section 1.5). However despite much investigation the role of PrP^c is still unclear.

This study focuses on the cellular isoform of the prion protein, PrP^c, and considers both the activity of the protein itself and the genetic mechanisms that control protein production. The primary aims are to elucidate the normal cellular methods of PrP^c regulation and metabolism, and to advance current understanding of its function. In addition, further emphasis is placed on determining how these factors may become altered in disease, and, where appropriate, consideration is given to potential therapeutic intervention.

1.1 Genetic Control of PrP^c Expression

PrP^c knockout mice are resistant to infection with scrapie (Weissmann *et al.*, 1994), and thus transmission of prion diseases and the resulting neurotoxicity requires the presence of PrP^c (Brown *et al.*, 1994; Brandner *et al.*, 1996). The level of PrP^c expression has been shown to influence the incubation period of the disease in mice (Scott *et al.*, 1989; Fischer *et al.*, 1996), and polymorphisms within the gene promoter alter PrP^c expression levels (Hills *et al.*, 2001; Sander *et al.*, 2005). Hence, the role of the promoter and expression control elements may be fundamental in both disease pathogenesis and control.

1.1.1 Overview of Eukaryotic Promoter Control

Regulation of protein expression is an essential function of all cells. A careful balance must be maintained for normal cellular homeostasis, and the ability to appropriately up or down-regulate specific proteins in response to stimuli is crucial to avoid damage to the individual cell or organ. Such is the importance of maintaining correct cellular expression levels that regulation occurs by mechanisms throughout the cell, acting on the gene itself, and all pathways through creation to destruction of the protein product. These regulatory mechanisms include; control of the transcription of mRNA from DNA by elements within the promoter sequence or up-stream of it; control of the translation of the mRNA by mRNA turnover (in turn influenced by the ability of the mRNA to form secondary structures to increase stability, by poly-adenylation, and by alternative splicing) or by micro RNAs (miRNAs) binding to sites within the mRNA sequence; and regulation of the protein itself by turnover mechanisms within the cell. The control of transcription is thought to be the most important factor for regulation of protein levels. A short description of eukaryotic promoter control is covered below.

Eukaryotic promoter control is extremely complex. A pre-initiation complex (PIC) must assemble around the appropriate sequence of DNA, functioning to first uncoil supercoiled DNA, and second to allow the attachment of DNA polymerase and other proteins forming the transcription apparatus, which unzips, transcribes and rezips the DNA of the gene. The PIC is a multi-protein complex, which includes general transcription factors, such as TFIIA - H, and DNA polymerase II. Many genes have a TATA box motif, which provides a binding site for transcription factors, located approximately 25 base pairs upstream of the transcription start site (TSS). For genes lacking a TATA box, prior to the TSS there is an initiator region and this determines the strength of the promoter. In addition to this

promoter region, genes may have other regulatory regions, which are usually (but not always) located 5' to the promoter region and may be thousands of base pairs away from the TSS. Depending on the transcription factors that bind them, these regions may enhance or inhibit protein expression (van Driel *et al.*, 2003; Sipos & Gyurkovics, 2005).

1.1.2 Features of the PrP Promoter

Early characterisation of the PrP gene (*prnp*) found that both prion isoforms (PrP^{c} and PrP^{sc}) were encoded by the same gene, and that no evidence of gene rearrangement was seen when comparing scrapie infected tissues to uninfected tissues (Basler *et al.*, 1986). This provided further evidence that the transition from PrP^{c} to PrP^{sc} was the result of post translational modification rather than a result of gene rearrangement or alternative splicing. The study by Basler *et al.* described the hamster *prnp*. The hamster gene was composed of two exons, the first was located 10kb upstream of the second, which encoded the entire uninterrupted open reading frame (ORF). In addition, several features typical of housekeeping genes were identified in the promoter (the region of DNA upstream of the putative transcription start site) including a GC rich region lacking a TATA box and three repeats of a sequence encoding Sp1 binding sites. Sp1 factors bind to these GC rich regions and, by direct protein–protein interaction of factors binding adjacent sites, loops the DNA to synergistically activate the gene by directly or indirectly recruiting proteins of the transcription apparatus (for review see Li *et al.*, 2004).

The structure of the prion gene has now been characterised in several species. In contrast to the initial study describing the two exon structure of hamster *prnp,* in most species it was found that the gene includes three exons with the third, final exon encoding the entire ORF (Inoue *et al.,* 1996; Saeki *et al.,* 1996; O'Neill *et al.,* 2003). The preceding two exons encode an mRNA 5' untranslated region (Westaway *et al.,* 1994). The human gene, however, was shown to have the same structure as the hamster gene, with two exons and one intron present, and the second exon encoding the ORF (Puckett *et al.,* 1991).

Following the determination of the three exon structure of mRNA from other mammalian species, Li & Bolton (1997) discovered the presence of a further exon in hamster mRNA, which showed significant sequence homology with exon 2 from other mammalian species. This data did not disprove the original finding that hamster mRNA was composed of two exons but instead showed there were two splice variants of the hamster mRNA, one with and one without the middle exon 2. In addition this study showed that the two variants

were expressed at different levels in different parts of the brain, with the two-exon structure favoured over the three exon structure, and that expression was altered during infection causing an increase in the levels of the three exon structure. This indicated that exon 2 may be involved in the regulation of PrP expression. The equivalent exon has also been found in humans (Lee *et al.*, 1998). This sequence has not been found in the mRNA transcript but sequence analysis of the gene, when compared to that of the mouse and sheep genes, shows a conserved region corresponding to the exon 2 sequence, which is flanked by splice sites. Since this exon has still not been identified in PrP mRNA transcripts it is thought that, like the hamster mRNA three exon transcript, expression levels of this mRNA variant may be considerably lower than its two exon counterpart and so remain undetected. An alternative theory is that exon 2 is redundant for the regulation of PrP expression, and so its loss from the mRNA transcript is of no consequence.

In agreement with the initial study, all characterised prion promoters lack a TATA box, are rich in GC sequences, and include Sp-1 binding sites. Other features of the prion promoter that have been identified include four highly conserved motifs, AP-1 and AP-2 binding sites, and an inverted CCAAT motif (not present in the bovine or ovine promoter), which can enhance or inhibit promoter activity dependant on what transcription factors bind to them (see Figure 1.1; Westaway *et al.*, 1994; Saeki *et al.*, 1996; Inoue *et al.*, 1997; O'Neill *et al.*, 2003). Promoter activity is further regulated by chromatin conformation, as shown by Cabral et al. (2002), who demonstrated the use of a histone deacetylase inhibitor could, though chromatin disassembly, cause a significant increase in promoter activity and an increased response to factors known to modulate the PrP promoter including nerve growth factor (NGF) and cAMP.

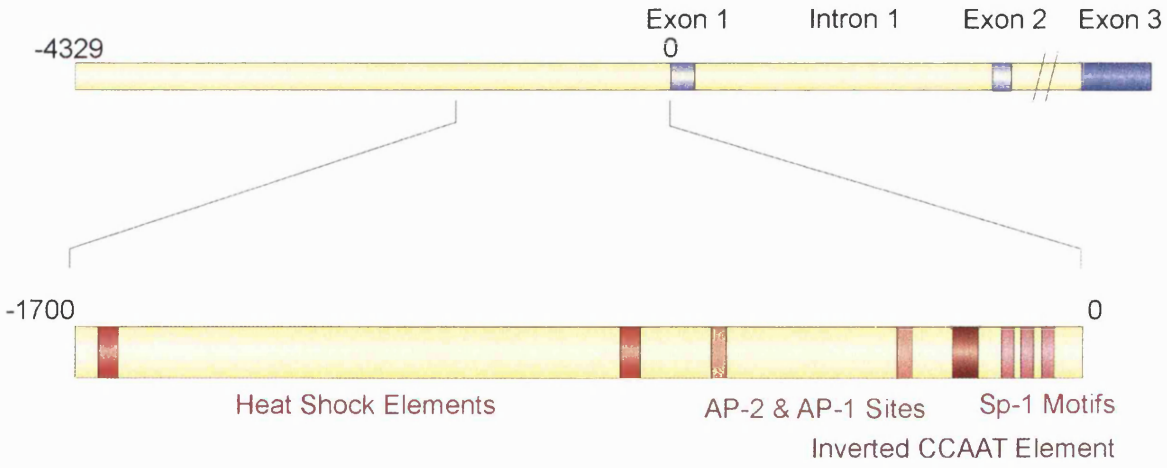

Figure 1.1 Gene structure of *prnp*. Shown are the documented regulatory domains of the promoter region. The long (over 10kb in most species) intron 2 is represented in a shortened form by two lines.

1.1.3 Prnp Non-Coding Region and Gene Regulation

In addition to the above promoter domains influencing expression, intron 1 is required for full activity of the promoter (Inoue *et al.,* 1997). The study by Inoue *et al.* using the bovine gene found that although intron 1 contributed to promoter activity, it was not an enhancer region. The authors suggest that intron 1 may be involved in tissue specific expression or synergistic control of the promoter. Intron 1 was not required for the full activity of the rat promoter. An area of promoter activity has been identified adjacent and 5' to exon 2 of the murine gene, and the intron 1 sequence was shown to contain two areas of potential transcription factor binding sites, however an mRNA transcript lacking exon 1 was not found (Baybutt & Manson, 1997). The implication is that this region may not have its own active TSS or that mRNA levels are so much lower than the full length mRNA that only this is detected. In addition, this area was shown to contain elements capable of suppressing activity of both the promoter and the intron 1 regulatory region.

The role of intron 1 in promoter control is further supported by evidence from Premzl *et al.* (2005). This study identified thirty-three potential regulatory elements within the non-coding region of human, mouse, bovine, ovine, and tamar wallaby *prnp*, seven of these elements occurred in all five species. Some were located in intron 1 and some in intron 2, indicating that the intron 2 sequence may also have regulatory function. Of the motifs conserved across all species tested were regions expected to bind myeloid zinc finger-1 (MZF-1), myocyte enhancer factor-2 (MEF2), Octamer 1 (Oct-1), myelin transcription factor 1 (MyT1), and nuclear factor of activated T-cells (NFAT).

1.1.4 Prnp and Cellular Stress

Heat shock has been shown to up-regulate both *prnp* mRNA and protein expression by 1.5 to 2.5 fold in human cells, and two heat shock elements have been detected in the rat prion promoter (Shyu *et al.,* 2000). Using repressors of transcription it was shown that this up-regulation occurs at a transcriptional level and is abolished or reduced when the heat shock elements are absent or mutated (Shyu *et al.,* 2002). In addition, heat shock proteins are up-regulated in the end stages of prion disease (Kenward *et al.*, 1994), indicating that PrP mRNA levels may also be up-regulated causing an increase of protein expression. Since disease progression is directly related to PrP^c expression this may, in part, account for the rapid progression of the disease in the end stage.

Using hyperbaric oxygen as a model of oxidative stress, it has been shown that oxidative stress can up-regulate both PrP mRNA and protein levels in mouse neuroblastoma cells (Shyu *et al.*, 2004). In this study up-regulation of heat shock protein 70 (hsp70) was also seen, indicating that oxidative insults may up-regulate *prnp* activity by the modulation of heat shock proteins. These would activate the promoter by binding to the previously described heat shock elements. Stress caused by hypoglycaemia has also been found to up-regulate PrP mRNA and protein through a heat shock mediated response, which may involve c-Jun N-terminal kinase (JNK), a signalling kinase that modulates transcription factor production and activity (Shyu *et al.*, 2005a).

Nitric oxide (NO) is a highly reactive radical used as a signalling molecule by cells. It has been found that PrP^c is up-regulated both at the mRNA and protein level in response to direct insult with NO or indirectly in response to lypopolysaccharide treatment, which caused up regulation of neurone specific nitric oxide synthase (nNOS: Wang *et al.*, 2005). Investigation into the mechanism of this up-regulation revealed that it was mediated by a signalling pathway utilising guanylyl cyclase, MEK, and p38 MAPK signalling proteins. This pathway is involved in cellular survival (Torii *et al.*, 2004; Sumbayev & Ysinska, 2005), implying PrP^c may be up-regulated as a cell survival response.

Copper up-regulates PrP^c at the protein level (Brown *et al.*, 1997a). Copper induced up-regulation of *prnp* is thought to involve activation of the promoter by metal response elements (MREs) or MRE-like sequences. Within the bovine *prnp*, an inverted MRE at position –2070 and two MRE-like elements at positions –2653 and -2599, differing from the MRE sequence by just one nucleotide, have been located by sequence analysis (Varela-Nallar *et al.*, 2005). However deletion studies using the bovine promoter find that the removal of these elements does not fully inhibit the ability of copper to up-regulate expression and activation was not mediated by MRE-binding transcription factor-1 (MTF-1), indicating that there may be other motifs and factors involved in regulation of the gene in response to copper. This, in turn, may indicate that the ability of the gene to become activated in response to copper is so important that several regions of the gene sequence are functional for copper induced regulation. A further finding of the study is that copper induced up-regulation is not mediated by the induction of a general stress response, which would activate the promoter by the induction of heat shock proteins. This implies a copper specific response.

The study described above is in contrast to a study by Toni *et al.* (2005), who find that copper down-regulates *prnp* activity at both the mRNA and protein level. The most likely reason for the difference, and a point raised by the Varela-Nallar study, is that response to copper is cell line specific. Since PrP^c expression is variable in dissimilar tissues it is most likely that genetic control mechanisms operate differently within these tissues, and both studies agree that copper is able to influence the activity of *prnp*.

1.1.5 Prnp and All-Trans Retinoic Acid

All-Trans Retinoic Acid (ATRA) is a drug used for the treatment of promyelocytic leukaemia. It is an effective treatment, sending the disease into remission by inducing terminal differentiation of the malignant clone. ATRA has been found to down regulate PrP^c expression (Rybner *et al.,* 2002). It is possible that ATRA exerts its effect on the PrP promoter by modulation of transcription factors involved in cellular differentiation. Myt1 is a transcription factor involved in cellular differentiation and, as discussed above (Section 1.13), a highly conserved Myt1 binding element is found in *prnp* from several species (Premzl *et al.*, 2005).

An alternative mode of action of ATRA could be activation of the retinoic acid receptor (RAR) allowing it bind to Retinoic Acid Response Elements (RAREs) either as a homodimer or as a heterodimer with Retinoic X receptor (RXR). The RAR can act as an enhancer or a repressor of transcriptional activity depending on the orientation in which it binds to DNA (for review see Bastien & Rochette-Egly, 2004). Once bound, protein interactions recruit transcription factors such as AP-1 and AP-2. However, as yet no RAREs have been identified in the *prnp*, indicating that ATRA may be more likely to exert a secondary effect through activation of transcription factors rather than direct interaction of RAR with *prnp*.

ATRA was also found to down regulate PrP expression by Cabral *et al* (2002), who propose that down regulation of PrP results through the activity of AP-2 transcription factors, their interaction with AP-1 transcription factors and the repression of c-fos, which is also involved in modulating gene expression. Similarly ATRA induces expression of MKP-1, which inactivates members of the mitogen activated protein (MAP) kinase family, including JNK. In turn, this results in reduced activation of c-Jun and c-fos and potent inactivation of AP-1 (Kitamura *et al.*, 2002). PrP may be down-regulated by ATRA using these pathways in the opposing way to that suggested for up-regulation by copper.

Given the correlation of disease progression with PrP^c levels, factors that down-regulate expression may have a potential role in disease therapy or management. It might be possible that ATRA and other similarly reacting agents could be used to slow the progression of the disease.

1.2 PrP^c Structure

PrP^c is a cell surface protein bound to the membrane by a glycophosphatidylinositol (GPI) anchor (Stahl *et al.*, 1987). It is a glycoprotein and can assume di, mono or unglycosylated states. N-linked glycosylation occurs on two asparagine residues, found at amino acid positions 180 and 196 in mouse PrP^c (Lehmann & Harris, 1997). The protein sequence also contains an N-terminal signal sequence (residues 1-23 in mice) for direction into the endoplasmic reticulum (ER) during synthesis, an octameric repeat region (51-89) and a hydrophobic domain (110-146). The linear structure of PrP^c is shown in figure 1.2.

Figure 1.2 Linear structure of unprocessed murine PrP. Shown are the characterised domains, di-sulphide bride and N-glycosylation sites.

The secondary structure of PrP^c from several species has been determined by nuclear magnetic resonance (NMR) spectroscopy. In mice PrP^c has three alpha helices at amino acids 114-154, 179-193, and 200-217, and a short anti-parallel beta sheet with amino acids 128-131 complementing 161-193 (Figure 1.3; Riek *et al.*, 1996). A disulfide bridge links the cysteine residues at positions 179 and 214 in mouse PrP^c, and by doing so tethers the start of helix 2 to the middle of helix 3. The N-terminus is predominantly unstructured and highly flexible (Donne *et al.*, 1997; Riek *et al.*, 1997), but may assume some secondary structure in the presence of copper binding (see below; Miura *et al.*, 1996).

Figure 1.3 Proposed three dimensional structure of murine PrP^c. Shown are the structure of the PrP^c C-terminus as determined by NMR spectroscopy (left), and the putative full length PrP^c structure with the flexible N-terminus assuming a coiled formation on copper binding (right). Adapted from Riek *et al.* (1996).

Despite small variations in the primary sequence, all characterised mammalian PrP^cs share the same tertiary structure, and the unstructured N-terminal section is highly conserved (Wopfner *et al.*, 1999). The structure is also maintained for chicken, turtle and frog PrP^c even though the amino acid sequences share only 30% homology with mammalian PrP^c (Calzolai *et al.*, 2005). The most conserved regions across mammalian, avian, reptilian and amphibian PrP^c are (with reference to mammalian PrP^c) the amino acid residues around positions 15-20 (which indicate the position of the N-terminal cleavage site), 100-110 at the start of the hydrophobic region, 112-119 of the hydrophobic domain, and the C-terminal structural domains. Such conservation indicates these regions are of importance to the function of PrP^c.

The octarepeat region has proved of much interest. In most mammalian species, it contains the amino acid sequence PHGGGWGQ repeated four times with a further incomplete repeat at the start of the region. Copper binds to this repeat sequence, with each repeat binding one copper molecule (Section 1.3). Despite the involvement of different amino acid motifs, a form of this repeat region is highly conserved across mammalian, avian and reptilian species, indicating it may be of considerable importance for the function of the

protein (Wopfner *et al.*, 1999; Calzolai *et al.*, 2005). However amphibian PrP^c lacks amino acid sequence homology of this region (Strumbo *et al.*, 2001).

In prion diseases, the C-terminal structure of PrP^c is altered such that the predominantly alpha helical structure of PrP^c is replaced by a higher beta sheet conformation (Pan *et al.*, 1993). This structural change is thought to be a post-translational modification of PrP^c catalysed by the presence of PrP^{sc}. The modification results in a change in solubility of the protein and partial resistance to digestion by proteinases (Prusiner, 1982).

1.3 PrP^c and Copper Binding

The octameric repeat domain has been proven to bind copper (II)/Cu^{2+} *in vitro* and *in vivo* (Hornshaw *et al.,* 1995a; Brown *et al.,* 1997b). The amino acid sequence PHGGGWGQ is repeated four times, with an incomplete repeat found at the start of the region, and is highly conserved among mammalian species. Each repeat has been shown to bind one Cu^{2+} molecule and this copper binding is relevant at physiological concentrations, with PrP^c binding becoming saturated at about 5 μM compared to the blood exchangeable concentration of 8 μM (Kramer *et al.,* 2001; Burns *et al.,* 2002). Jackson *et al* (2001) report that the octameric repeat region has a dissociation constant for copper (II) of 10^{-14}M, which is highly suggestive of copper binding under physiological conditions. In support of this, binding affinities of PrP^c for copper have been shown to lie between 10^8 and 10^{16} M^{-1} depending on the number of copper atoms bound (Thompsett *et al.*, 2005).

Cu^{2+} binding in the octameric repeat domain is five co-ordinated, and it is this co-ordination that is thought to give the PrP N-terminus its secondary structure when copper saturated. Of the repeat sequence, the HGGGW sequence is thought to be most important for copper binding, with all but the third glycine (G) acting to stabilise Cu^{2+} binding. Cu^{2+} is four co-ordinated by the residues of the octameric repeat domain, it binds with three nitrogen atoms and one oxygen atom. The nitrogens are donated from the histidine (H) imidazole and the de-protonated amides from the next two glycines, and the oxygen is donated from an additional binding to the second glycine involving the amide carbonyl (Figure 1.4; Stöckel *et al.*, 1998; Aronoff-Spencer *et al.*, 2000; Burns *et al.*, 2002; Chattopadhyay *et al.*, 2005). The four co-ordination of Cu^{2+} by the octameric repeats is planar. The five co-ordination arises from a further binding to the oxygen atom of a water

molecule that lies axially above the Cu^{2+} atom. The oxygen from the water molecule also forms a polar bond with the amine of the tryptophan (W) indole. The octameric repeats may associate with each other by interaction of the nitrogens from the histidine imidazole and the tryptophan of one octameric repeat with the backbone carbonyls of the histidine and the first glycine of the adjacent repeat (Burns *et al.*, 2002). This may result in a stacking effect, resulting in the acquired helical structure of the PrP^c N-terminus on copper binding.

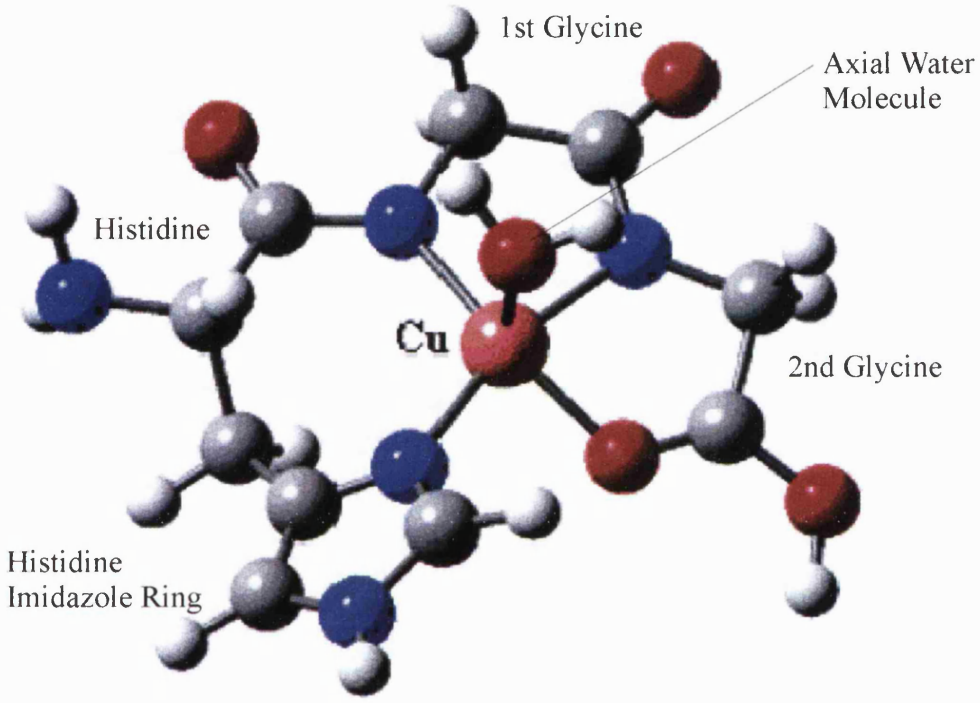

Figure 1.4 Proposed co-ordination of copper by amino acids HGG of a single octarepeat. Nitrogen atoms are shown in blue, oxygen in red, carbon in grey, and hydrogen in white. Adapted from Ji & Zhang (2004).

Two further copper binding conformations have been described (Aronoff-Spencer *et al.*, 2000; Chattopadhyay *et al.*, 2005). They are suggested to arise due to incomplete saturation of the octameric repeat region as a function of Cu^{2+} concentration, as opposed to the above description that is the conformation assumed by the octameric repeats in high copper concentrations (4 equivalents or greater) where full saturation occurs. An intermediate conformation occurs at 1-2 equivalent copper concentrations, where histidines from two adjacent repeats bind one Cu^{2+} molecule via their imidazole nitrogens and the Cu^{2+} is further bound by two oxygens from water molecules. The third conformation

occurs at low copper concentrations, and is thought to involve three or four of the histidine imidazoles.

Further evidence supporting the above secondary structure of the PrP^c N-terminus when saturated with copper was provided by theoretic computation of the binding energies (Ji & Zhang, 2004). This found that the structure proposed above has a higher binding energy for copper than other potential conformations of the octameric repeat region. This study also noted that the binding energy of ceruloplasmin, a serum protein involved in the transport of copper, is much lower than that of the octameric repeat region binding copper as a five co-ordinate. Therefore, it is likely that copper is incorporated most effectively into PrP^c when delivered chelated to serum proteins, as this is a more energetically favourable reaction than incorporation of free copper. Additionally, Brown (1999) showed that PrP^c specific uptake of Cu^{2+} by neurones required chelation, supporting that in a cell system incorporation of Cu^{2+} into PrP^c is more favourable when the copper ion is presented as a chelate, and Thompsett *et al.* (2005) show the binding affinity of PrP^c for copper is higher than that of ceruloplasmin, so PrP^c could effectively compete with transport proteins for bound copper ions.

In addition to the octameric repeat domain, a fifth binding site located between the octarepeat region and the structured C-terminus at amino acid residues 92-96 has been demonstrated (Hasnain *et al.*, 2001; Jackson *et al.*, 2001; Burns *et al.*, 2003). The histidine residue at amino acid position 96 thought to mediate this binding. Two co-ordination modes have been proposed for this site, the first suggests a six co-ordinate structure with histidine 96, glutamine 98, methionine 109, histidine 111, and two further bonds that may be provided by water (Hasnain *et al.*, 2001). The second theory proposes that only amino acids residues 92-96 are involved in Cu^{2+} co-ordination. In this model, Cu^{2+} is four co-ordinated, binding to four nitrogens provided by the histidine side chain and backbone, the threonine (95) and the glycine (94; Burns *et al.*, 2003). However co-ordination of this site does not occur when only these three amino acids (94-96) are present; the two glycines at positions 92 and 93 are required. Hence the authors suggest that one of these glycines may co-ordinate axially to the Cu^{2+} atom in a similar way to that seen for the water molecule and tryptophan in the octameric repeat region. Mutation of either histidine, at amino acid 96 or 111, to alanine results in the loss of one copper binding site from the full length protein (Thompsett *et al.*, 2005), indicating that both histidines are involved in copper coordination by the fifth site making the first proposed binding mode the most likely.

Copper binding to the fifth site is pH sensitive, and stability is lost at pH6.5. The importance of this fifth site remains to be determined, however Burns *et al.* (2003) offer the theory that it may simply be an extension of the copper binding octameric repeat domain. A further weak copper binding site may exist around amino acids 135-155 (Jackson *et al.*, 2001), but this has not yet been substantiated.

As a result of the association of PrP^c with copper molecules, copper binding has been implicated as an important factor in the disease process. Quaglio *et al.* (2001) demonstrated that Cu^{2+} could convert PrP^c into a protease resistant form that was not the same as the disease form. As such the authors suggest that copper binding may produce an intermediate form in the conversion of PrP^c to PrP^{sc}. However, more recently the binding of copper to full length recombinant PrP^c has been shown to prevent PrP^c conversion into the PrP^{sc} isoform and the formation of amyloid fibrils of PrP^{sc} at pH 7.2, which is the approximate pH of the extracellular environment (Bocharova *et al.*, 2005). Furthermore, PrP^c lacking the octameric repeat region was also found to be protected against conversion by the presence of copper, perhaps indicating that binding to the fifth site may play a role in this protection also. At pH 6, where binding of Cu^{2+} to the octameric repeats and the fifth site becomes unstable, the protection of Cu^{2+} against conversion is much less. The authors also showed that Zn^{2+} has a protective effect, although this is not as efficient as Cu^{2+}. Bocharova *et al.* explain the disagreement between the studies by the suggestion that Cu^{2+} binding stabilises a nonamyloidogenic proteinase K resistant form of PrP^c preventing it from undergoing disease specific structural changes.

With the wealth of data supporting copper binding by PrP^c the potential for binding other metals has been investigated. Stöckel *et al* (1998) report that binding is highly specific for copper, with other metals including Ca^{2+}, Co^{2+}, Mg^{2+}, Mn^{2+}, Ni^{2+}, and Zn^{2+} apparently having no affinity for the octameric repeat binding sites. However, Brown *et al* (2000) find that manganese (Mn^{2+}) can be substituted for copper and that over time Mn^{2+} loaded PrP^c develops protease resistance accompanied by alteration to a higher beta sheet structure. The affinity of PrP^c for other metals has also been demonstrated by Jackson *et al* (2001) who find that Ni^{2+}, Zn^{2+}, and Mn^{2+} bind three or more magnitudes more weakly than Cu^{2+} to the octameric repeats and six, seven and ten magnitudes more weakly (respectively) to the fifth site. Alteration in brain tissue metal ion concentrations is a feature of prion diseases and incorporation of metal ions other than copper into PrP^c may be involved in the disease pathogenesis (Wong *et al.*, 2001a).

1.4 PrP^c Trafficking and Metabolism

PrP^c has a wide distribution within the body with expression found in many tissues, including heart, lungs, spleen, kidney, skeletal muscle, uterus, and various glands, however highest expression is seen in neuronal tissues (Robakis *et al.*, 1986; Horiuchi *et al.*, 1995). In most tissues PrP^c has a short half-life, just 3-6 hours in neuronal cells and as little as 1.5 – 2 hours in splenocytes. The longest reported half-life is found in lymphocytes, where PrP^c persists for over 6 hours (Caughey *et al.*, 1989; Borchelt *et al.*, 1990; Parizek *et al.*, 2001; Li *et al.*, 2003). PrP^c is a cell surface glycoprotein and in neuronal tissues shows localisation to the synapses. It has been reported at synaptic terminals (Fournier *et al.*, 1995; Gohel *et al.*, 1999), and pre-synaptic (Herms *et al.*, 1999) and ubiquitous (Laine *et al.*, 2001) localisation have also been described.

1.4.1 Normal PrP^c Trafficking and Processing Within the Cell

To reach its cell surface location, PrP^c is directed co-translationally into the endoplasmic reticulum (ER) by the N-terminal signal peptide. Here the signal peptide is cleaved, as is the C-terminal GPI-anchor signal peptide, which is replaced with the GPI anchor. The mannose side chains are added, and converted into complex glycans within 30 minutes of addition. The correctly folded protein then exits the ER to the golgi, and from there is transported to the cell surface (Figure 1.5: Nunziante *et al.*, 2003; Winklhofer *et al.*, 2003).

PrP^c is associated with regions of the cell membrane known as lipid rafts. Protein localisation to lipid rafts is defined as partitioning with detergent resistant membranes (Sharma *et al.*, 2002). However the composition of these detergent resistant membrane domains varies and PrP^c shows a preference for regions rich in cholesterol, sphingomyelin and palmitolyoleoylphosphatidylglycerol (Mahfoud *et al.*, 2002; Brügger *et al.*, 2004; Critchley *et al.*, 2004). Mahfoud *et al.* found a sphingolipid-binding domain at amino acids 179-211 of the protein sequence, which may have a role in directing PrP^c into lipid rafts and determining its position in the cell membrane.

In addition to PrP^c localisation at the cell surface, it has been shown that PrP^c, as well as PrP^{sc} in disease, is secreted or shed from the cell surface. Secreted PrP^c lacks its GPI anchor, and is released by exosomes (Fevrier *et al.*, 2004). However there is still disagreement about whether the secreted form is actually secreted by the cell or if, instead, it is cleaved from the cell membrane at the anchor attachment site. There is evidence that

the amount of PrP^c found in cell culture media is reduced in the absence of serum, suggesting that serum enzymes such as phospholipase C or D may be involved in the cleavage of PrP^c from the cell surface resulting in an apparent secretory form (Parizek *et al.*, 2001; Parkin *et al.*, 2004).

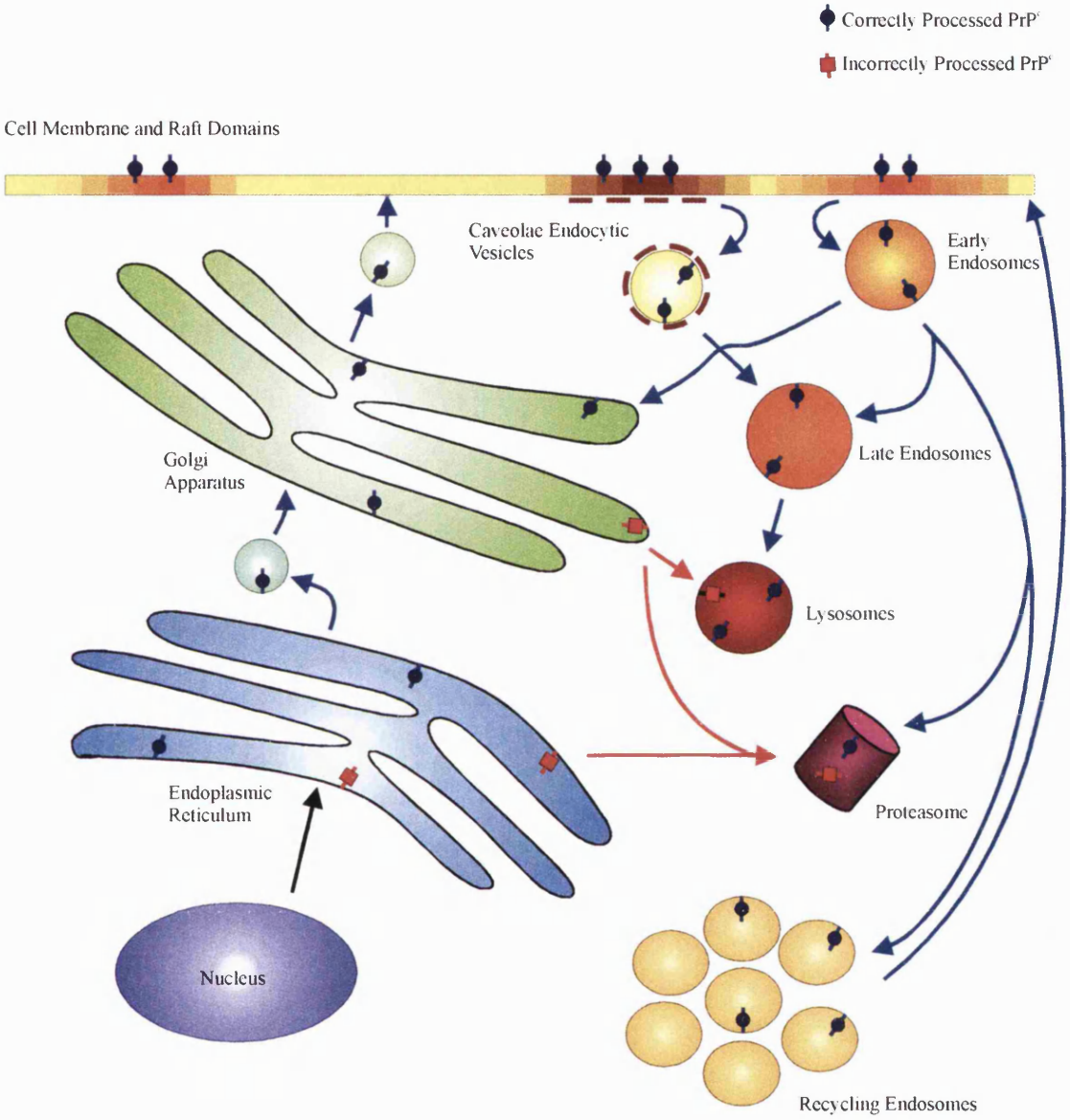

Figure 1.5 Cellular trafficking of PrP. Pathways of correctly folded (blue) and incorrectly folded (red) PrP trafficking to and from the cell surface.

Cell surface PrP^c is also metabolised by a different cleavage process to that which removes the GPI anchor. The flexible N-terminus is separated from the globular C-terminal region by cleavage at amino acids 111-112, located at the start of the palindromic region (Chen *et al.*, 1995). This cleavage is mediated by A Disintegrin And Metalloprotease 10 (ADAM10), Tumour necrosis factor α-Converting Enzyme (TACE), and zinc matrix

metalloproteases (MMPs; Vincent *et al.*, 2001; Parkin *et al.*, 2004). Zinc MMPs may, in turn, be activated by increased exogenous copper concentrations (Parkin *et al.*, 2004). Since the N-terminus of PrP^c binds copper and it is this region that is cleaved, the cleavage event may be relevant for the function of PrP^c. Cleavage is altered in infected cells, with the N-terminus cleaved at amino acids 88-89 by the calpain family of proteases (Chen *et al.*, 1995; Yadavalli *et al.*, 2004). Hence the metabolism of PrP may have an important impact on the disease progress, although it is not possible to say whether the alteration in metabolism causes or is a result of the disease pathology.

Although PrP^c is lost into the surrounding extracellular environment by shedding, the majority of cell surface PrP^c is internalised and directed into endosomes (Borchelt *et al.*, 1993). Internalisation has been suggested to occur by clathrin, dynamin-1 and caveolae mediated pathways (Shyng *et al.*, 1994; Magalhães *et al.*, 2002; Peters *et al.*, 2003). PrP^c internalised by both clathrin-coated vesicles and the dynamin-1 pathway is directed into early endosomes (Shyng *et al.*, 1994; Magalhães *et al.*, 2002) and from there may be directed back to the golgi (Magalhães *et al.*, 2002). PrP^c internalised by the caveolae-mediated pathway is transferred straight from the caveolae-containing endocytic vesicles into late endosomes and/or lysosomes so bypassing the classical early endosome internalisation pathway (Peters *et al.*, 2003). Caveolae is a type of raft protein involved in internalisation, therefore the localisation of PrP^c at the cell surface in different raft types may determine its mode of internalisation. In addition, internalised PrP^c is directed into recycling endosomes, from where it can be quickly relocated back to the cell surface if required (Magalhães *et al.*, 2002). Recycling endosomes are rich in lipid raft components (Gagescu *et al.*, 2000), therefore it is likely that the destination of PrP^c inside the cell is determined by the rafts to which it is directed. The internalisation pathways of PrP^c are shown in Figure 1.5.

The N-terminal region of PrP^c has been implicated in the control of PrP^c internalisation (Shyng *et al.*, 1995; Lee *et al.*, 2001; Nunziante *et al.*, 2003; Sunyach *et al.*, 2003). Shyng *et al.* (1995) proposed that the far N-terminus contains a domain capable of binding to other membrane proteins that would the target PrP^c to clathrin-coated pits for internalisation. This suggests that this form of internalisation could not happen in the absence of the N-terminal region. Specifically it has been found that movement out of raft domains for internalisation by non-caveolae pathways is dependant on the six N-terminal amino acid residues in the mature protein, NH_2-KKRPKP, at position 23-28 of the N-

terminus (Sunyach *et al.*, 2003). Hachiya *et al.* (2004) also found that these amino acids were important for intracellular trafficking of PrP^c by interacting with the microtubule-dependent motor proteins kinesin and dynein, allowing movement to and from the synapse. The C-terminus, in particular the final 14 residues, has also been implicated in the control of PrP^c internalisation. However, this region was suggested to direct PrP^c into a caveolae mediated internalisation pathway (Kaneko *et al.*, 1997).

1.4.2 Copper Induced Internalisation

Copper induces the internalisation of PrP^c. This response was shown to be rapid at 500 μM $CuSO_4$ and significant at 200 μM (Pauly & Harris, 1998; Lee *et al.*, 2001). The minimum concentration of $CuSO_4$ that produced a response was 100 μM. In addition, zinc (100 μM $ZnSO_4$) also significantly internalised PrP^c, but cobalt, manganese and iron at concentrations as high as 500 μM did not produce any effect. Miura *et al.* (2005) suggest that PrP^c at the cell surface binds Cu^{2+}, reduces it to Cu^+ before trafficking into endosomes, here the internal pH is low enough (pH 5.5-6.5) that the Cu^+ is released. The authors suggest that the complete intact octameric repeat region is vital for the reduction reaction and, therefore, for internalisation to occur.

N-terminal deletion of PrP^c and specifically deletion of the octameric repeat domain significantly inhibits copper induced internalisation (Pauly & Harris, 1998; Lee *et al.*, 2001). As suggested previously, it is likely that the role of the octameric repeat domain is to bind copper, thus binding produces the internalisation response. The importance of the histidines at amino acid positions 68 and 76 of the octameric repeat domain in copper co-ordination is seen by the abolition of internalisation in mutant constructs where these histidines have been replaced with glycine (Perera & Hooper, 2001). Moreover, disease associated mutation of the octameric repeat domain, where nine extra octameric repeats are present (PG14; found in patients with familial CJD), abolishes internalisation.

Copper and zinc stimulated internalisation directs PrP^c into early endosomes and to the golgi (Brown & Harris, 2003). However the preferred pathway for this reaction is still under debate. Brown & Harris conclude that copper and zinc induce internalisation via clathrin-coated pits. In contrast, Marella *et al.* (2002) find that copper induced internalisation occurs through a caveolin-dependant pathway in neurones and microglia. Further, it can be disrupted by the antibiotic filipin, which acts by binding membrane sterols and so disrupting lipid rafts where caveolae is found.

1.4.3 PrP^c Quality Control and Disease Associated Mutants

Cellular quality control mechanisms ensure that incorrectly assembled proteins are targeted for destruction so that they cannot exert a detrimental effect on cellular function. Incorrectly processed proteins are recognised in the ER, a ubiquitin protein tag is added by ubiquitin ligases in the ER membrane and the incorrectly folded proteins are directed by this tag to the proteasome via the ER associated destruction (ERAD) pathway (for review see Hampton, 2002). The correct folding and processing of PrP^c is important for it to reach its membrane position. Incorrectly processed PrP^c such as ^{Ctm}PrP (PrP^c inserted into the cell membrane and spanning the membrane via the hydrophobic region in the centre of the protein, with the C-terminus facing out of the cell and the N-terminal signal peptide remaining uncleaved) is retained in the ER (Stewart *et al.,* 2001). This suggests that incorrectly folded PrP^c is directed into ERAD for destruction. Further cellular quality control mechanisms operate beyond the ER. The pre-octameric repeat amino acid sequence was found to be highly important for recognition of misfolded PrP^c in post ER compartments and causes the incorrectly folded protein to be directed to lysosomes for destruction (Gilch *et al.*, 2004).

Disruption of either complex glycosylation or the addition of the GPI anchor interferes with PrP^c transport to the cell surface. Helix 1 has been identified as essential for the correct folding of PrP^c. The absence of this helix prevents the attachment of the GPI anchor and the complex glycans, and as a result prevents PrP^c from reaching the cell surface (Winklhofer *et al.*, 2003). The stabilisation of helix 1 by interaction of amino acids 140, 145, 148, and 149 with amino acid 204 of helix 3 (with reference to the murine primary sequence) is also involved in the correct processing of PrP^c. C-terminal membrane anchorage was found to be essential for complex glycosylation to occur, signifying that correct insertion into the cell membrane is important for the correct metabolism of PrP^c (Walmsley *et al.*, 2001). Additionally, disruption of the disulphide bridge prevents complex glycosylation and localisation to the cell surface (Yanai *et al.*, 1999).

Partial ER retention has been observed for some pathological mutations associated with the development of familial prion diseases including PG14 (Ivanova *et al.,* 2001). Two other pathological mutations associated with inherited disease are the substitution of glutamic acid at amino acid position 200 with lysine (PrP^{E200K}), found in familial CJD, and substitution of aspartic acid at position 178 with asparagine (PrP^{D178N}), associated with

FFI. Bovine representations of these two mutations, showed a lack of complex glycosyation and were retained within the ER (Negro *et al.*, 2001). The retention of the PrP^{E200K} mutant was not as severe as that seen for the PrP^{D178N} mutant, with cell surface localisation also seen. A mutant associated with GSS, where the glutamine at position 217 has been substituted for arginine, with also a valine at position 129 rather than methionine ($PrP^{Q217R\text{-}129V}$), is also retained inside the cell (Singh *et al.*, 1997). This mutant is found mostly within the ER but also in endosomes and lysosomes. Less than 45% of $PrP^{Q217R\text{-}129V}$ was found to reach the cell surface. In light of these studies, the role of ER processing and quality control is thought to play a significant part in diseases pathogenesis.

Two further pathological mutations associated with hereditary CJD, the substitution of threonine at amino acid position 183 with alanine (PrP^{T183A}) and the substitution of phenylalanine at position 198 with serine (PrP^{F198S}), have been shown to be misfolded, lack the GPI anchor and are not complex glycosylated (Kiachopoulos *et al.*, 2004). These mutants were not retained in the ER but were found to be secreted from the cell, most likely due to the lack of the GPI anchor and so lack of tethering to the cell surface. Since PrP^{sc} forms protein plaques in the brains of infected individuals this could be highly significant for the disease pathogenesis.

ERAD directed PrP^{c} degradation occurs in the proteasome (Yedidia *et al.*, 2001). It is still under debate how mutant PrP^{c} retained in the ER reaches the proteasome. Ma and Lindquist (2001) have found that PrP^{D178N}, as well as wild type PrP^{c}, reach the proteasome by retrograde transport to the cytoplasm. Jin *et al.* (2000) found that PrP^{Q217R} was associated with the ER chaperone BiP for an abnormally long time before being targeted to the proteasome for degradation. The authors suggest that PrP folding is promoted by BiP, which recognises misfolded PrP^{c} and mediates retrotranslocation to the proteasome. However, Drisaldi *et al* (2003) find that this is not the case, and that mutant and wild type PrP^{c} reach the proteasome via a pathway not as yet characterised that does not involve retrotranslocation from the ER. Studies of proteasome inhibition have shown that PrP^{c} accumulates in the cytosol. This accumulation of PrP^{c} results in neurotoxicity and cytosolic PrP^{c} forms aggregates of PrP^{sc}-like protein (Ma *et al.*, 2002; Ma & Lindquist, 2002). This may have implications for the disease process and further highlights the importance of cellular quality control in dealing with misfolded PrP^{c}.

1.5 The Elusive Function of PrP^c

Initial studies on transgenic mice showed that there is little effect on development and behaviour when *prnp* is knocked out (Büeler *et al.*, 1992; Weissmann *et al.*, 1994), signifying redundancy of the protein. However subtle effects are seen. Knockout mice display alterations in circadian rhythms, sleep disturbance, impaired learning ability, weakened exercise capability, and reduced anxiety response (Tobler *et al.*, 1996; Nishida *et al.*, 1997; Tobler *et al.*, 1997; Criado *et al.*, 2005; Nico *et al.*, 2005a; Nico *et al.*, 2005b) indicating that PrP may be involved in homeostatic systems. In addition, knock-out mice suffer increased susceptibility to oxidative stress (Klamt *et al.*, 2001; Brown *et al.*, 2002).

1.5.1 PrP^c in Copper Transport and Metabolism

Copper is an extremely toxic metal, present in high enough concentrations at the synapse to cause damage. Therefore the cell has an excess of mechanisms for copper metabolism (for review see Camakaris *et al.*, 1999; Bertinato & L'Abbè, 2004). As discussed in section 1.4.2, copper binding internalises PrP^c. This has led to the suggestion that PrP^c is involved in copper metabolism, possibly by binding and removing toxic copper ions or by delivering them to specific targets within the cell. Copper up-take has been shown to correlate with the level of PrP^c expression in mouse cerebellum (Brown, 1999). Copper binding to PrP^c is pH sensitive with stability lost as pH declines. Endocytosis into acidic organelles such as late endosomes and lysosomes may result in the release of copper (Burns *et al.*, 2002). The release of copper at the synapse on depolarisation is related to PrP^c expression (Brown, 1999), therefore PrP^c may have a role in containing synaptic copper fluctuations by binding copper ions and delivering them to storage vesicles. Copper liberated after internalisation may be utilised by other cellular proteins, or instead, PrP^c may not release copper on internalisation but deliver copper ions directly to intracellular proteins, thus functioning as a copper transport molecule. Alternatively, if PrP^c were to be directed to neutral cellular compartments, it would retain bound copper, and so might function as a sink in which excess copper is collected and stored to protect against cellular damage.

The up-regulation of *prnp* in response to increased exogenous copper supports a role of PrP^c in response to copper insults. PrP^c knockout neurones are more susceptible to copper induced toxicity than wild type (Brown *et al.*, 1998), and the octameric repeat region alone is able to rescue survival of these knockout neurones to a level equivalent to that of wild

type. Therefore the role of PrP^c in binding copper to its octameric repeat region might be to prevent the copper ions from damaging the cell. This would be of especial importance at the synapses, where local concentrations peak at high levels during depolarisation and would be likely to damage the cell in the absence of suitable protection mechanisms. This copper binding could, in turn, lower levels of hydrogen peroxide formed from copper ions undergoing Fenton or Haber-Weiss reactions and so indirectly protect cells from oxidative stress (Brown *et al.*, 1998; Nishimura *et al.*, 2004). PrP^c expression by astrocytes may also function to protect neurones from copper induced toxicity by taking up copper ions released from neurones (Brown, 2004).

A role for PrP^c as a storage or transport molecule for copper does not explain other properties associated with both the cellular and disease isoforms of the protein. For example, the increased susceptibility of scrapie infected cells to oxidative stress in the presence of redox active iron (Fernaeus *et al.*, 2005) is unlikely to be due to PrP^c chelating iron, as binding studies of the PrP^c octameric repeat domain and various metal ions have shown low affinity for this metal (Hornshaw *et al.*, 1995a; Hornshaw *et al.*, 1995b). This implies that the role of PrP^c extends to other cellular survival mechanisms such as oxidative stress response.

1.5.2 PrP^c and Cellular Antioxidant Activity

As stated above, PrP^c knockout mice show few developmental or biochemical irregularities. However, notable deviations from the wild type include an increased sensitivity to oxidative stress and reduced Cu/Zn superoxide dismutase (SOD) activity. Scrapie infected mice have compromised antioxidant function (Wong *et al.,* 2001b; Thackray *et al.,* 2002). This is also seen in scrapie infected neuronal cells, where increased levels of lipid peroxidation markers and decreased activity of SOD and glutathione dependant antioxidant mechanisms are observed (Milhavet *et al.*, 2000). Oxidative damage is a proposed method by which cells die during the progression of prion diseases (Guentchev *et al.*, 2002). This may be due to altered copper metabolism as suggested above but also might be a loss of function brought about by the change of PrP structure characteristic of prion disease.

PrP^c has been shown to be up-regulated and to accumulate at the site of damage in ischaemic brain injury in human tissue (McLennan *et al.*, 2004). This was also observed in mice (McLennan *et al.*, 2004) and rats (Shyu *et al.*, 2005b). In the mouse model, the

extent of injury in response to an equivalent insult was much greater in PrP^c knock out than wild type mice. Increases in inflammatory cytokines and reactive oxygen species (ROS) are found in ischaemic injury, and both of these may be involved in the up-regulation of PrP^c around the injury site. This data indicates that PrP^c may have a role in the protection against oxidative stress and inflammatory effects of ischaemia. The authors suggest that this protective effect is determined by the site of injury and is relative to the level of PrP^c expression.

A further effect of the absence of PrP^c is on mitochondria quantity and morphology (Miele *et al.*, 2002). Unusual mitochondrial morphology is observed on ablation of PrP^c and elevated levels of mitochondrial manganese-dependant SOD are found (Brown *et al.*, 2002; Miele *et al.*, 2002). Mitochondria produce the vast amount of the cell's energy and in doing so produce large quantities of free radicals, therefore it is likely that they would be greatly affected by an inability to deal with oxidative stress that may arise from a loss of PrP^c function. Mitochodria also play a significant role in apoptosis and so, if their physical condition is altered as a result of altered PrP^c activity in prion diseases, they may contribute to cell death and disease pathogenesis.

In knockout mice, alteration in antioxidant activity in tissues that would normally express PrP^c has been suggested to account for impaired ability to undergo strenuous exercise (Nico *et al.*, 2005b). Knockout mice have higher levels of ROS in muscle tissue as well as in neuronal tissue (Klamt *et al.*, 2001). The added oxidative insult from aerobic exercise may impair the ability of the muscle to function at the normal level. Additionally, Nico *et al.* note that, despite finding that mitochondrial respiration is unaltered in knockout mice, mitochondrial numbers are lower (Miele *et al.*, 2002), and so the mice may be unable to generate the energy muscles require for strenuous activity.

Early changes in the brains of infected mice include altered metal ion concentrations and this is associated with the decreased ability to deal with oxidative stress insults (Wong *et al.*, 2001b). A role for PrP^c in delivery or incorporation of copper into this enzyme has been suggested (Brown & Besinger, 1998). In cells selected for resistance to copper or oxidative stress insults, PrP^c is expressed at higher levels to those found in their unstressed counterparts (Brown *et al.*, 1997a). Loss of PrP^c mediated delivery of copper into Cu/Zn superoxide dismutase may account for the increased susceptibility of knock out mice to oxidative stress.

PrP^c has been suggested to have activity like that of SOD itself and this has been demonstrated using recombinant PrP^c *in vitro* (Brown *et al.,* 1999). The activity was dependent on copper binding to the octameric repeat domain and was directly proportional to the amount of copper bound. PrP^c has been shown to contribute to total SOD activity of mouse brain homogenates (Wong *et al.*, 2000). PrP^c immunoprecipitation from brain homogenates reduced total SOD activity of the remaining tissue proportionally to the quantity of PrP^c precipitated. Complementary to this data, PrP^c has been shown to have SOD-like activity *in vivo*. PrP^c isolated from mouse brain demonstrated SOD-like activity that was dependent on copper binding to the octarepeats (Brown *et al.*, 2001). At least two copper molecules must be bound for this activity to be significant. Although the octameric repeat domain is required for the reported SOD-like activity, a residual activity is observed using copper refolded recombinant protein lacking the octameric repeat region (Brown *et al.*, 1999). This may indicate that copper binding to the fifth site is also able to initiate some degree of antioxidant activity from recombinant PrP^c.

It should be noted that two studies show contrasting results with both PrP^c *in vivo* and recombinant PrP^c *in vitro* shown to have no antioxidant activity at all (Hutter *et al.*, 2003; Jones *et al.*, 2005). The disagreement most likely arises from differing experimental conditions. These experiments were carried out under conditions where copper was rendered biologically unavailable to PrP^c. Since the suggested PrP^c SOD-like activity is dependant on copper binding to the octameric repeat domain, it is doubtful that activity would be seen under these conditions. However, as a result of the disagreement, the SOD-like function of PrP^c remains highly controversial and further study is required to clarify if PrP^c is a genuine antioxidant.

The importance of the N-terminus in the response of PrP^c to oxidative stress is further emphasized by Zeng *et al.* (2003), who show that tethering the N-terminus to the cell membrane results in a neuronal phenotype which, despite displaying similar PrP levels to wild type, shows a decreased ability to deal with an oxidative stress insult. Sakudo *et al* (2003) also report that the octameric repeat domain is essential in regulating total cellular SOD activity and apoptosis. The authors found that cells expressing N-terminally truncated PrP^c, which lacks the octameric repeat region, show significantly higher levels of oxidative stress and apoptosis in response to serum deprivation than wild type cells. As well as the octameric repeat domain, the hydrophobic domain at the core of the structured C-terminus is also thought to be essential for PrP^c antioxidant activity (Cui *et al.*, 2003;

Sakudo *et al.*, 2005). Whereas the role of the octameric repeat domain is likely to involve copper binding, the role of the hydrophobic domain remains to be determined. This domain could be part of the enzyme active site or a structurally stabilising region of PrP^c.

The putative role of PrP^c as an antioxidant enzyme is supported by current knowledge of its gene structure and regulation. *Prnp* is up-regulated in response to cellular stress and shares a number of features with several mouse SOD genes (Premzl *et al.*, 2005) including the gene structure of two to three exons with the ORF entirely encoded by the final exon, and the lack of TATA box. In addition, MZF-1, for which binding sites have been found conserved in *prnp* across several species, is a negative regulator of some mouse SODs (Zelko & Folz, 2003).

A role for PrP^c as an antioxidant or a modulator of cellular stress is consistent with findings that it is involved in mouse embryogenesis (Manson *et al.*, 1992; Miele *et al.*, 2003). PrP^c is expressed in most adult tissues, although to varying extents depending on the tissue type. However during embryogenesis expression is more tightly regulated. The induction of PrP^c mRNA appears to coincide with the period of development where the embryo switches from anaerobic to aerobic metabolism and so is exposed to much higher levels of ROS. PrP^c may be induced to protect the developing embryo from oxidative stress insults during development.

1.5.3 Signal Transduction

PrP^c has been thought to have a role in lymphocyte signal transduction for some time (Cashman *et al.*, 1990). A PrP^c mediated signal cascade in lymphocytes is suggested to be involved in activation, as memory T lymphoctes express more PrP^c than immature cells, or in initiating response to proliferation signals (Li *et al.*, 2001; Bainbridge & Walker, 2005). In lymphocytes, the accumulation of crosslinked proteins in patches within the cell membrane (capping) involves lipid raft proteins. PrP^c is targeted to lipid rafts within the cell membrane and may become incorporated in these caps. The cross-linking of PrP^c that is potentially triggered by this close interaction has been suggested to cause activation of signal transduction pathways involving calcium signalling and MAP kinase activation (Stuermer *et al.*, 2004).

A role for PrP^c in signal transduction was strengthened by the finding that in mouse neuronal cells PrP^c could interact with signalling proteins including Fyn tyrosine kinase,

synapsin Ib and growth factor receptor-bound protein 2 (Grb2; Mouillet-Richard, 2000; Spielhaupter & Schätzl, 2001). Fyn is implicated in the control of cell growth. Synapsin Ib is part of a highly conserved family of synapsins, which are involved in synapse formation and neurotransmitter release. Grb2 is involved in transduction of signals from receptors at the cell membrane to intracellular signalling molecules. PrP^c binding to any of these molecules could, therefore, trigger signal transduction cascades. In addition a PrP^c-binding peptide has been found to activate cAMP and protein kinase A (PKA), and extracellular regulated protein kinase (ERK) pathways of neuroprotection (Chiarini *et al.*, 2002). This is also supported by data from Schneider *et al.* (2003), who propose a transduction cascade by which PrP^c stimulation activates ERK1 and ERK2. Overall this data suggests that PrP^c activation starts a cascade of cellular protective signals, which may explain the protective function of PrP^c in response to ROS. However it does not account for the role of copper in such a reaction. Activation of PrP^c in response to exogenous signalling molecules may require copper binding or the alteration in N-terminal secondary structure imparted by copper binding.

1.5.4 Other Suggested Functions

Other roles for PrP^c have been suggested but have received much less attention than those discussed above. PrP^c binds to neural cellular adhesion molecules (N-CAMs; Schmitt-Ulms *et al.*, 2001), and Mange *et al.* (2002) found that PrP^c overexpressing cells showed a greater tendency to aggregate than cells expressing normal levels of PrP^c, indicating a potential role for PrP^c as an adhesion molecule. Cleavage of cell surface PrP^c at the GPI anchor abolished this effect in cells overexpressing PrP^c but not in the wild type cells, signifying that under normal circumstances PrP^c would not be a dominant adhesion molecule. The authors also note that the PrP^c specific adhesion reaction occurs independently of Cu saturation but requires the N-terminus. The specific protein on the adjacent cell surface with which PrP^c may react is unknown, although it could potentially react with itself. There has been little further investigation into PrP^c as a cell adhesion molecule as it is plausible that the PrP^c specific adhesion was an artefact of overexpression.

Disrupted sleep patterns found in patients suffering from FFI along with the findings of altered sleep regulation in knockout mice compared to wild type, have advocated a potential role for PrP^c in promoting sleep continuity (Tobler *et al.*, 1996; Tobler *et al.*, 1997). The suggestion of a peptidase role for PrP^c has arisen because the structured C-terminus of murine PrP^c shares homology with the active site of rat signal peptidase

(Glockshuber *et al.*, 1998). Also, a role for PrP^c has also been proposed in serotonin homeostasis by regulating specific receptor couplings and cross-talk (Mouillet-Richard *et al.*, 2005).

1.6 Aims and Objectives

Despite the wealth of information generated by recent studies into many aspects of PrP^c, little is known about its genetic regulation and as yet there is no overall consensus on the function of the protein. The many properties of PrP^c provide confusing and sometimes misleading clues as to its role within the cell, and no single hypothesis is able to account for all the established characteristics of this protein. Overall, the aim of this work is to provide further understanding of the regulation, metabolism and function of the cellular isoform of the prion protein. The specific aims of this work are listed below.

The aims of studying the structure of the gene and control elements were;

- To investigate the regions of the gene important for driving the production of PrP mRNA.
- To determine the importance of the gene in tissue specific expression and how the underling tissue affects the expression of PrP^c at the genetic level.
- To determine the regions of the gene important for tissue specific expression
- To identify substances that alter *prnp* activity. Both for the purpose of determining the function of PrP^c as indicated by the factors that induce it, and for identifying substances that may be useful agents for disease management.
- To identify the regions of the gene important for responding to factors that are found to modulate expression.

PrP^c metabolism and function was investigated at the protein level with the following aims;

- To examine copper induced internalisation of PrP^c. Specifically to find the conditions under which internalisation occurs optimally and to determine the minimum concentration of copper that will induce internalisation.
- To determine if other metals can produce the same internalisation reaction as copper.
- To determine the regions of PrP^c important for the copper internalisation reaction.

- To investigate the protection PrP^c affords against copper toxicity, including if this protection is directed directly against the copper ion itself or if protection is by preventing oxidative stress that free copper can cause, and additionally, to identify the regions of PrP^c important for this protection.
- To investigate if PrP^c can protect against cell death induced by oxidative stress insults, and the regions of the protein important for protection against free radicals.

2 Materials and Methods

Reagents were purchased from Sigma (Poole, UK) unless otherwise stated.

2.1 Creation of Plasmid Constructs

2.1.1 Materials

Plasmids – Vector maps are shown in appendix A

pcDNA-3.1(+) – Invitrogen (Paisley, UK)

pEGFP-C1 – Clontech (Oxford, UK)

pd2-EGFP-1 – Clontech

pd2-EGFP-N1 – Clontech

DsRED-ER – Clontech

pProHGPrP(m)Sal – Kind donation from Dr Charles Weissmann (Fisher *et al.*, 1996)

PCR

Pwo Polymerase – Roche (East Sussex, UK)

dNTPs – New England Biolabs (NEB)

Dpn1 – Invitrogen

Nuclease Free Water – Promega (Southampton, UK)

Transformation

XL-2 Blue Ultra Competent Cells – Stratagene (Amsterdam, Netherlands)

LB Broth - Merck (Hertshire, UK)

Agar – Merck

Kanamycin Sulphate – Melford Laboratories (Ipswich, UK)

Carbenicillin

Mini-Prep

Qiagen Qia-Quick Spin Mini-Prep Kit – Qiagen (Crawley, UK)

Glycerol – Fisher (Loughborough, UK)

LB Broth – Merck

Nuclease Free Water – Promega

Primers – Purchased from either Helena (Sunderland, UK) or MWG (London, UK)

Primers for the introduction of mutations into PrP(m) through PCR mutagenesis are shown in table 2.1, and those for sequencing reactions are shown in table 2.2.

Mutation	F R	Primer Sequence
Δ23-38 (pcDNA-PrP)	F	5'GGA CTG ATG TCG GCC TCT GCC CCG GGC AGG GAA GCC CTG G 3'
	R	3'CCT GAC TAC AGC CGG AGA CGG GGC CCG TCC CTT CGG GAC C 5'
Δ23-38	F	5'CTA TGT GGA CAG ATG TCG GCC TCT GCT CAC CGG TCG CCA CCA TGG TGA GC 3'
	R	3' GAT ACA CCT GAC TAC AGC CGG AGA CGA GTG GCC AGC GGT GGT ACC ACT CG5'
Δ51-90	F	5' GGC AAC CGT TAC CCA GGA GGG GGT ACC CAT 3'
	R	3' CCG TTG GCA ATG GGT CCT CCC CCA TGG GTA 5'
Δ67-90	F	5' GGT GGC TGG GGA CAA GGA GGG GGT ACC CAT'3
	R	3' CCA CCG ACC CCT GTT CCT CCC CCA TGG GTA'5
Δ112-119	F	5' CCA AAA ACC AAC CTC AAG CAT GTG GTA GTG GGG GGC CTT GGT GGC 3'
	R	3' GGT TTT TGG TTG GAG TTC GTA CAC CAT CAC CCC CCG GAA CCA CCG 5'
Δ112-136	F	5' CCA AAA ACC AAC CTC AAG CAT GTG ATG ATC CAT TTT GGC AAC GAC TGG G 3'
	R	3' GGT TTT TGG TTG GAG TTC GTA CAC TAC TAG GTA AAA CCG TTG CTG ACC C 5'
Δ122-146	F	5' GCA GCT GGG GCA GTA GTG CGC TAC TAC CGT GAA AAC ATG TAC 3'
	R	3' CGT CGA CCC CGT CAT CAC GCG ATG ATG GCA CTT TTG TAC ATG 5'
Δ135-150	F	5' GGG AGC GCC GTG AGC GAA AAC ATG TAC CGC 3'
	R	3' CCC TCG CGG CAC TCG CTT TTG TAC ATG GCG 5'

Table 2.1 Primers used for the introduction of deletions into mouse PrP^c by site directed PCR mutagenesis. The sequences shown are for introduction of the mutation into pEGFP-C1-PrP(m) unless otherwise indicated.

Primer Name	Sequence
EGFP-N	5' CGT CGC CGT CCA GCT CGA CCA G 3'
EGFP-C	5' CAT GGT CCT GCT GGA GTT CGT G 3'
PrP F	5' AAA AAG CGG CCA AAG CCT GG 3'
PrP R	5' GGA TCT TCT CCC GTC GTA ATA G 3'
pEGFP-C1 base 527-547	5' GCG GTA GGC GTG TAC GGT GG 3'
T7	5' TAA TAC GAC TCA CTA TAG GG 3'

Table 2.2 Sequencing Primers.

Agarose Gel Electrophoresis

Agarose – Melford

TBE or TAE Buffer

Ethidium Bromide

10x Bluejuice loading dye – Invitrogen

λ - Hind III fragments – Invitrogen

2.1.2 Creation of Plasmids for PrP^c and PrP^c Mutant Studies

For the co-localisation, trafficking, and survival assays, seven GFP fusion constructs have been made using mouse PrP^c (accession number = M13685). The pEGFP-C1-PrP(m) plasmid was kindly donated from Marco Prado (Brazil). Mutations were introduced into this plasmid using PCR mutagenesis to give pEGFP-C1-PrP(m) Δ23-38, pEGFP-C1-PrP(m) Δ51-90, pEGFP-C1-PrP(m) Δ61-90, pEGFP-C1-PrP(m) Δ112-119, pEGFP-C1-PrP(m) Δ112-136, pEGFP-C1-PrP(m) Δ122-146 and pEGFP-C1-PrP(m) Δ135-150 (see figure 2.1). Δ51-90, Δ67-90, and Δ135-150 mutations were created previously by Kate Edwards (University of Cambridge). A pEGFP-C1-GPI control, the same construct as pEGFP-C1-PrP(m) but lacking all of PrP except the N-terminal signal peptide and GPI anchor, and pcDNA-3.1-PrP(m), a PrP expressing vector lacking the GFP tag, were created by Maki Daniels (University of Cambridge).

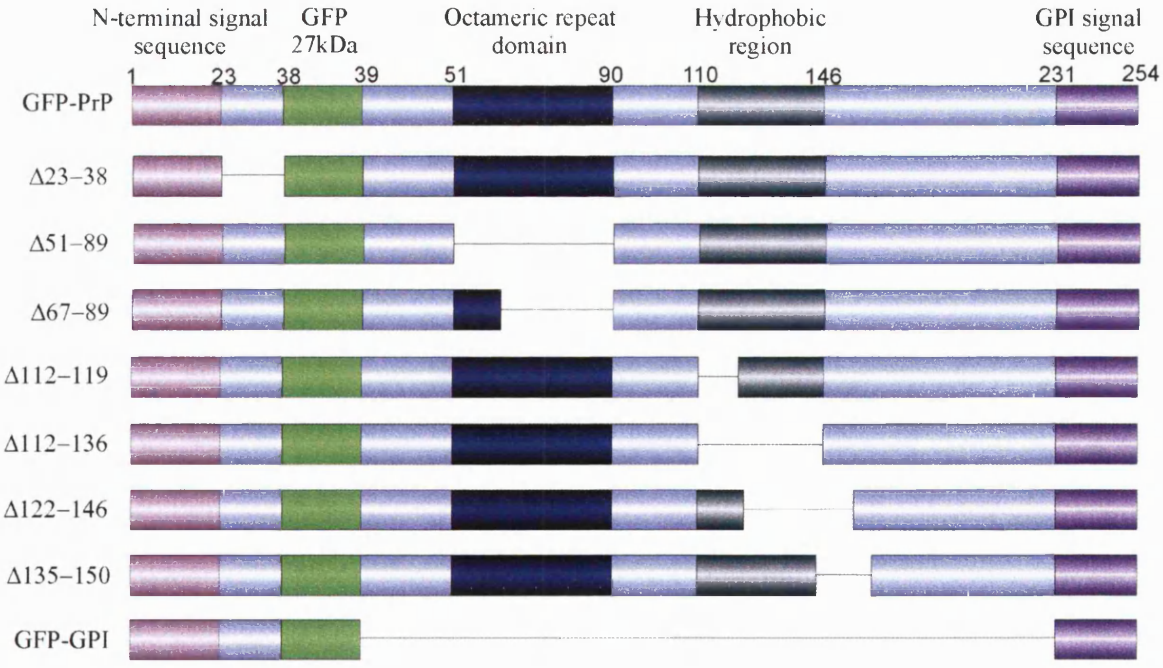

Figure 2.1 Diagrammatic representation of the construction of GFP-PrP^c showing the location of each of the deletion mutants.

To introduce the remaining mutations the following reaction was prepared, and carried out in a Thermo Hybaid PCR Sprint thermal cycler. 200 ng template DNA, 20 μM of each primer (see table 2.1), 0.5 μM dNTPs, and 10 μl 10x buffer (100 mM Tris-HCl [pH8.85 @ 20°C], 250 mM KCl, 50 mM $[NH_4]_2SO_4$, with or without 20 mM $MgSO_4$) were added into each reaction. When using the buffer without $MgSO_4$ reactions were set up with 10, 12, 14 and 16 μl 25 mM $MgSO_4$ (provided) added. Reactions were made up to 99 μl with nuclease free water. After a 10 minute hot start at 95°C, 5 units (1 μl) of Pwo polymerase were added to the reaction mixture, making a final volume of 100 μl reaction mix. Sixteen cycles of 97°C for 1 minute, 55°C for 1 minute, and 72°C for 3 minutes were performed. This was followed by one cycle of 95°C for one minute, 55°C for one minute, and 72°C for 10 minutes. The hold temperature was 4°C. Following PCR, samples were digested in Dpn1 to remove remaining parental DNA.

2.1.3 Creation of Plasmids for Promoter Studies

Plasmids for the promoter studies have been made using the bovine promoter sequence and include a promoter plus exons 1 and 2 construct (A), a promoter only construct(B), an exon 1 and exon 2 construct (C), a promoter plus exon 1 only construct (D), and an intron 1 and exon 2 only construct (E; see figure 2.2). Constructs D and E were made by Kate Edwards (University of Cambridge), and construct A was made by Andrea Holme (University of Bath). Constructs B and C were made by Lark Technologies Inc. (Essex – UK). All promoter constructs have been made in pd2-EGFP-1, a promoter-less vector containing destabilised GFP with a two hour half-life. The destabilised GFP reporter is a modified version of an enhanced variant of GFP (EGFP) made by fusing the C-terminal end of the EGFP with amino acids 422-461 of the degradation domain of mouse ornithine decarboxlyase, one of the shortest lived proteins in mammalian cells with a half life of just 30 minutes and no requirement of ubiquitination for destruction (Li *et al.*, 1998). The CMV promoter driven, and therefore constitutively expressed, pd2-EGFP-N1 vector was used as a control non-specific changes in fluorescence.

Constructs equivalent to A, and E were created using the mouse long incubation prion gene (accession number = U29187), by Lark Technologies Inc.

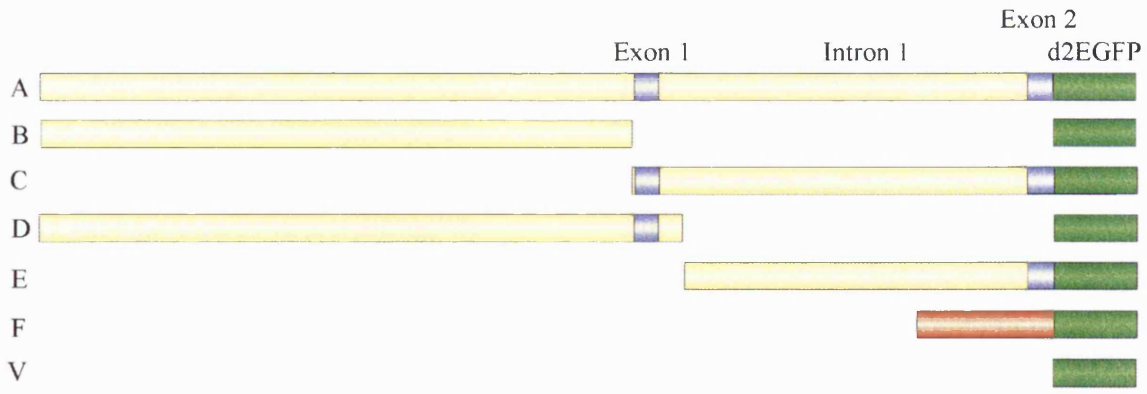

Figure 2.2 Bovine *prnp* constructs. A, promoter plus non-coding region; B, promoter only; C, non-coding region only; D, promoter plus exon 1; E, Intron one plus exon 2; F, CMV promoter control; and V, vector/background expression control.

2.1.4 Transformation

Transformations were done using XL-2 Blue Ultra Competent Cells. XL-2 Blue cells were thawed on ice. 35 µl of cells were transferred into pre-chilled 15 ml Falcon tubes and 0.7 µl of β-mercaptoethanol (provided) was added to this to give a final concentration of 25 mM. The cells were incubated on ice for 10 minutes with gentle mixing every 2 minutes. 5 µl PCR mutagenesis DNA or 10 µl ligation DNA was added to the cells and the cells were then incubated on ice for a further 30 minutes. After the 30 minute incubation, cells were heat shocked at 42°C for 30 seconds, then returned to the ice for 2 minutes. 965 µl LB broth, pre-heated to 42°C, was added to the cells, and then they were incubated at 37°C for 1 hour with shaking at 200 rpm. Cells were plated on LB agar plates containing 50 µg/ml kanamycin sulphate or carbenicillin as appropriate, and incubated at 37°C overnight.

2.1.5 Mini-preps

All reagents used were provided within the QIA-spin mini-prep kit to the recipes described in the product protocol. Several colonies from a transformation plate were picked and added to a 50 ml falcon tube containing 5 ml of LB broth with 50 µg/ml of relevant antibiotic. These were incubated overnight at 37°C with shaking at 200 rpm. Glycerol stocks were made of each new clone by adding 600 µl of cell suspension to 400 µl of glycerol diluted 1:1 in LB broth. Cultures were centrifuged for 10 minutes at 3220 xg in an Eppendorf 5810R centrifuge to collect the cells. The Qiagen Qia-Quick spin mini-prep kit was used to extract the plasmid as follows. The cell pellet obtained was resuspended in 250 µl of buffer P1 with RNase A (provided), and transferred to a micro-centrifuge tube.

250 µl of buffer P2 (lysis buffer) was added to this and mixed by inversion. The lysis reaction was stopped by the addition of 350 µl of buffer N3 and mixing as before. Tubes were centrifuged at >10 000 xg in a benchtop microfuge for 10 minutes. After centrifugation the supernatant was transferred to a mini-prep column and centrifuged at >10 000 xg for 1 minute, the flow through was discarded. The column was then washed by adding 750 µl of wash buffer with ethanol, centrifuging as before for one minute, discarding the flow through, and then centrifuging again for one minute. Plasmid DNA was eluted from the column by the addition of 30 or 50 µl of nuclease free water to the membrane (depending on the expected yield and desired concentration of the DNA), standing for one minute, transferring the column into a microfuge tube and then centrifuging as before.

2.1.6 Agarose Gel Electrophoresis

2-5 µl of mini-prep sample was mixed with 10x Bluejuice loading dye and loaded onto a 1% agarose gel (with 0.5 µg/ml ethidium bromide). The gel was electrophoresed using a BioRad mini-sub®cell GT gel tank and BioRad power pac 300, at 75 volts, for 1 hour. Gels were photographed under a long wave UV light box. Quantification was made by measurement of UV absorption at 260 and 280 nm or comparison of band intensity with λHindIII fragments of known concentration.

2.1.7 Sequencing

300-500 µg of mini-prep DNA was transferred into a micro-centrifuge tube with 5 pM of appropriate primer (see Table 2.2) and endonuclease free water to a final volume of 6 µl. Sequencing was performed by Paul Jones (University of Bath) using a PE Biosystems ABI 377 DNA Sequencer or by Gene Service Ltd (Cambridge, UK).

2.2 RNA Ligase Mediated Rapid Amplification of cDNA Ends (RLM-RACE)

2.2.1 Materials

RNA Extraction

Bovine brain tissue

Tri reagent

Chloroform

Isopropanol

Nuclease free water

RLM-RACE

FirstChoice® RLM-RACE Kit – Ambion (Huntingdon, UK)

Mouse total RNA – Ambion

Acid phenol:chloroform – Ambion

High fidelity PCR master – Roche

Isopropanol

Ethanol

Gene specific (GS) primers – MWG (see table 2.3)

Agarose

TAE buffer

100 bp ladder – NEB

200 µl thin wall PCR tubes – Fisher

Primer Name	Sequence
PrP(m) ex2 F	5' CTT TGA TGA AAG ACT CCT GAG 3'
PrP(m) GS outer	5' AAG CAG GAA GGC CTC CCT CA 3'
PrP(m) GS inner	5' AAG CAC GGT GCT GCT GGA TCT T 3'
PrP(b) ex2 F	5' CTT TGA TGA AAG ACT TCT GAA TAT AT 3'
PrP(b) GS outer	5' TCA CAG GAG GGG AAG AGA AGA 3'
PrP(b) GS inner	5' TGC TCC ACC ACT CGC TTC AT 3'

Table 2.3 Gene specific primers for RLM-RACE nested PCR reactions.

Cloning of RLM-RACE products

QIA-Quick Gel Extraction Kit – Qiagen

pGEM®-T-Easy Vector System I – Promega

XL-2 Blue Ultracompetent Cells – Stratagene

Agar – Merck

X-gal – Promega

IPTG

Carbenicillin

2.2.2 RNA Extraction

All equipment and work surfaces were treated to remove RNases, and RNase free plasticware and aerosol resistant tips were used throughout. 1ml of Tri reagent was added to approximately 1 cm^3 section of bovine brain and homogenised in a hand-held homogeniser. The resulting suspension was transferred to a 1.5 ml microcentrifuge tube and centrifuged at 15 300 xg for 10 minutes at 4°C. The supernatant was transferred to a new microcentrifuge tube and 200 µl chloroform added. This was agitated vigorously for 15 seconds then incubated at room temperature for 3 minutes before centrifuging at 15 300 xg for 10 minutes at 4°C. The upper aqueous phase was transferred to a new microcentrifuge tube and 500 µl isopropanol added. Tubes were mixed at room temperature for 10-15 minutes before centrifuging at 15 300 xg for 10 minutes at 4°C. The pellet was washed in 500 µl 100% ethanol, centrifuged at 15 300 xg for 2 minutes at 4°C, and then the ethanol was removed. The pellet was washed twice more in 70% ethanol as above. The ethanol was carefully removed and the pellet was allowed to air dry on ice for 10 minutes before resuspending in 100 µl nuclease free water. RNA was stored at –20°C until use. Just prior to use, RNA was quantified by reading a 1 in 50 dilution of the RNA in nuclease free water at 260nm in a Cary 50 UV-Visual spectrophotometer.

2.2.3 RLM-RACE

All reactions were carried out using nuclease free equipment as above. The FirstChoice® RLM-RACE kit was used for these reactions as described in the product instruction manual, all reagents except those listed in the materials above were supplied with the kit. To begin, the total RNA was incubated with calf intestine alkaline phosphatase (CIP) to remove free phosphate groups from the 5' ends of degraded mRNA, rRNA, tRNA and contaminating genomic DNA. 10 µg total RNA was incubated with 2 µl CIP, 2 µl 10x CIP

buffer, and nuclease free water to 20 µl total reaction. This was tapped to mix, spun briefly, then incubated at 37°C for 1 hour. To stop the reaction 15 µl ammonium acetate solution, 115 µl nuclease free water and 150 µl acid phenol chloroform were added to each tube. Samples were vortexed thoroughly, centrifuged at 17 950 xg in a benchtop microcentrifuge at room temperature, and the aqueous layer was transferred to a new tube. To this 150 µl of chloroform was added, samples were vortexed, centrifuged at 17 950 xg for 5 minutes, and the aqueous layer was transferred to a new microcentrifuge tube. 150 µl of isopropanol was added, tubes were vortexed and chilled on ice for 10 minutes. Samples were then centrifuged at 20 800 xg for 20 minutes at 4°C. The resulting pellets were washed with 500 µl cold 70% ethanol, centrifuged for a further 5 minutes at 20 800 xg and 4°C, then the ethanol was removed and discarded, and the pellets allowed to air dry. The pellets were resuspended in 11 µl of nuclease free water and stored on ice whilst the next reaction was prepared.

RNA from the CIP reaction was treated with tobacco acid pyrophosphatase (TAP) to remove the 5' cap from full length mRNA, leaving only a 5'-monophosphate to which the 5'RACE adapter was ligated. 5 µl of the CIP treated RNA was incubated with 2 µl TAP, 1 µl 10x TAP buffer, and 2 µl nuclease free water. The reactions were mixed by tapping, pulse centrifuged, and incubated at 37°C for 1 hour. To ligate the 5'RACE adapter 2 µl of the TAP reaction was incubated with 1 µl 5'RACE adapter, 1 µl 10x RNA ligase buffer, 2µl T4 RNA ligase, and 4 µl nuclease free water. Tubes were tapped to mix, pulse centrifuged, and incubated at 37°C for 1 hour.

After the addition of the 5'RACE adapter, cDNA was reverse transcribed from the RNA sample in the following reaction. 2 µl of the 5'RACE adapter ligated DNA or 2 µl of minus TAP control DNA were added to a new microcentrifuge tube with 4 µl of dNTP mix, 2 µl random decamer primers, 1 µl M-MLV Reverse Transcriptase (RT), 2 µl 10x RT buffer, 1 µl of RNase inhibitor, and 8 µl of nuclease free water. The reaction was tapped to mix, pulse centrifuged, and incubated at 42°C for 1 hour. Samples were stored at -20°C until use.

The cDNA from the RT reaction was used to set up the first, outer reaction for the nested PCR. The following reactions were set up in 200 µl thin wall PCR tubes; 1 µl RT reaction, 2 µl 5' RACE gene specific (GS) outer primer (10 µM), 2 µl 5' RACE outer primer, 25 µl

high fidelity PCR master mix, and 20 µl nuclease free water. Tubes were tapped to mix, spun briefly, and cycled in a PCR-sprint thermocycler, after a hot start of 3 minutes at 94°C. The PCR consisted of 35 cycles of 94°C for 30 seconds, 56°C for 30 seconds, and 72°C for 30 seconds. This was followed by 72°C for 7 minutes. The second, inner nested PCR was set up as follows; 2 µl of outer PCR product, 2 µl 5'RACE GS inner primer (10 µM), 2 µl 5'RACE inner primer, 25 µl high fidelity PCR master mix, and 19 µl of nuclease free water. This was cycled as for the outer PCR reaction. The products of the second PCR reaction, and control reactions, were run on a 2% agarose gel alongside a 100 bp ladder.

2.2.4 Cloning of RLM-RACE PCR Products

To characterise the products of the RLM-RACE reaction, the bands obtained from the second nested PCR were cut out of the gel and gel purified using the Qiagen QiaQuick gel extraction kit as described in the product protocol. Briefly, gel slices in 1.5 ml microcentrifuge tubes were incubated with 3 gel volumes buffer QG for 10 minutes (or until the gel was completely dissolved) at 50°C with vortexing every couple of minutes. One gel volume of isopropanol was added to this solution and mixed, the solution was then poured into a QiaQuick column and centrifuged in a benchtop microcentrifuge at 17 950 xg for 1 minute and the flow through discarded. The column was washed with 750 µl of wash buffer, centrifuged at 17 950 xg for 1 minute, the flow through was discarded and the column centrifuged again as before. To elute the DNA, 30 µl of nuclease free water was added to the membrane of the column, which was placed in a 1.5 ml microcentrifuge tube and centrifuged at 17 950 xg for one minute. DNA was stored at -20°C until use.

The Taq polymerase in the PCR master mix leaves A overhangs at the end of amplified products so a TA cloning vector, pGEM®-T Easy, was used to clone the PCR products. This vector and ligation reagents are provided as a kit and ligations were carried out as described in the product protocol. PCR products were ligated into the pGEM®-T Easy vector in the following reaction; 5 µl 2x rapid ligation buffer for T4 DNA ligase, 1 µl T4 DNA ligase, 1 µl pGEM®-T Easy vector, and 3 µl purified PCR product. Ligations were incubated at room temperature for 1 hour before transformation into XL-2 Blue ultracompetent cells as described in section 2.1.4.

The pGEM®-T Easy vector contains an ampicillin resistance selection marker and the LacZ operon allowing blue-white screening to be used to distinguish successfully ligated clones from vector religation due to loss of the T overhangs. The transformed cells were plated on agar plates containing 50 μg/ml carbenicillin and spread 30 minutes before use with 100 μl 10mM IPTG and 20 μl 50 mg/ml Xgal. White colonies were selected for overnight cultures and DNA purified by mini-prep as described in section 2.1.5. Plasmid DNA was sent for sequencing using T7 forward sequencing primers.

2.3 Cell Culture

2.3.1 Materials

Routine Culture

F14 and F21 cells (laboratory derived cell lines)

Cos-7 cells (Kind donation from Professors Harrison and Eisenthal, formerly of the University of Bath)

SH-SY5Y cells (Kind donation from Professor Wonnacott, University of Bath)

C8-D1A cells – ATCC (Middlesex, UK)

G8 cells – ATCC

Dulbecco's Modified Eagles Media – Calbiochem (Nottingham, UK)

Foetal Bovine Serum

Penicillin/Streptomycin Solution

Glutamine – Gibco (Paisley, UK)

Trypsin-EDTA

Cell dissociation buffer – Gibco

Transfections

FuGene 6 – Roche

Geneticin – Gibco

Chambered Coverslips – Labtek (Fisher, Loughborough - UK)

2.3.2 Routine Cell Culture

All cell lines were maintained at 37°C and 5% CO_2 in a humidified incubator.

2.3.2.1 F14 and F21 cells

F14 (PrP^c knockout mouse cerebellar-neuroblastoma fusion cells) and F21 (PrP^c wild type mouse cerebellar-neuroblastoma fusion cells). These cells lines were created in this laboratory by fusion of cerebellar suspension from PrP null mice with N18TG2 mouse neuroblastoma cells (Holme *et al*, 2003). Cells were cultured in Dulbecco's Modified Eagles Media (DMEM) of composition 4.5 g/L glucose, 1.5 g/L sodium bicarbonate, and without sodium pyruvate and glutamine. This was supplemented with 10% foetal bovine serum (FBS), and final concentrations of 1 U/ml penicillin and 0.5 mg/ml streptomycin (pen/strep). At approximately 95% confluency cells were detached from the culture flask by gentle tapping and passaged 1 in 3 or 1 in 4.

2.3.2.2 Cos-7 and SH-SY5Y cells

Cos-7 (African green monkey kidney cell line) and SH-SY5Y (human neuroblastoma) cells were cultured in DMEM of composition as described for the F14/F21 cells. Media was supplemented with 10% FBS, 2 mM glutamine, and pen/strep. At approximately 95% confluency, Cos-7 cells were passaged 1 in 20, and SH-SY5Y 1 in 10, by incubation in trypsin-EDTA until the cells detached from the base of the flask.

2.3.2.3 C8-D1A cells

C8-D1A (mouse type 1 astrocyte) cells were cultured in DMEM of composition 4.5 g/L glucose, 1.5 g/L sodium bicarbonate, and 4 mM L-glutamine. Media was supplemented with 10% FBS and pen/strep. Cells were passaged 1 in 5 at 90-95% confluency, by incubation with trypsin-EDTA until the cells detached.

2.3.2.4 G8 cells

G8 (mouse myoblast) cells were cultured in DMEM of composition as described for C8-D1A cells, supplemented with 10% FBS, 10% horse serum, and pen/strep. Cells were passaged 1 in 5 at approximately 90% confluency, by incubation with trypsin-EDTA until the cells detached, and were not allowed to reach confluency to avoid fusion into myotubules.

2.3.3 Transfection

All transfections were carried out using FuGene 6 transfection reagent.

2.3.3.1 Stable Transfection

Cells were plated at 50% confluency in 6-well plates the day before the transfection. To perform the transfection 100 µl of serum free media was pipetted into a micro-centrifuge tube. 3 µl of the FuGene 6 reagent was then added directly to this and mixed by gentle tapping. For each cell line to be created 1 µg of DNA was added to the mixture, mixed as before, and incubated at room temperature for 15 minutes. After this time the transfection mixture was added drop wise to the cells. The dish was swirled and returned to the incubator overnight. Cells were selected with 1 mg/ml geneticin 24 hours after transfection, then maintained in 0.5 mg/ml for routine culture.

2.3.3.2 Transient Transfection

Cells were plated in chambered coverslips at 35-50% confluency the day before transfection. To 20 µl of serum free media, 0.6 µl of FuGene 6 reagent was added and tubes were tapped to mix, then 0.2 µg of DNA was added to this and mixed again. The mixture was incubated for 15 minutes at room temperature before addition to the cells. To allow full expression and normal turnover of the plasmid product before the start of the experiment, cells were incubated under normal conditions for at least 24 hours after transfection.

2.4 Live Cell Imaging Studies

2.4.1 Materials

General Microscopy

Chambered Coverslips – Labtek (Fisher)

OptiMEM serum free, phenol red free media – Gibco

$CuSO_4$

Glycine – Fisher

Lyso-Tracker

Lyso-Tracker® Red – Molecular Probes (Invitrogen)

Mito-Tracker

Mito-Tracker® Red – Molecular Probes

DMSO

Golgi Probe

Sphingolipid Golgi Probe – Molecular Probes

Chloroform

Ethanol

HEPES

Defatted Bovine Serum Albumin (BSA)

Hanks

Endoplasmic Reticulum (ER) Probe

pDsRed-ER – Clontech

2.4.2 Co-localisation

Viable cells were required for the experiments, therefore cells were plated in chambered coverslips at 50% confluency and allowed to adhere before the start of the experiment. Images were captured using the Zeiss LS 550 confocal microscope.

2.4.2.1 Lyso-Tracker

Lysosomes were visualised using Lyso-Tracker® Red. Cells were incubated for half an hour at 37°C in normal media containing 50 nM probe, then rinsed in Hanks and transferred into pre-warmed OptiMEM.

2.4.2.2 Mito-Tracker

The Mito-Tracker® Red probe was dissolved in high quality anhydrous DMSO to a final concentration of 1 mM. For cell staining, 100 nM of Mito-Tracker in normal media was applied to the cells for 30 minutes. This was replaced with fresh pre-warmed OptiMEM and kept incubated under normal conditions until observation of the cells.

2.4.2.3 Golgi Probe

The sphingolipid golgi probe was prepared as a BSA complexed solution, as described in the product protocol. Briefly, the 250 μg of the probe provided was dissolved in 354 μl of 19:1 chloroform to ethanol solution to produce a 1 mM stock solution of probe. 50 μl of

stock solution was aliquoted into a small glass test tube and dried under a stream of nitrogen and then under vacuum for 1 hour. Dry probe was redisolved in 200 µl of absolute ethanol. 10 ml of Hanks with 10 mM HEPES (pH 7.4) was prepared in a 50 ml falcon tube. 3.4 mg of defatted BSA was added to this. The probe was added to the tube whilst agitating on a vortex mixer. The resulting solution is 5 µM sphingolipid – 5 µM defatted BSA solution. For staining, cells were washed in Hanks and then incubated in the probe solution at 4°C for 30 minutes. After this the cells were washed again then incubated in fresh culture media at 37°C for a further 30 minutes before being transferred into pre-warmed OptiMEM.

2.4.2.4 ER Probe

ER was visualised with the plasmid pDsRed-ER using transient transfections as described previously. Cells were transferred into pre-warmed OptiMEM before the start of the assay.

2.4.3 Trafficking Assays

For the copper internalisation assays, cells were plated in 4-well chambered coverslips at approximately 50% confluency. At time 0, test reagent was added and observations made at time zero, ten minutes and two hours. Images were captured as above.

2.5 Fixed Cell Imaging Studies

2.5.1 Materials

Indirect Immunofluorescence (IIF)

Slides

Coverslips

pcDNA-PrP(m)

Ethanol – Fisher

6-well plates – Nunc, Fisher

Hanks Buffered Salt Solution

Phosphate buffered saline (PBS)

Paraformaldehyde

Glycine – Fisher

Triton-X-100 – Fisher

Bovine serum albumin (BSA)

Foetal bovine serum (FBS)

DR1 anti-PrP antibody – Brown (2000)

FITC conjugated goat anti-rabbit antibody – Molecular Probes

Vectorshield hardset mounting media – Vector Laboratories (Peterborough UK)

2.5.2 IIF

Coverslips were sterilised in ethanol and placed in the wells of a 6-well plate. F14 cells stably transfected with the pcDNA-PrP(m) construct were then plated at 50% confluency and returned to the incubator overnight. At the start of the assay, test reagent was added to one well of a set of three (2 hour exposure), reagent was added to the second well 10 minutes from the end of the assay (10 minute exposure) and the third well was left untreated (time 0 control). 2 hours after the start of the assay, media was removed from the cells, and they were washed once in Hanks. Cells were fixed using 4% paraformaldehyde in PBS, and incubated for 30 minutes at room temperature. Following fixing, coverslips were transferred into a new 6-well plate and washed three times for 5 minutes in PBS. Fixed cells were permeablised in 0.1% Triton-X-100 in PBS for 10 minutes, washed again three times for 5 minutes in PBS, and then incubated for 10 minutes in 1% glycine in PBS. Cells were washed three times for 1 minute in PBS before blocking in 10% FBS and 0.5% BSA in PBS for 30 minutes. Coverslips were washed briefly in PBS, before incubating cells with the primary anti-PrP antibody (DR1, directed against amino acids 89-103) at a 1 in 500 dilution in 1% FBS and 0.5% BSA in PBS for a minimum of 2 hours at room temperature or overnight at 4°C. Cells were washed three times for 5 minutes in PBS to remove excess primary antibody, before addition of the secondary goat anti-rabbit FITC conjugated antibody in 1% FBS and 0.5% BSA in PBS. Incubation was for a minimum of 2 hours at room temperature or overnight at 4°C in the dark. Cells were washed again three times for 5 minutes before mounting in Vectorshield hardset mounting medium. Slides were stored at 4°C in the dark until viewing. Fluorescence was observed as described for live cell imaging. The final result was derived from studying a minimum of 18 cells over four separate experiments.

2.6 Survival Assays

The assay of cell viability used here is the MTT assay. Live cells metabolise tetrazolium salts into formazan by the succinate-tetrazolium reductase system producing a coloured precipitate. The precipitate can then be solublised and the intensity measured using a spectrophotometer.

2.6.1 Materials

MTT Assays

24 Well Plates – Corning (Fisher)

MTT Reagent

Hanks Buffered Salt Solution

Di-Methyl Sulphoxide (DMSO)

Copper Sulphate ($CuSO_4$)

Manganese Sulphate ($MnSO_4$)

Glycine

Histidine

Xanthine Oxidase

Xanthine

Catalase

Bovine Superoxide Dismutase (SOD)

N-acetyl Cysteine – Acros (Fisher)

2.6.2 MTT Assays

Cells were plated at approximately 40% confluency for metal assays and 80% confluency for oxidative stress assays, and incubated overnight before addition of the test reagent. The cells were then returned to the incubator until the time of the assay (4 days for metal assays, 24 hours for oxidative stress assays). At the time of the assay the media was removed from the cells and replaced by 200 µl of 200 µg/ml MTT reagent in Hanks. Plates were incubated for 30 minutes before the reagent was removed and 750 µl of DMSO was added to solublise the precipitate. Samples were read at 570 nm in a Cary 50 UV-visual spectrophotometer.

2.7 Cellular Stress Studies

Cellular stress was determined by measurement of either markers of lipid peroxidation or direct detection of free radicals.

2.7.1 Materials

Lipid Peroxidation Assays

Bioxytech ® LPO-586^{TM} – OxisResearch® (Portland, Oregon, USA)

HCl, 37%

Butylated hydroxytoluene (BHT)

Acetonitrile

Hanks Buffered Salt Solution

20 mM Phosphate Buffer (pH 7.4)

Reactive Oxygen Species Indicator Experiments

OptiMEM serum free, phenol red free media

Redox Red® Indicator – Molecular Probes

CM-H_2DCFDA

96-well plates – Nunc, Fisher

PBS

2.7.2 Lipid Peroxidation Assays

Lipid peroxidation is a mechanism of cellular injury caused by, and therefore a useful indicator of, oxidative stress. Lipid peroxides break down to form aldehydes, which may themselves be reactive and cause further oxidative stress insults. Break down products include malondialdehyde (MDA) and 4-hydroxyalkenals (HAE). The measurement of these is used to demonstrate oxidative stress injury of cells (Esterbauer *et al.*, 1991, Oxis product guide). Reaction of MDA or HAE with N-methyl-2-phenylindole results in a coloured product with an absorption maxima of 585nm. The intensity of the colour is directly related to the extent of the lipid peroxidation.

A homogenate of 5 x 10^7 cells was required per assay condition. This was achieved by using 4-6 T75 cell culture flasks of cells per condition. Cells were grown to be confluent at the time of extraction. Test reagent was added 2 days prior to this time. Cells were

collected by centrifugation at 1200 rpm for 10 mins, washed in Hanks, and then centrifuged again as before. The pellet was resuspended in 1.5 ml of 20 mM phosphate buffer (pH 7.4) and this was sonicated for 15 seconds to produce the homogenate. Immediately after sonication, 15 µl of 0.5 M BHT in acetonitile, to a final concentration of 0.5 mM, was added to the homogenate to prevent further lipid peroxidation occurring. Samples were then stored at –80°C until use.

The lipid peroxidation assay was carried out using the Bioxytech ® LPO-586^{TM} kit, as described in the product handbook. The provided MDA standard was diluted to create standards of final concentration 0, 0.5, 1, 2, 3, and 4 µM concentration in 200 µl. Samples were spun to remove cell debris and 200 µl of each sample was transferred into six 1.5 ml microcentrifuge tubes so that triplicates could be run for both the MDA and the MDA + HAE assays. Immediately prior to use, reagent R1 was diluted 3:1 in the provided diluent (18 ml R1: 6 ml diluent).

To start both the MDA and the MDA + HAE assays, 650 µl of diluted R1 was added to each tube (standards and samples) and mixed gently by vortexing. For the MDA assay, 150 µl of 37% HCl was added to each of the triplicates, and for the MDA + HAE assay, 150 µl of R2 reagent was added to each of the triplicates. The tubes were mixed well by vortexing. Tubes were then incubated at 45°C for one hour. Following incubation turbid tubes were centrifuged at 15 000 x g for 10 mins to obtain a clear supernatant. This was transferred into a plastic 1 ml cuvette and read using a Cary 50 UV-visual spectrophometer at 586 nm. The Cary software was used to plot the calibration curve and calculate sample concentrations. Following this a BCA assay (see section 2.8) was carried out on each sample to account for differences in protein concentration.

2.7.3 Direct measurement of free radicals – Microplate Assay

Direct measurement of reactive oxygen species (ROS) within cells was made using a microplate assay utilising CM-H_2DCFDA, which is a chemically reduced, acetmethoxy ester of 2',7'-dichlorofluorescein (DCF). This compound is colourless until the acetate groups are removed by intracellular esterases and oxidation occurs within the cell. CM-H_2DCFDA is cell permeable until it is oxidised to its fluorescent product inside the cell. Oxidation may be induced by hydrogen peroxide (with the assistance of endogenous metal ions), organic hydroperoxides, nitric oxide and peroxynitrite (Martin *et al.*, 1998)

F14 and F21 cells were plated in 96-well plates at 90-95% confluency and returned to the incubator overnight. Media was removed from test wells, and replaced by 50 µl of 5 µM probe in PBS, and incubated in the dark at 37°C for 20 minutes. Probe was removed from the cells and replaced by 100 µl of pre-warmed OptiMEM. Test reagent was added to 4 wells per experiment, and fluorescence intensity was measured using a microplate reader with excitation and emission wavelengths of 488 and 534 nm respectively, at time 0, 30 minutes, and 2 hours.

2.7.4 Direct Measurement of Free Radicals – RedoxSensor™ Red

RedoxSensor™ Red is a probe that passively enters live cells. Once inside the cell the non-fluorescent probe is oxidised to a red fluorescent product, which then accumulates in the mitochondria. Alternatively the non-fluorescent probe may be transported to lysozymes where it is oxidised to the fluorescent product. The intensity of the fluorescent signal is determined by the redox potential of the cytosol, with increased free radicals in the cytosol increasing the degree of oxidation of the probe (Chen & Gee, 2000).

Cells transfected with the GFP-PrP constructs were plated in chambered coverslips and allowed to adhere. Prior to the start of the assay, cells were incubated with 5 µM probe in normal media for 10 minutes, this was removed and cells washed once in Hanks, before addition of OptiMEM. Cells were observed by confocal microscopy at the start of the assay and 5, 10 and 15 minutes after the addition of test reagent.

2.8 Determination of Protein Concentration

2.8.1 Materials

Bicinchoninic acid (BCA)

4% (w/v) $CuSO_4$

Bovine serum albumin (BSA)

2.8.2 BCA assay

Using 1.5 ml micro-centrifuge tubes, protein standards of concentration 0, 200, 400, 600, 800, and 1000 µg/ml were made up using BSA to a final volume of 50 µl. A volume of sample buffer equal to that of the diluted sample was included in this preparation to

account for any interference of the buffer on the assay. Samples were diluted appropriately to a final volume of 50 µl in deionised H_2O, in triplicate. The BCA reagent and 4% (w/v) $CuSO_4$ were mixed in a 50:1 ratio respectively. 1 ml of this reaction mix was added to each tube and mixed by vortexing. Samples and standards were incubated at 37°C for 30 minutes. The standards and samples were transferred to 1 ml plastic cuvettes and read at 562 nm in a Cary UV-visual spectrophotometer. The Cary software was used to plot the calibration curve and calculate the concentration of the samples.

2.9 Native Polyacrylamide Gel Electrophoresis (PAGE)

2.9.1 Materials

Native PAGE

30% acrylamide – Protogel (Fisher)

1.5M Tris pH 8.8

Ammonium Persulphate (APS)

N,N,N',N'-Tetramethylethylene-diamine (TEMED)

4x Loading Dye (2.35 ml dH_2O, 1.25 ml 0.5M Tris-HCl pH6.8, 6.0 ml glycerol, 0.4 ml 0.5% w/v bromophenol blue)

Running Buffer (188 g glycine, 30.2 g Tris base, dH_20 to 1L)

Transfer

Methanol

Marvel Dry Semi-Skimmed Milk

PVDF membrane – Millipore (Watford, UK)

Blotting paper – Fisher

2.9.2 Native PAGE

To preserve the protein in its native form, non-denaturing conditions were used throughout. Cells were extracted by first washing in Hanks, then incubated in extraction buffer consisting of 20 mM tris acetate, 0.27 M sucrose, 1 mM EDTA, 1 mM EGTA, 10 mM sodium-B-glycerophosphate (pH 7.4), and 1% triton-X-100, with protease inhibitors 1 mM sodium orthovandate, 2 mM phenylmethylsulphonylfluoride (PMSF), and 1 mM benzamidine, for 20 minutes at 37°C. Cell lysates were collected and briefly spun to

separate the cell debris from the soluble protein. BCA assays (section 2.8) were used to quantify protein so equal amounts could be loaded onto the gel. Lysates were mixed 3:1 with 4x native loading buffer.

Gels were prepared and run using an ATTO (US) gel tank system. 12% native gels were mixed using 3.39 ml H_20, 4 ml 30 % acrylamide, 2.5 ml 1.5 M Tris (pH 8.8), 100 µl 10% (w/v) ammonium persulphate, and 10 µl TEMED per gel, added in the order the reagents are listed. 50 µg of protein was loaded in each well and gels were run at 30 mA per gel for approximately one hour until the loading dye reached the bottom of the gel. Gels were removed from the chamber and read under a Fujifilm FLA-5000 phosphoimager using excitation and emission wavelengths of 488 and 530 respectively (optimum wavelengths for GFP). Protein was transferred onto a PVDF membrane as described below.

2.9.3 Transfer

Protein from the gel was transferred to a PVDF membrane by a semi-dry transfer protocol. Blotting paper was soaked in transfer buffer (500 ml 1x running buffer, 200 ml methanol, and 300 ml deionised H_2O). On top of this was placed PVDF membrane pre-wetted in methanol. This was positioned with care to ensure there were no bubbles between the paper and the membrane. The gel was placed on top of this with equal care, and a final piece of blotting paper was positioned on the top of the sandwich, which was wetted with transfer buffer. The transfer was run for 1 hour 30 minutes using 50 mA per gel in a Biorad semi-dry blotter. Following transfer, membranes were placed in 5% (w/v) milk powder in TBS with 0.1% (v/v) tween (TBS-t) for 1 hour at room temperature with shaking or overnight at 4°C to block the membrane.

2.10 Western Blot

2.10.1 Materials

Marvel non-fat milk powder

Tris Buffer Saline

Tween 20

Primary Antibodies (see Table 2.4)

Goat anti-mouse HRP secondary antibody – Dako (Ely, UK)

Goat anti-rabbit HRP secondary antibody – Dako

ECL-plus developing kit – Amersham (Buckinghamshire, UK)

Hyperfilm XL – Amersham

Antibody	**Dilution**	**Protein Binding Site**	**Source**
PrP C-terminal antibody (5C3)	1 in 1 000	PrP amino acids 90-145	Professor Man-Sun Sy
Anti α-tubulin Clone B-5-1-2	1 in 10 000	C-terminus	Sigma

Table 2.4 Primary antibodies used for western blot.

2.10.2 Western Blotting

Membranes were blotted for PrP using a C-terminal antibody directed against amino acids 149-165 of the protein (kind gift from Professor Man-Sun Sy). As a loading control alpha-tubulin was also blotted. Following transfer membranes were blocked in 5% non-fat milk – tris buffered saline with 0.1% tween (TBS-t) for 1 hour at room temperature or overnight at 4°C. Membranes were rinsed in TBS-t before incubation with the primary antibody in 1% milk – TBS-t, for a minimum of 1 hour at room temperature. Two 2 minute, one 15 minute and three 5 minute washes removed excess primary antibody. Membranes were incubated in secondary goat anti-mouse HRP conjugated antibodies, in 1% milk TBS-t for a minimum of 1 hour. Membranes were developed using the ECL-plus kit and film exposure times were between 30 seconds and 5 minutes. A Compact X-ray processor was used to develop the films.

2.11 Computer Modelling of Promoter Regions

Gene sequences of the bovine and mouse PrP genes were entered into BIMAS Proscan database, the Eukaryotic Promoter Database, SignalScan, TFsearch, and the Transcription Element Signal Search (TESS) in Fasta format. The results are accurate as of August 2005.

2.12 Data Analysis

Data for microscopy experiments was collected over a minimum of four different experiments, each of which aimed to collect ten different fields of cells per experimental condition. Intensity measurements of live cell experiments were made using the Zeiss LSM software. Band intensity measurements for native page and western blots were made using Scion imaging software. For all intensity measurements background signal was subtracted from the reading to eliminate interference. Statistical analyses were performed with Minitab 12 statistical software. General linear model, using dose as a covariate, or one-way ANOVA were used for determining significant data trends or point differences, respectively, of normally distributed multivariate data, and Tukey's secondary test was used to determine the significant responses. T-tests were used where only two conditions, with samples of small size fitting a normal distribution, were to be analysed. Data not fitting a normal distribution was analysed using the non-parametric Mann Whitney test for comparison of two data sets, or the Kruskal-Wallis test for multiple comparisons.

3 Genetic Modulation of PrP Expression

The PrP^c gene (*prnp*) has now been sequenced and analysed in several species including humans, cattle, sheep, mice, hamsters and rats (Basler *et al.*, 1986; Puckett *et al.*, 1991; Saeki *et al.*, 1996; Inoue *et al.*, 1997; O'Neill *et al.*, 2003). Despite regulatory regions such as heat shock elements being identified, little is known about the regulation of PrP at the genetic level. Since PrP^c is necessary for disease progression and appears to be up-regulated in disease, the regulation of *prnp* is an area that may prove invaluable for understanding and potentially managing the disease.

Prnp has a three exon structure in all characterised species. However, in hamsters and humans the second exon may not be spliced into the final mRNA sequence (Li & Bolton, 1997; Lee *et al.*, 1998). The third and final exon encodes the entire open reading frame (ORF) of the protein. Various motifs involved in promoter control have been identified within the promoter region (Section 1.1.2, Figure 1.1), and intron 1 has been identified as essential for full promoter activity (Inoue *et al.*, 1997).

The presence of heat shock elements allows the *prnp* promoter to become activated in response to forms of cellular stress (Shyu *et al.*, 2000; Shyu *et al.*, 2002), indicating that total levels of PrP^c within the cell would be up-regulated as the cell attempted to combat the stress insult. The observed up-regulation of the *prnp* promoter as a result of stress induced by nitric oxide (NO) radicals (Wang *et al.*, 2005), oxidative stress induced by hyperbaric oxygen (Shyu *et al.*, 2004), and hypoglycaemia (Shyu *et al.*, 2005a) also provides evidence of a role for PrP^c in dealing with stress insults. In addition to this up-regulation, down-regulation of the *prnp* promoter has also been observed in response to ATRA (Rybner *et al.*, 2002), an effect that may be due to direct interaction with the promoter or be an indirect response to ATRA modulation of transcription factors.

Eukaryotic gene regulation is highly complex with even the most basic promoter sequences requiring numerous transcription factors to recruit and form the transcription apparatus.

Protein expression in eukaryotic cells is regulated at several levels, including the DNA sequence itself, control elements within the mRNA, and by protein turnover. All of these factors can be influenced by many other control mechanisms within the cell. Given that so many factors can influence the levels of protein within a cell, measurement of total protein does not accurately indicate the activity of the promoter. By replacing the ORF of *prnp* with a GFP variant of known half-life it has been possible to look at the genetic control of expression. In this way changes in the level of GFP signal indicate changes in gene activity not changes in protein turnover.

A recurring problem with previous studies into the factors affecting *prnp* activity is the variability of responses between different cell culture systems. This has lead one group to conclude that copper down regulates the *prnp* promoter (Toni *et al.*, 2005), but other researchers to conclude the exact opposite; that copper up-regulates promoter activity (Armendariz *et al.*, 2004; Varela-Nallar *et al.*, 2005). This study attempts to address this problem by considering several cell lines derived from different lineages with different phenotypes. As PrP^c is expressed to various extents in separate tissues of the body, the underlying cell type was expected to influence the activity of the promoter both at the basal expression level and in response to stimuli that regulate activity.

The aims of this work were to elucidate regions of the *prnp* promoter that were important for genetic regulation and to determine the influence of the underlying cell line on expression. In addition, copper, DMSO and ATRA were tested on the promoter sequences to determine how they may affect gene regulation. This was both for the purpose of determining potential functions of PrP^c and determining potential compounds that might be used in the management of disease progression. The results presented highlight the importance of intron 1 in the control of promoter activity and show that this region may have its own promoter activity. Copper, DMSO and ATRA were found to alter promoter activity in a cell line specific manner, and the regions of the gene sequence that mediate these reactions were demonstrated.

3.1 *Prnp* region activity

Prnp has three exons, of which only the final exon encodes the open reading frame (ORF), indicating that the other exons may have another role. In addition intron 1 has previously

been reported to be essential for the full function of the promoter region (Inoue *et al.*, 1997). On the basis of this several bovine *prnp* constructs were made to investigate the ability of the gene regions to drive mRNA (and the resulting protein) production. The constructs include the whole promoter and non-coding region (construct A), the promoter on its own (B), the non-coding region without the promoter (C), the promoter and exon 1 (D), intron 1 and exon 2 on their own (E), and the CMV promoter as an expressing control (F, figure 3.1A). Each construct was cloned into pd2EGFP-1, a promoterless vector, where insertion of a sequence with promoter activity into the multiple cloning site drives the production of a destabilised EGFP with a half-life of two hours. Changes in gene activity can be measured quickly by looking for changes the level of GFP production. These constructs were transfected into several different cell types including F14 (mouse fusion – PrP null), F21 (mouse fusion – wild type PrP), SH-SY5Y (human neuroblastoma), C8-D1A (mouse astrocyte), G8 (mouse myoblast), and Cos-7 (African green monkey kidney). Stable cell lines were selected. In this way the activity of the constructs could be determined and compared across the cell lines.

3.1.1 Comparison of Promoter Constructs Expression Levels

To assess the basal level of expression of each construct, cells were observed under the LSM 550 confocal microscope with images captured using wavelengths for GFP (excitation 488nm, emission 530nm). GFP intensity was quantified using Scion imaging software.

The different promoter constructs transfected into different cell lines showed different expression levels. Considering first the F14 (PrP^c null) cells, the greatest activity, as measured by the intensity of GFP compared to the CMV driven control, was seen for construct A indicating that the promoter and the non-coding region are important for the full activity of the gene (Figure 3.1). However construct B showed significant activity demonstrating that this the promoter is active in isolation but enhanced in the presence of the non-coding region. Of interest is that construct D showed reduced activity. The level of expression of this construct is significantly lower than the construct containing the promoter region alone (B; $W = 2100$, $p < 0.001$) and not significantly different to that of the vector control ($W = 64$, $p = 0.112$), indicating that the promoter is effectively switched off when followed by just exon 1 of the non-coding region. The exon may, therefore, have a yet undiscovered negative regulatory role. Since there are two splice variants of this exon, but it is not part of the coding region, a role in regulating protein expression is likely.

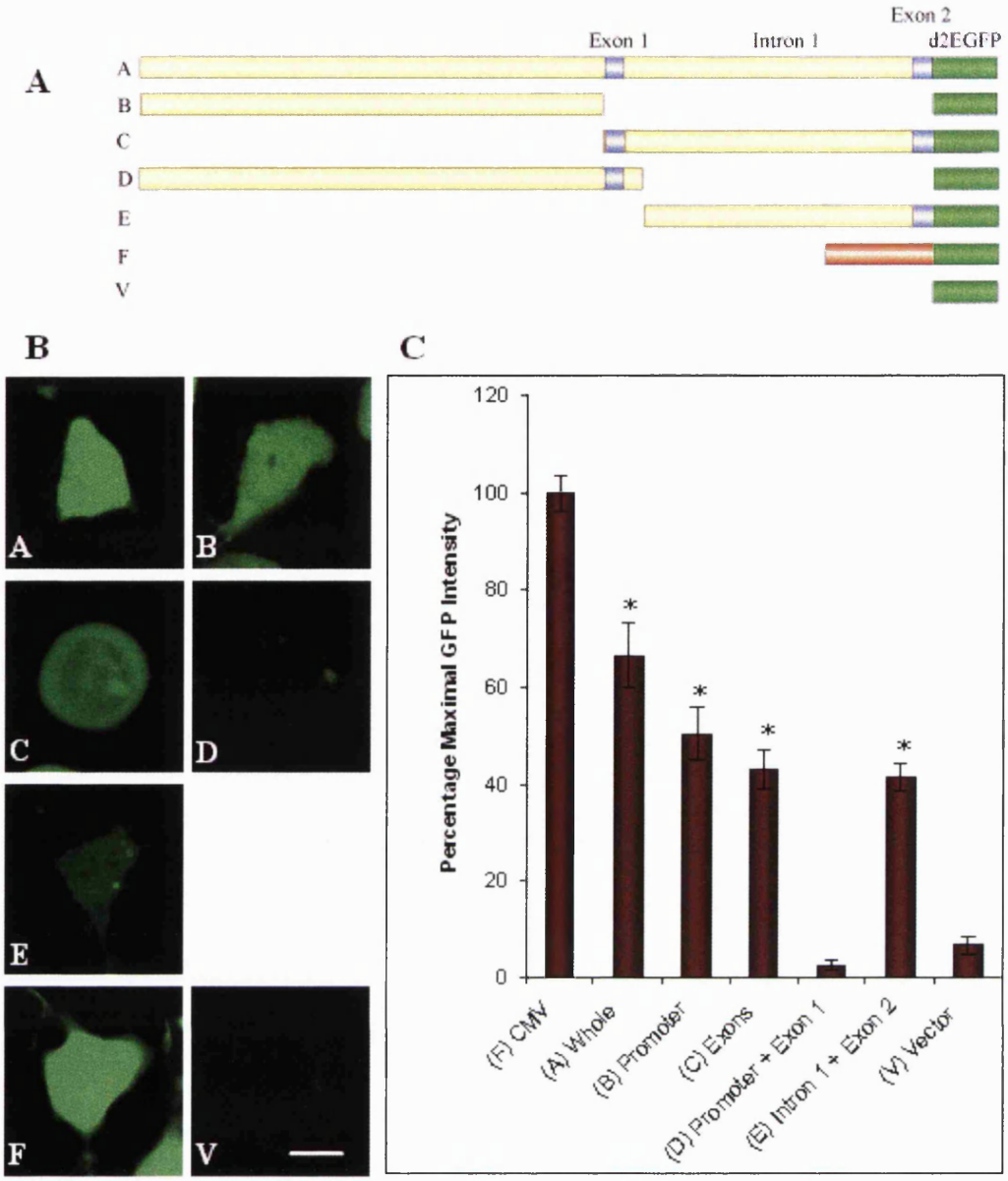

Figure 3.1 Relative intensity of PrP promoter–GFP fusion construct protein products in F14 (PrP null mouse neuroblastoma-fusion) cells. (A) PrP Promoter and non-coding region constructs cloned into pd2EGFP-1, as described in section 2.1.3, were transfected into F14 cells and stable cell lines established. (B) GFP expression levels driven by each of the promoter constructs as detected by fluorescence microscopy. Cells were grown on chambered coverslips and observed live. Images shown are representative of the fluorescence levels observed over four experiments. Scale bar = 10 µm. (C) Quantification of GFP intensity by measurement of fluorescence intensity when expression is driven by each of the promoter constructs expressed relative to the maximal expression of the CMV promoter driven control. Analysis of the raw data intensities found that the test constructs indicated by * showed significant ability to drive GFP production above the level observed for the vector/background control. $H = 109.81$, $p < 0.001$, $n = 206$ cells.

A further interesting observation is that the constructs C and E exhibit significant GFP expression, indicative of promoter activity of this region. This effect appears to be independent of exon 1, since construct E lacks this exon but still drives GFP production, and is most likely mediated by intron 1, which has been previously reported to be important for promoter activity (Inoue *et al.*, 1997).

3.1.2 Comparison of Promoter Construct Expression by Cell Line

The pattern of expression described for the F14 cells is also observed for the Cos-7 cell line (Figure 3.2). However a different pattern of expression of the constructs is seen for the F21 (Figure 3.3), C8-D1A (Figure 3.4), and SH-SY5Y (Figure 3.5). The full length construct A in these cells does not express as highly as in the F14 and Cos-7 cells, and the promoter alone (B) and exons (C) constructs are (with the exception of construct C in the F21 cells) expressed higher than the full length construct. Expression of construct D is consistent across all of the cell lines. It shows the lowest expression and by comparison with the vector control appears to be unable to drive the production of the GFP mRNA.

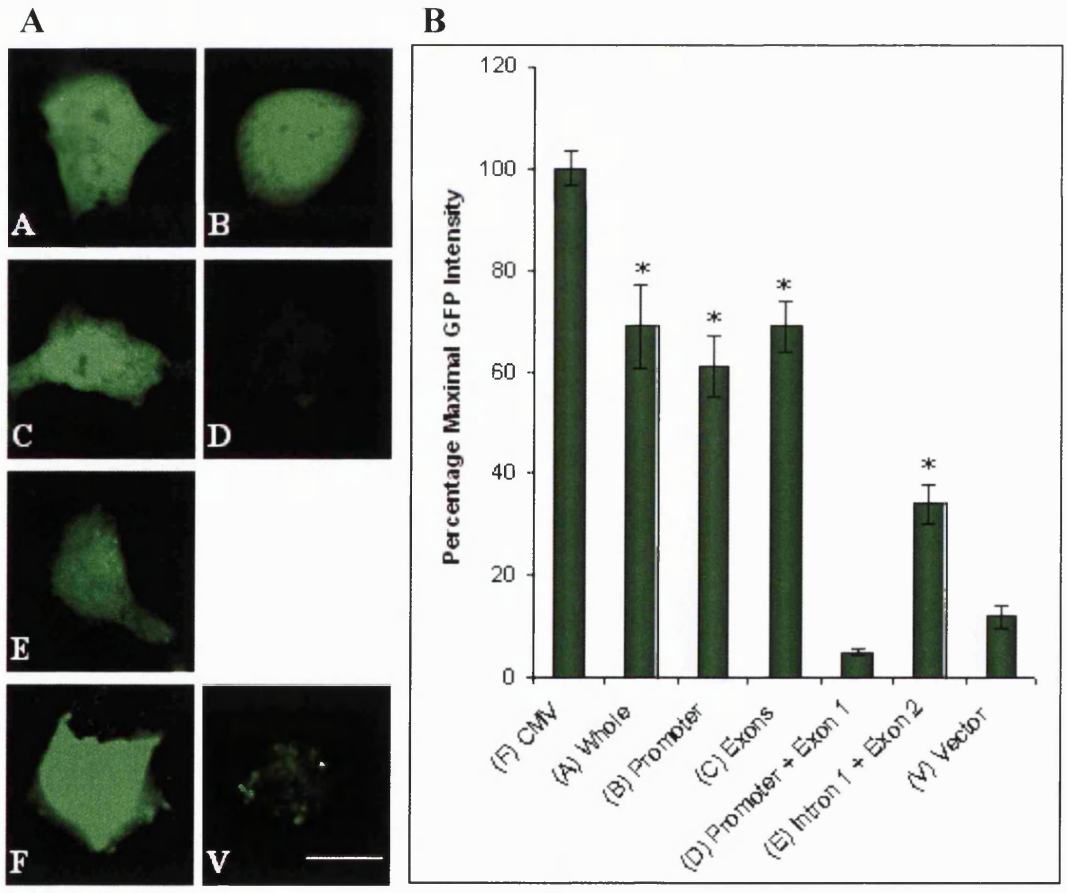

Figure 3.2 Expression of promoter constructs in Cos-7 cells. PrP Promoter and non-coding region constructs cloned into pd2EGFP-1, as described in section 2.1.3, were transfected into Cos-7 monkey kidney cells and stable cell lines established. (A) GFP expression levels driven by each of the promoter

constructs as detected by fluorescence microscopy. Cells were grown on chambered coverslips and observed live. Images shown are representative of the fluorescence levels observed over four experiments. Scale bar = 20 µm. (B) Quantification of GFP intensity by measurement of fluorescence intensity when expression is driven by each of the promoter constructs expressed relative to the maximal expression of the CMV promoter driven control. Lowest expression is seen for constructs D and V, and similar expression is seen for constructs A, B, and C. Analysis of the raw data intensities found that the test constructs indicated by * showed significant ability to drive GFP production above the level observed for the vector/background control. $H = 87.07$, $p < 0.001$, $n = 142$ cells.

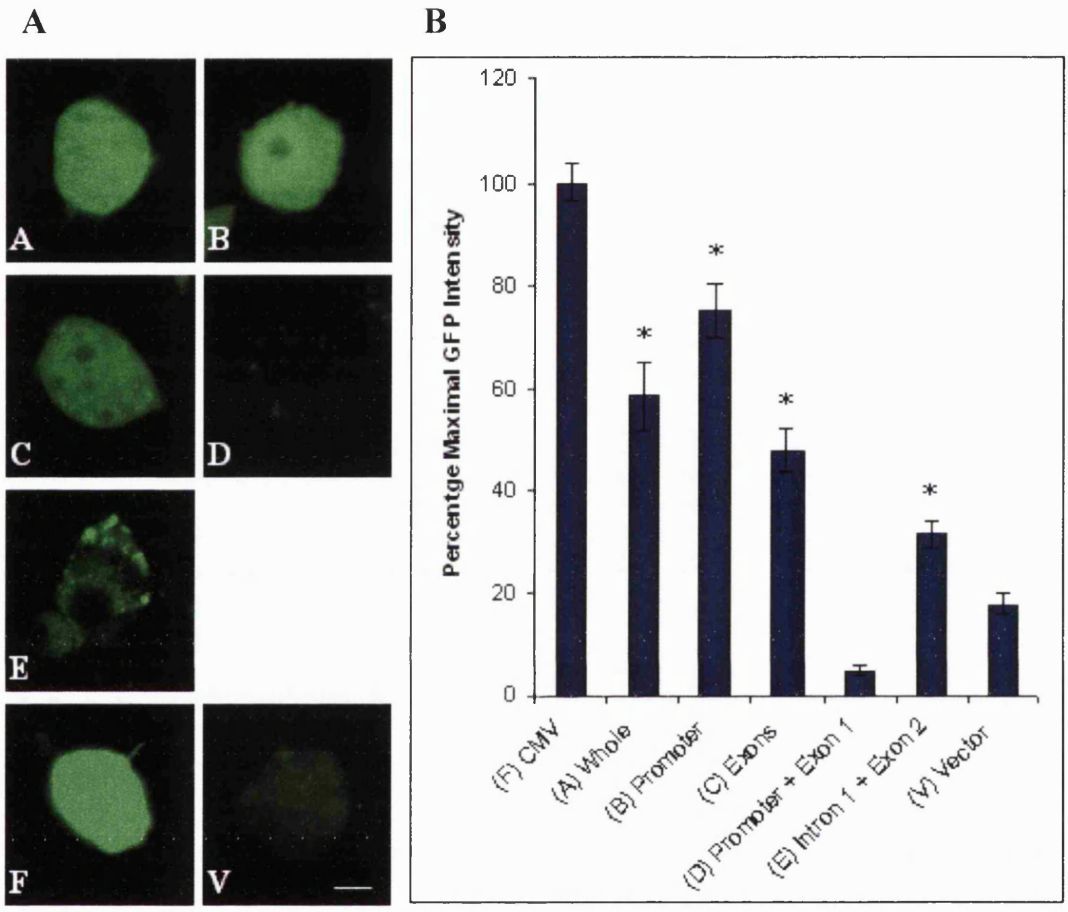

Figure 3.3 Expression of promoter constructs in F21 cells. PrP Promoter and non-coding region constructs cloned into pd2EGFP-1, as described in section 2.1.3, were transfected into F21 (PrP^c wild type mouse neuroblastoma fusion) cells and stable cell lines established. (A) GFP expression levels driven by each of the promoter constructs as detected by fluorescence microscopy. Cells were grown on chambered coverslips and observed live. Images shown are representative of the fluorescence levels observed over four experiments. Scale bar = 5 µm. (B) Quantification of GFP intensity by measurement of fluorescence intensity when expression is driven by each of the promoter constructs expressed relative to the maximal expression of the CMV promoter driven control. Lowest expression is seen for constructs D, V, and E, with similar expression levels seen for constructs A, B, and C. Analysis of the raw data intensities found that the test constructs indicated by * showed significant ability to drive GFP production above the level observed for the vector/background control. $H = 112.75$, $p < 0.001$, $n = 189$ cells.

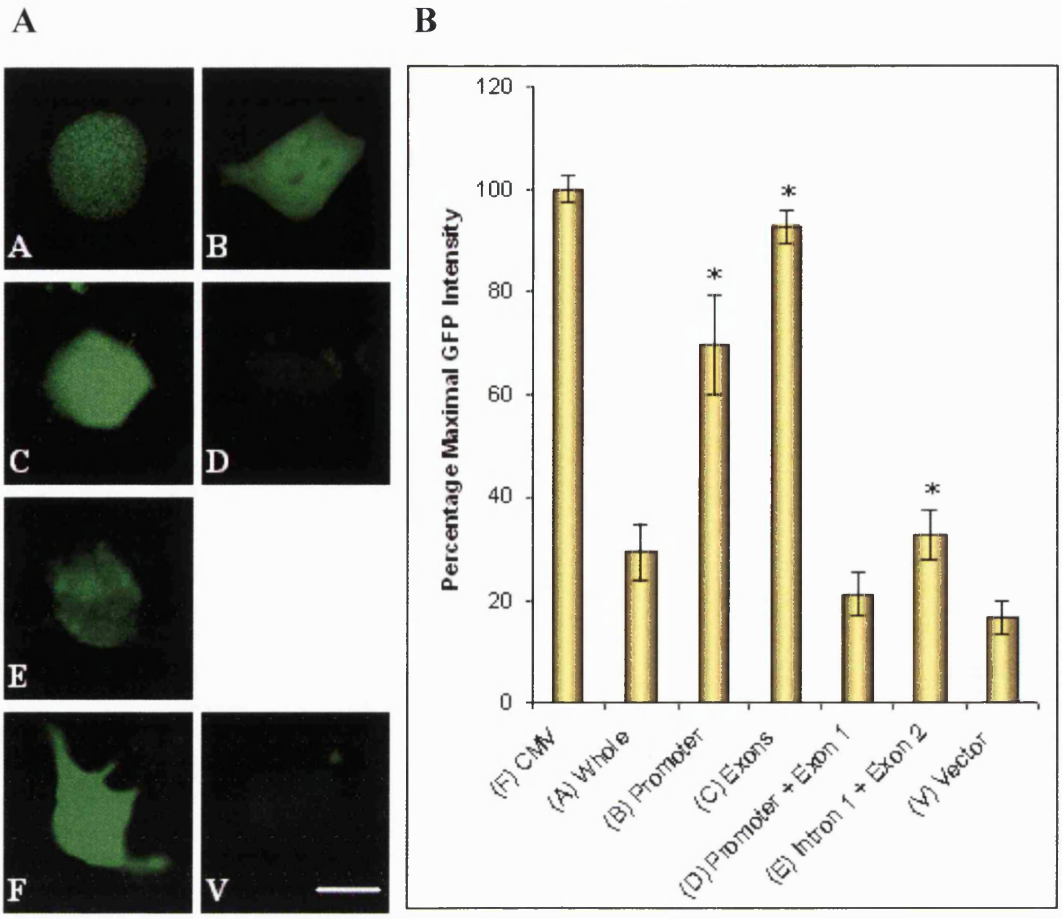

Figure 3.4 Expression of promoter constructs in C8-D1A cells. PrP Promoter and non-coding region constructs cloned into pd2EGFP-1, as described in section 2.1.3, were transfected into C8-D1A type 1 astrocyte cells and stable cell lines established. (A) GFP expression levels driven by each of the promoter constructs as detected by fluorescence microscopy. Cells were grown on chambered coverslips and observed live. Images shown are representative of the fluorescence levels observed over four experiments. Scale bar = 10 µm. (B) Quantification of GFP intensity by measurement of fluorescence intensity when expression is driven by each of the promoter constructs expressed relative to the maximal expression of the CMV promoter driven control. Lowest expression is seen for constructs A, D, E, and V. Constructs B and C have significantly higher expression levels than all but the CMV control (construct F) . Analysis of the raw data intensities found that the test constructs indicated by * showed significant ability to drive GFP production above the level observed for the vector/background control. $H = 104.42$, $p < 0.001$, $n = 173$ cells.

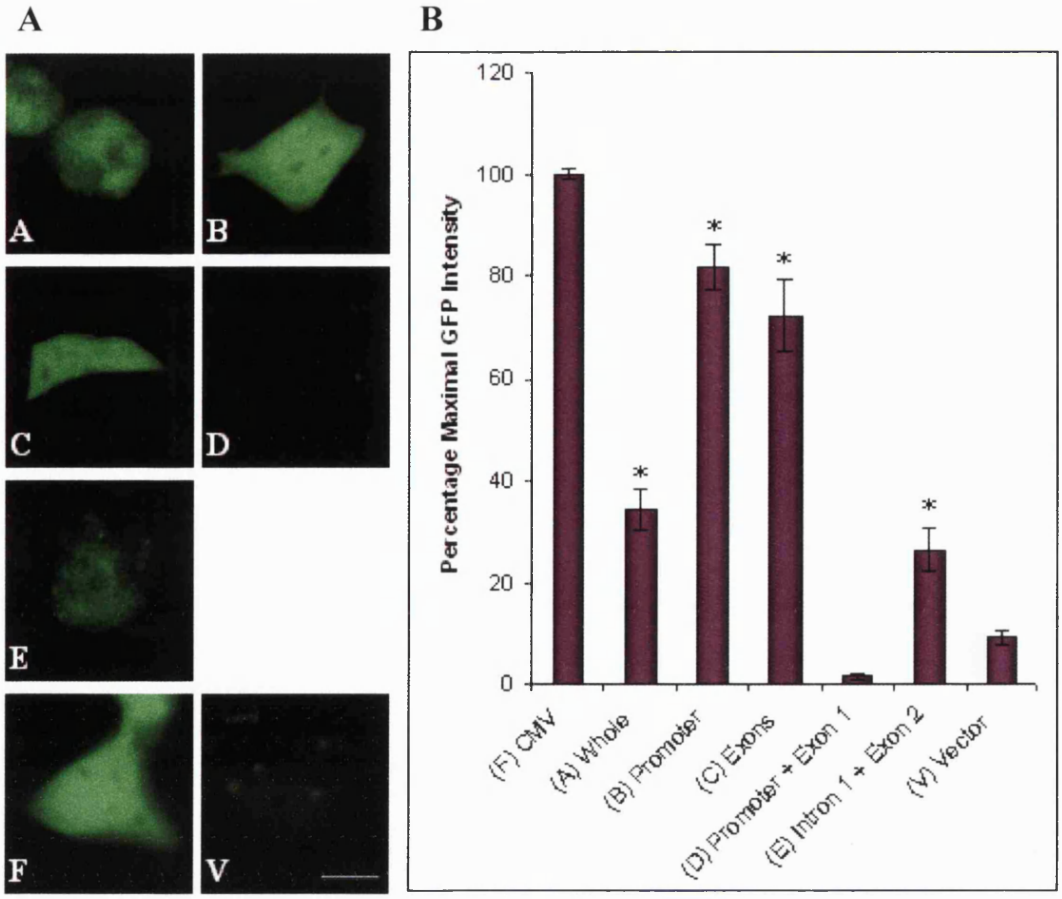

Figure 3.5 Expression of promoter constructs in SH-SY5Y cells. PrP Promoter and non-coding region constructs cloned into pd2EGFP-1, as described in section 2.1.3, were transfected into SH-SY5Y human neuroblastoma cells and stable cell lines established. (A) GFP expression levels driven by each of the promoter constructs as detected by fluorescence microscopy. Cells were grown on chambered coverslips and observed live. Images shown are representative of the fluorescence levels observed over four experiments. Scale bar = 10 µm. (B) Quantification of GFP intensity by measurement of fluorescence intensity when expression is driven by each of the promoter constructs expressed relative to the maximal expression of the CMV promoter driven control. Lowest expression levels are seen for constructs D and V. Highest expression levels are observed for constructs B and C. Analysis of the raw data intensities found that the test constructs indicated by * showed significant ability to drive GFP production above the level observed for the vector/background control. $H = 100.13$, $p < 0.001$, $n = 116$ cells.

A further different pattern of expression was observed for the G8 myoblastoma cell line. This cell line showed the highest expression for the full length construct, much lower expression levels for constructs B and C, and expression is again seen for construct E (Figure 3.6). Consistent with all the other cell lines, the construct containing just the promoter and exon 1 (construct D) showed no significant expression of GFP compared to

the vector only cells (W = 75.0, p = 0.224), indicating the this construct is likely to be inactive regardless of the underlying cell type.

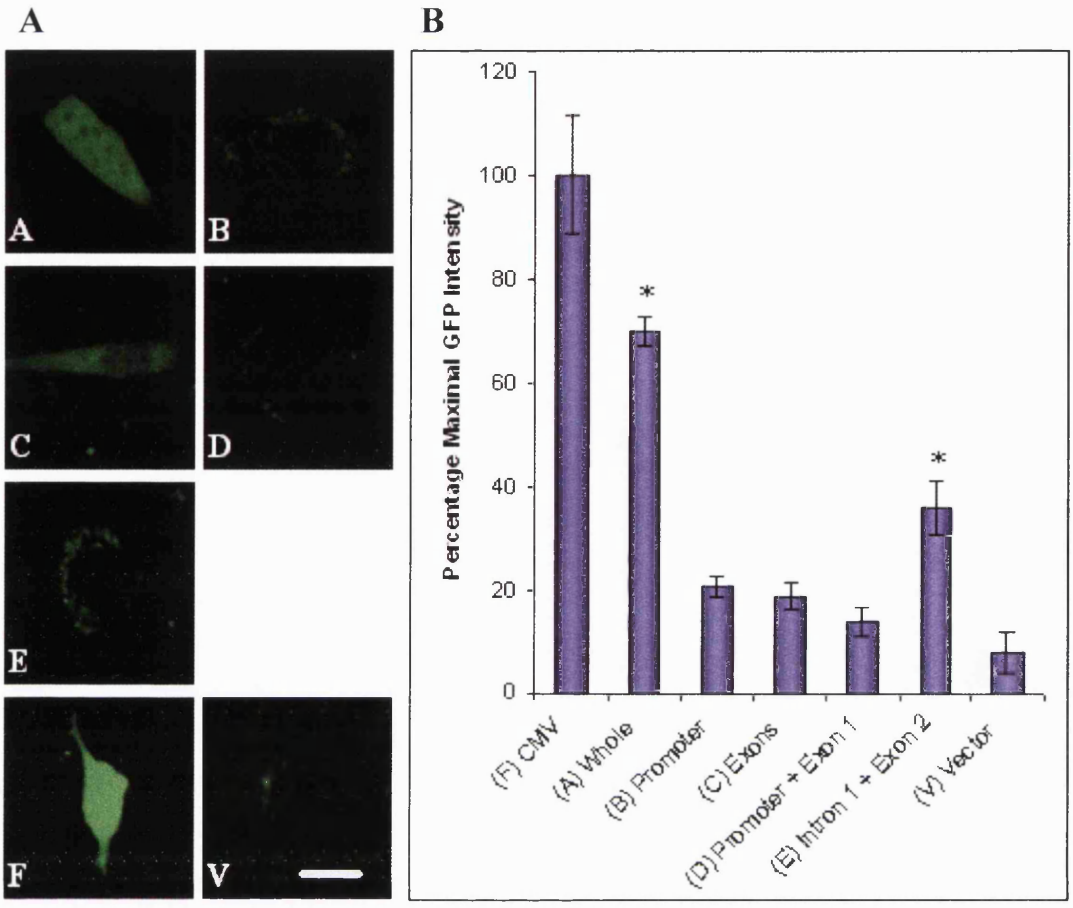

Figure 3.6 Expression of promoter constructs in G8 cells. PrP Promoter and non-coding region constructs cloned into pd2EGFP-1, as described in section 2.1.3, were transfected into G8 mouse myoblast cells and stable cell lines established. (A) GFP expression levels driven by each of the promoter constructs as detected by fluorescence microscopy. Cells were grown on chambered coverslips and observed live. Images shown are representative of the fluorescence levels observed over four experiments. Scale bar = 10 µm. (B) Quantification of GFP intensity by measurement of fluorescence intensity when expression is driven by each of the promoter constructs expressed relative to the maximal expression of the CMV promoter driven control. Highest expression is observed for construct A and all other constructs show significantly lower expression, however construct E is significantly higher than the vector control (V). Analysis of the raw data intensities found that the test constructs indicated by * showed significant ability to drive GFP production above the level observed for the vector/background control. H = 73.88, $p < 0.001$, n = 97 cells.

3.1.3 Murine Promoter Expression

Since the constructs studied above are bovine and they have been expressed in several murine cell lines, they may suffer from different expression patterns due to the differences between the cellular control mechanisms from different species. Therefore, two murine promoter constructs have been created, the whole promoter and non-coding sequence (construct A) and the intron 1 and exon 2 sequence (construct E). These have been used to determine if the bovine sequence is expressed differently to the murine sequence in murine cells (Figure 3.7). No detectable expression was seen for either of the murine constructs in the human derived SH-SY5Y cells, most likely due to species difference.

Expression levels of the murine constructs in F14 cells are very similar to the levels seen for the bovine constructs (Figure 3.1 and 3.7). Expression of the murine construct A is lower in the F21 cells than the bovine construct, and higher in the C8-D1A cell line than seen for the bovine. This may reflect species-specific transcription control mechanisms within these cells, which recognise different genetic signals (or respond differently to the same genetic signals) and so influence basal expression levels of the constructs. Again construct E is able to drive expression of GFP, indicating that intron 1 of the mouse gene sequence also contains control elements. However this is only significant in the F14 cells, perhaps indicating that this region is less important for control of expression of murine *prnp* than for bovine. Alternatively, the genetic control mechanisms of the underlying cell type may act differently on the bovine control elements within this region compared to the mouse, thus affecting expression.

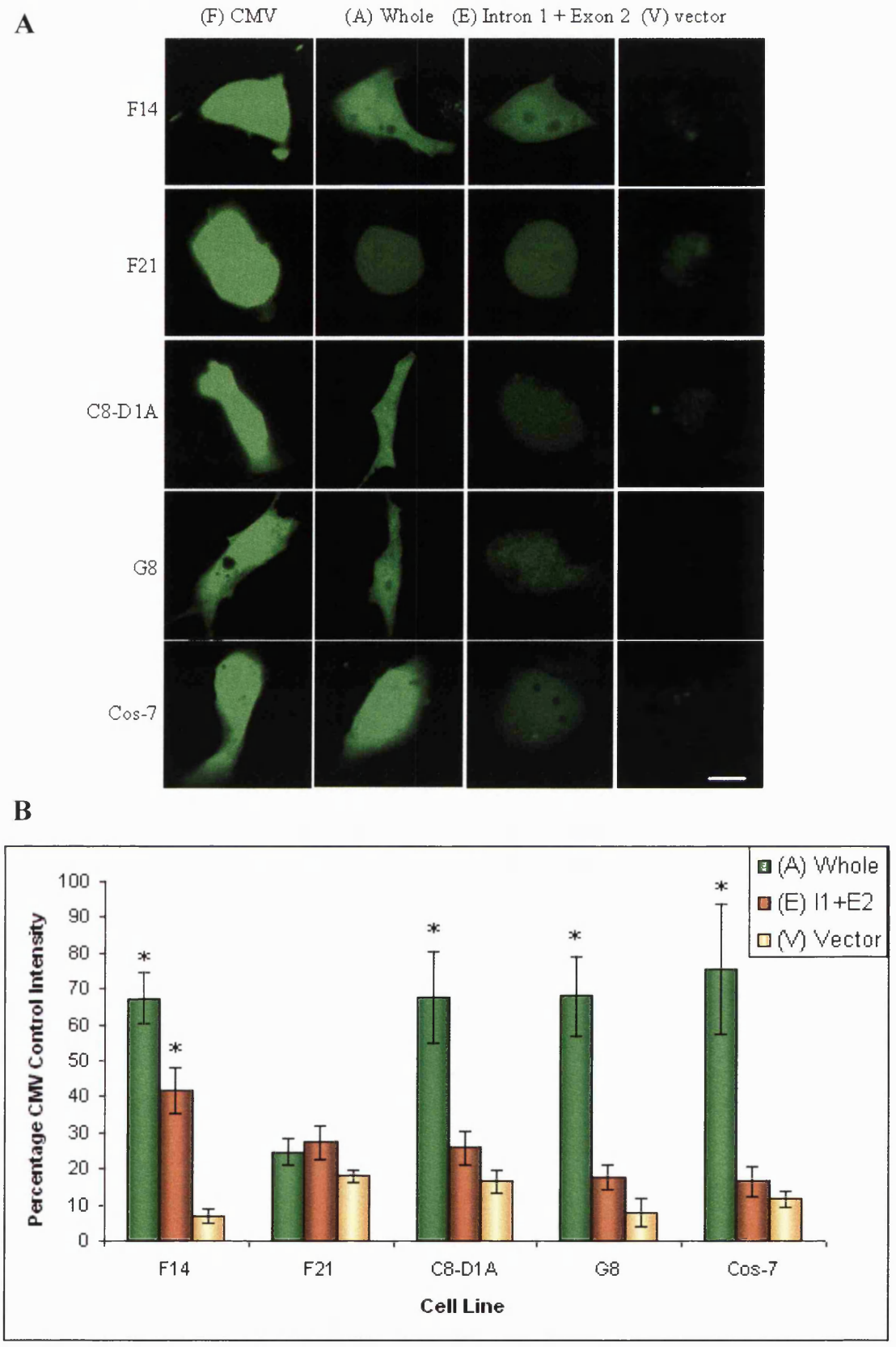

Figure 3.7 GFP Intensity of the mouse promoter constructs in each of the cell lines where expression can be detected. (A) Individual cell pictures. Scale bar = 10 µm. (B) Quantification with respect to the CMV promoter driven control. Analysis of the raw data intensities found that the test constructs indicated by * showed significant ability to drive GFP production above the level observed for the vector/background control. $H = 228.14$, $p < 0.001$, $n = 334$ cells.

3.2 Modelling of the Promoter Region Within Intron 1

Various databases have been developed for evaluating eukaryotic signal sequences within regions of genes that may have high regulatory function. Such databases use defined signal sequences to identify regions of coding sequence recognised by RNA polymerise II and include programmes such as PROSCAN, the Eukaryotic Promoter Database (EPD; Périer *et al.*, 2000), and Promoter 2.0 prediction server of the Centre for Biological Sequence Analysis. In addition, databases can recognise sequences of DNA that encode binding sequences of transcription factors and enhancer or repressor sequences. The Transcription Element Search System (TESS; Schug & Overton, 1997) uses TRANSFAC (Wingender *et al.*, 2000), IMD, and CBIL-GibbsMat databases to predict the position of transcription factor binding sites. Signal Scan is a further database that carries out this function (Prestridge, 1991).

3.2.1 Promoter Predictions

Analysis of mRNA has previously shown two splice variants of PrP mRNA and defined the position of the PrP promoter by mapping the exon sequences. However as shown previously (for constructs C and E), the non-coding region is able to drive GFP production on its own, indicating that the transcription apparatus can be activated by signal sequences within this region. To investigate potential signal sequences the bovine and murine *prnp* sequences were entered into the PROSCAN, EPD, and Promoter 2.0 databases. The results obtained are accurate as of the end of August 2005.

The results consistently show a region of promoter activity in intron 1 (see Table 3.1, and diagrammatical representation in Figure 3.8). Using PROSCANv1.7, the presence of a TATA box at position 1610 of the bovine post origin sequence inside intron 1 was predicted. This is highly significant, in so much as PrP has often been classified as a house-keeping gene due to its lack of TATA box. When the long incubation mouse sequence is analysed by the same methods a TATA box is not found but strong promoter activity is predicted within the same region. Interestingly, however, even if this TATA box is active, previous studies that have determined the position of the promoter based on the mRNA species would indicate that it is secondary to the promoter region preceding exon 1. This may indicate that the function of the gene product is so important that several mechanisms are required to ensure that protein production can be initiated when required.

An alternative explanation considering the experimental data described in this chapter is that different initiation methods may be used by different cell types.

	Bovine		**Mouse**	
Transcription Complex Binding sites.	Type	Location	Type	Location
	TFIID	1372	JCV repeated Sequence	1919
	TFII-I	1403		
	Oct-Factors	1541	MLTF	2131
	IgHC.2	1548	CP1	2151
	TFIID	1581	Oct-Factors	2155
	TATA	1610	IgHC.2	2157
			Oct-Factors	2157
				2164
			OTF-2A	2165
Promoter Region		1359-1609		1921-2171
Estimated TSS		1610		Unknown

Table 3.1 Identification of putative promoter sites inside intron 1 by consideration of binding sites for the transcription apparatus. Bovine (accession number AF163764) and long incubation murine (accession number U29187) gene sequences were entered into the PROSCAN v1.7 database and regions of probable promoter activity calculated by this database. For both gene sequences a promoter region inside of intron 1 is found in addition to the known promoter site preceding exon 1. The binding sites for the transcription apparatus are listed with their locations are expressed relative to the previously determined transcription start site (TSS) of each sequence.

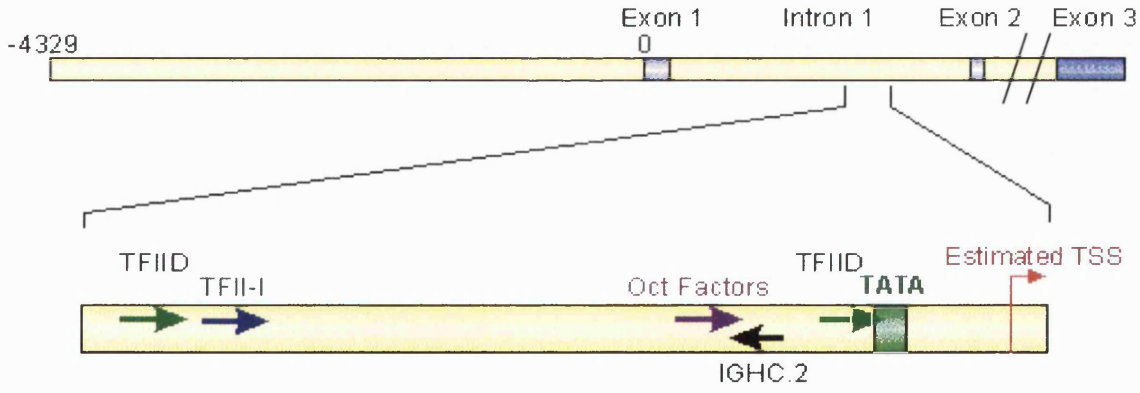

Figure 3.8 Diagrammatic representation of the putative promoter region within intron 1 of bovine *prnp*. The data obtained by entering the bovine (accession number AF163764) and murine (accession number U29187) gene sequences into the PROSCAN v1.7 database are shown relative to their position within the *prnp* gene sequence.

3.2.2 Transcription Factor Predictions

To look at the transcription factor binding sites found within the bovine and mouse sequences, the sequences were entered into the TESS and Signal Scan databases and are accurate to the end of August 2005.

Transcription factor analysis of the bovine sequence shows four regions of high intensity transcription factor binding sites, indicating that these regions are of considerable importance to the genetic control of expression (figure 3.9A). The first two are located in the promoter sequence, with one just before exon 1 and the other slightly further up-stream around the area where the heat shock factors are found in the rat gene. The second two sites are inside intron 1, one of which corresponds with the site that may have promoter activity within this region and the other occurs immediately before the start of exon 2.

Binding sites in the mouse sequence are not as localised as the bovine sequence (figure 3.9B). The promoter sequence appears of greater importance for mouse gene regulation with several high intensity sites, two of which correlate with equivalent sites in the bovine promoter region. In addition the intron 1 sequence appears less active for gene regulation. Although it does have several areas of high frequency of binding sites, these are not as intense as for the bovine intron 1 region.

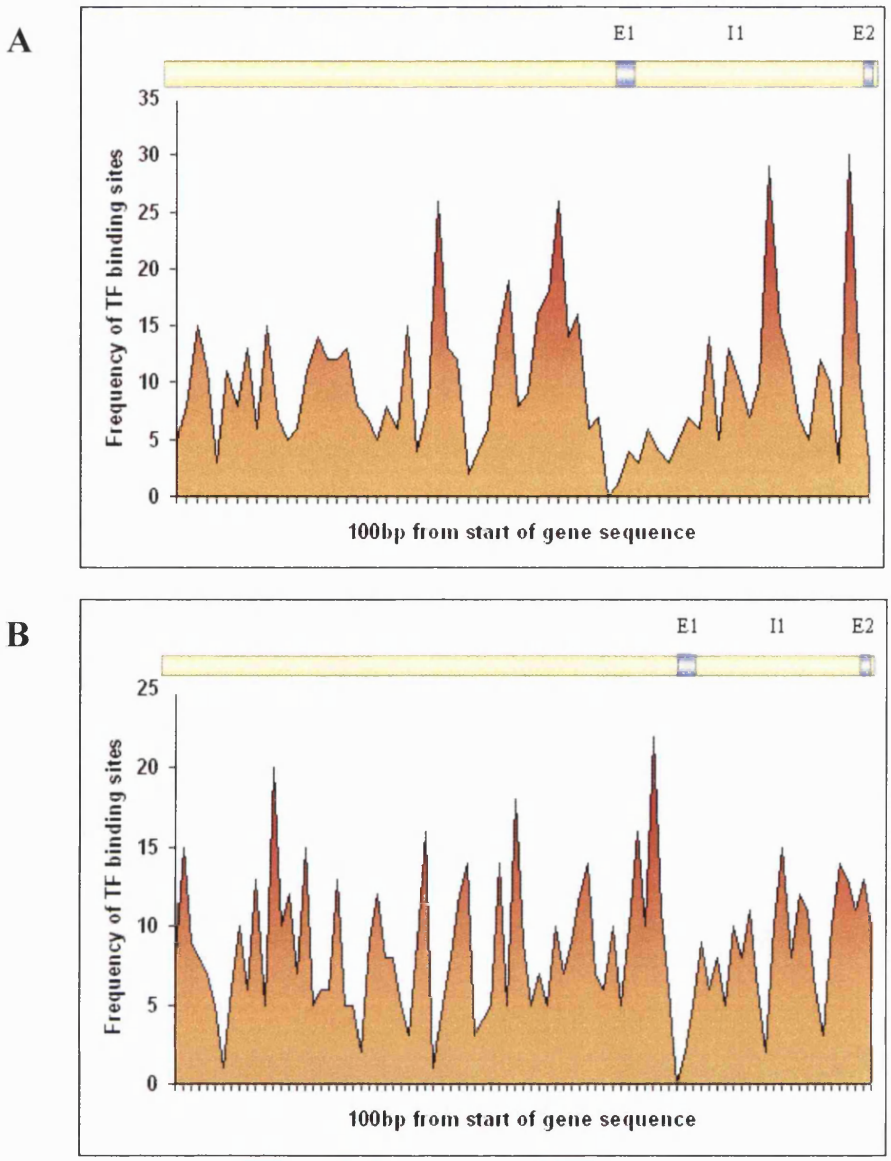

Figure 3.9 Frequency of transcription factor (TF) binding sites throughout the bovine and murine genes from the start of the published gene sequence to the end of exon 2. The bovine (A; accession number AF163764) and murine (B; accession number U29187) gene sequences were entered into TFSearch with a minimum acceptable homology value of 0.85. The plots show the frequency of binding sites per 100 bases. Shown above each plot is the gene to indicate the position of the exons and intron 1.

For both sequences it is found that there are no transcription factor binding sites within exon 1. Since construct D, composed of the promoter and exon 1 only, showed no ability to drive GFP production in any of the cell lines this is likely to be significant. It may suggest that the influence of this region on gene activity is not a repressor effect but rather a result of the lack of transcription factor binding sites.

3.3 mRNA variants

Since the GFP constructs and the database predictions both show a potential area of promoter activity in intron 1, the existence of an mRNA species that was lacking exon 1 was investigated. For this, an RT-PCR based method, RNA-ligase mediated rapid amplification of cDNA ends (RLM-RACE) was used. This method specifically targets full length capped mRNA and adds an adaptor onto the 5' end. This ensures that the species that are found are the result of full length mRNA, not degradation products. A nested PCR using adapter and gene specific primers is then used to identify variations in the 5' ends of mRNA (section 2.2). Since a species lacking exon 1 may be rare, an additional primer overlapping the end of the adapter with a short gene specific sequence was also used to avoid such a species being missed. mRNA from bovine (n = 3) and murine (n = 1) total brain tissue were tested (Figure 3.10).

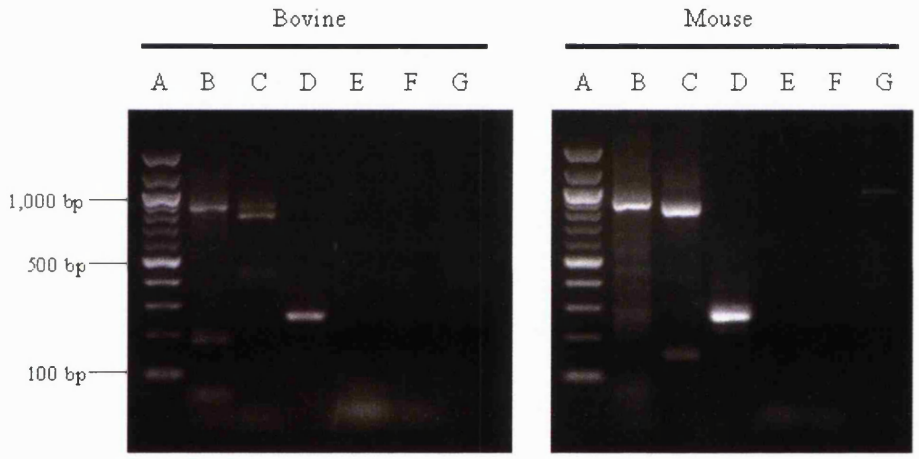

Figure 3.10 RLM-RACE identification of bovine and murine 5' mRNA splice variants. Total RNA was extracted from bovine and murine brain samples. The total RNA was treated to add an adapter RNA sequence to the 5' end of only mature capped mRNA. A reverse transcription reaction was used to create cDNA from the RNA sample and the mRNA of interest was amplified using a nested PCR reaction, with primers directed against the adaptor sequence (or part of the adaptor sequence) and against the PrP mRNA to ensure only full length species of PrP mRNA were detected. To visualise the PCR reaction products 10 µl of each reaction mixture was electrophoresed on a 2% agarose gel containing ethidium bromide, and the DNA-ethidium bromide detected by viewing under a long range UV light box. A) 100 base pair DNA ladder. B) Adapter primer nested PCR reaction. C) Adapter-Exon 2 Specific primer nested PCR. D) GAPDH positive control reaction. E) PCR mix negative control. F) Minus adapter negative control. G) First nested PCR result.

The results showed that the PCRs had worked correctly with the positive control lane (D) showing a band corresponding to GAPDH, and the negative control lanes (E & F) clear of contamination. Several bands are seen in lane B, where the 5' adapter primer was used, these are likely to correspond to different splice variants of PrP mRNA. From this lane it is unclear if an exon 2 only splice variant is present. However, a band is observed in lane C, where the adapter-gene specific primer was used. This band is of the correct size to correspond to a variant lacking exon 1 for both the bovine and murine tissues. To confirm that this band was a mRNA splice variant lacking exon 1, the PCR products were sequenced. Example results of the bovine and murine sequencing are shown in Figures 3.11 and 3.12 respectively.

The sequencing results obtained from the PCR products of the RLM-RACE reactions show that a splice variant lacking exon 1 can be found in both bovine and murine brain tissue. The bovine full length clones aligned with exon 1b (subject base pair number 4330-4382) and exon 2 (subject base pair number 6826-6923), and murine clones aligned with exon 1 (subject base pair number 6205-6251) and exon 2 (subject base pair number 8442-8539). Splice variants lacking exon 1 aligned with the exon 2 sequence only.

A. Bovine exons 1 + 2

Query = Bovine clone, 842 bases

Subject = Bos taurus prion protein PrP (PrnP) gene, alternatively spliced, promoter, exons 1a, 1b, and 2, partial sequence. Accession number = AF163764

Exon 2 alignment

```
Query: 645  atctgctgtgattcagctcaagttggatttgtgtctctgggaagacagatgcttcggctt 704
            ||||||||||||||||||||||||||||||||||||||||||||||||||||||||||||
Sbjct: 6923 atctgctgtgattcagctcaagttggatttgtgtctctgggaagacagatgcttcggggc 6864


Query: 705  ggttgaaactgttcagttttcaaatatattcagaagtcct 744
            |||||||||||||||||| ||||||||||||||||||||
Sbjct: 6863 ggttgaaactgttcagtttgcaaatatattcagaagtcct 6824
```

Exon 1 alignment

```
Query: 742  cctgcttctgcgagagagaagacgctctcagctctgcggctgtcagcgactg 793
            ||||||||||||||||||||||||||||||||||||||||||||||||||
Sbjct: 4383 cctgcttctgcgagagagaagacgctctcagctctgcggctgtcagcgactg 4332
```

B. Bovine exon 2 only

Query = Bovine clone, 840 bases

Subject = Bos taurus prion protein PrP (PrnP) gene, alternatively spliced, promoter, exons 1a, 1b, and 2, partial sequence. Accession number = AF163764

Exon 2 alignment

```
Query: 656  atctgctgtgattcagctcaagttggatttgtgtctctgggaagacagatgcttcggctt 715
            ||||||||||||||||||||||||||||||||||||||||||||||||||||||||||||
Sbjct: 6923 atctgctgtgattcagctcaagttggatttgtgtctctgggaagacagatgcttcggggc 6864


Query: 716  ggttgaaactgtncagttttcaaatatattcagaagtc 753
            |||||||||||| |||||| ||||||||||||||||||
Sbjct: 6863 ggttgaaactgttcagtttgcaaatatattcagaagtc 6826
```

Figure 3.11 Bovine RLM-RACE sequencing results. Clones from the RLM-RACE reactions were sequenced using a PE Biosystems ABI 377 DNA sequencer (Gene Service Ltd, Cambridge). Examples of clones obtained from the bovine RLM-RACE reactions were aligned with bovine *prnp* using NCBI BLAST. A) Variant containing exon 1b. B) Variant lacking exon 1. Exon sequences are indicated in red. Slight variations may be seen between the published and obtained sequences due to the accuracy of the sequencing reaction, mutations introduced by the PCR Tac polymerase, or polymorphisms in the gene sequences, which are more common in untranscribed sequences such as introns where the mutation is likely to be silent and so not affect the gene function.

A) Murine exons 1 + 2

Query = Murine clone, 830 bases

Subject = Murine long incubation prion protein. Accession number = U29187

Exon 2 alignment

```
Query: 686  agtctgcttggctctcctaaattggactggtaccactaggaaggcagaatgcttcagctc 745
            ||||||||||||||||||||||||||||||||||||||||||||||||||||||||||||
Sbjct: 8539 agtctgcttggctctcctaaattggactggtaccactaggaaggcagaatgcttcagctc 8480


Query: 746  ggttgaaatggttcagttctgaaatatactcaggagtcct 785
            |||||||||||||||||||||||||||||||||||||||
Sbjct: 8479 ggttgaaatggttcagttctgaaatatactcaggagtcct 8440
```

Exon 1 alignment

```
Query: 783  cctgccaccgatgcgacgcagcgcccagaatcngtc 818
            |||||||||||||||||||||||||||||| |||
Sbjct: 6252 cctgccaccgatgcgacgcagcgcccagaatcggtc 6217
```

B) Murine exon 2 only

Query = Murine clone, 800 bases

Subject = Murine long incubation prion protein. Accession number = U29187

Exon 2 alignment

```
Query: 688  agtctgcttggctctcctaaattggactggtaccactaggaaggcagaatgcttcnnctc 747
            ||||||||||||||||||||||||||||||||||||||||||||||||||||||  |||
Sbjct: 8539 agtctgcttggctctcctaaattggactggtaccactaggaaggcagaatgcttcagctc 8480


Query: 748  nggttgaaaatggttcanttctgaaatatactcngg 783
              ||||| |||||||||| |||||||||||||| ||
Sbjct: 8479 -ggttg-aaatggttcagttctgaaatatactcagg 8446
```

Figure 3.12 Murine RLM-RACE sequencing results. Clones from the RLM-RACE reactions were sequenced using a PE Biosystems ABI 377 DNA sequencer (Gene Service Ltd, Cambridge). Examples of clones obtained from the murine RLM-RACE reactions were aligned with murine *prnp* using NCBI BLAST. A) Variant containing exon 1. B) Variant lacking exon 1. Exon sequences are indicated in red. Exon sequences are indicated in red. Slight variations may be seen between the published and obtained sequences due to the accuracy of the sequencing reaction, mutations introduced by the PCR Tac polymerase, or polymorphisms in the gene sequences, which are more common in untranscribed sequences such as introns where the mutation is likely to be silent and so not affect the gene function.

3.4 Exogenous Factors Affecting Promoter Activation

The genetic control of PrP^c expression is very likely to be affected by factors related to protein function and, in turn, factors that regulate promoter activity might be valuable clues to the function of the protein. PrP^c has previously been linked to cellular stress response and earlier studies have shown that the rat promoter is up-regulated in response to heat shock (Shyu *et al.*, 2000; Shyu *et al.*, 2002). Given that PrP^c binds copper and has been implicated in oxidative stress response, copper, DMSO (to induce oxidative stress) and ATRA, were chosen to be investigated for the effect on gene activity in the different cell lines.

The GFP variant used to monitor expression driven by the promoter constructs is destabilised, it has a half-life of just 2 hours as opposed to the 24 hour half-life of normal enhanced GFP reporters. Therefore any changes in gene expression should quickly become evident by monitoring changes in the GFP signal. Due to the instability of the GFP variant, transient changes should be detected as well as persistent alterations in activity. All of the following experiments have been run at least in triplicate and up to twelve times for confirmation of positive results.

3.4.1 Promoter Response to Cu

Stably transfected cell lines were plated in six well plates and allowed to adhere before the start of the experiment. Cells were treated with 100 μM $CuSO_4$ for 2, 4, 8, 24, 48 hours or left untreated. Following treatment, cells were washed in Hanks and extracted in native extraction buffer (see Methods, section 2.9). For this the 100 μl extraction buffer was distributed over the cell monolayer, incubated for 20 minutes at 37 °C and the lysates collected. Equal amounts of protein were run on a native gel and observed under a phosphorimager at optimum wavelengths for GFP detection (excitation 488, emission 530), before being transferred onto a PVDF membrane and blotted for tubulin as a loading control.

Examples of the levels of GFP detected for the full-length construct A are shown in figure 3.13 and the quantification of this data shown in figure 3.14. The only cell line to show a significant response to copper when compared to the CMV promoter driven control was the PrP^c null F14 cell line. In the F14 cells GFP intensity driven by construct A starts to

increase after 4 hours exposure, begins to plateau after 8 hours exposure and is significant after 24 hours with activity about 1.5 times that of the untreated cells ($F = 4.88$, $p = 0.037$). Small fluctuations are seen for some of the other cell lines but these are not significant when compared to fluctuations of the CMV control ($F = 0.24$, $p = 0.994$). The vector control was also tested by this method to rule out a background response. No expression of the vector was found in any of the cell lines in response to copper at any time point (data not shown).

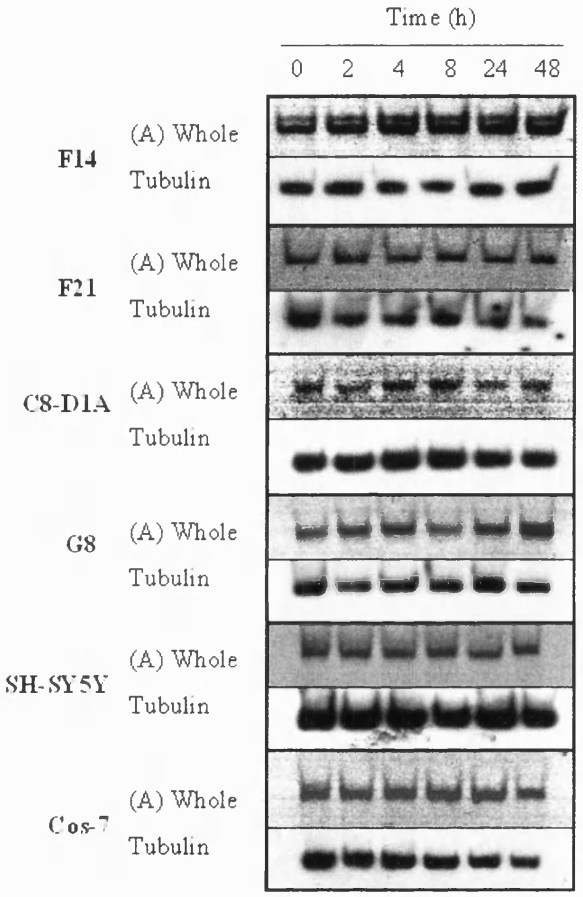

Figure 3.13 Direct detection of GFP signal driven by the whole promoter and non-coding region construct A in each of the cell lines in response to copper treatment. Cell lines stably transfected with the destabilised GFP reporter vector driven by whole bovine *prnp* gene construct (A; containing the promoter and non coding sequence up to the end of exon 2), were treated with 100 μM $CuSO_4$ for 2, 4, 8, 24, or 48 hours, or left untreated for the time 0 control. Equal quantities of the extracted protein were separated by electrophoresis on a 12% native acylamide gel and detected by excitation of the GFP and recording the intensity of the emitted light. Samples were then transferred onto a PVDF membrane and blotted for tubulin as a loading control. The GFP detection is shown compared to the respective tubulin loading control.

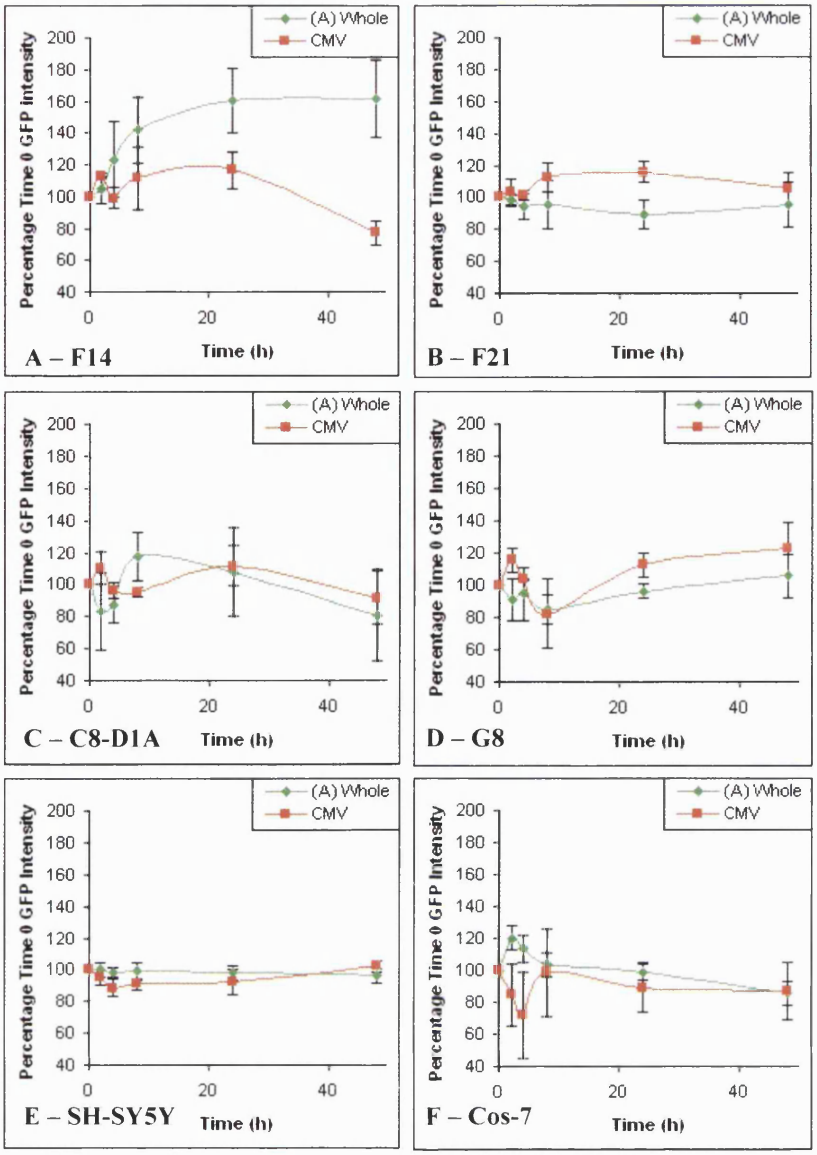

Figure 3.14 Quantification of *prnp* copper response. Cell extracts were electrophoresed on 12% native acrylamide gels, GFP was excited at light wavelength 488 nm and the intensity of emission at 530 nm measured. Protein was then transferred onto a PVDF membrane and blotted for tubulin as a loading control. The tubulin blots were quantified by densitometry. The GFP signal driven by the whole gene (promoter and non coding region up to the end of exon2) construct A is shown in comparison to that driven by the CMV promoter control in A) F14, B) F21, C) C8-D1A, D) G8, E) SH-SY5Y, and F) Cos-7 cell lines in response to treatment with 100 μM $CuSO_4$ for 2, 4, 8, 24 and 48 hours. Expression is shown relative to the time 0 GFP intensity and quantified with respect to tubulin as a loading control. Shown are the mean and SEM. The F14 cells showed a significant change in construct A activity compared to the CMV control ($F = 4.88$, $p = 0.037$), the remaining cell lines showed no significant response ($F = 0.24$, $p = 0.994$). n = min 3, max 12 individual time series.

To investigate the regions of *prnp* that were responsible for the reaction to copper all of the gene part constructs were tested in the same way as construct A and the CMV control. Despite the lack of reaction of construct A in most of the cell lines, copper was tested in all

of the cell lines to avoid a significant response being missed. Examples of only the cell lines and constructs showing significant alterations in activity are shown in figure 3.15 and the quantification of all of the constructs that could be detected by this method are shown in figure 3.16. The constructs that did not express highly enough to be quantified have not been included since it would have been inaccurate to attempt to quantify beyond the limitations of the software.

Most of the constructs showed a lower signal to background ratio than was seen for construct A. This effect is most likely to be due to the lower basal level of activity of these constructs compared with that of the full length construct A in most of the cell lines.

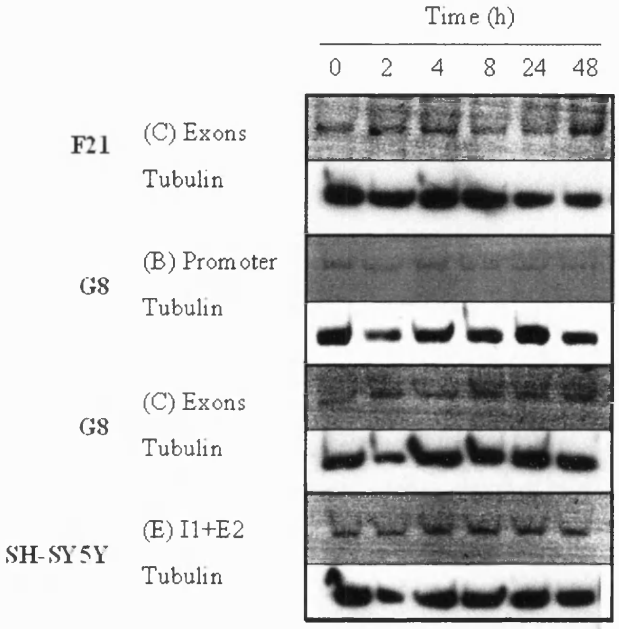

Figure 3.15 Direct detection of GFP signal driven by the constructs that showed a significant response to copper ($F = 2.73$, $p < 0.001$). Cell lines stably transfected with the destabilised GFP reporter vector driven by each of the bovine *prnp* gene constructs (B, containing the promoter only; C, containing the non-coding sequence from the start of exon 1 to the end of exon 2; D, the promoter plus exon 1; E, intron 1 and exon 2), were treated with 100 μM $CuSO_4$ for 2, 4, 8, 24, or 48 hours, or left untreated for the time 0 control. Equal quantities of the extracted protein were separated by electrophoresis on a 12% native acylamide gel and detected by excitation of the GFP and recording the intensity of the emitted light. Samples were then transferred onto a PVDF membrane and blotted for tubulin as a loading control. The GFP detection is shown compared to the respective tubulin loading control. Only the cell lines and constructs that showed a reaction significantly different to that of the CMV promoter driven control cell lines have been shown.

Up-regulation of GFP signal is shown by exons containing construct C in the F21 ($T = 3.23$, $p = 0.001$) and G8 ($T = 2.52$, $p = 0.012$) cell lines. This effect only becomes

significant at 48 hours post exposure. The promoter region on its own (construct B) only showed a significant effect in the G8 cells ($T = -3.33$, $p = 0.001$) and this effect peaked at 4 hours post exposure, dropping rapidly away by 8 hours to a level lower than that of the CMV control. In the SH-SY5Y cells the intron 1 and exon 2 only construct (E) was able to up-regulate GFP expression from 4 hours post exposure ($T = 3.39$, $p = 0.001$). Clearly the underlying cell line makes a considerable difference to how the promoter is regulated. Since some of the cell lines did not show a response of the full length construct A to the copper insult, but sections of the gene did react, this suggests that the response of the gene involves both the promoter region and the intron 1 region interacting with each other. The finding that increases in GFP expression by construct C were only significant after 48 hours may suggest that prolonged exposure to copper causes secondary cascades to become activated, resulting in different gene expression mechanisms controlling expression.

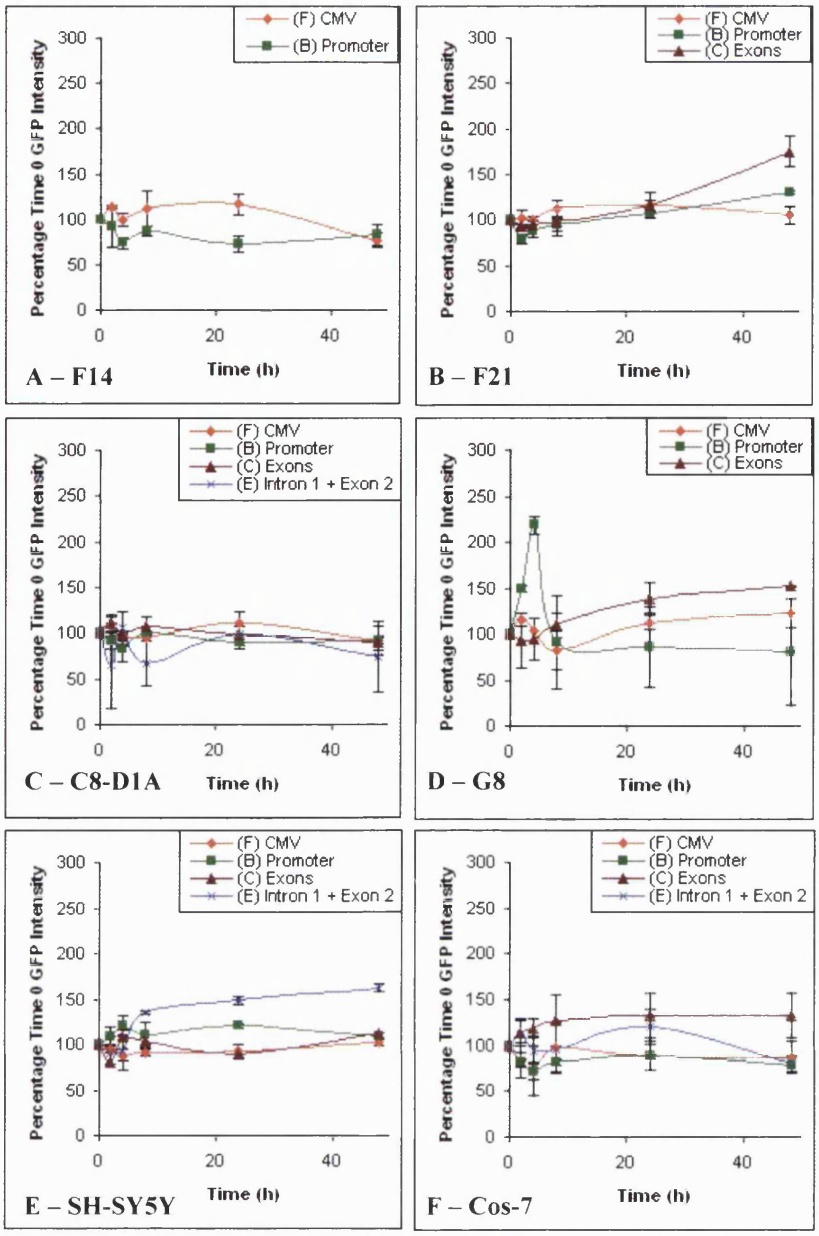

Figure 3.16 Quantification of truncated *prnp* copper response. Cell extracts were electrophoresed on 12% native acrylamide gels, GFP was excited at light wavelength 488 nm and the intensity of emission at 530 nm measured. Protein was then transferred onto a PVDF membrane and blotted for tubulin as a loading control. The tubulin blots were quantified by densitometry. The GFP signal driven by each of the bovine *prnp* gene constructs (B, containing the promoter only; C, containing the non-coding sequence from the start of exon 1 to the end of exon 2; D, the promoter plus exon 1; E, intron 1 and exon 2) is shown in comparison to that driven by the CMV promoter control in A) F14, B) F21, C) C8-D1A, D) G8, E) SH-SY5Y, and F) Cos-7 cell lines in response to treatment with 100 μM $CuSO_4$ for 2, 4, 8, 24 and 48 hours. Expression is shown relative to the time 0 GFP intensity and quantified with respect to tubulin as a loading control. Only those constructs that expressed highly enough to be quantified within the limits of the software have been plotted. Shown are the mean and SEM. n = min 3, max 12 individual time series.

3.4.2 Promoter Response to DMSO

DMSO was used to look at the effect of oxidative stress on the PrP promoter in the stably transfected cells. DMSO is a versatile molecule. It can act as an oxygen radical scavenger and so has been implicated in protection from oxidative stress. However, the incorporation of oxygen radicals into the DMSO molecule initiates its breakdown, during which process further radicals are released. These are mostly methyl radicals (although at higher concentrations methyl sulphoxide radicals are produced by pyrolysis) and in an aqueous system can react with oxygen to form peroxyl radicals, thus inducing oxidative stress (Mišík & Riesz, 1996; Lee *et al.*, 2004). In addition to these qualities, DMSO can also initiate apoptosis by collapsing the mitochondrial membrane potential and the subsequent activation of caspases 3 and 9. It can induce cellular differentiation of some malignant clones, and alter expression of various cell surface antigens (for review see Santos *et al.*, 2003). Cells were prepared similarly to the method described for $CuSO_4$ treatment. At the same time points as described for Cu, cells were treated with 1% DMSO, and extractions were as previously described. The response of the whole *prnp* construct A in each of the cell lines is shown in figure 3.17 and the quantification of this shown in figure 3.18.

Significant increases in GFP intensity driven by construct A are seen in the C8-D1A ($T = -1.52$, $p = 0.014$) and Cos-7 ($T = -4.51$, $p < 0.001$) cell lines, with this effect significant as early as four hours post exposure, but dropping back to the level of the CMV control in the C8-D1A cells by 24 hours post exposure, perhaps reflecting the ability of the cells to deal with the insult. The G8 cells show a variable result; an initial drop in activity is seen, followed by an increase in activity that then steeply drops away to a significant decrease in expression. This reaction is made more significant by the response of the CMV control, which is increased after 24 hours exposure indicating non-specific up-regulation of cellular proteins but PrP specific down regulation ($T = 3.19$, $p = 0.002$). The F14 and SH-SY5Y cells do not appear to respond to DMSO at all.

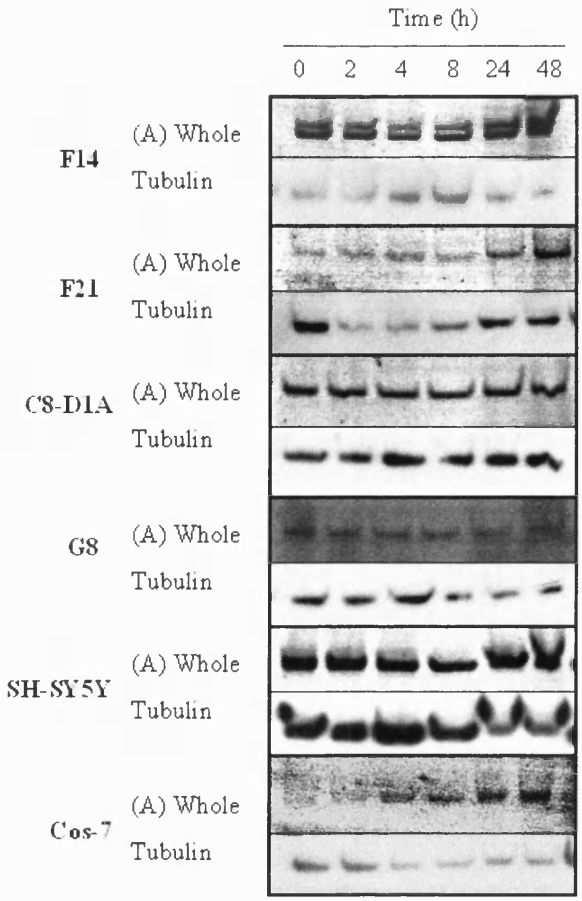

Figure 3.17 Direct detection of GFP signal driven by the whole promoter and non-coding region construct A in each of the cell lines in response to 1% DMSO treatment. Cell lines stably transfected with the destabilised GFP reporter vector driven by whole bovine *prnp* gene construct (A; containing the promoter and non coding sequence up to the end of exon 2), were treated with 1% DMSO for 2, 4, 8, 24, or 48 hours, or left untreated for the time 0 control. Equal quantities of the extracted protein were separated by electrophoresis on a 12% native acylamide gel and detected by excitation of the GFP and recording the intensity of the emitted light. Samples were then transferred onto a PVDF membrane and blotted for tubulin as a loading control. The GFP detection is shown compared to the respective tubulin loading control.

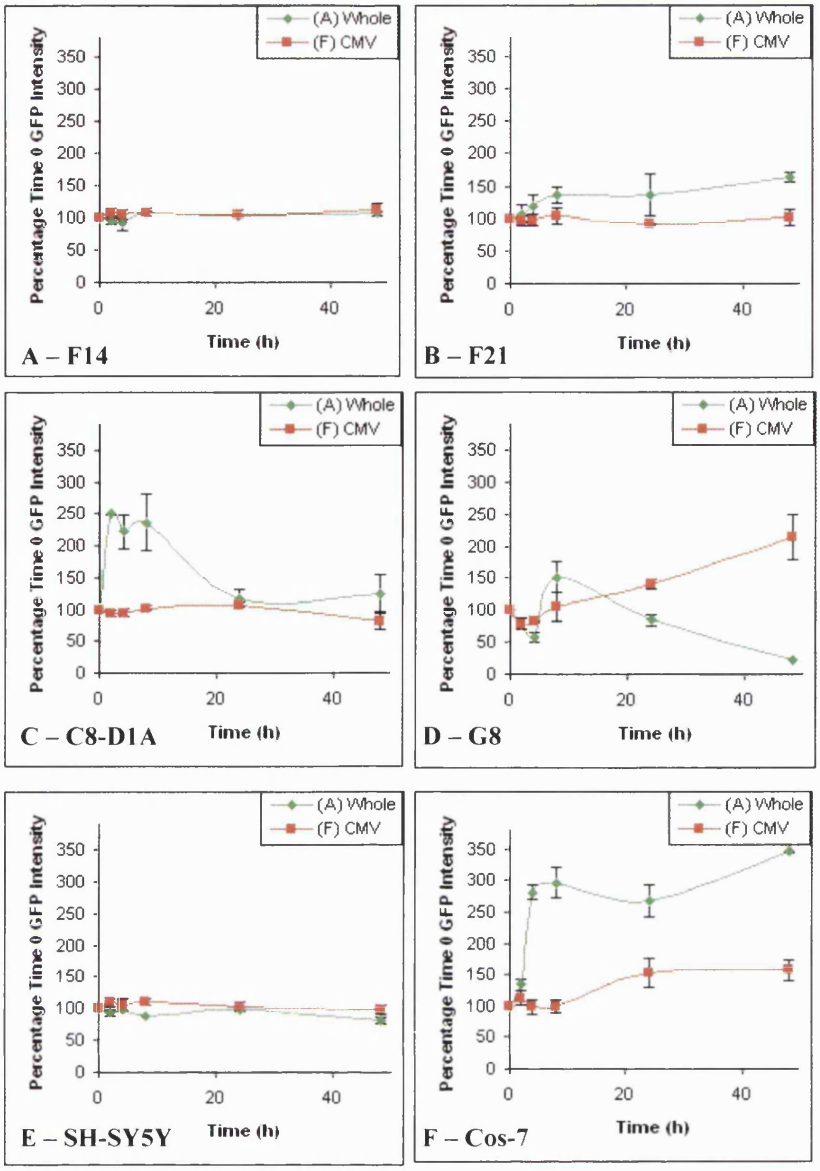

Figure 3.18 Quantification of *prnp* DMSO response. Cell extracts were electrophoresed on 12% native acrylamide gels, GFP was excited at light wavelength 488 nm and the intensity of emission at 530 nm measured. Protein was then transferred onto a PVDF membrane and blotted for tubulin as a loading control. The tubulin blots were quantified by densitometry. The GFP signal driven by the whole gene (promoter and non coding region up to the end of exon2) construct A is shown in comparison to that driven by the CMV promoter control in A) F14, B) F21, C) C8-D1A, D) G8, E) SH-SY5Y, and F) Cos-7 cell lines in response to treatment with 1% DMSO for 2, 4, 8, 24 and 48 hours. Expression is shown relative to the time 0 GFP intensity and quantified with respect to tubulin as a loading control. Shown are the mean and SEM. Construct A responds significantly differently to the CMV control in the C8-D1A, G8 and Cos-7 cell lines ($F = 6.01$, $p < 0.001$). n = min 3, max 12 individual time series.

As for the copper experiments, the other constructs were tested in all the cell lines to look for the regions of the gene that are activated/deactivated by DMSO. The constructs that showed a significant response are pictured in figure 3.19 and the quantification is shown in figure 3.20.

For all of the constructs that responded to DMSO the reaction only became significant after 48 hours exposure, much later than for the cell lines in which construct A reacted. Again this suggests that control of *prnp* relies on the interaction of the promoter with the sequence that follows it. This is further supported by the reaction of constructs C and E showing a significant increase in the F14 cells ($T = 3.48$, $p = 0.001$ and $T = 3.18$, $p = 0.014$ respectively) and construct E showing a significant increase in the G8 cells ($T = -3.66$, $p < 0.001$). The reaction of construct E in these cell lines is especially significant since its expression was virtually undetectable by phosphorimager detection until the addition of DMSO. The promoter region (construct B) was also found to up regulate the GFP signal in the C8-D1A ($T = -2.28$, $p = 0.023$) and Cos-7 ($T = -2.3$, $p = 0.02$) cells. The F21 cells that showed an up-regulation of construct A in response to DMSO only showed a small increase in the activity of construct C, and the SH-SY5Y cells demonstrated no reaction to the DMSO.

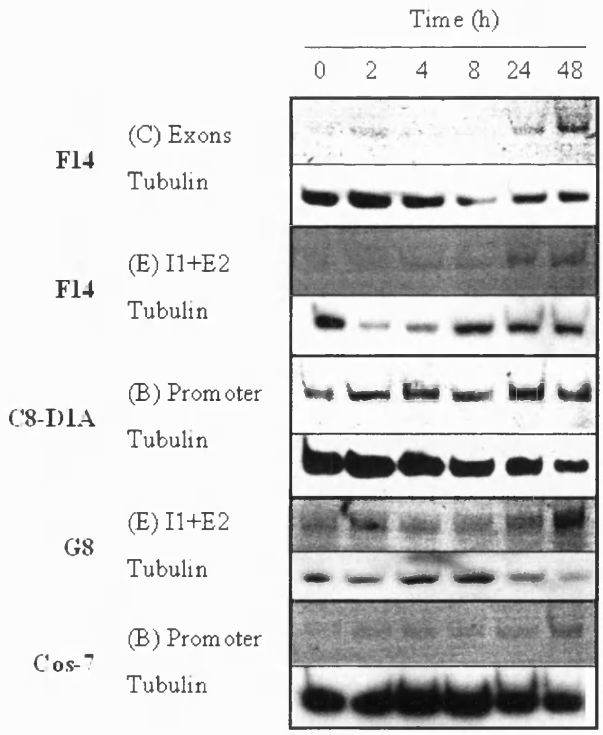

Figure 3.19 Direct detection of GFP signal driven by the constructs that showed a significant response to DMSO ($F = 4.6$, $p < 0.001$). Cell lines stably transfected with the destabilised GFP reporter vector driven by each of the bovine *prnp* gene constructs (B, containing the promoter only; C, containing the non-coding sequence from the start of exon 1 to the end of exon 2; D, the promoter plus exon 1; E, intron 1 and exon 2), were treated with 1% DMSO for 2, 4, 8, 24, or 48 hours, or left untreated for the time 0 control. Equal quantities of the extracted protein were separated by electrophoresis on a 12% native acylamide gel and detected by excitation of the GFP and recording the intensity of the emitted light. Samples were then transferred onto a PVDF membrane and blotted for tubulin as a loading control. The GFP detection is shown compared to the respective tubulin loading control. Only the cell lines and constructs that showed a reaction significantly different to that of the CMV promoter driven control cell lines have been shown.

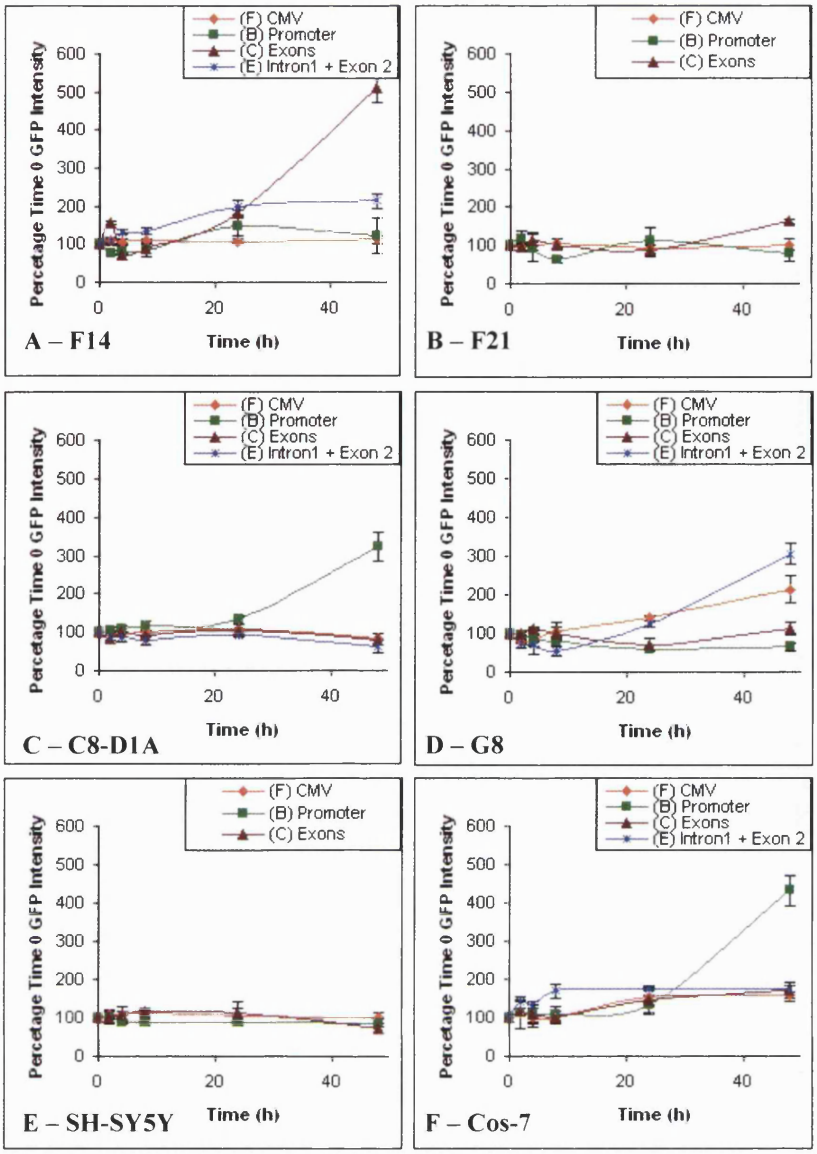

Figure 3.20 Quantification of truncated *prnp* DMSO response. Cell extracts were electrophoresed on 12% native acrylamide gels, GFP was excited at light wavelength 488 nm and the intensity of emission at 530 nm measured. Protein was then transferred onto a PVDF membrane and blotted for tubulin as a loading control. The tubulin blots were quantified by densitometry. The GFP signal driven by each of the bovine *prnp* gene constructs (B, containing the promoter only; C, containing the non-coding sequence from the start of exon 1 to the end of exon 2; D, the promoter plus exon 1; E, intron 1 and exon 2) is shown in comparison to that driven by the CMV promoter control in A) F14, B) F21, C) C8-D1A, D) G8, E) SH-SY5Y, and F) Cos-7 cell lines in response to treatment with 1% DMSO for 2, 4, 8, 24 and 48 hours. Expression is shown relative to the time 0 GFP intensity and quantified with respect to tubulin as a loading control. Only those constructs that expressed highly enough to be quantified within the limits of the software have been plotted. Shown are the mean and SEM. n = min 3, max 12 individual time series.

3.4.3 Promoter Response to ATRA

In addition to factors that increase promoter activity, factors that decrease activity and so would down regulate cellular PrP^c levels are also of interest. Factors that may down regulate PrP^c are of especial interest with respect to managing the progression of the disease. Since PrP^c is up-regulated as part of the disease pathogenesis and is required for disease progression, the disease could potentially be managed by maintaining reduced levels of PrP^c if an agent could be found to produce this effect. Rybner *et al.* (1997) found that ATRA down-regulates PrP^c expression in white blood cells, therefore this agent is of interest to this study.

Cells were prepared similarly to that described for $CuSO_4$ treatment. At the same time points as described for copper, cells were treated with 1 μM ATRA, and extractions were as previously described. Examples of the levels of GFP detected for the full-length construct A are shown in figure 3.21 and the quantification of this data shown in figure 3.22.

A significant down-regulation of the GFP signal is seen in the F14 ($T = 2.93$, $p = 0.004$) and F21 ($T = 3.61$, $p = 0.001$) cells, this is significant as early as 4 hours post exposure and maintained from then the final 48-hour measurement. Down-regulation is also seen in the G8 cells but this is not significant until 48 hours post exposure. The remaining cell lines show no significant change in expression compared to the CMV promoter control ($F = 0.23$, $p = 0.636$).

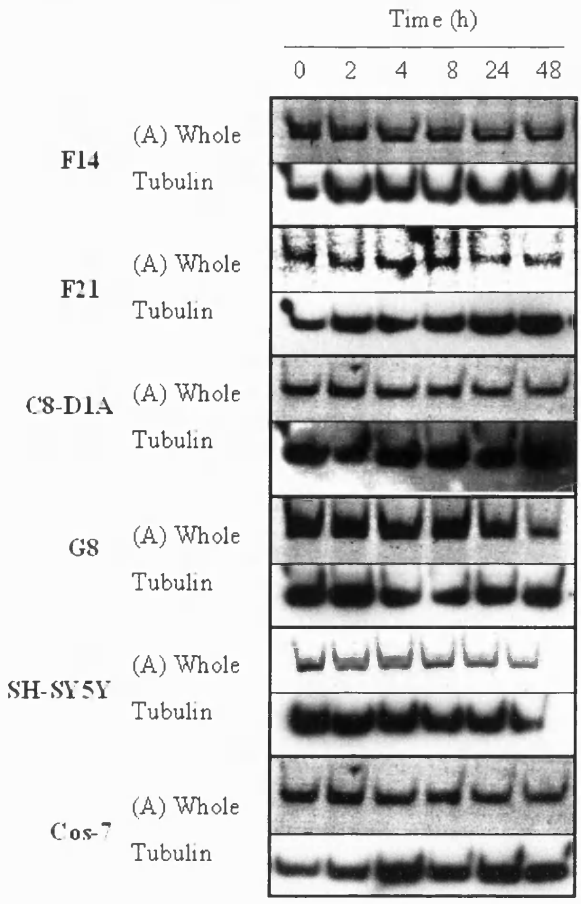

Figure 3.21 Direct detection of GFP signal driven by the whole promoter and non-coding region construct A in each of the cell lines in response to ATRA treatment. Cell lines stably transfected with the destabilised GFP reporter vector driven by whole bovine *prnp* gene construct (A; containing the promoter and non coding sequence up to the end of exon 2), were treated with 1 μM ATRA for 2, 4, 8, 24, or 48 hours, or left untreated for the time 0 control. Equal quantities of the extracted protein were separated by electrophoresis on a 12% native acylamide gel and detected by excitation of the GFP and recording the intensity of the emitted light. Samples were then transferred onto a PVDF membrane and blotted for tubulin as a loading control. The GFP detection is shown compared to the respective tubulin loading control.

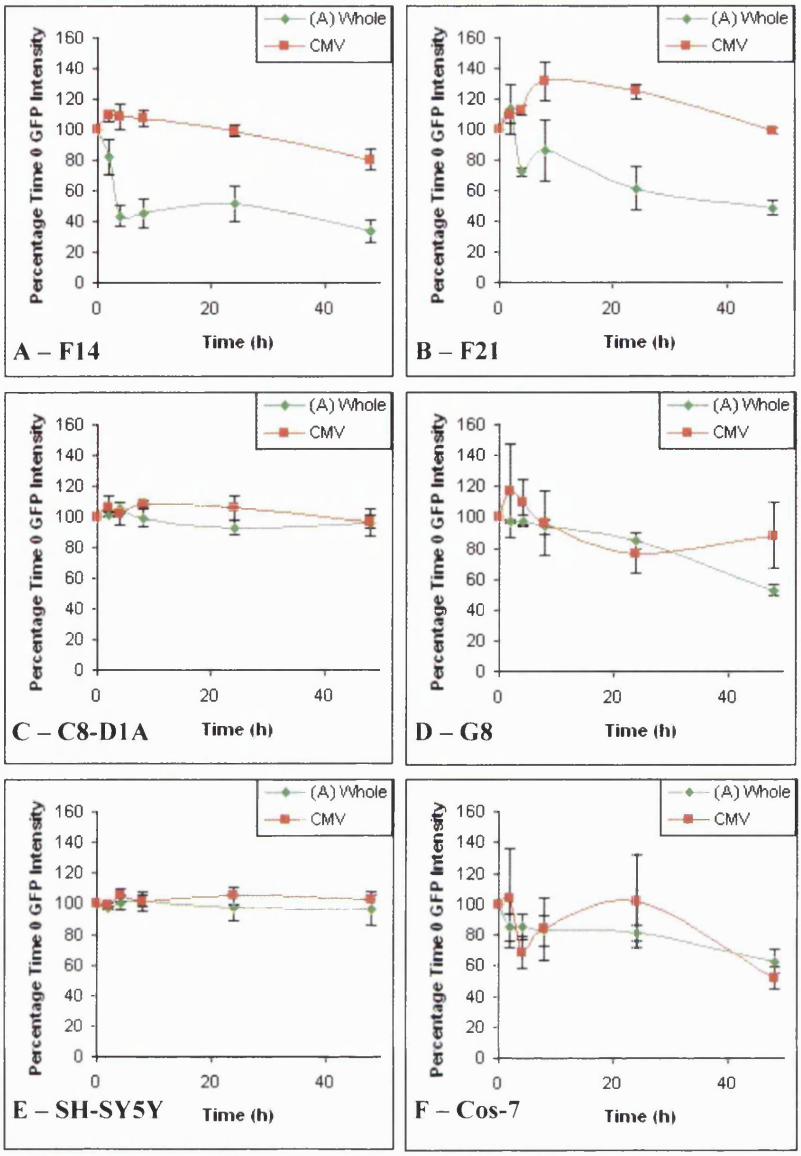

Figure 3.22 Quantification of *prnp* ATRA response. Cell extracts were electrophoresed on 12% native acrylamide gels, GFP was excited at light wavelength 488 nm and the intensity of emission at 530 nm measured. Protein was then transferred onto a PVDF membrane and blotted for tubulin as a loading control. The tubulin blots were quantified by densitometry. The GFP signal driven by the whole gene (promoter and non coding region up to the end of exon2) construct A is shown in comparison to that driven by the CMV promoter control in A) F14, B) F21, C) C8-D1A, D) G8, E) SH-SY5Y, and F) Cos-7 cell lines in response to treatment with 100 μM $CuSO_4$ for 2, 4, 8, 24 and 48 hours. Expression is shown relative to the time 0 GFP intensity and quantified with respect to tubulin as a loading control. Shown are the mean and SEM. Construct A expressed in F14 and F21 cells shows a significant down-regulatory response compared to the CMV control ($F = 5.18$, $p = 0.001$). n = min 3, max 12 individual time series.

The other promoter constructs were tested for their response to ATRA as before. The constructs showing a significant change in GFP expression are shown in figure 3.23 and the quantification of these reactions is shown in figure 3.24.

The F14 and F21 cells expressing the full-length construct A showed a significant down-regulatory response to ATRA, however no response was detected for any of the truncated constructs. This suggests that the response of these cell lines requires the interaction of the promoter with the intron 1 control sequences. The G8 cells, which show down-regulation of construct A after 48 hours exposure, show a significant down-regulation response of both construct B ($T = 2.73$, $p = 0.01$) and construct C ($T = 2.66$, $p = 0.013$) at 48 hours indicating that both of these regions are independently able to respond to ATRA. The SH-SY5Y cells, which did not show an alteration in the regulation of construct A in response to ATRA, show an increase in the GFP signal produced by the activity of construct C ($T = 4.1$, $p < 0.001$), containing the non coding region. This suggests that in these cells ATRA is able to activate regulatory pathways, which produce a different effect on the activation of the non-coding region of *prnp*. In addition an initial, significant increase in signal is seen for promoter only (construct B) in the Cos-7 cells before activity drops resulting in a significant down-regulation ($F = -1.96$, $p = 0.042$). This activity is not sustained and expression returns to normal levels by 48 hours post exposure.

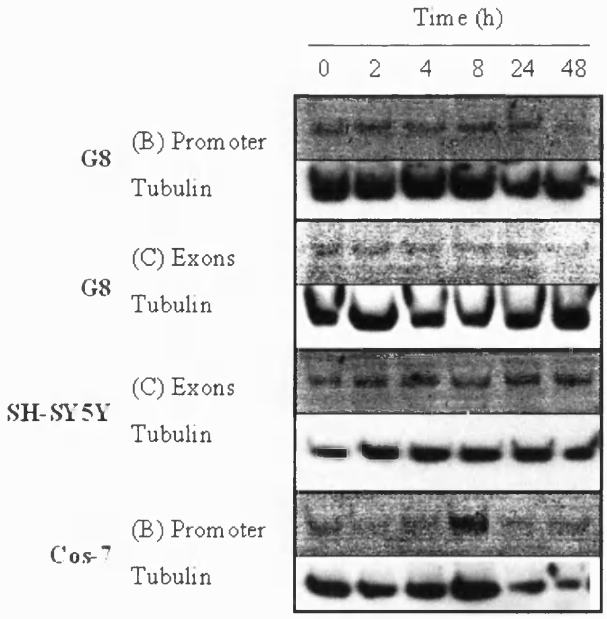

Figure 3.23 Direct detection of GFP signal driven by the constructs that showed a significant response to ATRA ($F = 1.89$, $p = 0.017$). Cell lines stably transfected with the destabilised GFP reporter vector driven by each of the bovine *prnp* gene constructs (B, containing the promoter only; C, containing the non-coding sequence from the start of exon 1 to the end of exon 2; D, the promoter plus exon 1; E, intron 1 and exon 2), were treated with 1 μM ATRA for 2, 4, 8, 24, or 48 hours, or left untreated for the time 0 control. Equal quantities of the extracted protein were separated by electrophoresis on a 12% native acylamide gel and detected by excitation of the GFP and recording the intensity of the emitted light. Samples were then transferred onto a PVDF membrane and blotted for tubulin as a loading control. The GFP detection is shown compared to the respective tubulin loading control. Only the cell lines and constructs that showed a reaction significantly different to that of the CMV promoter driven control cell lines have been shown.

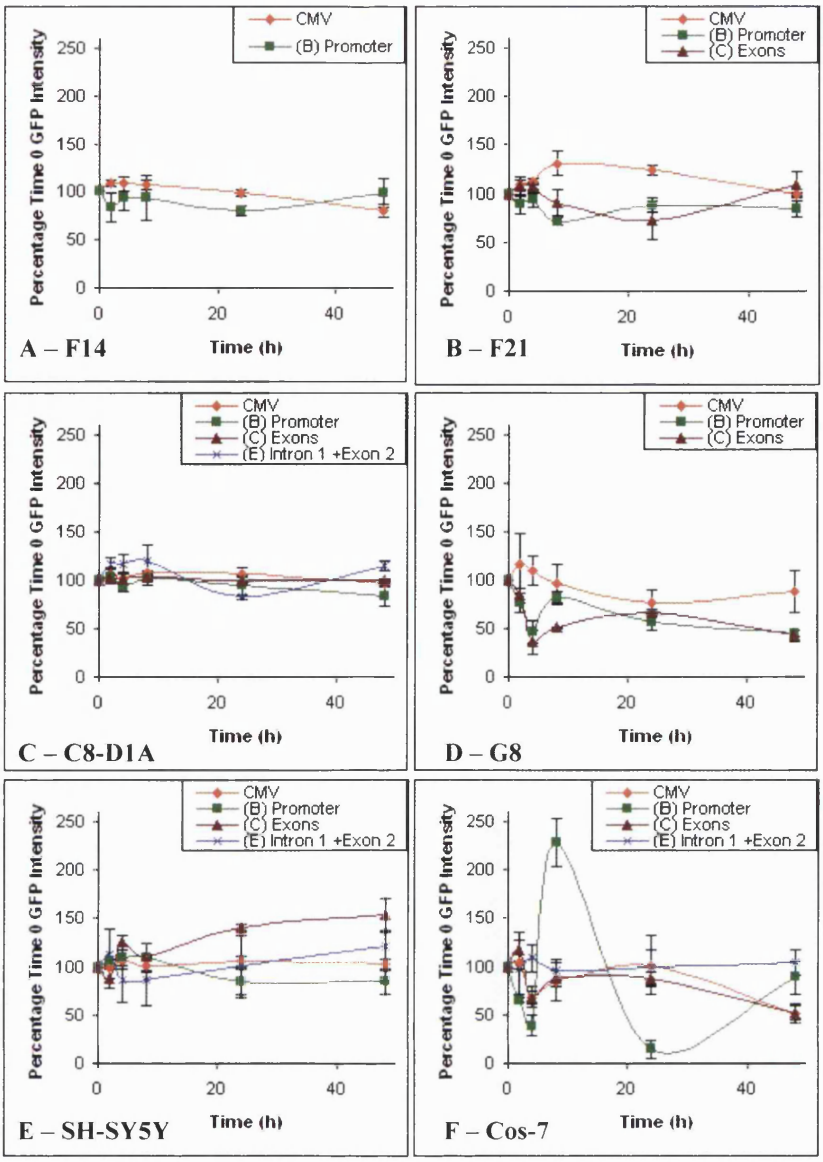

Figure 3.24 Quantification of truncated *prnp* ATRA response. Cell extracts were electrophoresed on 12% native acrylamide gels, GFP was excited at light wavelength 488 nm and the intensity of emission at 530 nm measured. Protein was then transferred onto a PVDF membrane and blotted for tubulin as a loading control. The tubulin blots were quantified by densitometry. The GFP signal driven by each of the bovine *prnp* gene constructs (B, containing the promoter only; C, containing the non-coding sequence from the start of exon 1 to the end of exon 2; D, the promoter plus exon 1; E, intron 1 and exon 2) is shown in comparison to that driven by the CMV promoter control in A) F14, B) F21, C) C8-D1A, D) G8, E) SH-SY5Y, and F) Cos-7 cell lines in response to treatment with 1 μM ATRA for 2, 4, 8, 24 and 48 hours. Expression is shown relative to the time 0 GFP intensity and quantified with respect to tubulin as a loading control. Only those constructs that expressed highly enough to be quantified within the limits of the software have been plotted. Shown are the mean and SEM. n = min 3, max 12 individual time series.

3.4.4 Prnp Promoter Response to Recombinant PrP^c

The differences in expression and response to stimuli of the F14 (null) cell line compared to the F21 (wild type) cell line, when transfected with the different constructs, indicated the presence of PrP^c in the cell was having an effect on its own regulation. To investigate if recombinant PrP^c could alter promoter activity, F14 and F21 cells expressing the whole bovine sequence (construct A) and the CMV and vector controls were incubated for 24 hours with 0.25 or 0.5 ng of water refolded recombinant PrP^c. The water refolded PrP^c is likely to lack the secondary structure that copper gives the N-terminus but there is no risk of a confounding effect caused by the release of copper into the cellular environment causing a change in promoter activity and GFP production. The results of this treatment are shown with the CMV and vector only controls in figure 3.25.

Recombinant PrP^c caused a significant up-regulation of the full length construct A in the F14 cells in response to both recombinant PrP concentrations tested ($T = 2.49$, $p = 0.017$). The CMV control showed no response (F14 cells $T = -1.23$, $p = 0.224$; F21 cells $T = -1.6$, $p = 0.118$) and no measurable fluorescence was observed for the vector control cells. An up-regulation is also seen in the F21 cells, however this is not significant ($T = 3.01$, $p = 0.057$).

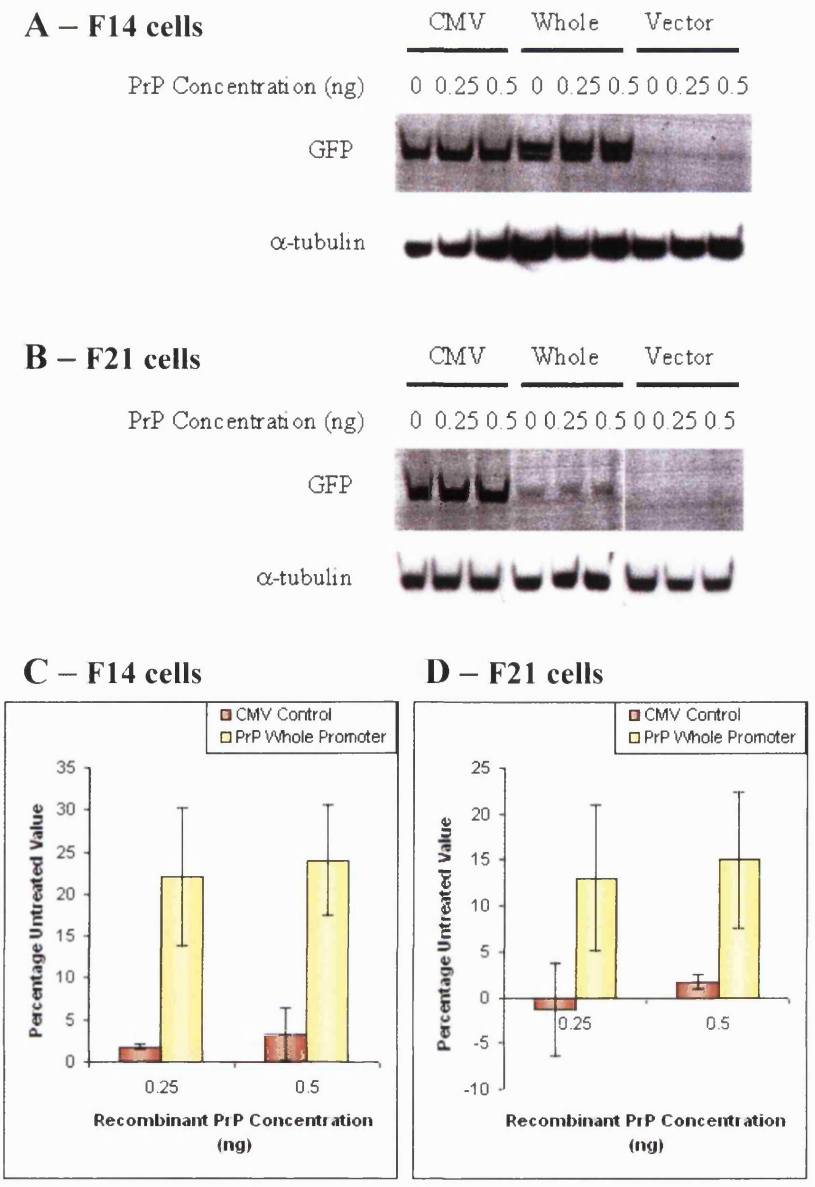

Figure 3.25 Effect of recombinant PrP^c on *prnp* activity in F14 and F21 cells. Cell extracts were electrophoresed on 12% native acrylamide gels, GFP was excited at light wavelength 488 nm and the intensity of emission at 530 nm measured. Protein was then transferred onto a PVDF membrane and blotted for tubulin as a loading control. The tubulin blots were quantified by densitometry. Response of A) F14 cells and B) F21 cells expressing the CMV control, the whole gene construct (A; promoter and non coding region up to the end of exon2), and the vector control when treated with 0.25 or 0.5 ng of water refolded recombinant PrP for 48 hours. C and D represent the quantification of the CMV and the *prnp* construct A response of the F14 and the F21 cells respectively, expression is shown relative to the time 0 GFP intensity and quantified with respect to tubulin as a loading control. Shown are the mean and SEM. In the F14 cells construct A shows significant up-regulation in response to recombinant PrP compared to the other CMV control and the F21 cells ($F = 4.73$, $p = 0.042$). $n = 5$ individual time series.

3.5 Conclusions

The requirement of endogenous PrP^c for infection and disease progression (Brown *et al.*, 1994; Brandner *et al.*, 1996) and the influence of the level of expression of PrP^c on the incubation period (Scott *et al.*, 1989; Fischer *et al.*, 1996) suggest that the control of PrP^c expression may be an important consideration in the pathogenesis of the TSEs. Factors regulating PrP^c expression may be important therapeutic targets. Potentially, factors producing a down-regulation of PrP^c could be used to slow disease progression as part of disease management and therapy.

The finding that the intron 1 region has its own promoter activity and contributes to the full activity of the gene sequence is in agreement with previous studies (Baybutt & Manson, 1997; Inoue *et al.*, 1997; Premzel *et al.*, 2005). However, no previous studies have been able to find evidence to suggest that a construct lacking exon 1 may exist. Here it is shown that both bovine and murine splice variants lacking exon 1 can be found by the use of RLM-RACE. This technique targets only full length, properly capped mRNA, so virtually eliminating the possibility that this splice variant has only been detected due to the presence of degraded mRNA species.

The finding of control elements inside intron 1 is not unusual. Many genes have conserved regulatory regions located within the intron sequences, which may contribute to the control of gene expression (Jonsson *et al.*, 1992; Rohrer & Conley, 1998; Hural *et al.*, 2000; Chamary & Hurst, 2004). Control elements are preferentially found located in the 5' introns with less control elements found in the introns located further down stream. The enhancer effects of these control regions are so essential that some genes will not be expressed in their absence. In addition, these control elements may be involved in the tissue specific expression of the gene product. Of specific interest here is the identification of a putative TATA box within this region of the bovine gene. *Prnp* has often been classified as a house-keeping gene due to its lack of TATA box, this data may suggest that this is not the case and that *prnp* regulation is much more complicated. Different control mechanisms may be employed depending on the requirements of the cell; a basal level of expression may be maintained by the promoter region and specific induction driven by the intron 1 region.

This is the first study to show that exon 1 may also be involved in *prnp* regulation. None of the cell lines tested showed any significant activity of the construct containing just the promoter and exon 1 despite the full promoter sequence being present, indicating that the exon 1 region was interfering with expression. Alternatively, a further part of the sequence may be required for promoter activation, however this is unlikely as the promoter alone is able to drive expression. Analysis of putative transcription factor binding sites within *prnp* from both bovine and murine genes shows a complete lack of potential binding sites within exon 1, indicating that this may be a region of completely inert DNA sequence. As such it may be that it does not interact to inhibit PrP^c expression but that despite the presence of the promoter sequence the transcription apparatus cannot remain correctly assembled on the DNA or does not recognise this region as active DNA without the sequence that follows it. An alternative theory is that the exon 1 containing mRNA is produced but that exon 1 has mRNA regulatory regions, which prevent the mRNA from being translated into DNA. Investigation to determine the presence or absence of a GFP mRNA transcript containing exon 1 from cells transfected with the promoter and exon 1 construct would clarify which theory is correct. Further work could be directed toward determining the importance of both exons in the control of mRNA turnover. Database analysis of the untranslated regions, followed by mutational studies could be used for this purpose.

Cell line specific variation in expression of both the full length *prnp* promoter with the non-coding region and the truncated constructs was expected since different expression levels are seen in different body tissues. This is most likely to be due to the varied mechanisms that different cells use to regulate their protein expression depending upon their function and their underlying state of health. The F14 and the F21 cell lines exhibit differences in their basal stress levels (see chapter 5, part 5.3.3). This may result in different activation levels for the factors that control expression of proteins related to stress responses including PrP^c, which is known to be up-regulated in response to cellular stress via heat shock factors in the region preceding the promoter sequence (Shyu *et al.*, 2000; Shyu *et al.*, 2002).

The differences in the expression of the murine constructs compared to the equivalent bovine constructs in the cell lines studied may be due to different species utilising different control mechanisms. However, it is also likely they arise from the differences in the gene sequence. Despite the high conservation of the exons the remainder of the gene sequence is not highly conserved across species and, as is shown here by the variation in number and

location of transcription factor binding sites, the differences in sequence means that some variation in gene expression is expected due to the ability to bind different transcription factors.

Copper and oxidative stress alter *prnp* activity. *Prnp* regulation in response to copper and oxidative stress insults relies on both the promoter and the control elements within intron 1. When only one of these regions is present the ability to drive mRNA production is different to when the gene is complete, and this may reflect the ability of the DNA to coil and allow protein-protein interaction of transcription factors. The reaction of each of the constructs in all of the cell lines is shown in table 3.2. Varela-Nallar *et al.* (2005) reported that copper up-regulates the prion promoter. This is in agreement with the findings presented here, however the authors did not consider the effect of intron 1 on expression. The data presented here indicate that this region is highly important in maintaining the appropriate response to metal imbalance. In addition Varela-Nallar *et al.* find that the response to copper is cell line specific with responses seen in pheochromocytoma (PC12) cells but not glioma (C6) cells. This supports the data presented here, which shows that the changes in *prnp* activity in response to both copper and oxidative stress are influenced by the underlying cell line. Cell line specific modulations in expression induced by copper also explain why the study by Toni *et al.* (2005) showed down-regulation of PrP in response to copper. This study also used high exogenous levels of copper, well beyond that found physiologically, it is therefore likely that at these high concentrations the cells that are surviving are quiescent cells with much lower metabolic activity and so much less normal PrP^c production. It would be interesting to determine what effect lower concentrations of copper have in their culture system.

Previous studies found that ATRA could down regulate PrP^c expression (Rybner *et al.*, 2002; Cabral *et al.*, 2002). The data presented here show that *prnp* is significantly down-regulated in mouse neuroblastoma and myoblast cells, with the neuroblastoma cells showing rapid down-regulation within four hours of exposure. It is also found that the different gene regions of *prnp* interact to produce this effect (table 3.2). Down-regulation effects are seen by part constructs in some of the cells lines but the effect happens at a much slower rate (after 24 hours) than for the full length construct. The finding that the full length construct down-regulates so rapidly suggests that ATRA may be able to interact directly, perhaps by the activation of RAR and RAREs or by activation of transcription factors already present, as opposed to by activation of cascades to induce production of

specific transcription factors. This would be expected to produce a much slower down-regulation and may account for the down-regulation effects observed for the truncated constructs. Also noted is that in the cells showing a rapid down-regulation response, the effect is sustained up to the 48 hour time point. ATRA is highly labile, and will degrade quickly once in culture media at 37°C. For the effect to be sustained, either the down-regulation is induced by a more stable breakdown product or ATRA is activating further pathways to induce expression of transcription factors that bind to the promoter and maintain the effect. This also agrees with the slower down-regulation seen in some of the cell lines with the truncated constructs.

	Construct									
	A - Whole		B - Promoter		C - Exons		E - I1+E2		F - CMV	
F14	Cu	↑	Cu	↔	Cu	n/d	Cu	n/d	Cu	↔
	DMSO	↔	DMSO	↔	DMSO	↑	DMSO	↑	DMSO	↔
	ATRA	↓	ATRA	↔	ATRA	n/d	ATRA	n/d	ATRA	↔
F21	Cu	↔	Cu	↔	Cu	↑	Cu	n/d	Cu	↔
	DMSO	↔	DMSO	↔	DMSO	↔	DMSO	n/d	DMSO	↔
	ATRA	↓	ATRA	↔	ATRA	↔	ATRA	n/d	ATRA	↔
C8-D1A	Cu	↔	Cu	↔	Cu	↔	Cu	↔	Cu	↔
	DMSO	↑	DMSO	↑	DMSO	↔	DMSO	↔	DMSO	↔
	ATRA	↔	ATRA	↔	ATRA	↔	ATRA	↔	ATRA	↔
G8	Cu	↔	Cu	↑	Cu	↑	Cu	n/d	Cu	↔
	DMSO	↓	DMSO	↔	DMSO	↔	DMSO	↑	DMSO	↑
	ATRA	↔	ATRA	↓	ATRA	↓	ATRA	n/d	ATRA	↔
SH-SY5Y	Cu	↔	Cu	↔	Cu	↔	Cu	↑	Cu	↔
	DMSO	↔	DMSO	↔	DMSO	↔	DMSO	n/d	DMSO	↔
	ATRA	↔	ATRA	↔	ATRA	↑	ATRA	↔	ATRA	↔
Cos-7	Cu	↔	Cu	↔	Cu	↔	Cu	↔	Cu	↔
	DMSO	↑	DMSO	↑	DMSO	↔	DMSO	↔	DMSO	↔
	ATRA	↔	ATRA	↑↓	ATRA	↔	ATRA	↔	ATRA	↔

Table 3.2 Response of *prnp* constructs expressed in all cell lines to Cu, DMSO and ATRA stimuli. Up-regulatory responses are shown by ↑, down-regulatory responses are shown by ↓, and no response is shown by ↔. Where expression levels were too low to be detected by phosphorimaging n/d represents not detectable.

The finding that PrP has the ability to regulate its own expression is likely to be highly significant for disease pathogenesis. If the metal imbalances associated with the onset of the disease were to cause up-regulation of PrP^{c}, and it then continued to up regulate itself, a self exacerbating cycle could be started providing more PrP^{c} and so more substrate for conversion into PrP^{sc}. The ability of recombinant PrP to up-regulate *prnp* is not likely to arise from direct interaction of the recombinant PrP with endogenous PrP^{c}, due to the more pronounced effect seen in the PrP^{c} null F14 cells. Instead it is likely that PrP interacts with another protein on the cell surface causing the activation of a signal transduction cascade, which in turn activates transcription factors that bind *prnp*. These results would further suggest that factors that would down regulate PrP^{c} expression could have a place in disease management.

Overall the findings presented here highlight the importance of the non-coding post promoter sequence in the control of PrP expression. The effect of the underlying cell line is shown to be a significant factor in baseline PrP expression as well as in the response to external stimuli. Cellular stress, induced by copper and DMSO, alter *prnp* activity producing an overall up-regulation of the gene, and ATRA also affects *prnp* activity with a down regulatory reaction. In addition, *prnp* appears to be able to influence its own expression, providing a potential therapeutic target for the control of disease progression. The control of *prnp* is highly complex, involving interaction of various gene domains with each other under the influence of the genetic control mechanisms of the underlying cell type.

4 Copper and PrP^c Internalisation

PrP^c is a cell surface protein, bound to the outer leaflet of the cell membrane by a GPI anchor. PrP^c is trafficked to the cell membrane via the exocytic pathway. First it is directed into the ER by the N-terminal signal peptide, folded, and modified by the addition of the sugar chains in the ER and through the golgi. The mature PrP^c is then transported to the cell surface (Nuziante *et al.*, 2002; Winklehofer *et al.*, 2003). At the membrane PrP^c is localised to lipid rafts (Mahfoud *et al.*, 2002; Brügger *et al.*, 2003).

The octameric repeat domain of the PrP^c N-terminus is able to bind four copper molecules, with a fifth copper binding site located adjacent, and C-terminal, to the repeat domain (Hornshaw *et al.*, 1995; Brown *et al.*, 1997; Hasnain *et al.*, 2001; Jackson *et al.*, 2001). Previous studies have shown that PrP^c is readily internalised from the cell membrane in response to 500 μM Cu, a reaction that was significant at concentrations as low as 200 μM Cu (Pauly & Harris, 1998; Lee *et al.*, 2001). However, although copper concentrations at the synapse can reach this high during depolarisation, this level of copper is at the peak of conditions found in normal metabolism. For a reaction to be considered relevant physiologically it would have to readily occur at much lower concentrations of copper (Vassallo & Herms, 2003). Perera and Hooper (2003) found internalisation would readily occur at 100 μM copper if applied as a chelate with histidine. Zinc (100 μM) has also been shown to internalise PrP, but 500 μM cobalt, manganese or iron had no effect on PrP^c localisation (Pauly & Harris, 1998).

Copper induced internalisation is abolished in the absence of the octameric repeat domain (Lee *et al.*, 2001). In addition, a disease-associated mutation of the octameric repeat domain (PG14) abolishes the copper induced internalisation response (Perera & Hooper, 2001). Since this mutation has nine extra octameric repeats inserted into the octameric repeat region, it may be that excessive copper binding is as detrimental to trafficking as the abolition of copper binding to this domain. The six most N-terminal amino acids of PrP^c have also been suggested to be essential for internalisation (Sunyach *et al.*, 2003).

The present study was concerned with the internalisation of PrP^c in response to copper. The effect of copper chelation on copper induced internalisation and the range of copper concentrations within which an internalisation reaction could be measured were considered to determine how likely the internalisation response was to occur under physiological conditions. To investigate the regions of PrP^c important for internalisation and normal cellular processing, domain deletion mutants of PrP^c were assessed for the ability to internalise. In addition the potential of PrP^c to internalise in response to other redox metals was evaluated.

4.1 Cellular Location of GFP-PrP^c and GFP-PrP^c Mutants

GFP-PrP^c wild type and domain deletion fusion constructs have been used throughout this investigation to assess the response of PrP^c to various stimuli. It was, therefore, important to confirm that the fusion constructs would be correctly processed and that presence of the GFP tag would not affect the metabolism of PrP^c. Incorrect processing would be likely to detrimentally affect the function of the construct. PrP^c is a GPI anchored cell surface glycoprotein. So to ensure GFP-PrP^c was correctly processed, it was first studied in the presence or absence of organelle probes, to ensure it was reaching the cell surface. The location of a GPI anchored GFP control was also determined. Following this, the GFP-PrP^c mutant constructs were observed to identify their localisation.

4.1.1 Location of GFP-PrP^c and GFP-GPI

Wild type GFP-PrP^c and null GFP-GPI constructs were transfected into F14 (PrP^c null cells) and stable cell lines established. Cells were observed by confocal microscopy under phase and FITC wavelength (excitation 488 nm, emission 530 nm) settings. The pattern of GFP localisation is shown in Figure 4.1.

Both the wild type GFP-PrP^c and the null GFP-GPI construct were expressed at the cell surface as shown by the GFP fluorescence following the cell membrane that is seen under the phase. Both constructs also showed a similar intracellular staining pattern. The apparent perinuclear clump is thought to be a region of recycling endosomes (Magalhães *et al.*, 2002), which may store GPI anchored proteins until they are needed at the cell surface.

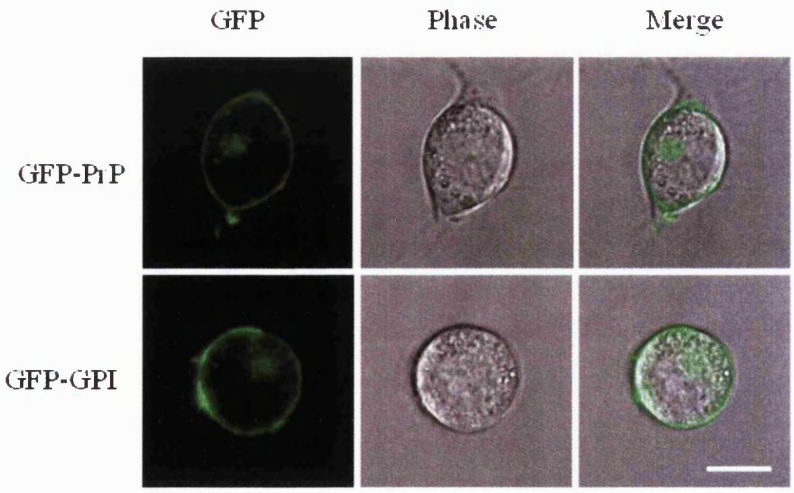

Figure 4.1 Localisation of GFP in cells expressing GFP-PrP^c or GFP-GPI constructs. The GFP-PrP^c and GFP-GPI constructs were transfected into F14 (PrP^c null mouse neuroblastoma fusion) cells, and stable cell lines established. Images were produced using a Zeiss LS 550 confocal laser scanning microscope and show a section through the cells. Cell surface localisation can be seen by the green fluorescence following the contours of the cell. Scale bar = 10 μm

To investigate further the intracellular distribution of PrP^c, live cell intracellular organelle probes were used to look for golgi apparatus, lysosomal, and mitochondrial localisation, and a plasmid with ER direction and retention sequences (pDsRed-ER) was used to look for ER localisation. The results are shown in Figure 4.2.

Both the GFP-PrP^c and GFP-GPI constructs showed low levels of localisation in the ER and golgi. This represents constant production and trafficking through the exocytotic pathway to the cell surface, consistent with normal protein turnover. Consistent with the cell membrane localisation of PrP^c, no co-localisation is seen with the mitotracker probe. A difference between the GFP-PrP^c and GFP-GPI cell lines is seen with the lysotracker probe. A higher level of co-localisation of the GFP-GPI construct is seen with the lysotracker probe than for the GFP-PrP^c construct. This is due to PrP^c being degraded primarily by the proteosome, as opposed to the lysosome to which most GPI anchored proteins are targeted.

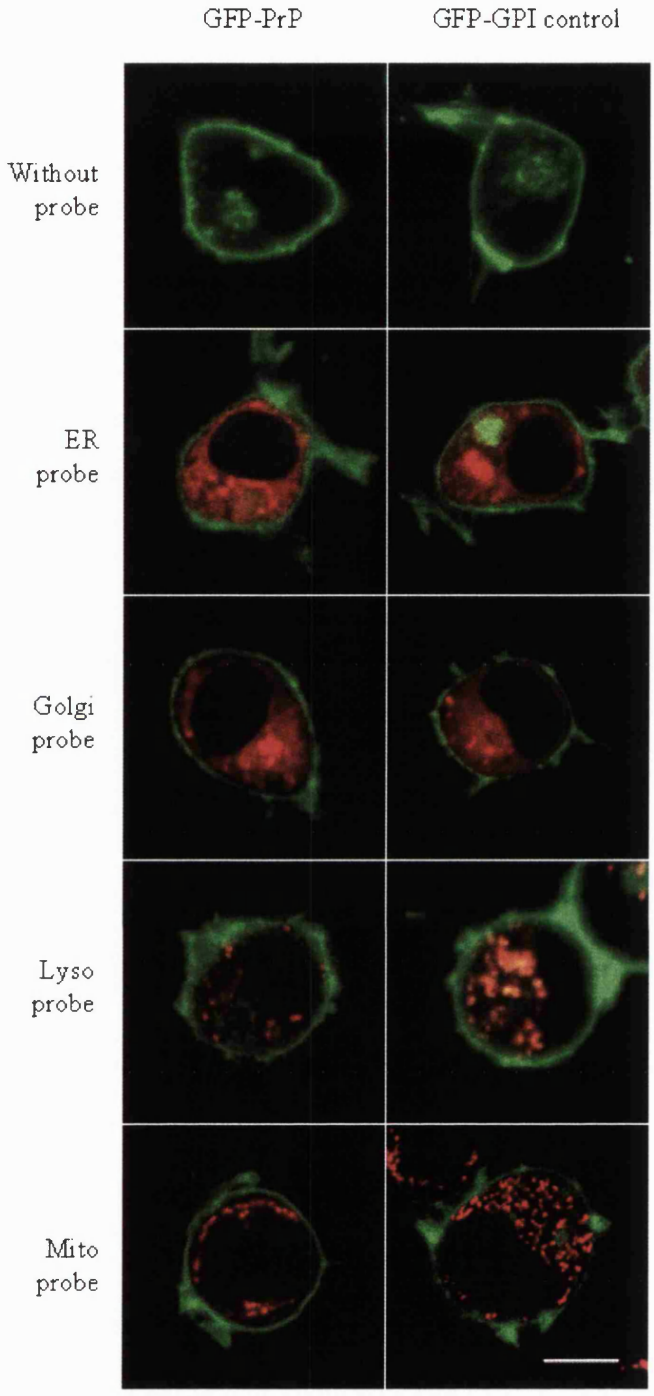

Figure 4.2 Cellular localisation of GFP signal in GFP-PrP^c and GFP-GPI expressing cells. F14 cells stably transfected with the GFP-PrP^c and GFP-GPI constructs were incubated with a sphingolipid golgi probe, and Lyso-Tracker® Red and Mito-Tracker® Red organelle probes to look for co-localisation with the GFP signal. ER localisation was probed using co-transfection with the pDsRed-ER plasmid (Clontech). Scale bar = 10 μm.

4.1.2 Cellular Location of Mutant PrP^c Constructs

The cellular localisation of the deletion mutants was determined as described for the GFP-PrP^c and GFP-GPI constructs.

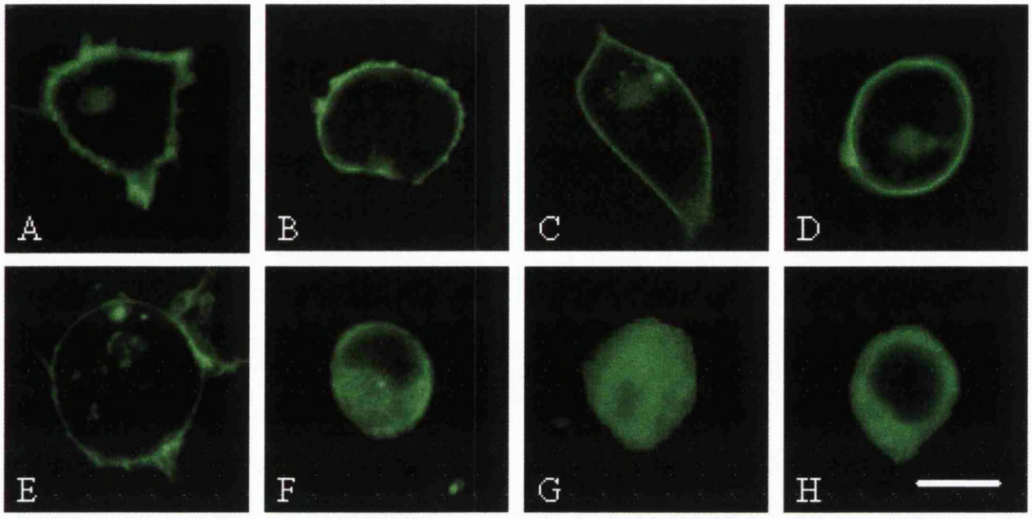

Figure 4.3 Cellular location of A) GFP-PrP^c, and PrP^c mutants B) Δ23-38, C) Δ51-89, D) Δ67-89, E) Δ112-119, F) Δ112-136, G) Δ122-146, H) Δ135-150. GFP-PrP^c and GFP-PrP^c mutant constructs were transfected into F14 cells and stable cell lines established. Pictures of GFP localisation were captured using a Zeiss LS 550 confocal microscope. Mutants B-D show cell surface localisation in the same pattern as that of GFP-PrP^c, mutant E also reaches the cell surface but shows some intracellular retention, and mutants F-H are fully retained inside the cell. Scale Bar = 10 μm.

The N-terminal deletion mutants (Δ23-38, Δ51-89, Δ67-89) were localised to the cell surface following the same pattern as the wild type GFP-PrP construct (see Figure 4.3). The Δ112-119 deletion mutant was also localised to the cell surface but showed slightly higher retention inside the cell, as seen by the presence of green vesicles inside the cell. This is a result of increased direction to the lysosomes compared to the wild type (Figure 4.4). In contrast, the C-terminal deletion mutants (Δ112-136, Δ122-146, Δ135-150) did not reach the cell surface and the green fluorescence was confined to the inside of the cell (Figure 4.3). When the cells were incubated with organelle probes, the internally localised mutants were shown to co-localise to the ER (Figure 4.4). The merging of the fusion construct GFP signal with the red fluorescence of the pDsRed-ER probe demonstrating ER localisation is shown for each of the internals mutants in figure 4.5.

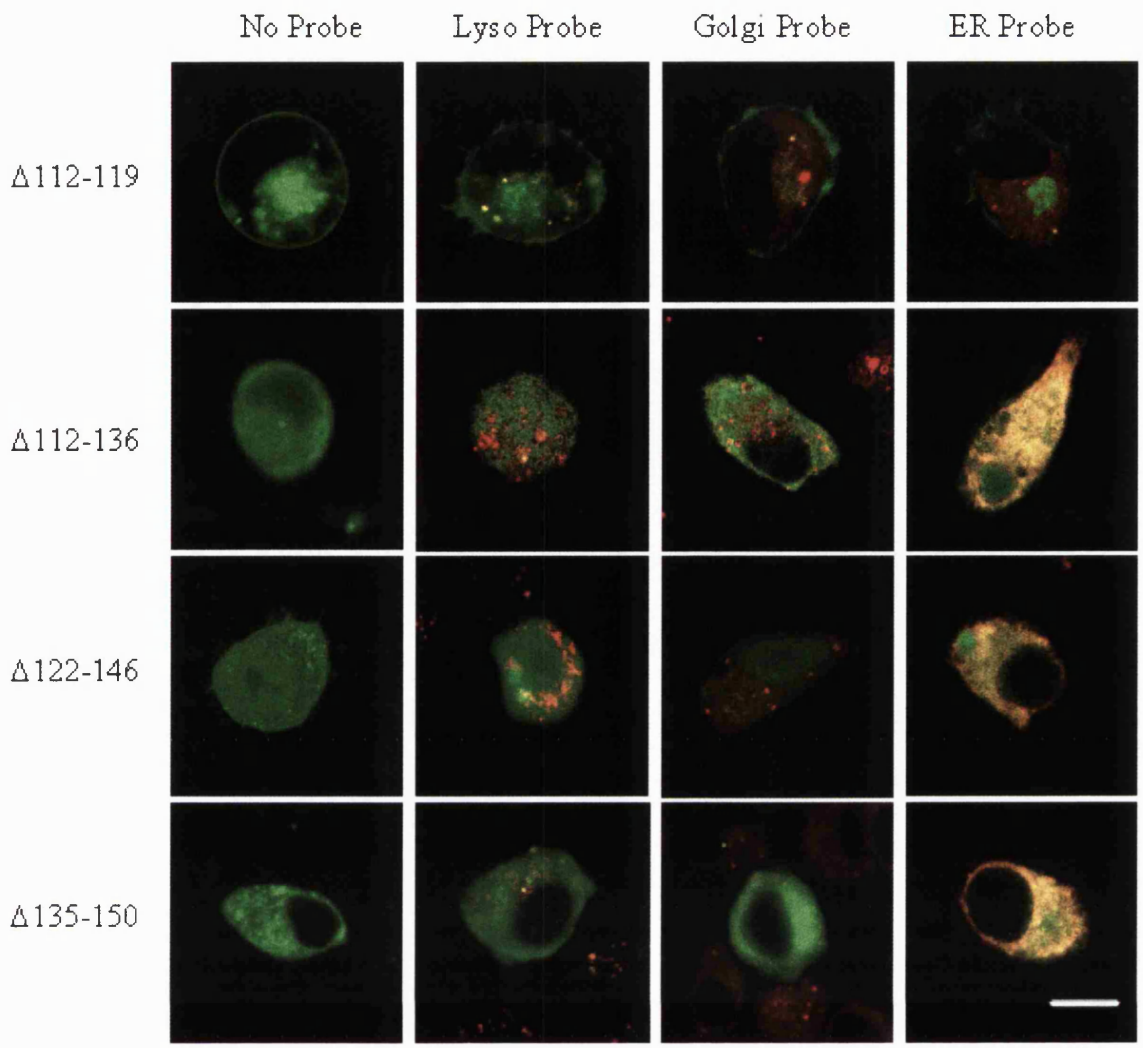

Figure 4.4 Localisation of PrP^c mutant constructs that show retention inside the cell. The stable cell lines established with the mutant constructs Δ112-119, Δ112-136, Δ122-146, and Δ135-150 show internal localisation, which is different from the cell surface localisation of wild type GFP-PrP^c. These cell lines were incubated with the sphingolipid golgi probe, lyso-Tracker® Red, and Mito-Tracker® Red probes to determine where the GFP was expressed. ER localisation was determined by transient co-transfection of the plasmid containing the mutant PrP^c with pDsRed-ER. Images were captured using a Ziess LS 550 confocal microscope. The Δ112-119 mutant shows a slight co-localisation to the lysosomes and the remaining three mutants show co-localisation with the ER probe as seen the orange-yellow staining of the cells where the two probes merge. Scale bar = 10 μm.

ER retention of the C-terminal deletion mutants may have occurred for a variety of reasons. The removal of this region may have removed a binding site for the chaperones that move PrP^c through the secretory pathway to the cell surface, so preventing its correct transport. Alternatively, the removal of these amino acids may have caused the protein to misfold resulting in ER retention due to redirection of the mutants into the ER Associated Degradation (ERAD) pathway. Since these mutations are within the structured C-terminus

of the protein, and specifically around the hydrophobic region, which is located inside of the protein, it is likely that the protein is not maintained as strongly in its correct conformation as the wild type due to the weakening of the bonds that maintain this conformation. Regions of the hydrophobic domain are likely to be located in the interior of mature protein resulting in their amino acid sequences being inaccessible to chaperones, suggesting that the second proposed internal localisation theory is most likely.

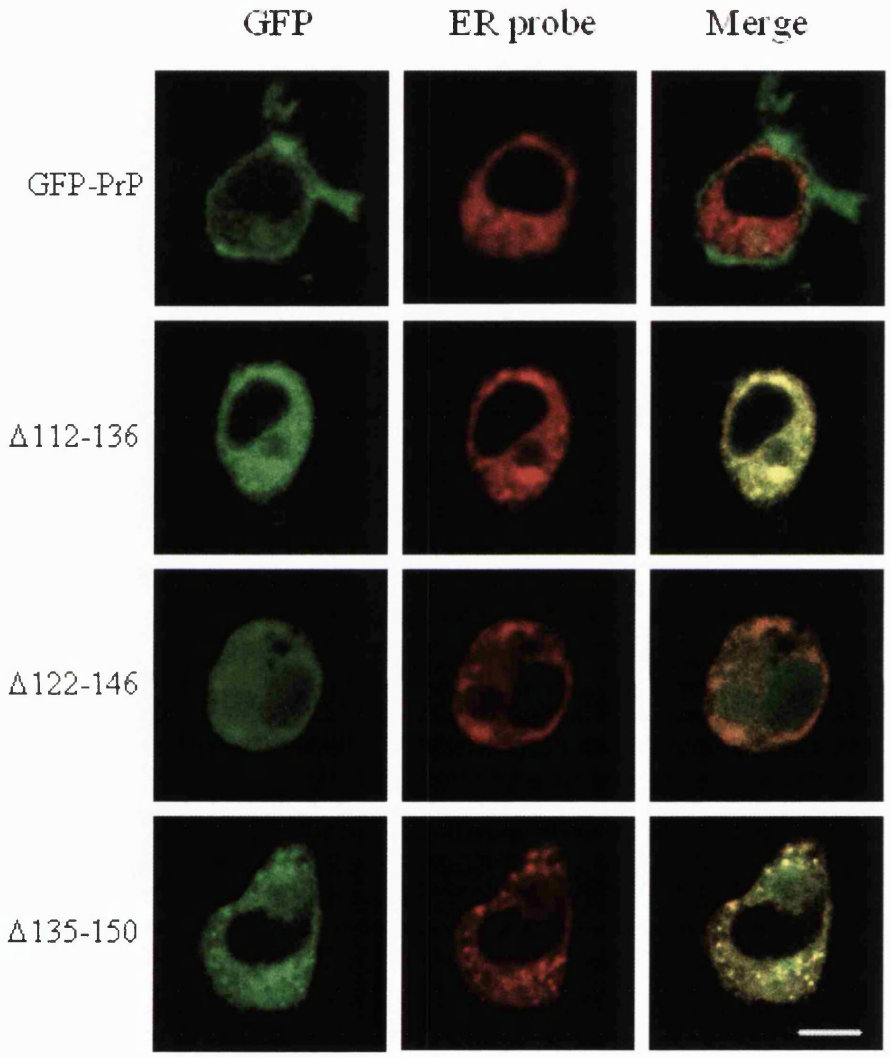

Figure 4.5 ER localisation of internal PrP^c mutant constructs. F14 cells were transiently co-transfected with GFP-PrP^c, or with the internally retained Δ112-136, Δ122-146, or Δ135-150 constructs, and with the ER probe pDsRed-ER. The individual GFP and DsRed channels are shown along with the merged pictures. Co-localisation of the internal mutants can be seen by the overlap of the green and red signals producing a yellow signal. Scale bar = 10 μm.

4.2 Copper and PrP^c Trafficking

Copper is bound by the octameric repeat domain within the N-terminus of PrP^c. Previously, it has been shown that high exogenous concentrations of copper cause PrP^c to move away from the cell surface. However the concentrations reported were 200-500 μM, which are of limited relevance physiologically. When applied as a chelate with histidine, internalisation has been reported at concentrations as low as 100 μM copper (Perera & Hooper, 2001), suggesting that this reaction is of physiological relevance. The aims of this study were first to confirm that copper internalises the GFP-PrP^c construct but not the GFP-GPI control, and second to determine the if lower copper concentrations would significantly internalise PrP^c to confirm the physiological relevance of this reaction.

4.2.1 Copper, Glycine, and PrP^c Internalisation

Copper is rarely found in its free, unbound form in physiological systems. Copper in the blood or extracellular fluid is transported bound to proteins such as ceruloplasmin, ferritin and albumin, thus protecting the cells within the system from its potentially toxic effects. To reproduce the effect of bound copper glycine was premixed with $CuSO_4$ in a 1 $CuSO_4$: 4 Glycine molar ratio (Cu-4xGly). Glycine binds copper but with low enough affinity to readily release it to amino acids with stronger affinity such as the histidines found in the copper binding octarepeat domain of PrP^c. The assays were carried out on stably transfected F14 GFP-PrP^c and GFP-GPI cells, using the mixed population to allow expression levels to be considered. Live cells were cultured in chambered cover slips and incubated in OptiMEM serum free and phenol red free media. Reagent was added at time 0, cellular response to the reagent were observed by confocal microscopy, and images were captured at time 0, 10 minutes and 2 hours. Internalisation of PrP^c was measured by the change in cell surface intensity of the GFP signal.

A concentration of 500 μM $CuSO_4$ significantly increased the internalisation of PrP^c after 10 minutes exposure (see Figure 4.5). This reaction was also significant at 100 μM $CuSO_4$ after 2 hours exposure. However, as previously stated, free copper is not usually found in physiological systems so copper complexed to glycine was used to replicate the effect of chelated copper. Using the pre-mixed Cu-4xGly, 100 μM Cu produced a more rapid reaction than the 500 μM $CuSO_4$. This indicates that copper may be more effectively delivered into PrP^c when it is chelated, thus causing a greater reaction. 400 μM glycine on

its own had no significant effect on PrP^c. No effects of any of the tested reagents were seen on the GFP-GPI construct, with cell surface fluorescence remaining constant throughout all the treatments and time points. The lack of response of the GFP-GPI construct eliminated the possibility of a non-specific internalisation effect or metal quenching of the GFP at the cell surface.

To eliminate the possibility that the internalisation is an effect of over expression, the percentage change in fluorescence was plotted against the time 0 intensity to look for trends. No trends caused by the over expression of PrP^c were found (figure 4.7). The implication is that the effect of copper on GFP-PrP^c cells is not a result of over expression of PrP^c.

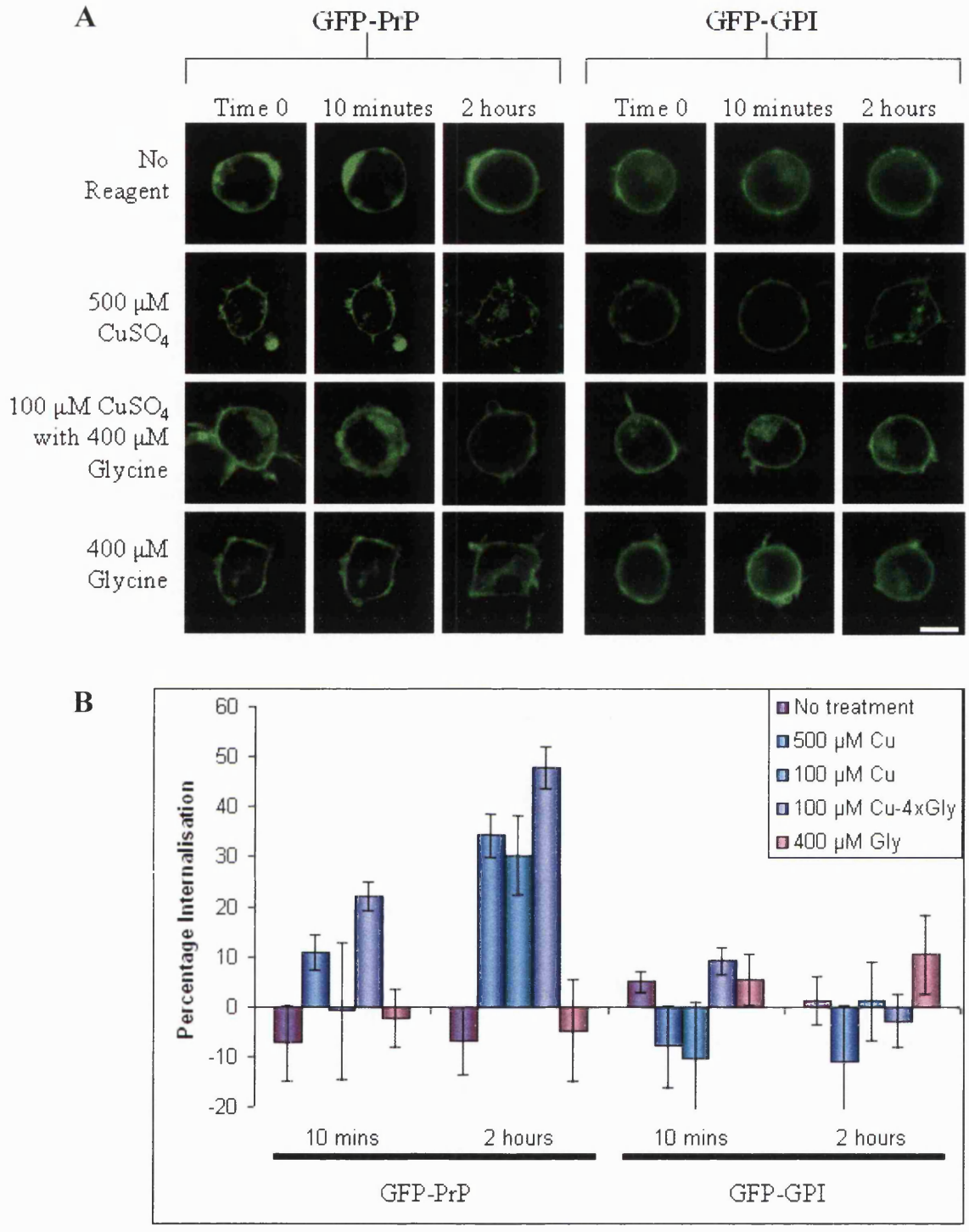

Figure 4.6 Copper and copper glycine trafficking of GFP-PrP^c and GFP-GPI cells. A) shows individual cell responses at time 0, 10 minutes and 2 hours after addition of reagent. Scale bar =10 µm. B) shows the percentage internalisation compared to the fluorescence measured by recording GFP intensity at the cell surface at time 0. Significant internalisation is seen for the GFP-PrP^c construct in response to 100 µM $CuSO_4$ (after 2 hours), 500 µM $CuSO_4$ and 100 µM Cu-4xGly ($F = 6.04$, $p < 0.001$). Shown are the mean and SEM. n = min 12, max 22 cells.

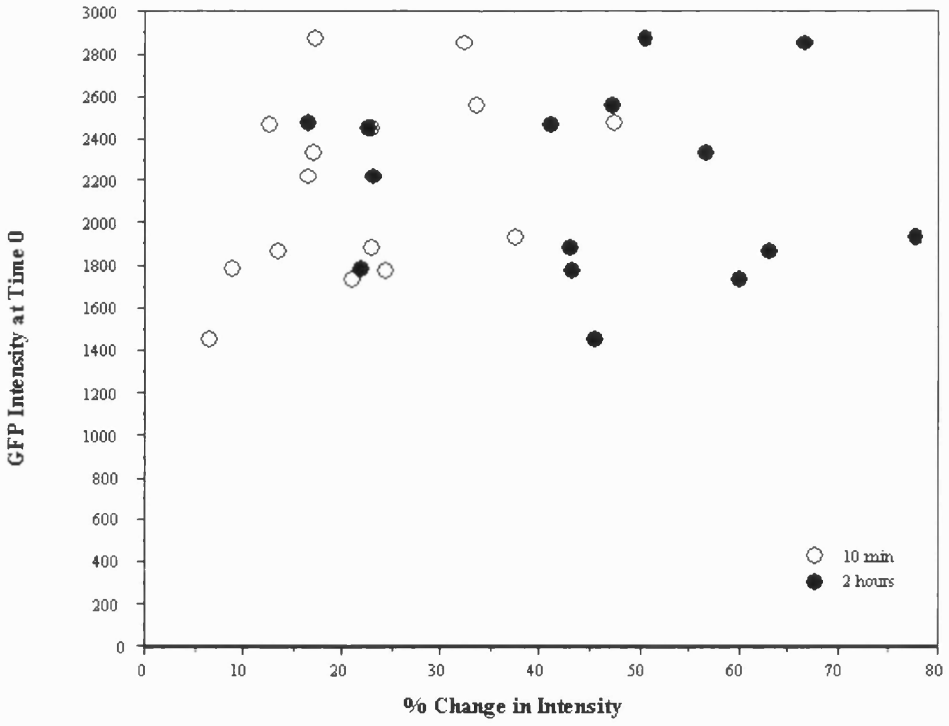

Figure 4.7 Effect of expression levels on internalisation response. Difference at 10 minutes (open circles) and 2 hours (black circles) between cells treated with 100 μM $CuSO_4$ with 4x glycine compared to raw intensity at time 0. The spread of data points in this plot shows that the rate of internalisation in response to copper is not influenced by the expression level of the cell.

4.2.2 Copper Dose Response

The difference in the rate of internalisation when using 100 μM Cu-4xGly as opposed to 100 μM Cu alone is pronounced, but this concentration of copper is at the higher end of concentrations that may be relevant physiologically. An internalisation reaction at 100 μM Cu could only occur at a significant rate during depolarisation of the neurone. At the synapse copper concentrations can reach 300 μM on depolarisation. However, resting concentrations are more like 15 μM and there is a blood exchangeable level of 8 μM (Kramer *et al.*, 2001; Vassallo & Herms, 2003). For a reaction to be physiologically significant it would have to be readily proceeding within these limits. Therefore, further assays were carried out as above with lower copper concentrations (5, 20, and 50 μM Cu-4xGly).

The dose-response curves (figure 4.8) show that in 10 minutes there is a significant internalisation response to 20 μM Cu-4xGly ($F = 7.21$, $p < 0.001$) and after 2 hours this

response is significant at levels as low as 5 μM Cu-4xGly ($F = 14.09$, $p < 0.001$). This indicates that, as copper levels at the synapse spike during depolarisation, the rate of internalisation of PrP^c would rise significantly. Under the normal range of copper in the extracellular fluid copper induced internalisation would occur but at a slower rate.

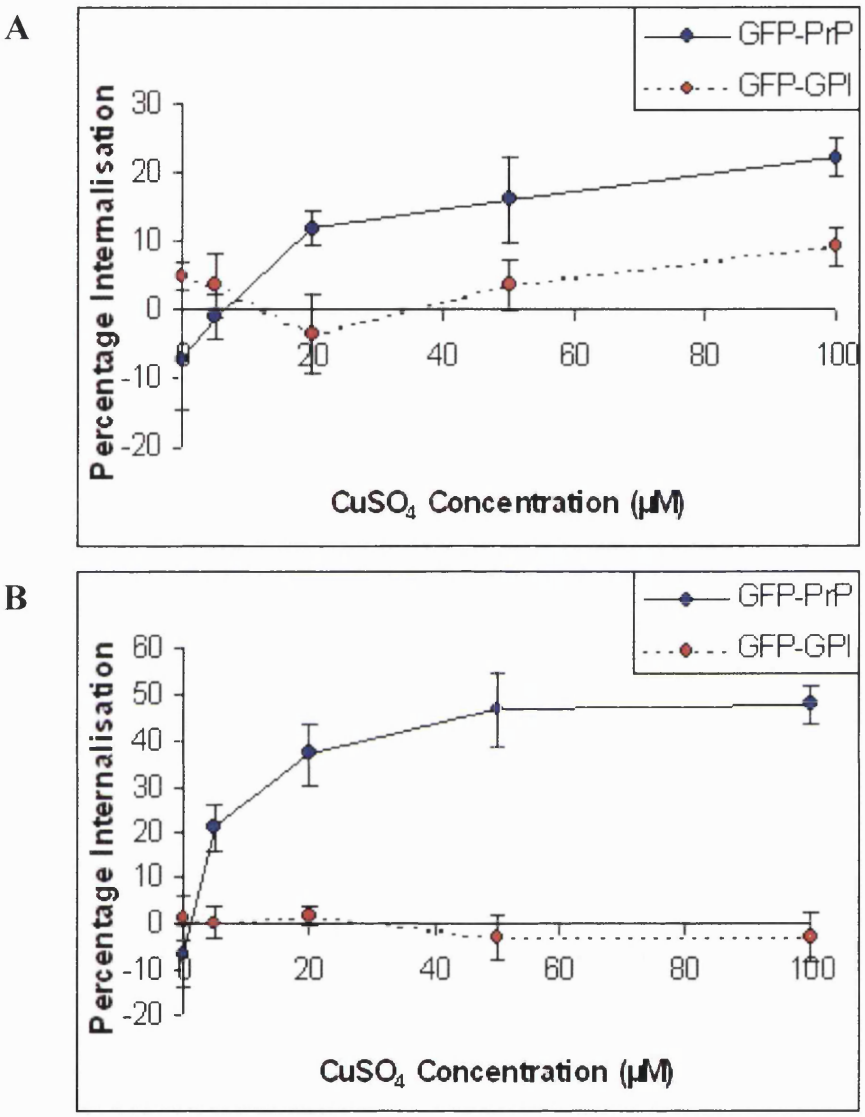

Figure 4.8 Dose response curves for Cu treatment of cells expressing GFP-PrP^c and GFP-GPI. Cells were treated with 5 μM, 20 μM, 50 μM or 100 μM Cu-4xGly. Percentage Internalisation, measured as decrease in GFP signal compared to that at time 0, is shown for the GFP-PrP^c and GFP-GPI cell lines at (A) 10 minutes and (B) 2 hours. Shown are the mean and S.E.M. n = 18 cells.

4.3 The Destination of Copper Internalised PrP^c

Internalisation of PrP^c has been measured in this study by the decrease in GFP signal at the cell surface. However, as the signal is internalised, it decreases, making the determination of its destination difficult. The destination of the internalised PrP^c was investigated by indirect immunofluorescence. This method allowed for the assessment of PrP^c levels in acidic organelles where GFP fluorescence may be quenched.

F14 cells were stably transfected with pcDNA-PrP(m), a mammalian expression vector containing a DNA insert encoding murine PrP^c without the GFP reporter. The transfected cells were cultured on coverslips. Cells were treated for 10 minutes or 2 hours with 100 μM Cu, Cu-4xGly, Gly only, or were left untreated, before fixing and staining PrP^c with a FITC antibody probe. Cu-4xGly treated cells showed a vesicular pattern emerging inside the cell, while the signal of PrP at the cell membrane was decreased and not as smooth and continuous as the untreated cells (Figure 4.9). The glycine only treated cells showed the same pattern throughout. This indicates that the internalised PrP^c was being directed into acidic vesicles, most probably early endosomes, where the reduced pH may have resulted in quenching of the GFP signal in the GFP-PrP^c cells.

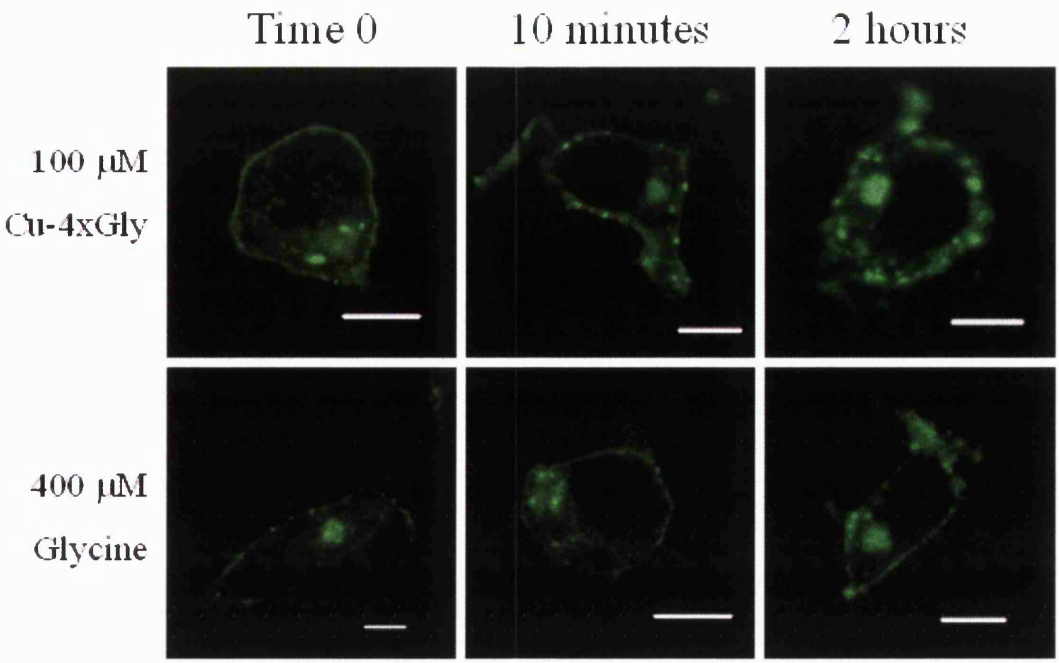

Figure 4.9 Indirect immunofluorescence staining of PrP^c in F14 cells. F14 cells were transfected with pcDNA 3.1 PrP^c. PrP^c was detected using the rabbit DR1 primary antibody directed against amino acids 89-103 of the PrP^c sequence, and visualised with a secondary FITC conjugated anti rabbit antibody. Images were captured using a Zeiss LS 550 confocal microscope using excitation and emission wavelengths of 488 nm and 530 nm respectively. Shown are untreated cells representing localisation at time 0, and cells treated for 10 mins and 2 hours with 100 μM Cu-4xGly or 400 μM glycine. Internalisation is seen in the PrP^c expressing cells by the development of a punctuate pattern as the PrP^c moves from the cell surface into endocytic vesicles. Scale bar = 10 μm.

It was also possible that the reduction in PrP^c at the cell surface was due to PrP^c being shed or cleaved from the cell surface. Matrix metalloproteinases (MMPs) may be activated by Cu and these have previously been shown to cleave PrP^c when activated (Parkin *et al.*, 2004). As a result part of the loss of the signal may have been due to the loss of the N-terminal domain (containing the GFP signal) into the surrounding media due to cleavage. Since some GFP could be seen inside the cell this would be occurring alongside the internalisation reaction. To investigate the destination of PrP^c, extracts from cells that were cultured in OptiMEM and incubated for 2 hours untreated, treated for the whole 2 hours or for only the final 10 minutes with 100 μM Cu4xGly were collected. Native PAGE gels were run, GFP intensity measured using a phosphorimager at GFP wavelengths (excitation 488 nm and emission 530 nm), and proteins were transferred onto a nitrocellulose membrane. Membranes were blotted for PrP^c levels using an antibody that detected a C-terminal epitope of PrP^c. Following blotting, membranes were stripped and

tubulin immunodetected. Quantification was made with respect to tubulin as a loading control (figure 4.10).

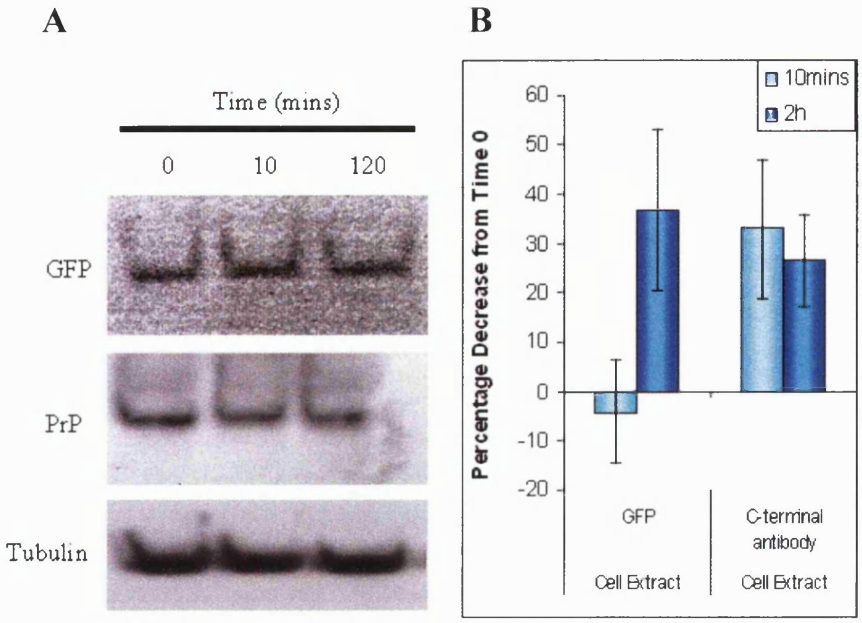

Figure 4.10 Total PrP^c levels in F14 cells following 100 µM Cu-4xGly treatment. (A) Western blots of F14 GFP-PrP^c cells treated with 100 µM Cu-4xGly. Protein was extracted from the cells at 10 minutes and 2 hours, and untreated cells were used as time 0 controls. Samples were electrophoresed on a 12% native acrylamide gel. GFP signal was detected using a phosphorimager and PrP^c or tubulin detected by western blot. n = 3. (B) Blots were scanned and band intensities quantified by densitometry. Direct linear ANOVA was used to look for differences in the trend of detection of GFP and PrP^c C-terminus in the cell extract. No significant difference was seen (F=0.53, p=0.469, n=3). Shown are the mean and S.E.M.

The measured GFP and PrP^c signals showed a decrease in total signal, however this response was variable and is not statistically significant. Whilst the decrease in signal suggests there may increased turnover of PrP^c or loss into the media (Figure 4.10), the lack of significance requires further investigation be made. Therefore the GFP and PrP^c levels in the medium surrounding the cells was analysed.

To investigate the potential loss of PrP^c into the surrounding media, the medium from the above experiments was collected at the time of harvesting the cells, spun to collect the protein and the protein pellet separated by native PAGE as for the cells extracts. Quantification of GFP and PrP^c in the media extracts was made with respect to the total cell number plated. The intensities measured showed a decrease of both PrP^c and GFP in

the media, which was returned almost to normal levels by the addition of protease inhibitors (Figure 4.11). This would suggest that extracellular proteases are activated by the increased exogenous copper resulting in higher degradation of PrP^c expelled in to the media, but that there is no significant change to the quantity of PrP^c secreted or released by cleavage into the media.

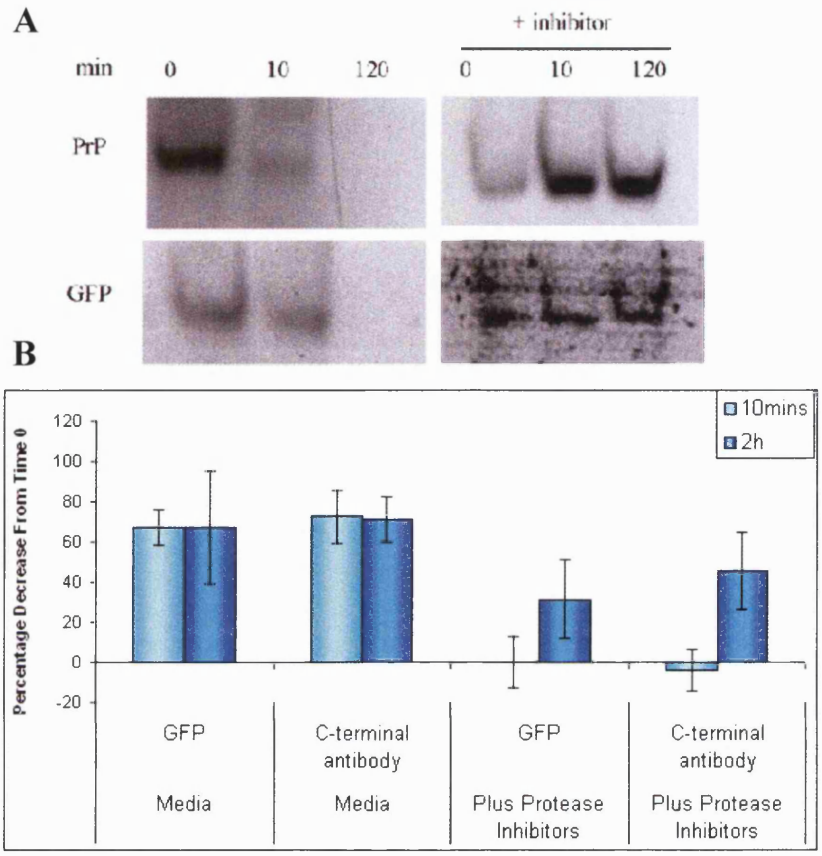

Figure 4.11 Protease inhibition of PrP^c degradation in culture medium. (A) F14 GFP-PrP^c expressing cells treated with 100 μM Cu-4xGly, in the presence and absence of protease inhibitors, 2 mM PMSF and 1 mM benzamidine. Extracts were prepared at time 0, 10 minutes and 2 hours after treatment with Cu. Following native PAGE, GFP was detected using a phosphorimager and PrP^c detected by western blotting. (B) Quantification of the blots. Two-sample *t* tests were used to look for significant differences between the Cu experiments carried out with/without the protease inhibitors present. The media harvested from the Cu only treated cells shows a significant decrease in the detected of either GFP or PrP ($F = 3.88$, $p = 0.039$). Following protease inhibition treatment significant differences were seen in comparison to untreated samples for both the GFP ($t = 3.24$, $p = 0.048$) and the PrP^c detection ($t = 10.78$, $p = 0.002$). Neither the GFP or the PrP detected was significantly decreased in the media after protease inhibition. Shown are the mean and S.E.M. $n = 3$.

4.4 PrP^c Functional Regions and Copper Internalisation

Copper binds to the octameric repeat domain and the absence of this domain abolishes copper induced internalisation (Lee *et al.*, 2001). In addition the N-terminal domain following the signal peptide, specifically amino acids 23-28, is thought to be essential for PrP^c trafficking (Nunziante *et al.*, 2003). To investigate more fully the domains of PrP^c important for internalisation several mutant constructs were employed. Deletions, shown in figure 2.1, included the far N-terminus of the mature protein (Δ23-38), the octameric repeat region (Δ51-89), most of the octameric repeat region but leaving one complete repeat intact (Δ67-89), the palindromic region (Δ112-119), and three mutations of the hydrophobic domain (Δ112-136, Δ122-146, Δ135-150). The stably transfected mutant cell lines were exposed to 100 μM Cu-4xGly. This concentration was chosen since it provides the maximal response to copper (see figure 4.7), and so it is likely that a decreased response should not be overlooked due to too low a concentration being used. Internalisation could only be measured in those mutants that were expressed at the cell surface. However the internal mutants were observed under the same conditions to look for any response.

4.4.1 Cell Surface Mutants and Copper

As previously reported, removing the octameric repeat region completely abolished internalisation (Figure 4.12 and 4.13b). After 2 hours the Δ51-89 mutant showed increased GFP signal at the cell surface. Such an increase may be due to the cell mobilising the PrP^c to the surface in an attempt to deal with the copper insult. This indicates that for copper induced internalisation of PrP^c, copper binding to the octameric repeat domain is more significant than that binding to the fifth site. The Δ67-89 mutant demonstrated reduced ability to internalise compared to the wild type but it did significantly internalise. This shows that just one octameric repeat is required for this reaction to proceed, although not fully, and further emphasizes the importance of the octameric repeat domain for copper induced internalisation. The Δ23-38 N-terminal deletion mutant was expected not to react to copper. However it did internalise significantly, with a rate equalling that shown by the Δ67-89 mutant. Therefore copper binding to the octameric repeat region overrides the role of this region in internalisation. The final cell surface mutant, Δ112-119, lacking the palindromic region thought to be a cleavage site, showed no internalisation in response to copper. This was unexpected, and shows for the first time that this region is involved in

copper induced internalisation. PrP^c may need to be cleaved before it can internalise, or alternatively, this region may directly react with Cu or the octameric repeat region to induce internalisation.

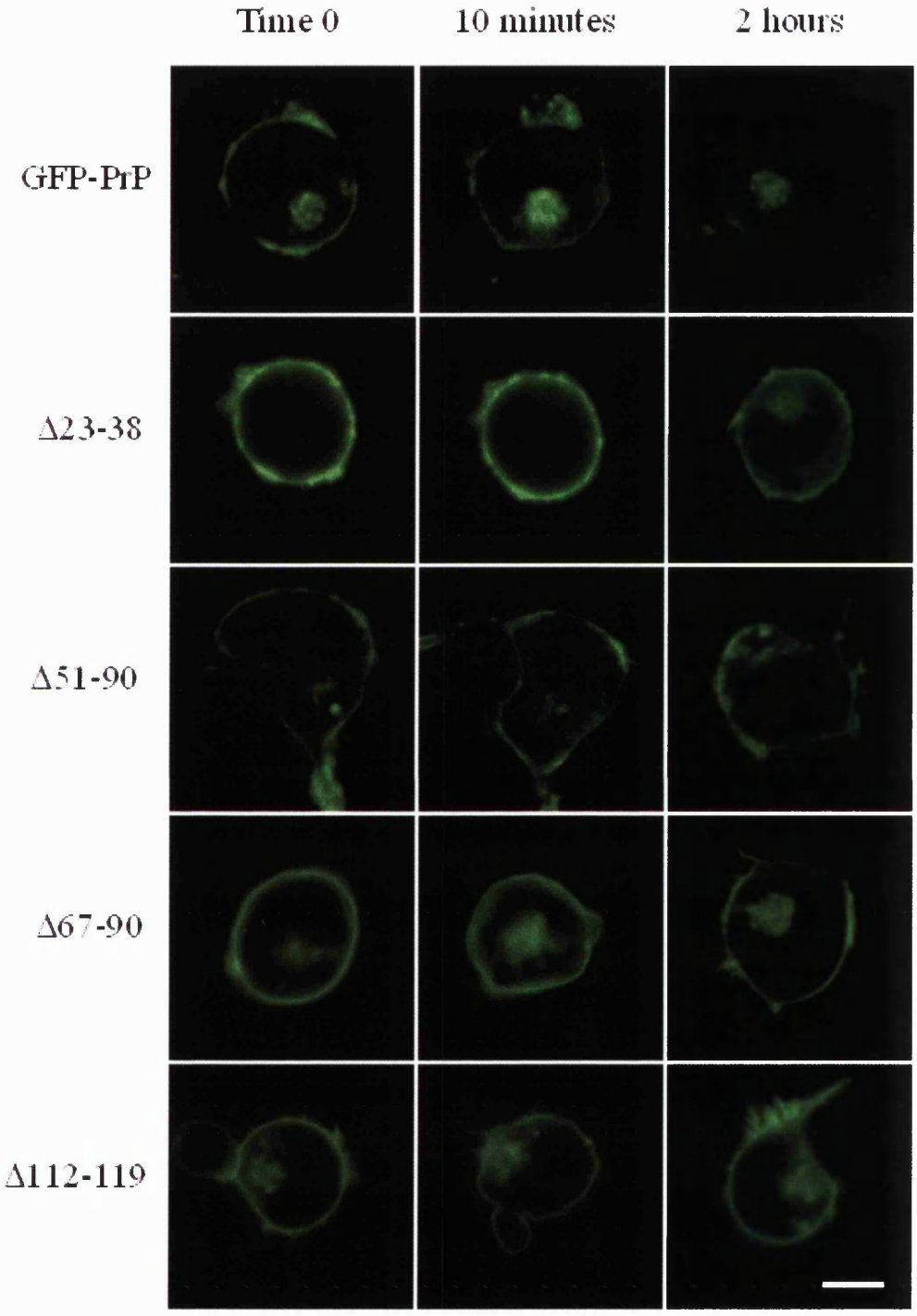

Figure 4.12 Change in wild type and mutant GFP-PrP^c cell surface expression following Cu treatment. Cells were treated with 100 μM Cu-4xGly, and images captured using a Zeiss LS 550 confocal microscope at time 0, 10 minutes, and 2hours. Shown are individual F14 cells expressing either GFP-PrP^c, or GFP-PrP^c mutants Δ23-38, Δ51-89, Δ67-89, or Δ112-119. Significant internalisation was seen as a decrease in membrane intensity of the GFP signal for the Δ23-38 and Δ67-89 mutants but not for the Δ51-89 and Δ112-119 mutants. Scale bar = 5 μm.

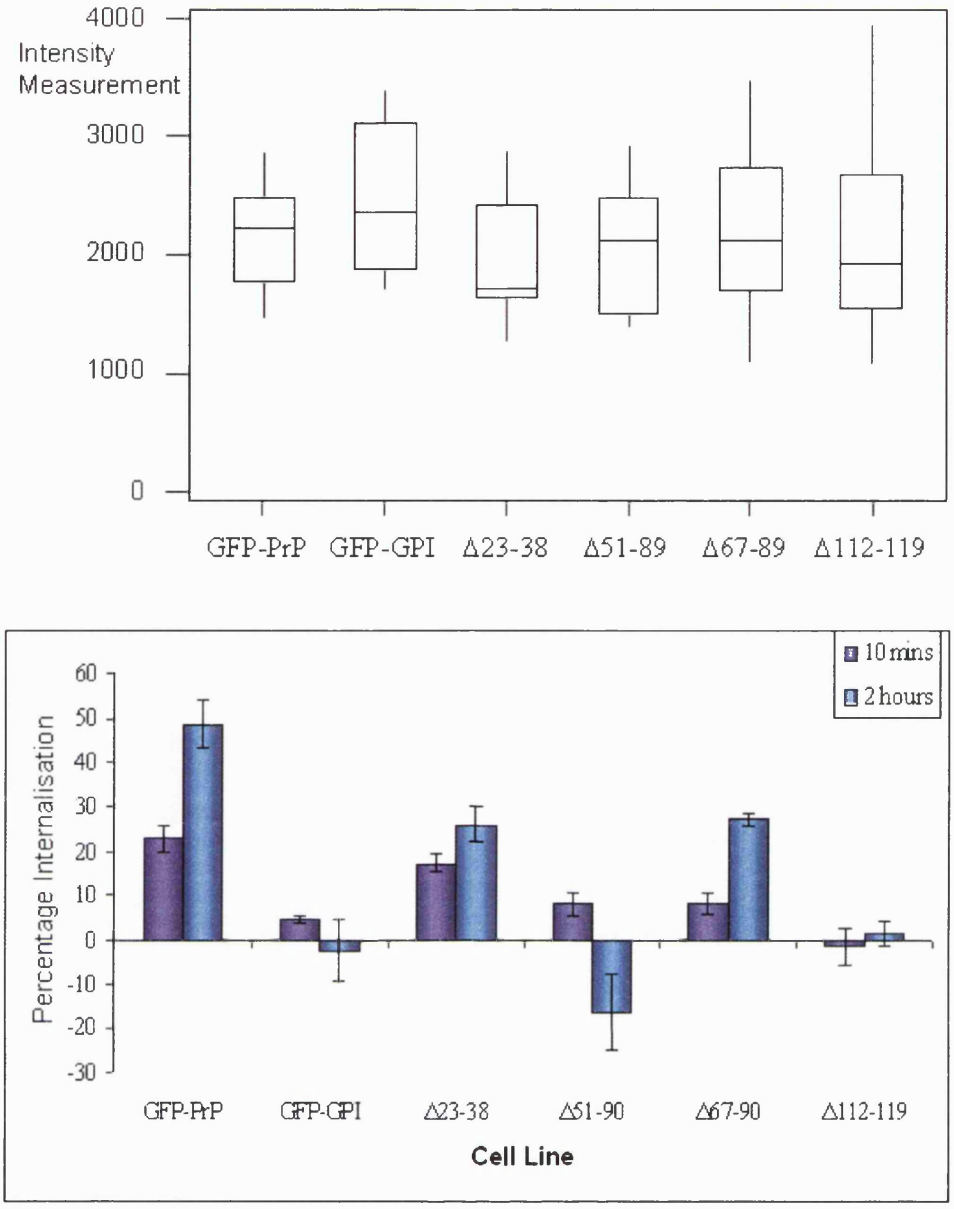

Figure 4.13 Effect of mutations on basal GFP expression levels and response to Cu. (A) Boxplot of basal expression levels of each of the membrane localised constructs. The box represents the mean and inter-quartile range. One-way ANOVA was used to test for significant differences in basal expression of the constructs; no significant difference is seen (F = 1.14, p = 0.346). (B) The percentage internalisation, compared to the time 0 membrane intensity, of each of the membrane localised mutant constructs compared to the GFP-PrP^c and GFP-GPI cell lines. Significant internalisation is seen for the Δ23-38 and Δ67-89 cell lines compared to the GFP-PrP^c and GFP-GPI cell lines (F = 21.26, p <0.001, n = min 12, max 18), but not for the Δ51-89 and Δ112-119 cell lines. The Δ51-89 mutant is seen to increase at the cell surface. Untreated and glycine treated controls showed no significant difference to basal expression (shown in appendix C).

Based on the evidence of previous studies (Nunziante *et al.*, 2003), the deletion of the far N-terminus was expected to abolish internalisation, but this was not seen. To confirm this, immunofluorescent staining was carried out on cells expressing a PrP^c construct containing the same mutation but without the GFP tag (Figure 4.14). This showed that this mutation does have a pronounced effect on trafficking but that it is trafficking to the cell surface rather than away from it that is most affected. PrP^c minus the N-terminus still locates to cellular membranes but predominantly those inside the cell, including the nuclear membrane, which can be seen clearly by the perinuclear staining. Since this mutant appears not to be trapped in the ER in the same way as the C-terminal deletion mutants, it is likely that it is not retained in the cell to be directed into ERAD. Instead it may lack a region where chaperones that are involved in the movement of PrP through the cell to the cell surface would normally bind. In the GFP tagged model, there may be sites within GFP that are in some way able to compensate for this, or the cell surface expression may be clearer due to the more acidic pH of internal organelles quenching the GFP signal.

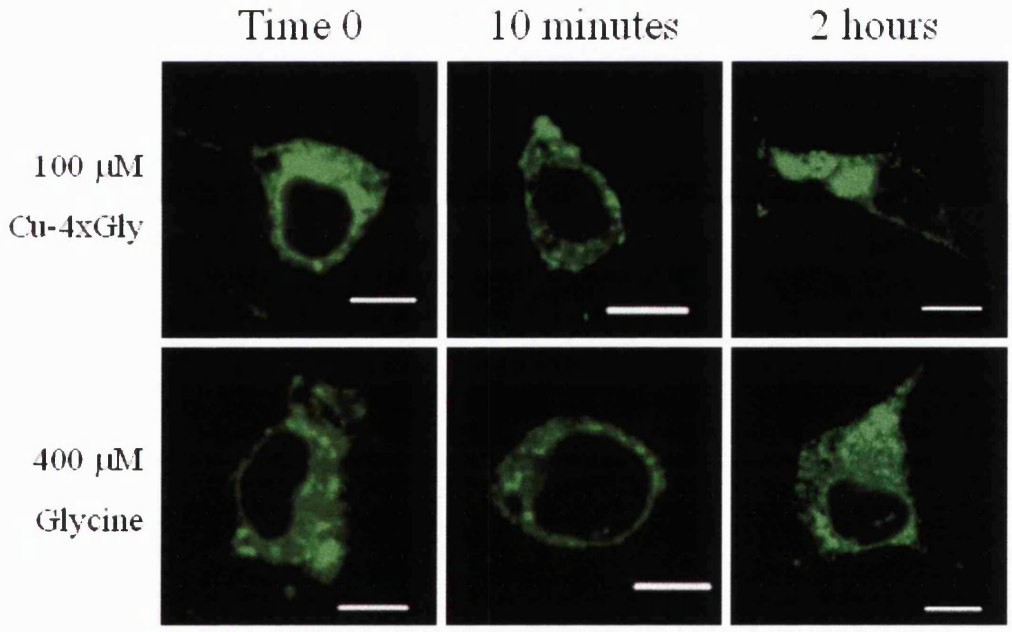

Figure 4.14 Immunofluorescent staining of F14 cells expressing pcDNA-3.1 PrP(m)Δ23-38. F14 cells were transfected with pcDNA 3.1 PrP^c. PrP^c was detected using the rabbit DR1 primary antibody directed against amino acids 89-103 of the PrP^c sequence, and visualised with a secondary FITC conjugated anti rabbit antibody. Images were captured using a Zeiss LS 550 confocal microscope using excitation and emission wavelengths of 488 nm and 530 nm respectively. Shown are untreated cells representing localisation at time 0, and cells treated for 10 mins and 2 hours with 100 µM Cu-4xGly or 400 µM glycine. An internal staining pattern is seen by the localisation of the FITC signal inside the cell. Scale bar = 10 µm.

4.4.2 Internal Mutants and Copper

The Δ112-136, Δ122-146, and Δ135-150 mutants are predominantly located in the ER. Basal intensity is not significantly different between the cell lines ($F = 0.51$, $p = 0.482$). However, the signal is much lower at the cell surface than inside the cell (figure 4.16b). The cell surface signal measured may be due to PrP^c in organelles next to the cell surface rather than PrP^c expression at the membrane. To see if these mutants would show any response to Cu treatment, cells were treated as for the cell surface mutants and readings were taken from both the cell surface and the interior. No change in the location or the intensity of the GFP signal was observed for any internal mutant following copper treatment (Figure 4.15 and 4.16b), although a slight decrease in membrane intensity was seen for the Δ112-136 mutant, which is most likely to be an artefact of the very low intensity of GFP at the surface. It is likely that even if the externally applied copper reaches the mutant protein and becomes incorporated, it is still targeted for destruction and so does not move from its position in response to copper.

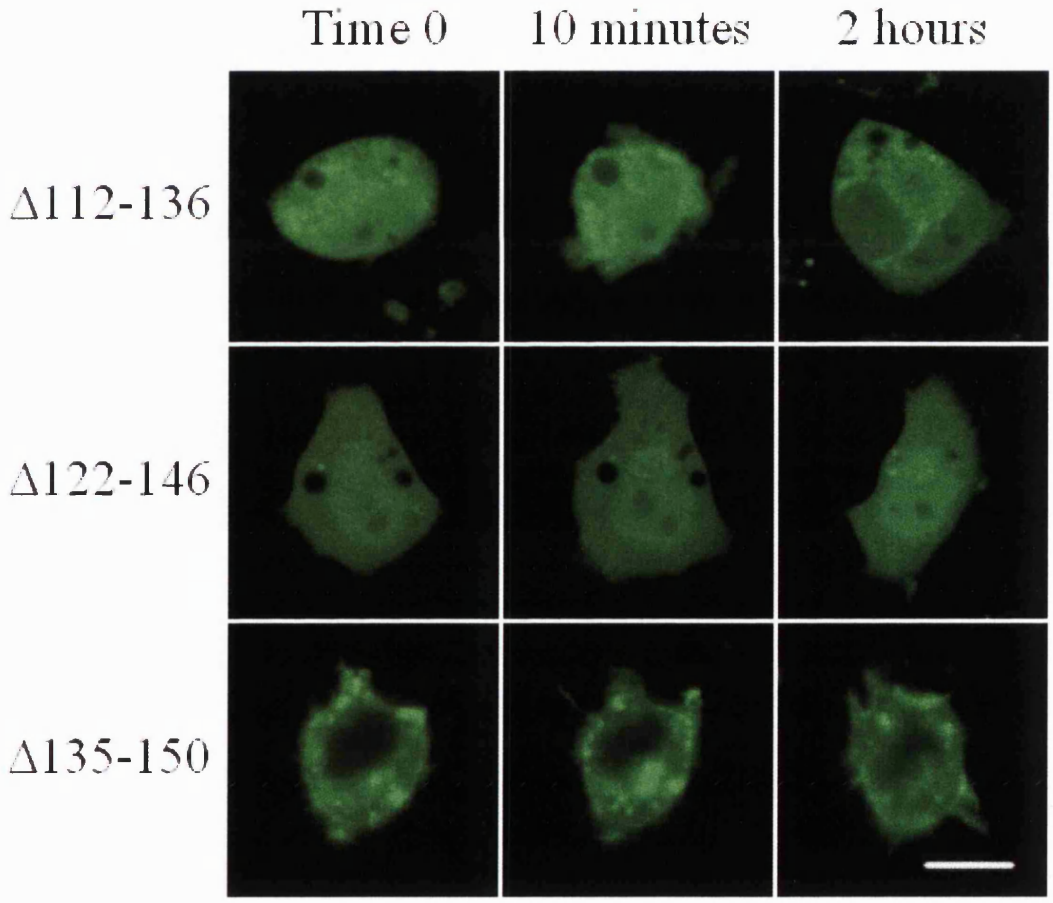

Figure 4.15 Response of internally localised mutants to 100 μM Cu-4xGly. F14 cells stably transfected with the GFP-PrP^c mutants Δ112-136, Δ122-146, and Δ135-150 were treated with 100 μM Cu-4xGly, and images captured using a Zeiss LS 550 confocal microscope at time 0, 10 minutes, and 2hours. The location and intensity of the GFP signal show no significant change. Scale bar = 10 μm.

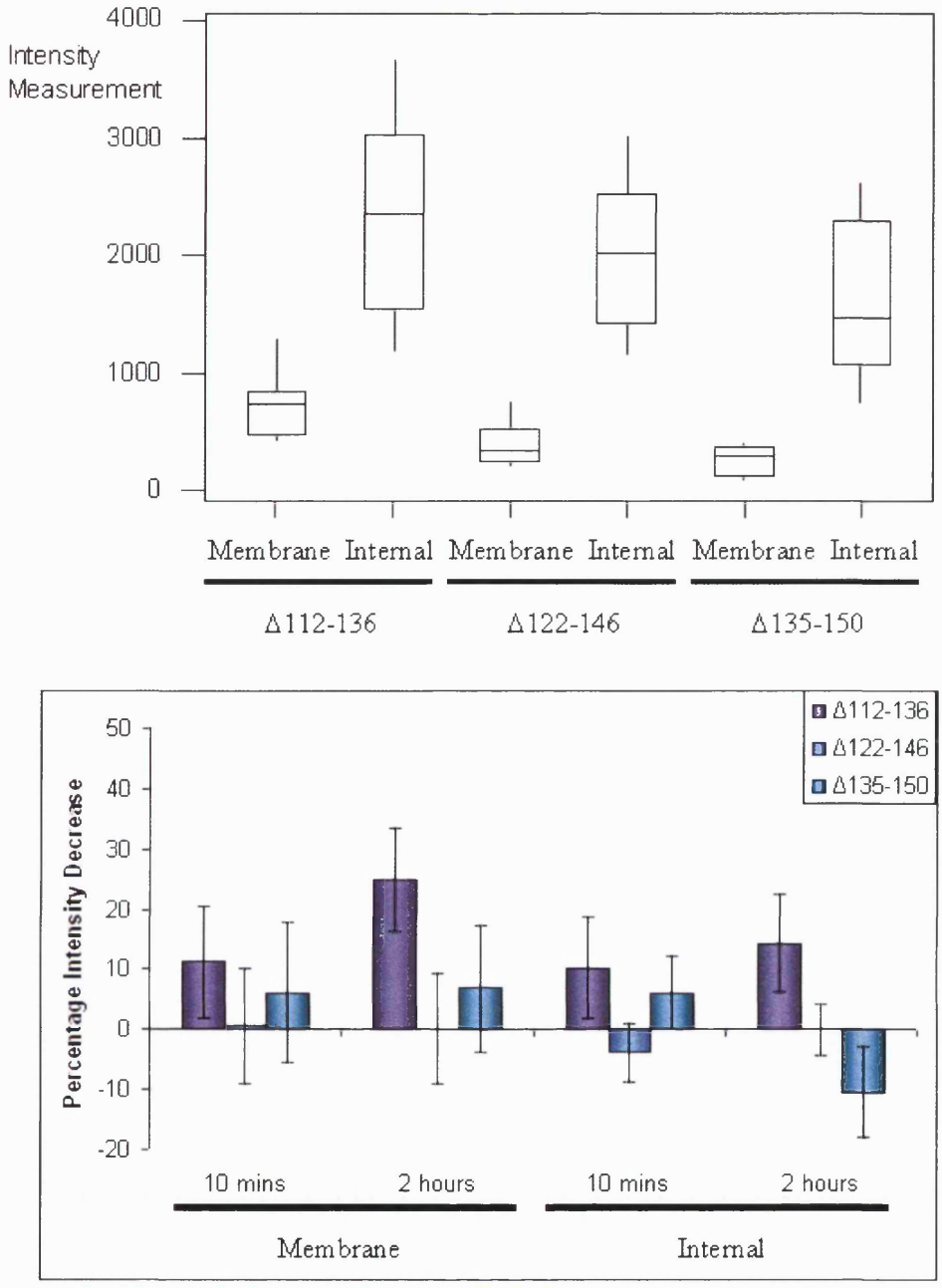

Figure 4.16 Effect of internal mutations on GFP-PrP^c expression levels and response to Cu. (A) Boxplot of basal expression levels of each of the ER localised constructs in F14 cells. The box represents the mean and inter-quartile range. (B) The percentage intensity decrease, compared to the time 0 membrane intensity, of each of the ER located mutant construct cell lines. Shown is the change both at the membrane and inside the cell where the protein is found. No significant change in location or intensity of GFP signal is seen. F = 2.3, p = 0.097, n = 12. Untreated and glycine treated controls showed no significant difference to baseline expression (F = 1.67, p = 0.333, appendix C).

4.5 PrP^c Internalisation and Other Metal Ions

Perera and Hooper (2001) and Brown and Harris (2003) also reported PrP^c internalisation with zinc (Zn). Zn and manganese (Mn) have been reported to bind to the octameric repeat domain of PrP^c. For this reason the ability of these metals to internalise PrP^c was investigated. The assays were carried out as described above. Mn is much more toxic to cells than Cu or Zn, therefore a lower concentration of Mn was used (20 μM) to produce an elevated exogenous concentration that was not high enough to kill the cells. At the start of the assay the cells were incubated with 20 μM $MnSO_4$ or 100 μM $ZnSO_4$, and observations made at time 0, 10 minutes and 2 hours. In addition, given that the Cu induced internalisation reaction proceeds much faster when Cu is delivered to the cells, a four molar excess of glycine premixed with each metal was also assayed.

Neither Mn nor Zn alone or complexed to glycine caused PrP^c to internalise. No significant reaction of either the GFP-PrP^c or GFP-GPI cells was seen to either metal ($F = 0.10$, $p = 0.748$; Figure 4.17), indicating that PrP^c may not be binding these metals or that binding does not cause internalisation. This could possibly be due to metal binding to a different site on the protein or a different fit in the sites of the octameric repeat region.

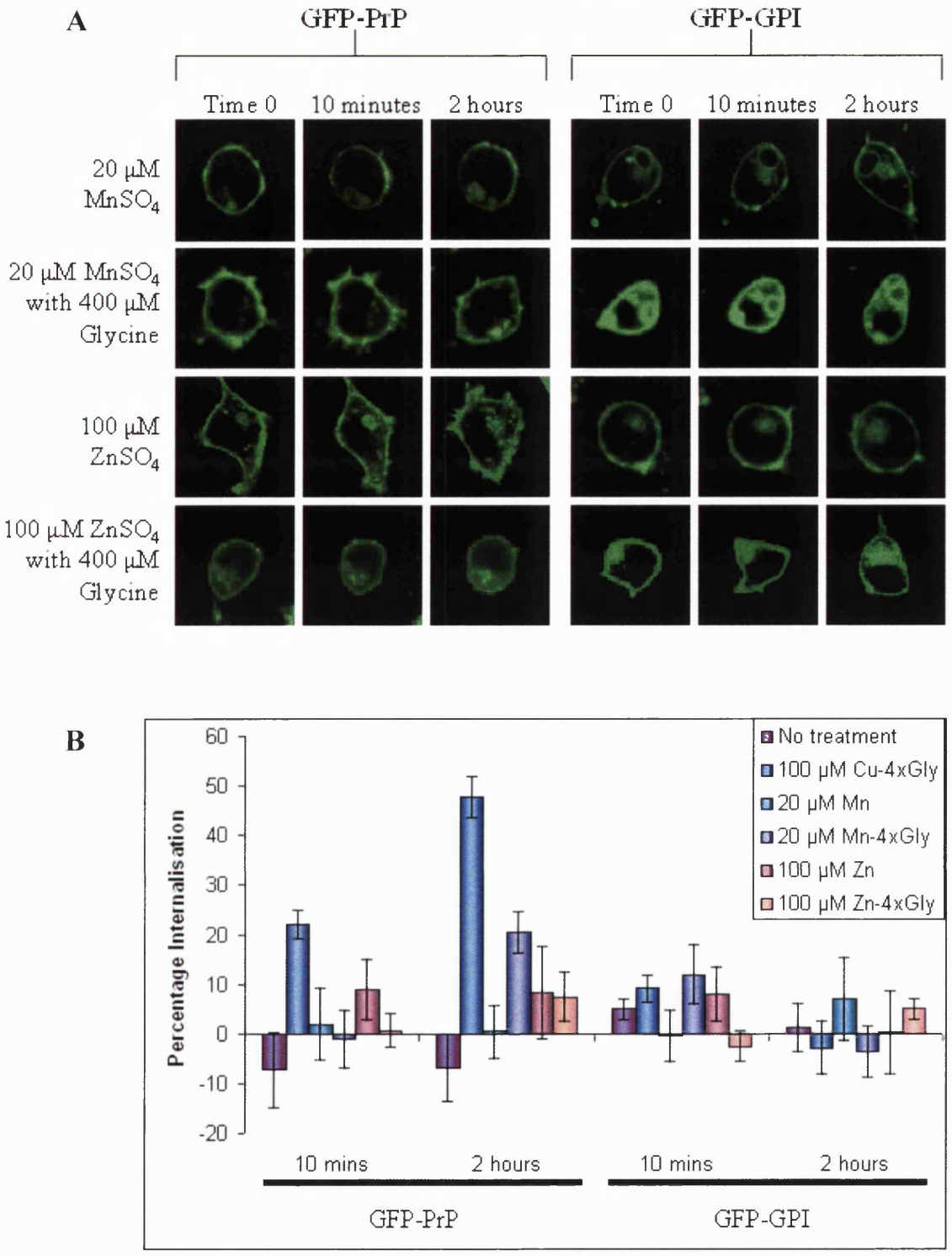

Figure 4.17 The response of GFP-PrP^c and GFP-GPI to treatment with Mn and Zn. A) shows individual cell responses at time 0, 10 minutes and 2 hours after addition of reagent. Scale bar =10 µm. B) shows the percentage internalisation compared to the GFP intensity measured at the cell surface at time 0. Percentage internalisation in response to Mn and Zn and respective chelates is shown compared to the 100 µM Cu-4xGly results. No significant internalisation is seen in response to any of the stimuli (F = 0.10, p = 0.748). Shown are the mean and SEM. n = min 12, max 18 cells.

4.6 Conclusions

The aims of this study were to address if copper could stimulate PrP^c internalisation under conditions that would arise physiologically, to determine the domains of the protein important for this function, and to consider whether other metals could produce the same reaction.

Previous studies have show that high exogenous concentrations of copper induce internalisation of PrP^c (Pauly & Harris, 1998; Brown & Harris, 2003). However, the concentrations reported are extremely high (200-500 μM) and, whilst these concentrations may be seen during neuronal depolarisation, to conclude that the reaction would occur physiologically requires that it would proceed at much lower concentrations. The data presented here shows that copper induced internalisation occurs much more readily when copper is delivered to the cell as a chelate. Copper is transported in the body chelated by transport proteins including ceruloplasmin, ferritin and albumin, and would also preferentially bind amino acids than remain unbound, and so copper induced internalisation of PrP^c is much more likely to occur under conditions resembling those found physiologically. The function of the glycine may be to provide more efficient delivery into PrP^c or it may maintain the Cu ion in the redox state preferable for PrP^c binding. The finding that glycine facilitates internalisation is in agreement with previous studies that suggest histidine facilitates uptake of radioactive Cu into neurones and astrocytes (Brown, 1999; Brown, 2004).

Using copper as a chelate, this investigation has found that concentrations as low as 5 μM can induce significant internalisation of PrP within two hours, and at 20 μM this reaction is significant as early as ten minutes after exposure. The blood plasma exchangeable concentration of Cu is 8 μM (Kramer *et al.*,2001; Burns *et al.*, 2002), and at the synapse Cu concentrations are reported to be around 15 μM, rising to 100-300 μM during neuronal depolarisation (Vassallo & Herms, 2003). This suggests the exogenous levels of Cu at the synapse would be causing a constant low level of PrP^c internalisation reaction, and that on depolarisation of the neurone, and subsequent increase in exogenous Cu, PrP^c at the cell surface would be rapidly internalised. There may be several reasons for this. The internalisation reaction may be a part of maintaining the environmental balance at the synapse so that the released metal ions can do no damage to the cells. Alternatively, PrP^c

may be an intermediate in Cu trafficking and incorporation into cellular proteins (Brown, 1999). Another explanation is that the binding of Cu may be involved in the activation of PrP^c either by directly binding to PrP^c or by activation of proteases at the cell membrane that then cleave and activate PrP^c (Parkin *et al.*, 2004).

The fate of PrP^c in response to copper is still unclear. The concentration of PrP^c in cells treated with copper is decreased compared to untreated cells, indicating that either PrP^c is cleaved from the cell surface or routed for degradation once inside the cell. No increase in the concentration of PrP^c was seen in the media taken from the copper treated cells compared to untreated cells after treatment with protease inhibitors. Certain proteases at the cell surface are involved in PrP^c cleavage and may become activated in response to copper (Parkin *et al.*, 2004). Therefore, protease inhibitors were applied to cells during copper treatment to prevent PrP^c expelled in the media being degraded. Since no change in the concentration of PrP expelled into the media was seen, it is likely that the reason for the decrease in cell extracts in response to copper is due to increased turnover of PrP^c. Cell permeable inhibitors of the proteosome or lysozomal enzymes could be employed to determine if PrP^c destruction is increased.

The trafficking of PrP^c to the cell surface appears to be highly dependant on the integrity of the hydrophobic region of the protein. The PrP^c mutants lacking part of the hydrophobic domain (Δ112-136, Δ122-146, and Δ135-150) are not correctly trafficked to the cell surface and localise to the ER. Hydrophobic regions usually stabilise protein folding by forming the core of the protein, therefore this region of PrP^c is likely to be important for maintenance of PrP^c tertiary structure. As a result, it is likely mutations of the hydrophobic domain do not reach the cell surface due to protein misfolding and redirection into ERAD. Cui *et al.* (2003) have previously shown that mutations in this region exert little if any effect on the secondary structure of PrP^c, with the alpha helical content showing little variation. However two of the hydrophobic domain mutants (Δ112-136 and Δ122-146) are lacking amino acids that form part of the beta sheet, 128-131 (Riek *et al.*, 1996), and so in their absence the beta sheet will not form correctly. This suggests that the beta sheet may stabilise PrP^c structure. The Δ135-150 mutation lacks most of helix 1 (located at amino acid positions 144-154), and although this does not affect the overall alpha helical content as shown by Cui *et al.*, its position at the C-terminal end of the hydrophobic region may result in a pronounced effect on tertiary structure. An alternatively theory is that sites within the hydrophobic domain provide epitopes for chaperone binding, which would

direct PrP^c to the cell membrane. This may explain the slight internal retention observed for the Δ112-119 mutation. However, the hydrophobic domain is expected to be hidden inside the protein and so inaccessible to chaperones. Accordingly the deletions would be most likely to affect tertiary structure and, by do so, remove or reposition motifs recognised by chaperones.

In addition the far N-terminus has a pronounced effect on the transport of PrP^c to the cell surface. When amino acids 23-38 are missing, the protein is trafficked into the intracellular membranes of the cell, and less reaches the cell surface. Since this region is unstructured, and perinuclear localisation is seen as well as to ER localisation, it is likely that, rather then misfolding causing ERAD, the protein is missing a binding site for a chaperone that is involved in movement through the exocytotic pathway to the cell surface.

Whereas trafficking to the cell surface is dependent on the hydrophobic region, trafficking away from the cell surface is reliant on the N-terminal regions. In agreement with previous studies (Lee *et al.*, 2001; Perera & Hooper, 2001), the octameric repeat domain is essential for copper induced internalisation. The absence of this region not only completely abolishes internalisation, but also produces a significant accumulation of PrP^c at the cell surface after 2 hours. It is possible that this mutation affects not only the ability of the protein to internalise, but also the regulation of its movement through the secretory pathway, resulting in increased mobilisation of the protein in response to Cu. In addition to the octameric repeat region, a fifth copper binding site has been identified (Jackson *et al.*, 2001). However the results of this investigation would indicate that this site is not involved in the internalisation of PrP^c in response to Cu. The importance of the octameric repeats is further emphasised by the finding that just one repeat is sufficient to restore a significant, although reduced, reaction.

A unique discovery of this investigation is that the palindromic region (amino acids 112-119) is essential for Cu induced PrP^c internalisation. Previous studies have found that that this region is necessary for the proposed antioxidant function of the protein (Cui *et al.*, 2003), and it has been shown that PrP^c is cleaved at this site (Chen *et al.*, 1995). This region may be necessary for the movement of PrP^c into membrane microdomains or clathrin coated pits, or PrP^c may have to be cleaved before it can move away from the membrane. In addition, PrP^c mutants lacking this domain have been shown to be resistant to conversion into PrP^{Sc}, signifying this domain may be involved in PrP^{sc} formation by

initiating the association with PrP^c that allows conversion (Hölscher *et al.*, 1998; Norstrom & Mastrianni, 2005).

Previous studies of PrP internalisation have suggested that the far N-terminus is essential for internalisation (Lee *et al.*, 2001; Nunziante *et al.*, 2003; Walmsley *et al.*, 2003). In contrast, this study found that although deletion of this region (amino acids 23-38) does slow copper induced internalisation, it does not abolish it. Mutation of amino acids 23-38 had a much more pronounced affect on trafficking to the cell surface. A further study showed that the very N-terminal amino acid residues, KKRPKP, are an essential recognition sequence for movement toward specific membrane microdomains and coated pits (Sunyach *et al.*, 2003). Although the finding that internalisation can be induced by copper when amino acids 23-38 are missing is in contrast to the findings published by Sunyach *et al.*, the studies do both agree that movement to the cell surface is impaired in the absence of this region. Taylor *et al.* (2005) found that this far N-terminal region was required for PrP^c movement at the cell membrane, facilitating passage out of lipid rafts and subsequent internalisation by clathrin coated pits. PrP^c has also been shown to be internalised by a caveolae-mediated pathway (Peters *et al.*, 2003). This may explain the discrepancy between the results presented here and those previously reported. In the absence of the N-terminal region copper induced PrP^c internalisation is slowed, since the clathrin pathway is effectively blocked, however internalisation does occur due to the calveolae-mediated pathway remaining active. The regions of PrP important for copper induced internalisation are summarised in Figure 4.18.

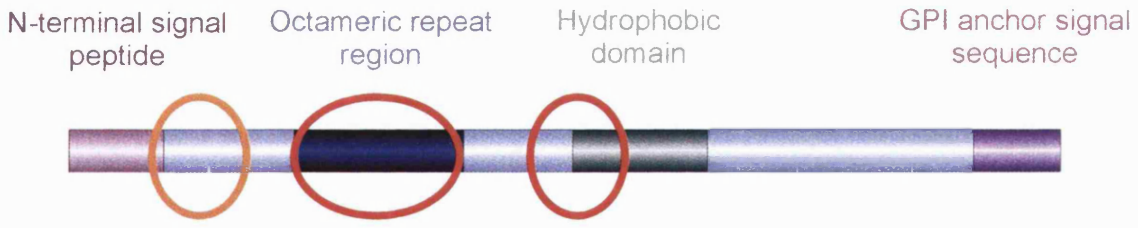

Figure 4.18 Domains of PrP^c important for copper induced internalisation. Essential domains are shown in red and the N-terminal region found to alter but not stop internalisation is shown in amber.

Studies by Perera and Hooper (2001) and Brown and Harris (2003) also found that zinc could induce internalisation of PrP. These findings were not repeatable in this study either when Zn was administered as a chelate or alone. The concentration used here was

considerably lower than that used by Brown and Harris, 100 μM and 250 μM $ZnSO_4$ respectively, however some effect would have been expected. This suggests that, although Zn induced internalisation may occur, Cu is the more dominant metal in initiating the internalisation process. No internalisation effect of PrP^c was seen in response to Mn, suggesting that if Mn is binding it is not producing the same response as copper.

From the evidence presented here it is apparent that the copper induced PrP^c internalisation reaction would happen readily under physiological conditions. This suggests that copper induced internalisation is relevant for PrP^c function. PrP^c may be delivering copper into storage vesicles to remove it from the exogenous environment, where it may be able exert potentially toxic effects. Copper delivery could be into cellular enzymes such as SODs or into storage molecules for later incorporation into enzymes. Copper could potentially activate a PrP^c signal transduction cascade, where internalisation is the first response and PrP^c goes on to activate other, possibly protective, proteins. Much further investigation is needed to clarify what role copper induced internalisation of PrP^c does play within the cell, clarifying where PrP^c is directed within the cell and if it interacts with other proteins may help to determine the function of PrP^c.

In conclusion, the prion protein internalises in response to copper, this reaction is preferential and swift under conditions that arise physiologically. PrP^c is located to the synapse, and as such would internalise rapidly in response to synaptic fluctuations in Cu. Cu induced PrP^c internalisation is dependant on the presence of the octameric repeat and palindromic domain but also influenced by the far N-terminus. Furthermore, the far N-terminus and the hydrophobic region have a pronounced effect on PrP transport to the cell surface.

5 Cellular Protection and PrP^c

Early changes in prion disease include altered metal ion concentrations in the brain and an associated inability to deal with oxidative stress insults (Wong *et al.*, 2001b; Thackray *et al.*, 2002). Therefore, a role as a protective molecule has been suggested for PrP^c. PrP^c protects neurones against copper toxicity (Brown *et al.*, 1998). This protective effect can be extended to PrP^c null neurones by incubation with a peptide corresponding to the copper binding octameric repeat domain of PrP^c. This suggests that by incorporation of copper into itself PrP^c protects cells against the deleterious effects of this metal ion.

Incorporation of copper into PrP^c may protect cells against death by preventing copper from generating free radicals by switching redox states, as occurs during the Fenton reaction (Brown *et al.*, 1998; Nishimura *et al.*, 2004). However, the incorporation of copper into PrP^c may have a more functional role. The internalisation of PrP^c in response to copper (Pauly & Harris, 1998) has lead to the theory that PrP^c acts as a copper chaperone, delivering the metal ion to enzymes within the cell such as SODs, which mediate the cellular protective response against oxidative stress (Brown & Besinger, 1998). In addition, PrP^c has been shown to have SOD-like activity both *in vitro* and *in vivo* (Brown *et al.*, 1999; Wong *et al.*, 2000; Brown *et al.*, 2001), so may itself impart a cellular protective response at the cell membrane.

The SOD-like response of PrP^c is dependant on copper binding to the octameric repeat region and requires at least two copper molecules to be bound (Brown *et al.*, 2001). In addition to the octameric repeat domain the hydrophobic domain has been reported to be essential for PrP^c antioxidant activity (Cui *et al.*, 2003; Sakudo *et al.*, 2005). PrP^c also shares several features with mouse SOD genes (Premzel *et al.*, 2005), and is up-regulated in response to ischaemic brain damage, accumulating at the site of damage where high concentrations of ROS are found (McLennan *et al.*, 2004). However conflicting results, suggesting that PrP^c has no SOD-like activity, have been reported (Hartter *et al.*, 2000; Jones *et al.*, 2005), leaving the putative SOD-like function of PrP^c still highly debated.

Alternative to PrP^c acting an antioxidant enzyme itself, it has been suggested that PrP^c is a cell surface receptor for oxidative stress, which on activation can start a signal transduction

cascade (Mouillet-Richard, 2000; Spielhaupter & Schätzl, 2001, Watt *et al.*, 2005). The pathways that would be activated by such a cascade may include PKA and ERK pathways of neuroprotection (Chiarini *et al.*, 2002; Schneider *et al.*, 2003), explaining the protective effect of PrP^c.

The role of PrP^c in protection against cellular stress remains to be defined, and the suggestion that PrP^c functions as an anti-oxidant is still a matter of controversy. To investigate the role of PrP^c in protection against cellular stress, its ability to protect cells against metal imbalance was investigated. In addition, given the suggestion that PrP^c is a superoxide dismutase, the potential to protect against direct oxidative stress insults was investigated and the mechanisms of protection against metal ion insult were then examined. The domains of PrP^c important for each protective reaction were considered.

5.1 Metal Toxicity and PrP^c Protection

The high binding affinity of PrP^c for Cu implies that the role of PrP^c involves Cu. As suggested above, such roles may include Cu transport, signal transduction, or protection against sources of cellular stress including metal ion fluctuations or ROS. The ability of PrP^c to protect against the toxicity of Cu was investigated and the important functional regions of the protein considered. Other metals, including Mn and Zn, have been suggested to bind to PrP^c (Brown *et al.*, 2000; Jackson *et al.*, 2001), therefore the ability of PrP^c to protect against toxicity of these metals was also investigated.

5.1.1 Copper Toxicity and PrP^c Protection

Cu is rarely found in its free, unbound form in biological systems, so in these experiments Cu chelated by a four times molar excess of glycine (Cu-4xGly) was used to replicate the effect of endogenous bound Cu. Stable cell lines were established by transfecting F14 cells with GFP-PrP^c (wild type) and GFP-GPI (null) constructs, and these were treated with 0-200 μM of $CuSO_4$, Cu-4xGly, and 0-800 μM glycine only concentrations for four days then assayed for viability using an MTT assay. The results are shown in Figure 5.1.

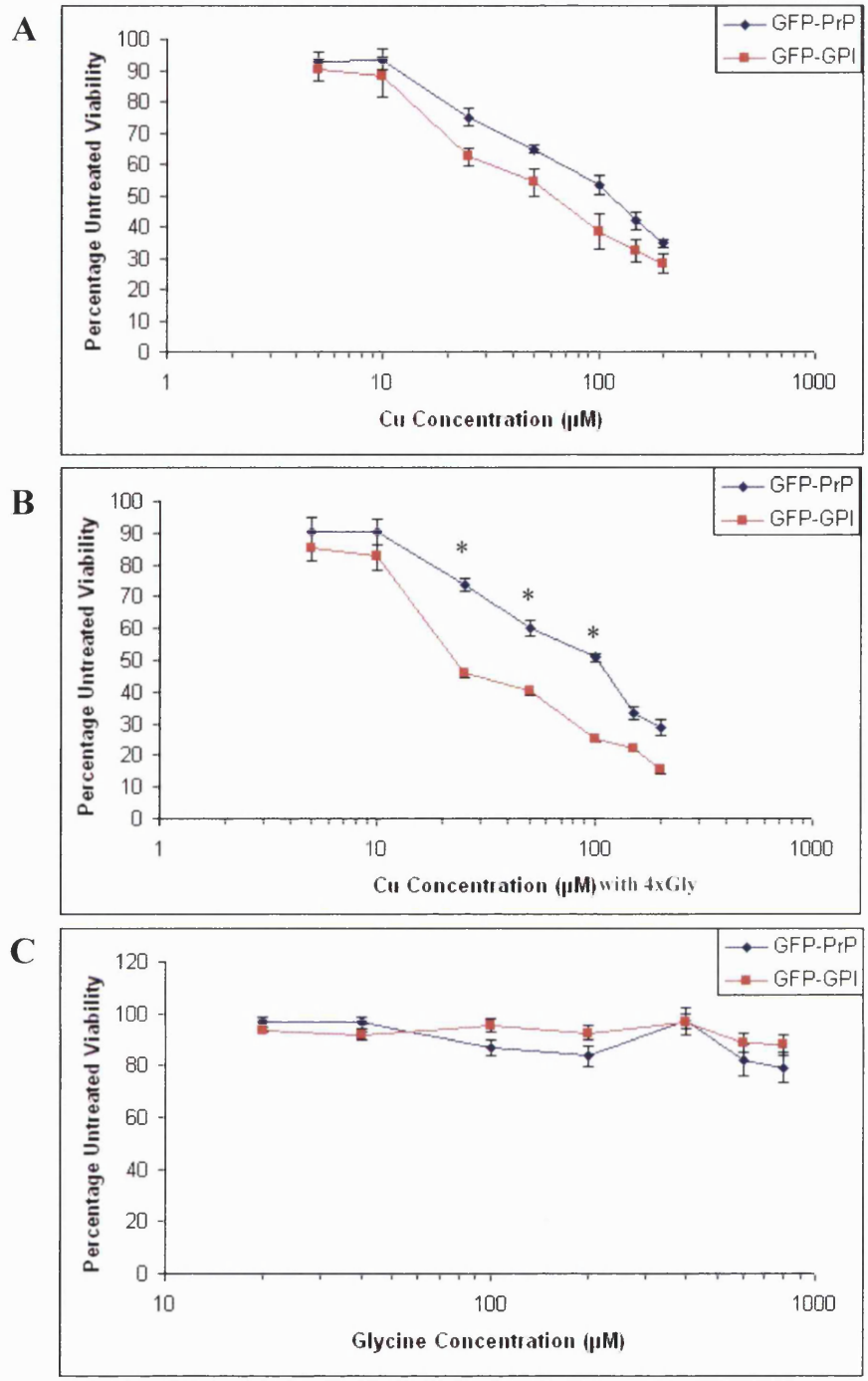

Figure 5.1 Viability GFP-PrP^c and GFP-GPI cells treated with copper alone, Cu-4xGly or glycine alone. Survival of GFP-PrP^c and GFP-GPI transfected F14 cells was determined by MTT assay after treatment with A) $CuSO_4$, B) Cu-4xGly, or C) glycine alone for four days, as shown by the percentage viability of the cells compared to that of untreated cells monitored in parallel. Shown are the mean and SEM. GFP-PrP^c significantly protects against copper induced cell death compared to the GFP-GPI null cells in the range of 25-100 μM, but only when copper is delivered as a chelate with glycine ($F = 13.61$, $p < 0.001$, * indicates significant results). n = 4 repeats, each of 3 replicates.

When treated with the free copper ($CuSO_4$), a small but non-significant protective effect is exhibited by the PrP^c expressing cells compared to the null cells ($F = 0.52$, $p = 0.815$; see Figure 5.1a). In contrast when the Cu is applied complexed to glycine, the protective effect is much more pronounced and can then be seen to be statistically significant ($F = 13.61$, $p < 0.001$; Figure 5.1b). Glycine on its own had no effect ($F = 0.02$, $p = 0.88$; Figure 5.1c).

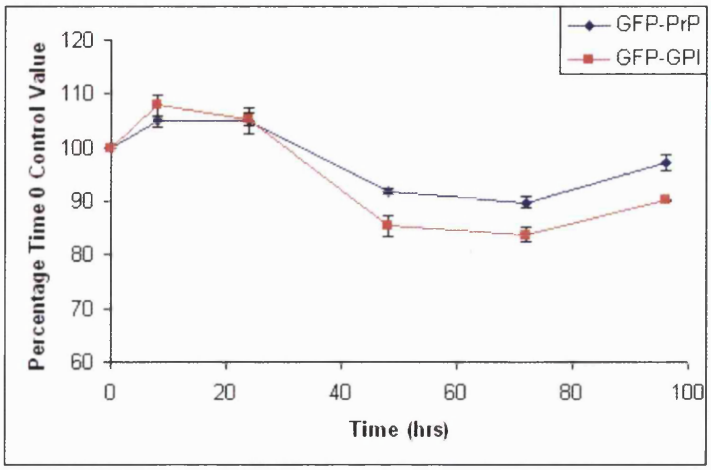

Figure 5.2 Viability of GFP-PrP^c and GFP-GPI cells at various time points up to 4 days when treated with 50 µM Cu-4xGly. F14 cells stably transfected with GFP-PrP^c and GFP-GPI constructs were treated for 8, 24, 48, 72, or 96 hours with 50 µM Cu-4xGly then assayed for viability using the MTT assay. Results are shown compared to untreated cells representing a time 0 value. Shown are the mean and SEM. n = 4 repeats, each of 3 replicates.

To be sure that the reaction seen was significant after four days incubation, the GFP-PrP^c and GFP-GPI cells were treated at 8, 24, 48, 72, and 96 hour time points with 50 µM Cu-4xGly. The results show a significant difference between the cell lines from 48 hours onwards ($T = 3.58$, $p = 0.037$). At the 96 hour time point used for these assays the cells are beginning to recover but the difference between the cell lines is still significant ($T = 3.69$, $p = 0.019$). A slight difference in viability is seen between the data shown in Figure 5.1B and 5.2, this is due to the passage number of the cells used. The cells have a finite life and later passages lose the phenotype. Therefore, care was taken that all subsequence assays used cells at passage 10 or less in age.

When the Cu and Cu-4xGly treatments are compared within the same cell line it can be seen that the increased difference in viability of the cell lines (figure 5.1) is due to more death of the GFP-GPI cells in response to Cu chelated with glycine as opposed to an

increased protective effect of PrP^c when copper is administered this way (figure 5.3). The viability of the GFP-PrP^c cells is only slightly altered when both treatments are compared indicating that the glycine neither significantly enhances nor diminishes the protective effect of PrP^c ($F = 1.32$, $p = 0.256$), but causes Cu to be more toxic to null cells than when it is unbound ($F = 2.48$, $p < 0.001$).

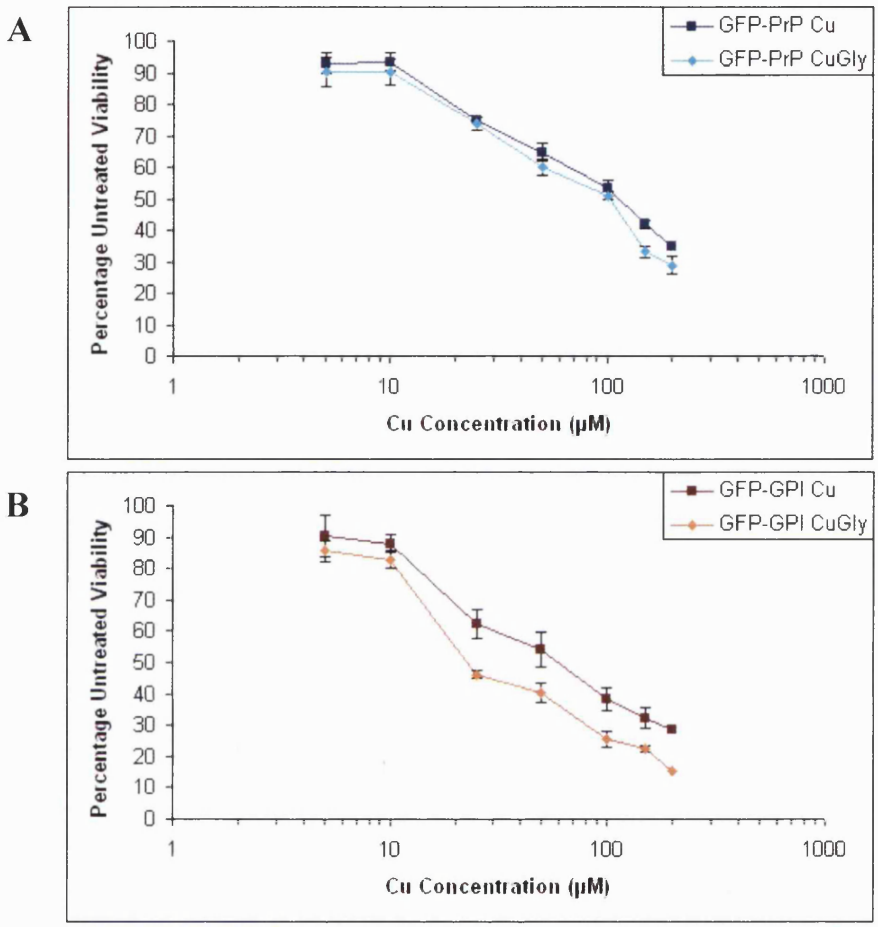

Figure 5.3 Copper-glycine is more toxic to PrP^c null cells than to wild type cells. Comparison of survival of F14 cells stably transfected with A) GFP-PrP^c and B) GFP-GPI cells treated with Cu and Cu-4xGly as measured by the MTT viability assay. GFP-GPI cells show a significantly reduced survival when treated with the Cu-4xGly compared to the Cu only, whereas the GFP-PrP^c cells show little change. Shown are the mean and SEM. n = 4 repeats, each of 3 replicates.

5.1.2 Domains of PrP^c Functional in Protection Against Copper Toxicity

Since Cu binds to the octameric repeat domain it was expected that this region would be essential for the protective effect of PrP^c. Deletion mutants (previously described and shown in figure 2.1) were used to investigate the regions of PrP^c important for this protective function. F14 cells, stably transfected with the mutant PrP^c constructs, were

treated with $CuSO_4$, Cu-4xGly, and Gly only as for the GFP-PrP^c and GFP-GPI cell lines, and viability measured by MTT assay. The results are grouped by significance, figure 5.4a shows cell lines that responded significantly differently ($F = 7.85$, $p < 0.001$) and figure 5.4b shows cell lines that did not respond significantly differently to the wild type.

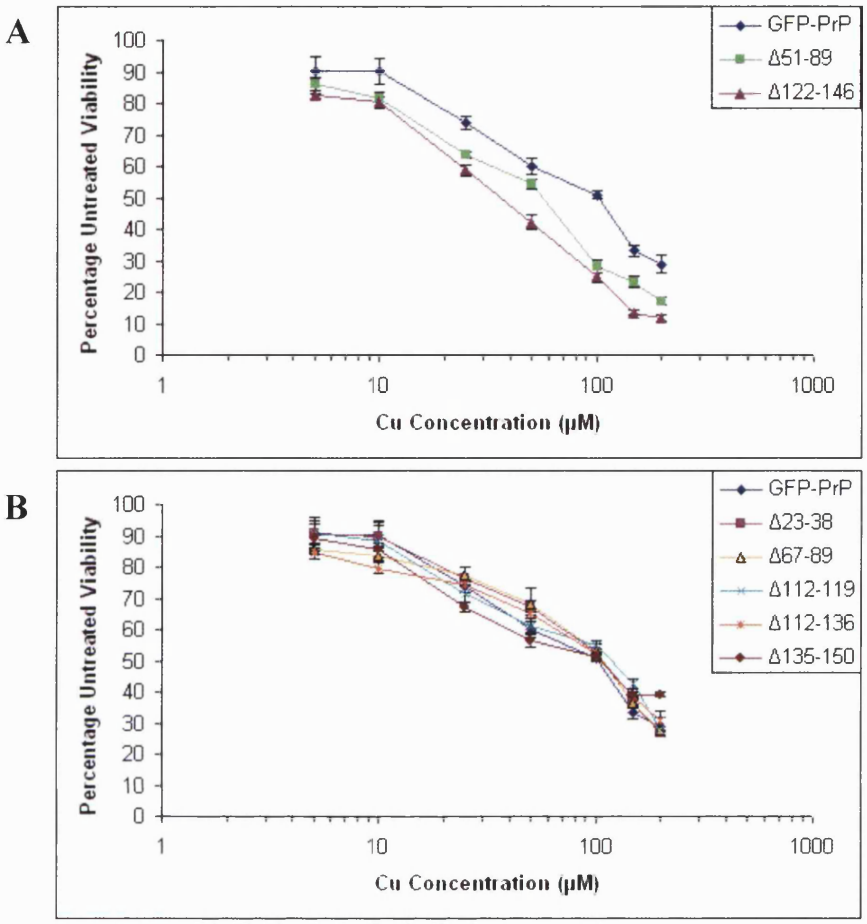

Figure 5.4 The response of PrP^c mutant cell lines treated with Cu-4xGly. F14 cells stably transfected with GFP-PrP^c and GFP-PrP^c mutant constructs were treated for four days with a range of Cu4xGly concentrations and assayed by MTT assay. Results are expressed relative to the 100 % value of the untreated controls. The octameric repeat deletion (Δ51-89) and the hydrophobic domain section deletion (Δ122-146) show significantly decreased survival compared to the wild type $F = 7.85$, $p < 0.001$ (A), whereas the remaining cell lines showed no significant decrease in survival in response to copper (B). Shown are the mean and SEM. n = 4 repeats, each of 3 replicates.

The deletion of the octameric repeat domain (51-89) abolished the protective effect of the protein in response to the copper insults (Figure 5.4a). The presence of just one octameric repeat appears to re-establish the protection that PrP^c affords, indicating that even one repeat is sufficient for the PrP^c protective response.

In addition, the deletion mutant lacking amino acids 122-146 of the hydrophobic domain showed significantly decreased survival compared to the wild type protein (Figure 5.4a), indicating that this domain is also important for protection of cells against copper toxicity. The requirement for this region suggests that the protection against copper toxicity may not be simply due to PrP^c chelating Cu within its octameric repeat region, but that further mechanisms may be involved. PrP^c could potentially be also protecting against copper toxicity by reducing the oxidative stress that a redox metal such as copper may induce. This will be considered in Section 5.3. The remaining mutant cell lines did not show any significant difference from the wild type (Figure 5.4b).

5.1.3 Manganese Toxicity and PrP^c Protection

Mn is a much more toxic metal than copper. Since PrP^c may bind Mn and the above results show it protects against copper toxicity, the toxicity of Mn on the GFP-PrP^c and GFP-GPI cell lines was investigated. Mn is weakly bound by glycine, therefore Mn was prepared complexed to glycine in a 1Mn:4Glycine molar ratio as used for Cu. $MnSO_4$ and Mn-4xGly were added to GFP-PrP^c and GFP-GPI cells, and cells were incubated for four days then viability measured by MTT assay.

A significant protective effect is seen by increased viability of the GFP-PrP^c cells compared to the GFP-GPI cells ($F = 14.72$, $p < 0.001$; figure 5.5), showing that PrP^c protects against Mn toxicity. This effect only becomes apparent at high manganese concentrations. This may be due to the octameric repeat domain of PrP^c having a higher affinity for Cu, so Mn concentrations would have to appreciably exceed copper concentrations before Mn can complete for the octameric repeat binding sites. If this were the case PrP^c would be protecting against the Mn insult by the chelation of the Mn ions. PrP^c could also be protecting against the oxidative stress caused by the Mn ions undergoing redox reactions, which would become considerably more toxic to cells at higher concentrations of Mn. In contrast to the Cu results, the Mn complexed to glycine produced the same pattern of survival of each cell line as the unbound, free Mn ($F = 8.35$, $p < 0.001$). The most likely reason for this effect is that glycine binds to Cu with much greater affinity than it does to Mn. The stability constants for the two metals at pH 7.4 are Cu $K_1 = 5.87$, and Mn $K_1 = 0.67$ (Dawson *et al.*, 1994). With Mn having a low affinity, it is likely that the protective effect observed is primarily due to protection against free manganese, which is released from the glycine once it is added to the medium. Also Mn incorporation into PrP^c may not be more efficient if Mn is chelated than if it is not.

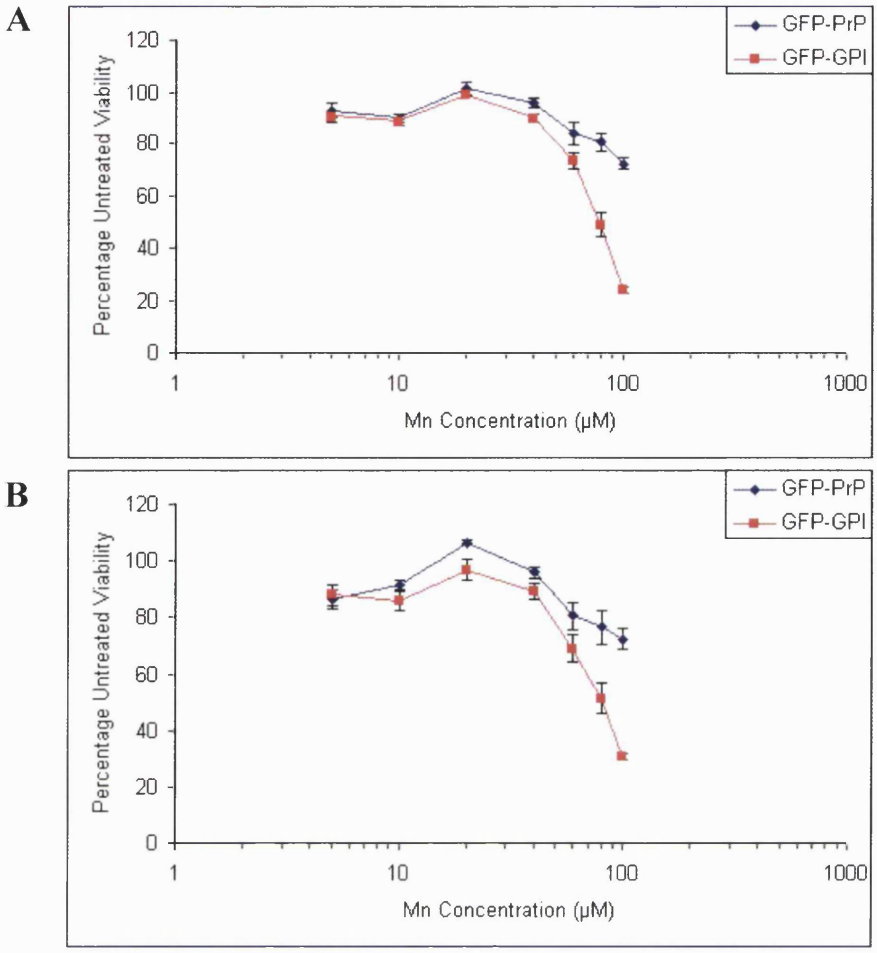

Figure 5.5 Mn treatment of PrP^c null and wild type cell lines. F14 cells stably transfected with GFP-PrP^c and GFP-GPI constructs were treated for four days with A) $MnSO_4$ and B) $MnSO_4$ with a four times molar excess of glycine and viability determined by MTT assay. GFP-PrP^c protects significantly against cell death induced by either treatment compared to the GFP-GPI cells, however there is no significant difference between the effects seen for Mn or Mn-4xGly. Shown are the mean and SEM. n = 4 repeats, each of 3 replicates.

5.1.4 PrP^c Protection Against Other Metals

There is evidence that PrP binds other metals such as Zn, Fe and Ni (Jackson *et al.*, 2001). To investigate the protective ability of PrP^c against these metals 0-200μM $ZnSO_4$, $NiSO_4$, and Fe_2SO_4 were used to treat GFP-PrP^c and GFP-GPI cells. No significant protective effect was seen to any of these metals, for Zn $F = 0.30$, $p = 0.587$, for Ni $F = 1.85$, $p = 0.112$, and for Fe $F = 0.58$, $p = 0.451$ (figure 5.6).

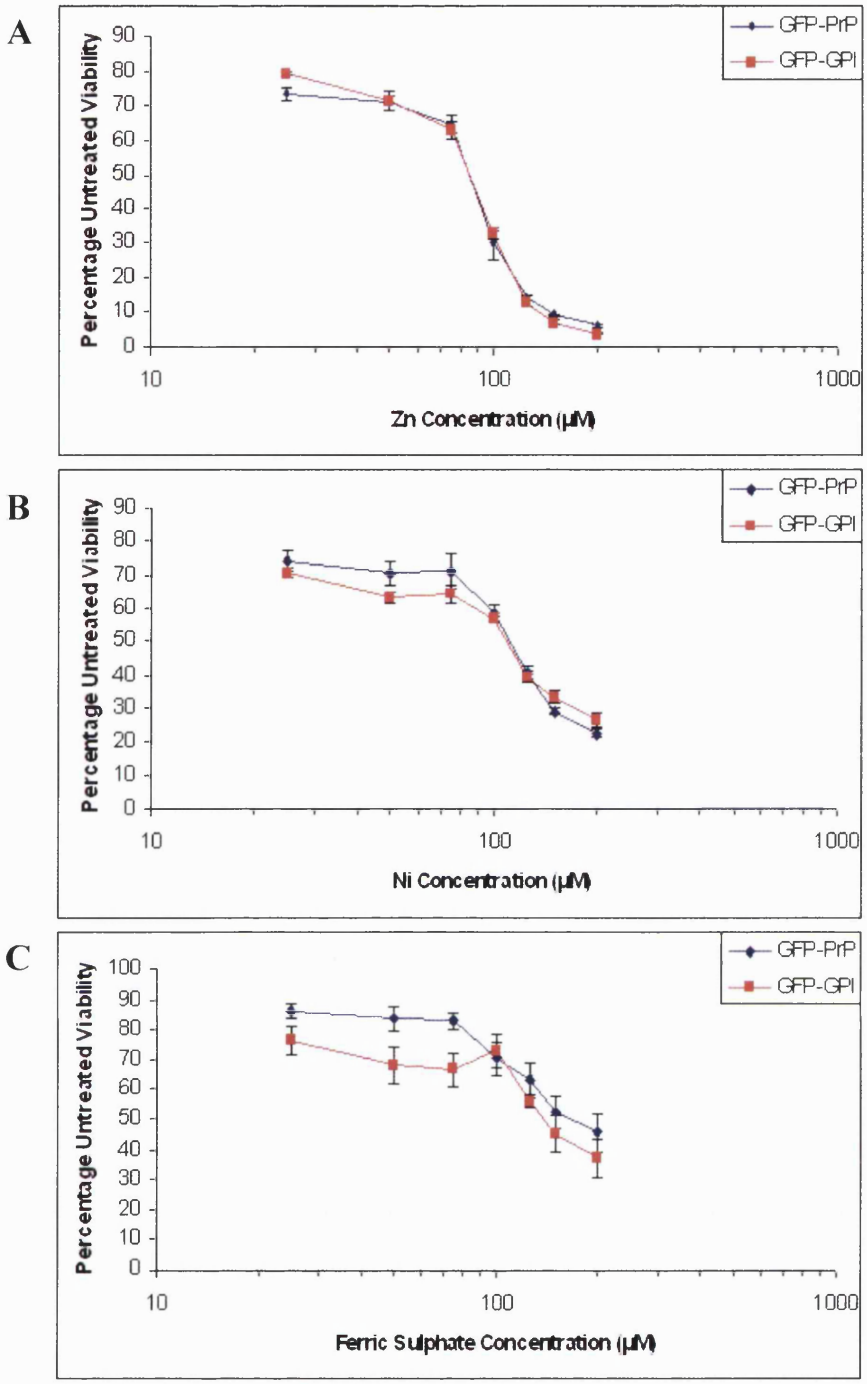

Figure 5.6 Response of PrP^c null and wild type cells to treatment with Zn, Ni, and Fe. F14 cells stably transfected with GFP-PrP^c and GFP-GPI constructs were treated with A) $ZnSO_4$, B) $NiSO_4$, and C) Fe_2SO_4 for four day and then viability measured using the MTT assay. No significant differences in survival are seen between the GFP-PrP^c and GFP-GPI cell lines in response to any of the treatments. Shown are mean and SEM. n = 4 repeats, each of 3 replicates.

The lack of PrP^c protective effect against these metals may be due to lower binding affinity of PrP^c for these metals, or that the protective function of PrP^c does not involve these metal ions. It is also possible the method of protection is the reason for the lack of response. If

the protective effect shown by PrP^c is a response to the oxidative stress caused by active redox metals such as Cu and Mn, it may not be able to respond to less redox active metals, which cause toxicity primarily via the metal ion itself.

5.2 PrP^c and Protection Against Oxidative Stress

5.2.1 PrP^c Protection Against DMSO and Xanthine Oxidase Insults

PrP^c has been suggested to have SOD-like activity itself. To consider if this capability is sufficient to protect the cells from death induced by oxidative stress dimethyl sulphoxide (DMSO) and xanthine oxidase were used to induce oxidative stress insults. At the start of the assay 0-3% DMSO (Figure 5.7a) or 0-50 mU xanthine oxidase (Figure 5.7b) with 50 μM xanthine (included in control wells also), was added to the cells and after 24 hours treatment cell viability was measured using the MTT assay.

PrP^c protected against insults induced by DMSO ($F = 4.8$, $p < 0.001$) and xanthine oxidase ($F = 4.32$, $p < 0.001$) indicating that the oxidative protection observed is not restricted to just that caused by metal ions. This indicates that the protective effect of PrP^c against metals may not just be due to the chelation of the metal ion preventing oxidative stress but potentially also due to the removal of any oxidative insult directly.

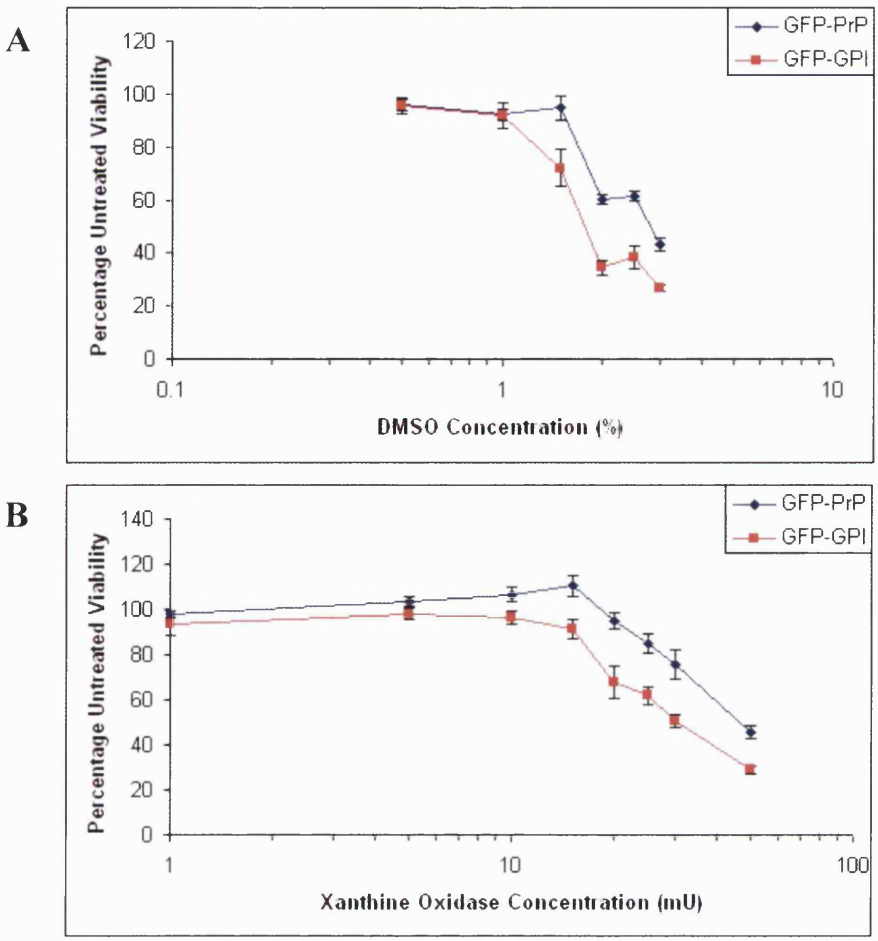

Figure 5.7 Response of PrP^c null and wild type cells to oxidative stress insults. F14 cells stably transfected with GFP-PrP^c and GFP-GPI constructs were treated for 24 hours with A) DMSO and B) xanthine oxidase to induce oxidative stress. Viability was determined by the MTT assay. An increased survival of the GFP-PrP cell line is seen by an increased viability compared to the GFP-GPI cell line. Shown are the mean and SEM. n = 4 repeats, each of 3 replicates.

5.2.2 PrP^c Functional Domains for Protection Against Oxidative Stress

The domains important for PrP^c function were considered using the deletion mutants. For this the cells were exposed to DMSO (figure 5.8) or xanthine oxidase (figure 5.9) as for the GFP-PrP^c and GFP-GPI cell lines, and assayed as before.

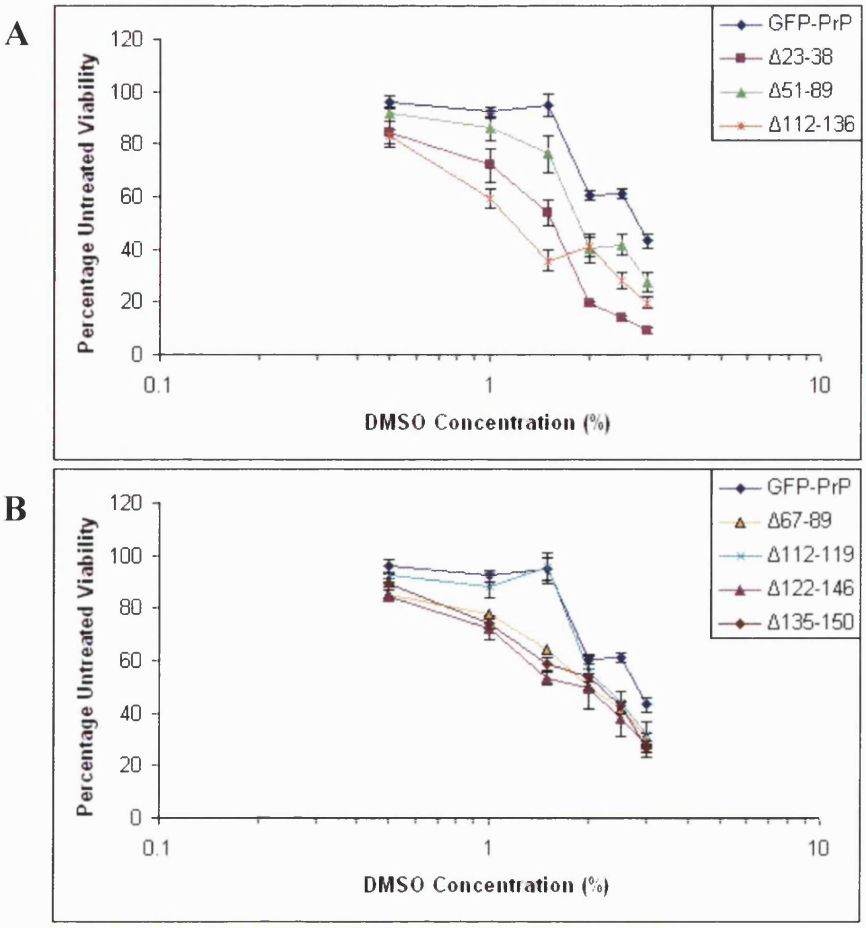

Figure 5.8 PrP^c mutant cell lines treated with DMSO. F14 cells stably transfected with GFP-PrP^c and GFP-PrP^c deletion mutants were treated for 24 hours and viability determined by MTT assay. Deletion of amino acids 23-38, 51-98, and 112-136 produced the most significant decrease in cellular survival compared to the wild type GFP-PrP^c cells (A), however all the remaining mutants show some degree of reduced survival (B). Shown are the mean and SEM. n = 4 repeats, each of 3 replicates.

All of the mutant cell lines showed some degree of reduced survival compared to the wild type when treated with DMSO (Figure 5.8). For most of the cell lines reduced survival is seen at 2% DMSO but overall viability is not significantly different to wild type, however for cell lines expressing the mutants Δ23-38, Δ51-89, and Δ112-136 survival was significantly reduced from that of wild type ($F = 4.92$, $p < 0.001$).

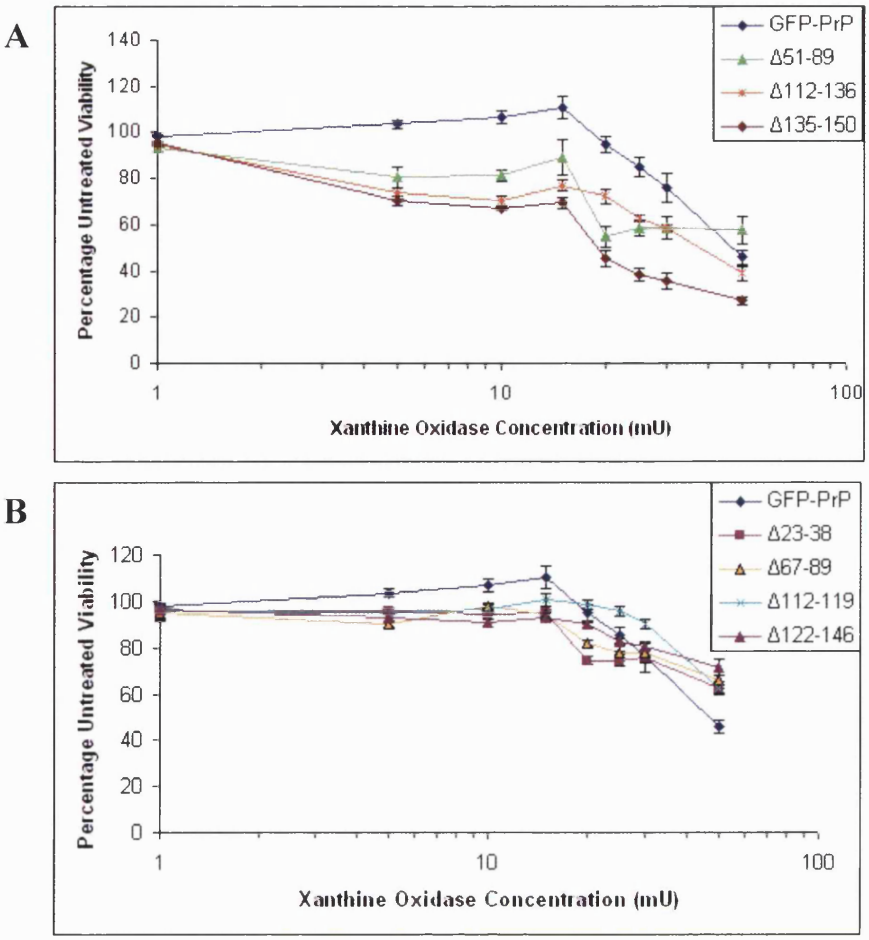

Figure 5.9 PrP^c mutant cell lines treated with xanthine oxidase. F14 cells stably transfected with GFP-PrP^c and GFP-PrP^c deletion mutants were treated for 24 hours to induced oxidative stress and viability determined using the MTT assay. Mutants lacking amino acids 51-89, 122-136, and 135-150 showed the most reduced survival compared to the GFP-PrP^c cells $F = 5.14$, $p < 0.001$ (A). The remaining mutants did not show significantly reduced survival (B). Shown are the mean and SEM. n = 4 repeats, each of 3 replicates.

Consistent with the findings of the DMSO assays, deletion of the octameric repeat domain removes the ability of the protein to respond to oxidative stress induced by xanthine oxidase (Figure 5.9a). The protective effect is also lost with the removal of the hydrophobic domain and the area immediately following it. The remaining deletion mutants showed no significant reduction in survival when treated with xanthine oxidase (Figure 5.9b).

5.3 Method of PrP^c Protection Against Copper

As suggested previously PrP^c may protect against cellular injury from Cu by several methods. The octameric repeat region binding and chelating the Cu ions may prevent them from binding to other cellular proteins causing damage, and also may prevent oxidative stress by keeping Cu static in one oxidation state. Alternatively the protection may be due to the ability of PrP^c to act as an anti-oxidant and so remove the stress that the Cu ion is causing to the surrounding environment. There is also the possibility that both methods could act together for the overall protection of the cell. The evidence presented so far suggests that PrP^c protects against the Cu ion itself but also against the oxidative stress that the ion may induce, therefore further investigation is needed to more fully characterise the role of PrP^c in protection against Cu induced cellular death. To this end several methods have been employed, both indirectly looking for markers of oxidative stress and directly measuring reactive oxygen species.

5.3.1 PrP^c, Copper, and Anti-Oxidants

The first approach considered to elucidate the mechanism of action of PrP^c was the use of anti-oxidants for the purpose of restoring the viability of the GFP-GPI cells to that of the GFP-PrP^c cells. Restoration to a similar viability level would be likely if the protective effect of PrP^c was a result of removing the oxidative stress caused by the Cu ion as opposed to just chelation of the ion itself. F14 (null) and F21 (wild type) cells were used for this comparison. Cells were treated for four days with Cu plus bovine SOD, catalase, N-acetyl cysteine, or a combination of these, and then tested for viability using the MTT assay.

Using the anti-oxidants on the cells in conjunction with the Cu treatment did not produce any effect on either cell line ($F = 0.72$, $p = 0.619$; figure 5.10). Thus indicating that the protective effect is not likely to be due solely to PrP^c anti-oxidant activity.

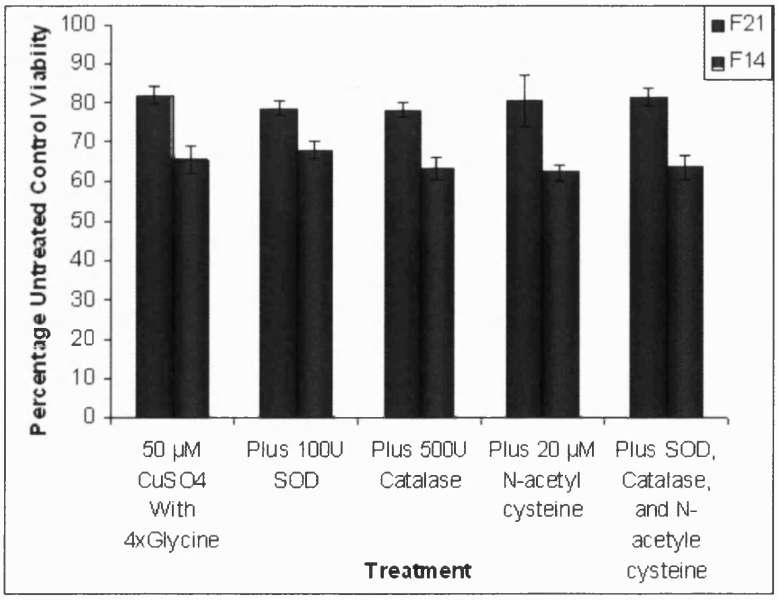

Figure 5.10 Rescue effect of anti-oxidants on copper treated F14 and F21 cells. Cells were treated with 50 µM Cu-4xGly with or without SOD, catalase, N-acetyl cysteine, or all of these antioxidants to assess if null cell survival could be rescued to that of wild type. Cells were treated for four days then viability determined by MTT assay. No antioxidant, or combination of anti-oxidants, had any significant effect on the survival of the cell lines. Shown are the mean and SEM, n = 4 repeats, each of 3 replicates.

5.3.2 PrP^c, Copper, and Markers of Oxidative Stress

Lipid peroxidation is a mechanism of cellular injury in response to oxidative stress, and lipid peroxides can themselves inflict further damage on cells. Lipid peroxide species malondialdehyde (MDA) and 4-hydroxyalkenyls (HAE) can be detected by two variations on the same assay, the first of which is specific for MDA and the second that is less specific for MDA but also detects HAE. Cells were treated for 48 hours with 5 µM Cu-4xGly, 50 µM Cu-4xGly, 200 µM Gly, 50 µM $CuSO_4$, or left untreated. These concentrations were decided by considering viability differences between the GFP-PrP^c and GFP-GPI cells (figure 5.11), and concentrations at which copper may occur physiologically. Cells were collected by centrifugation and washed, before homogenisation in 20 mM phosphate buffer (pH 7.4). The assays were carried out using the Bioxytech ® LPO-586^{TM} kit from Oxis Research.

Significant concentrations of lipid peroxidation markers were only seen in the GFP-GPI cells in response to 50 µM $CuSO_4$ ($F = 3.9$, $p = 0.04$). Significant increases in peroxidation markers were not seen with the equivalent concentration of Cu-4xGly. The chelation of the

Cu ion by the glycine may prevent it changing redox states, which would cause oxidative stress and lipid peroxidation of cells, whereas the free copper is not restrained in this way. Alternatively the incorporation of Cu into PrP^c may occur much more readily when Cu is complexed to glycine so PrP^c may be able to chelate much more of the glycine bound copper than the free copper. Thus allowing free Cu to remain free and induce oxidative stress. A further possibility is that the glycine itself is protecting against oxidative stress. Glycine has been reported to have the ability the remove reactive oxygen species (Senthilkumar *et al.*, 2003), and so may be removing the reactive oxygen species that Cu creates. The glycine on its own showed no significant increase or decrease in oxidative stress markers. An anomalous result is seen for 5 μM Cu-4xGly when MDA and HAE are measured. Since this is not seen for MDA detection it is likely that HAE markers are responsible for this increase and may signify that at low concentrations Cu is able to cause oxidative damage even when chelated. This may be due to the cell not activating protection mechanisms because the Cu levels are not high enough to be detected as toxic.

The evidence so far suggests that PrP^c is able to protect against the oxidative stress that free Cu can cause. Direct detection of radical levels is required to confirm that it is acting to removing the ROS insult.

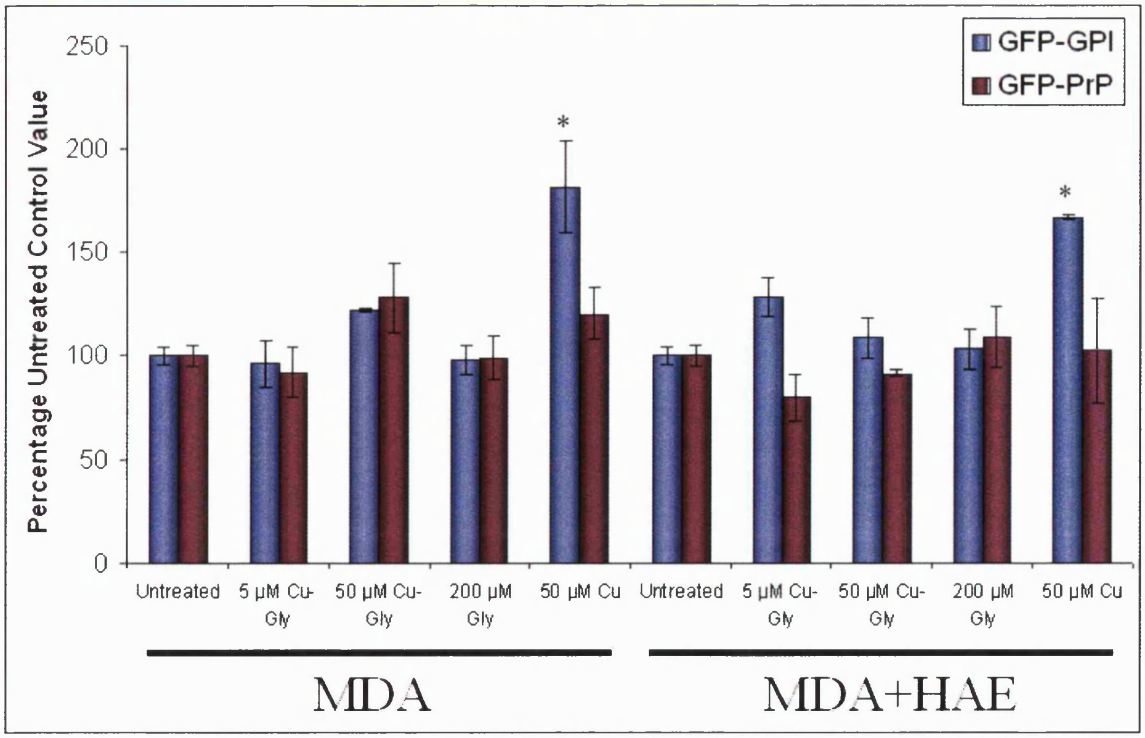

Figure 5.11 Detection of lipid peroxidation markers malondialdehyde (MDA) and 4-hydroxyalkenyls (HAE) in GFP-PrP^c and GFP-GPI cells following copper treatments. F14 cells stably transfected with GFP-PrP^c and GFP-GPI constructs were grown to produce approximately 5 x 10^7 cells per condition at the time of extraction. Cells were treated for 48 hours with 5 or 50 µM Cu-4xGly, 50 µM $CuSO_4$, 200 µM Glycine, or left untreated for basal marker levels. Two variations of the LPO-586^{TM} assay (OxisResearch®, Portland, USA) were then used to quantify MDA alone or MDA with HAE. Significantly increased markers (*) are only seen in the GFP-GPI cell line when treated with 50 µM $CuSO_4$. Shown are the mean and SEM compared to the untreated values. n = 4 repeats, each of 3 replicates.

5.3.3 PrP^c, Copper, and Direct Detection of Free Radicals

The direct detection of free radicals allows for the measurement of both the oxidative stress that Cu is able to induce and the ability of PrP to control cellular levels of ROS. Two methods were employed to look for free radicals inside cells. Individual cells expressing GFP-PrP^c or GFP-GPI constructs were monitored using RedoxSensor® Red stain, allowing the GFP signal and the red signal of the probe to be detected together, and a population response was determined using CM-H_2DCFDA probe.

5.3.3.1 GFP-PrP^c, Copper, and Free Radical Detection by Redox Sensor Red

GFP-PrP^c and GFP-GPI transfected cells were incubated with RedoxSensor® Red probe for 10 minutes prior to the start of the assay. Assays were carried out in OptiMEM, with

100 μM $CuSO_4$, 100 μM Cu-4xGly, or 400 μM glycine added at time 0 and images captured at 0, 5, 10, and 15 minutes. Untreated cells were followed in parallel to account for basal changes in oxidative stress. F14 cells were also assayed to monitor the differences in response that might arise due to transfection and selection pressure.

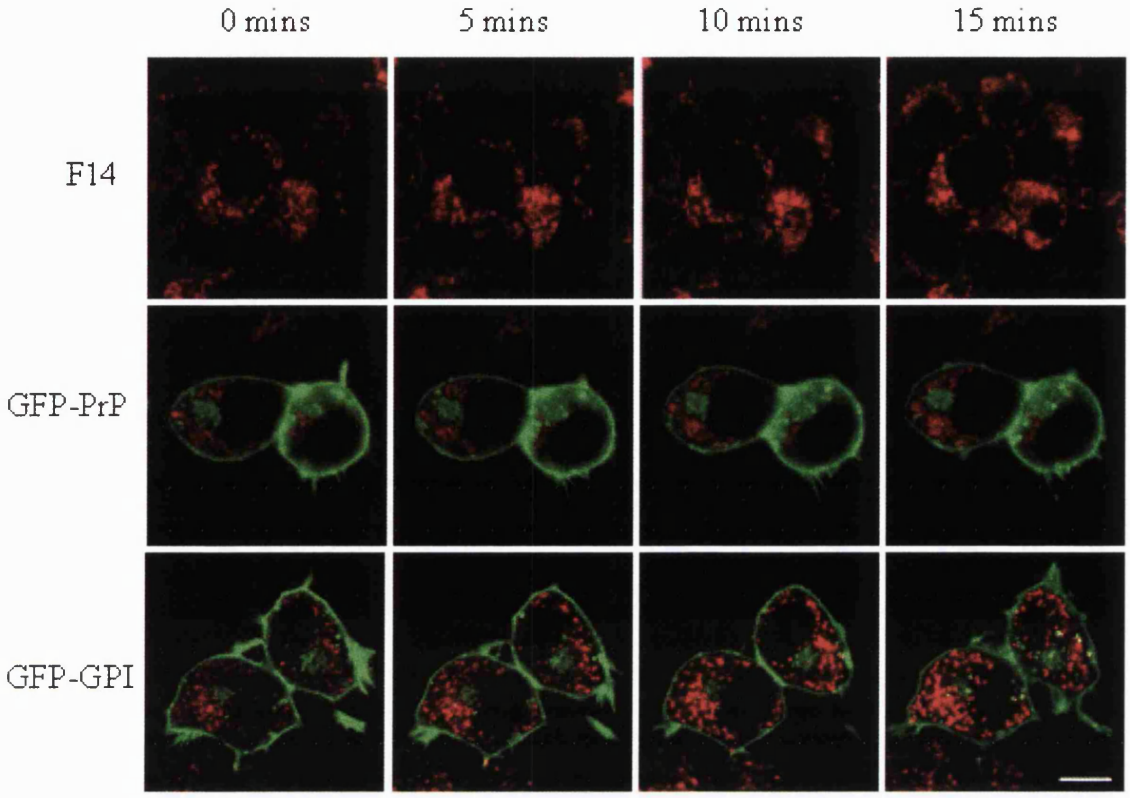

Figure 5.12 Images of F14 cells and F14 cells stably transfected with GFP-PrP^c and GFP-GPI constructs stained with redox sensor red probe and incubated for 15 minutes with 100 μM $CuSO_4$. Images were captured using a Zeiss LS 550 confocal microscope. Increased ROS is seen by an increase in signal of the probe, with the GFP-GPI (null) cells showing a greater increase in signal than the GFP-PrP^c (wild type) cells. Scale bar = 20 μm.

A significant increase in the intensity of the redox red sensor is seen in the F14 and GFP-GPI cells compared to the GFP-PrP^c cells in response to free Cu indicating that the oxidative stress levels in the PrP^c expressing cells are less affected by the stress insult induced by Cu than GFP-GPI cells ($F = 4.23$, $p = 0.043$; Figure 5.12 and 5.13). Therefore the PrP^c that is present is helping regulate the oxidative conditions within the cell.

As seen for the LPO assay, the Cu-4xGly and glycine only treatments had no significant effect on the intracellular level of oxidative stress of any of the cell lines after 15 minutes

exposure (Figure 5.13c and 5.13d respectively). This further argues that only free Cu induces an oxidative stress response that PrP^c null cells are unable to remove.

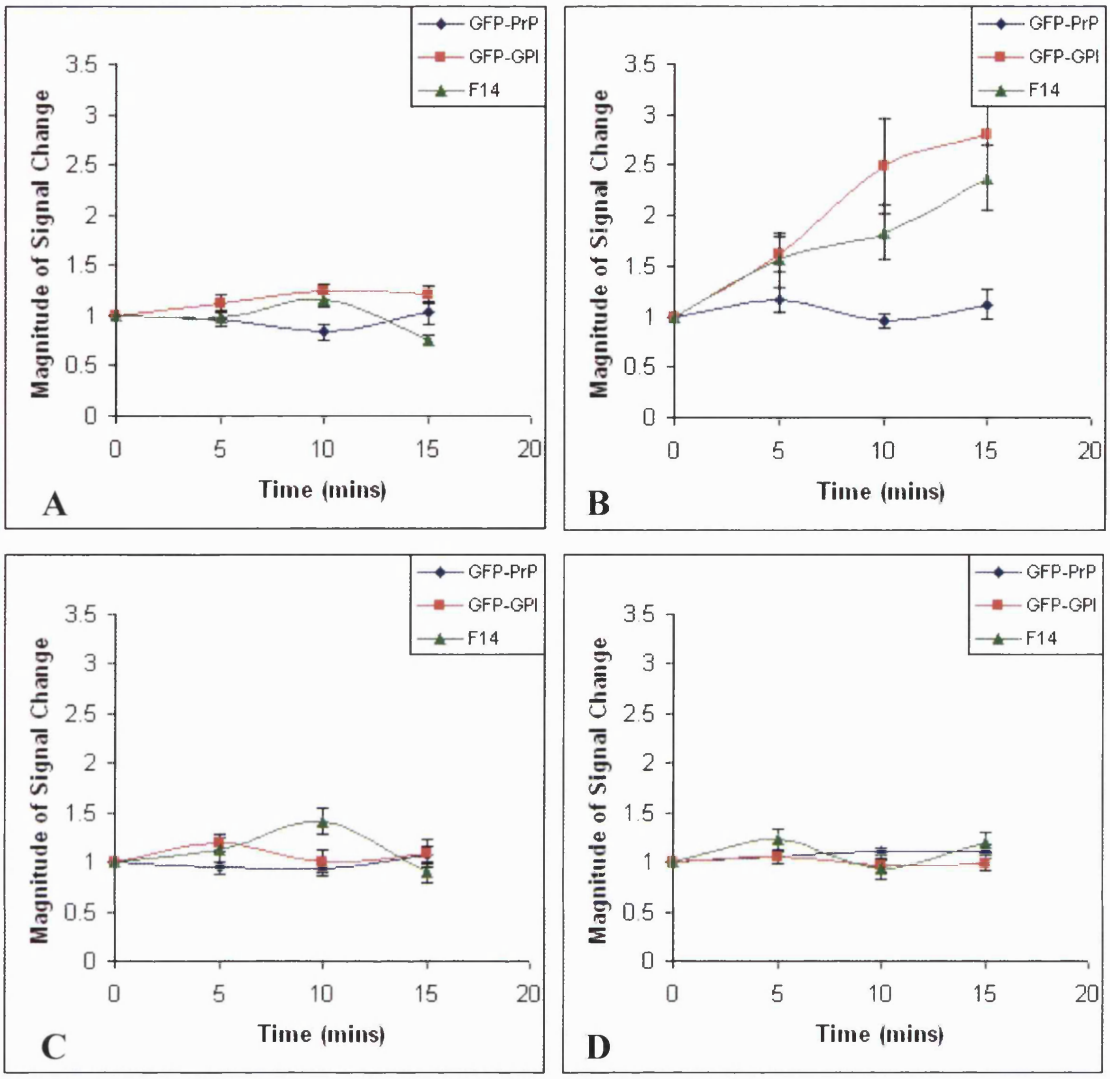

Figure 5.13 Quantification of Redox Red probe signal intensity in untransfected F14 cells and cells stably transfected with GFP-PrP^c and GFP-GPI constructs treated with A) no reagent, B) 100 μM CuSO4, C) 100 μM Cu-4xGly, and D) 400 μM Glycine. The change in signal intensity (measured at the time of image collection by the Zeiss LSM software) is expressed as a ratio of time point value: time 0 value, to show the magnitude of signal change comparable to the time 0 reading. n = min 12, max 25 cells.

5.3.3.2 GFP-PrP^c mutants, Copper, and Free Radical Detection by RedoxSensor® Red

To look at how the different mutants were able to deal with the stress insult, the N-terminally expressed mutants (Δ23-38, Δ51-89, Δ67-89, Δ112-119) were stained with the redox sensor probe and the assays carried out as described above. Only the N-terminal mutants were examined due to the internal localisation of the C-terminal mutants interfering with the redox red signal (see Section 4.1.2).

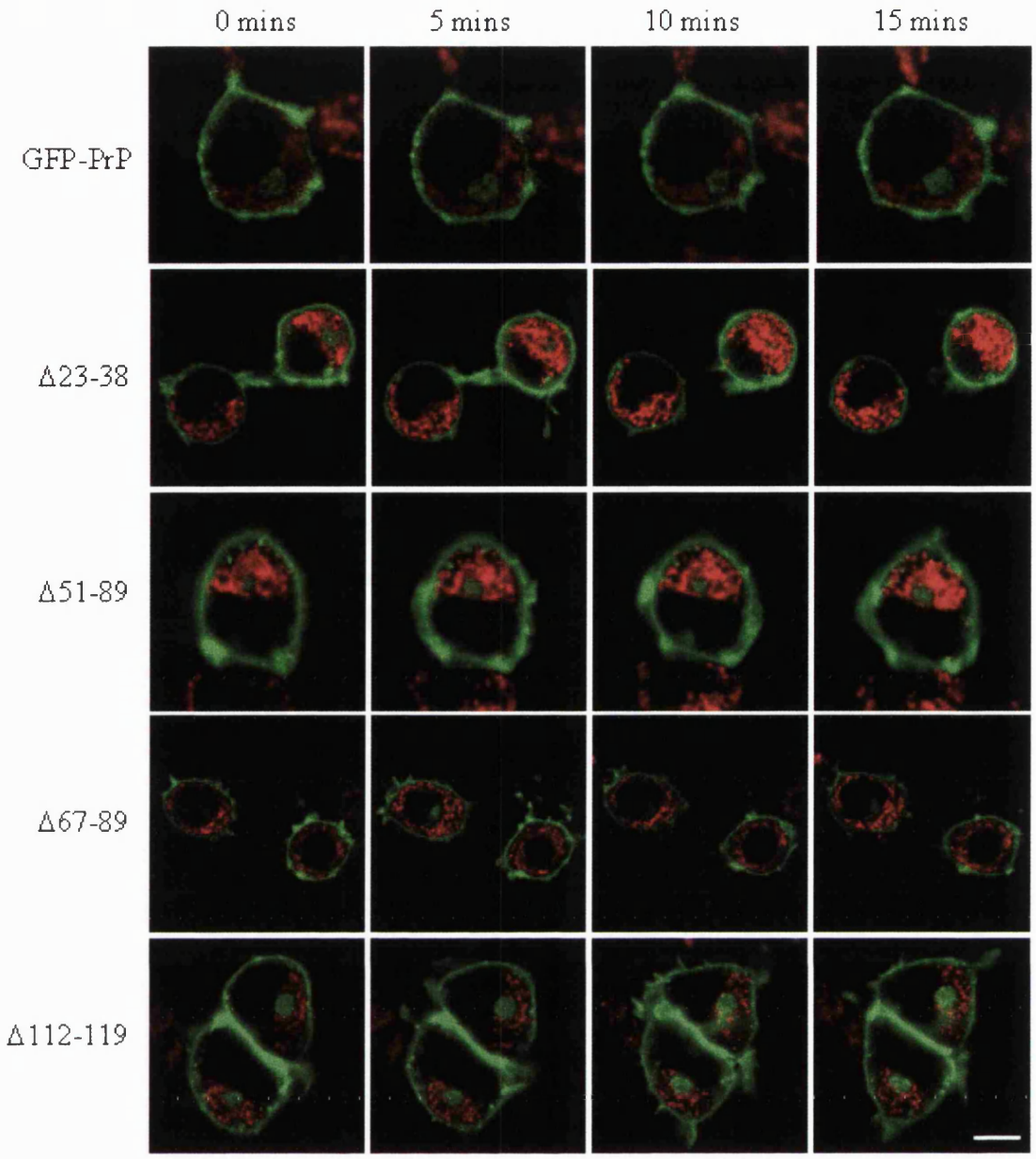

Figure 5.14 F14 GFP-PrP^c and cell surface F14 GFP-PrP^c mutants stained with redox sensor red and incubated for 15 minutes with 100 μM $CuSO_4$. Images were captured at 0, 5, 10, and 15 minutes using a Zeiss LS 550 confocal microscope. Deletion of the octameric repeat domain (Δ51-89) showed the greatest increase in probe signal with the other mutants unaffected. Scale bar = 10 μm.

An increase in oxidative stress is seen in the cells expressing the deletion of the octameric repeat region (Δ51-89), shown by significantly increased probe intensity in response to Cu treatment ($F = 6.58$, $p = 0.008$). The remaining mutants, deletions of the far N-terminus (Δ23-38), all but one octameric repeat (Δ67-89) and the palindromic region (Δ112-119), showed no significant increase in oxidative stress compared to the GFP-PrP construct (see figure 5.14 and 5.15). Cu-4xGly and glycine only treatments showed no significant change

in the level of intracellular free radicals in any of the cell lines (figure 5.15 c and d respectively).

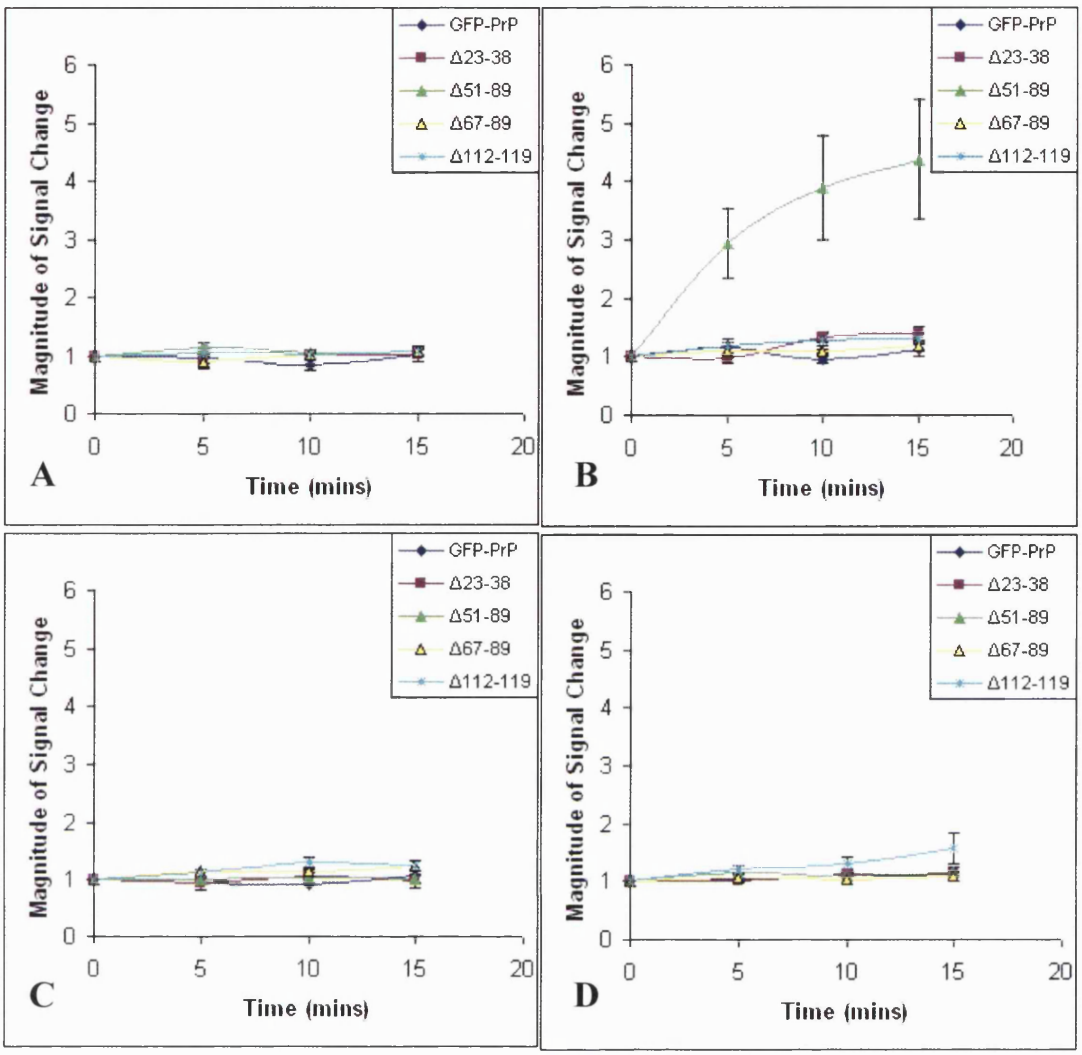

Figure 5.15 Quantification of Redox Red probe signal intensity in F14 GFP-PrP^c and cell surface mutant cell lines, in response to A) no treatment, B) 100 μM CuSO4, C) 100 μM Cu-4xGly, and D) 400 μM Glycine. The change in intensity (as recorded by the Zeiss LSM software at the time of image collection) is expressed as a ratio of time point value: time 0 value, to show the magnitude of the signal change comparable to the time 0 reading. A significant increase in intracellular oxidative stress is seen only with the deletion of the octameric repeat domain (Δ51-89) in response to the free Cu insult. n = min 12, max 25 cells.

5.3.3.3 F14 and F21 cells, Copper, and Free Radical Detection by DCFDA Assay

F14 and F21 cells were used to look at the effect of PrP^c on the ROS caused by Cu. Cells were prepared in microtitre plates, stained with CM-H_2DCFDA probe, and reagent (100 μM CuSO4, 100 μM Cu-4xGly, 400 μM Gly) was added at time 0, with readings taken by a fluorescence microplate reader at time 0, 30 minutes and 2 hours.

The background rate of conversion of the probe to a fluorescent signal by ROS is significantly higher in the F14 (PrP null) cells than in the F21 cells ($F = 6.17$, $p = 0.006$; figure 5.16a), demonstrating that the F14 cells are unable to deal as well as the F21 cells with the ROS produced during metabolism and so suffer a greater basal level of oxidative stress than the F21 cells. The presence of ROS rises in the F14 cells F21 cells treated with free Cu (figure 5.16b), this is significantly greater in the F14 cells ($F = 26.62$, $p < 0.001$). No increase in the levels of ROS above basal metabolism is seen for either treatment with Cu-4xGly ($F = 0.13$, $p = 0.72$) or glycine alone ($F = 0.02$, $p = 0.884$), and these treatments appear to reduce the difference in stress levels between the cell lines, an effect that may be due to protection against the free radicals by glycine (figure 5.16c and d respectively).

As for the individual cell data from the redoxsensor® red probe, this data is in agreement with the LPO results for oxidative stress markers, which showed that significant markers were seen for the null cells in response to free Cu but not for the Cu-4xGly. This data shows that endogenous PrP^c directly protects against oxidative stress induced by increased Cu levels, and also that PrP^c helps control free radical levels within the cell during normal respiration.

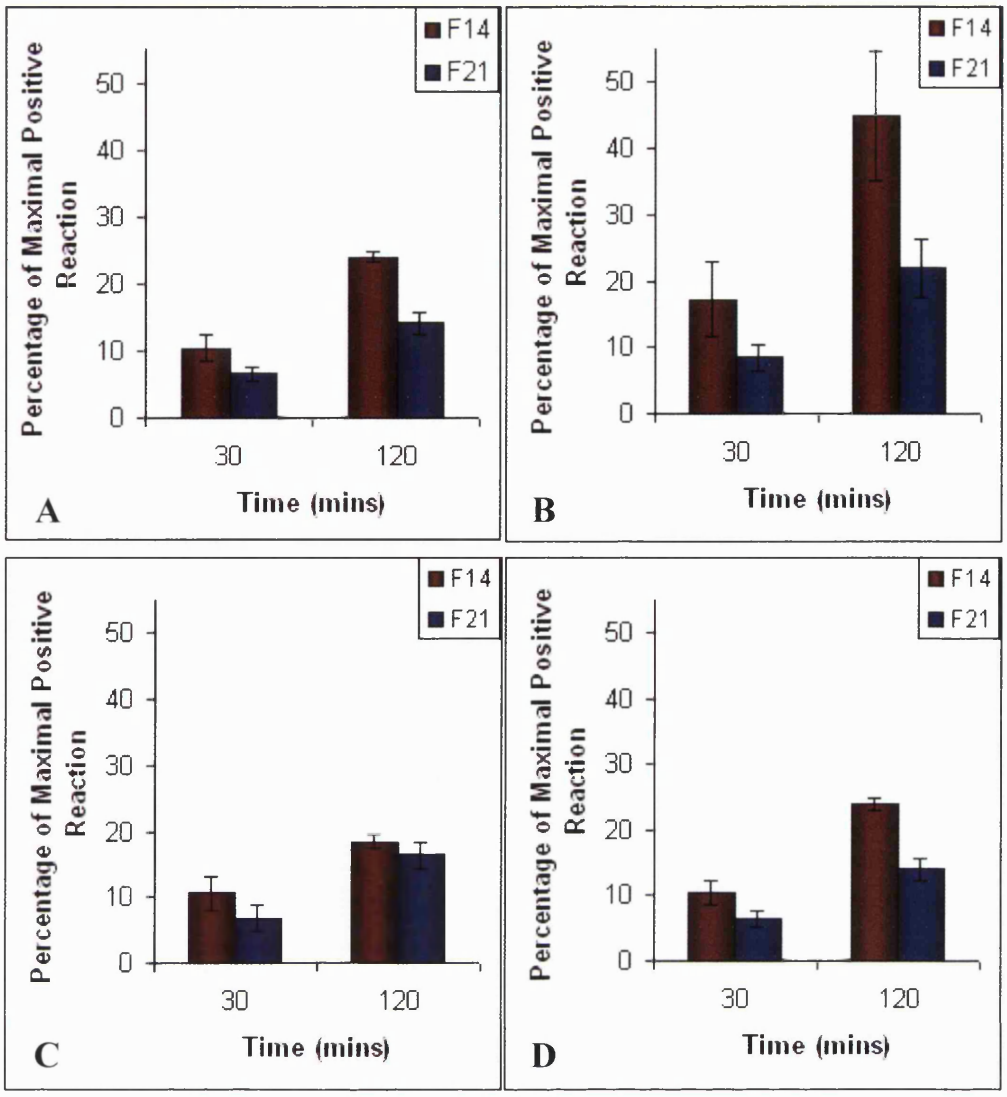

Figure 5.16 F14 and F21 cell oxidative stress measured by DCFDA assay when cells are A) untreated, or treated from time 0 with B) 100 μM CuSO4, C) 100 μM Cu-4xGly, or D) 400 μM glycine alone. The increase plotted has been calculated as a ratio of time point value:time 0 value, to show the magnitude of the increase comparable to the time 0 reading. Shown are the mean and SEM. n = 5 repeats, each of 6 replicates.

To ensure that the Cu-4xGly was unable to induce oxidative stress and that there was not a time delay in radical production F14 and F21 cells were treated with 100 μM Cu-4xGly for 24, 48, 72, or 96 hours, or left untreated, then assayed using the CM-H_2DCFDA assay to look for changes in the oxidative stress levels of the cells. Results are shown in Figure 5.17, and are corrected for viability of the cells.

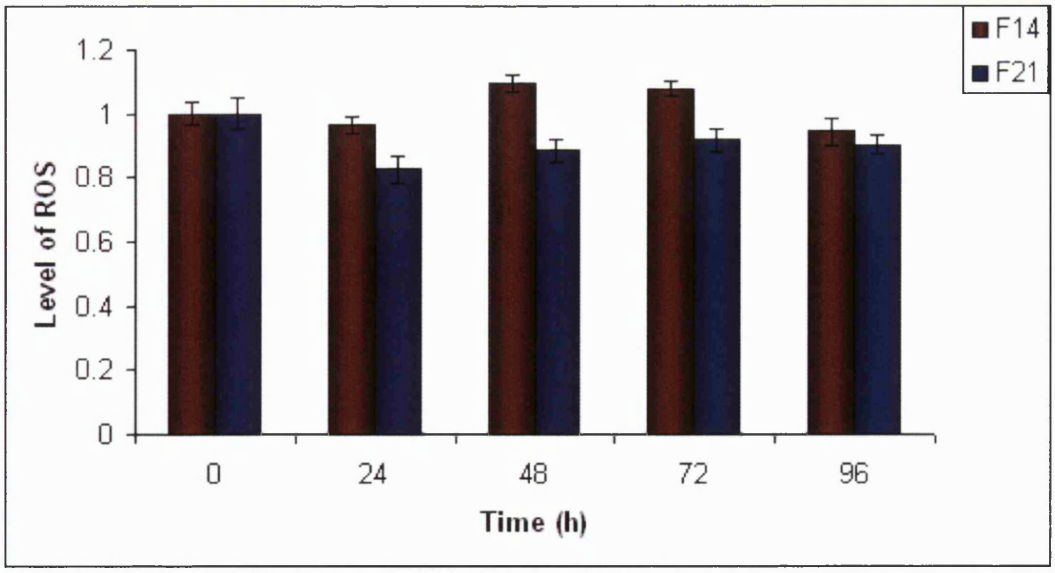

Figure 5.17 F14 and F21 cells were treated for 0, 24, 48, 72, or 96 hours with 100 μM Cu-4xGly, then intracellular oxidative stress levels were measured by DCFDA assay. The level of ROS plotted has been calculated as a ratio of time point value:time 0 value, to show the magnitude of the change comparable to the time 0 reading. Shown are the mean and SEM. No significant change in oxidative stress is seen (F = 0.6, p = 0.44). n = 4 repeats, each of 6 replicates.

Since Cu-4xGly is not inducing oxidative stress at any time point but the concentrations used caused significant death by four days (see section 5.1), it is unlikely that the mechanism by which PrP^c protects against bound copper is removal of an oxidative stress insult. Instead it is likely that the protection that PrP^c exhibits against copper induced cell death, when copper is administered as a chelate, is due to the ability of PrP to bind the metal ion thereby preventing copper ions binding to and denaturing cellular proteins resulting in cell cycle arrest and cell death.

The potential for PrP^c to regulate levels of ROS in response to 50μM MnSO4, which, like copper, is a highly reactive redox metal, was investigated. Also, to determine if PrP^c could act against a direct ROS insult, and not just prevent oxidative stress by metal binding, oxidative stress was induced using 1 % DMSO, 20 mU xanthine oxidase, and also 100 μM hydrogen peroxide, which is an extremely potent ROS releasing agent (figure 5.18).

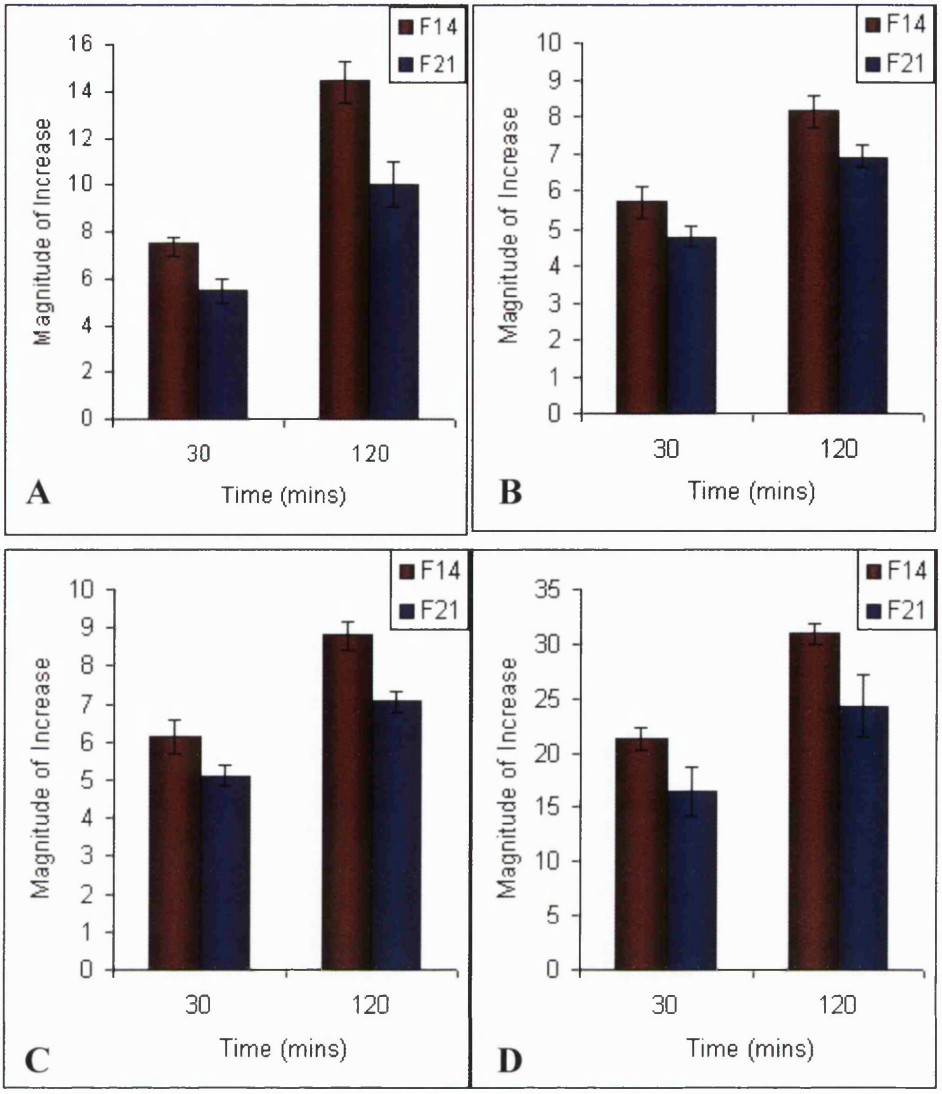

Figure 5.18 ROS detected in F14 and F21 cells in response to Mn, and agents inducing oxidative stress. Cells were treated for 2 hours with (A) Mn, (B) DMSO, (C) xanthine oxidase and (D) hydrogen peroxide. Measurement of ROS was made at time 0, 30 minutes and 2 hours using the DCFDA assay. Shown are mean and SEM. n = 5 repeats, each of 4 replicates for Mn, n = 6 repeats, each of 4 replicates for oxidative stress agents.

In addition to the effect of Cu on intracellular oxidative stress levels, Mn, DMSO, xanthine oxidase and hydrogen peroxide all cause an increase in oxidative stress in both cell lines. The F21 cells showed a much lesser increase in ROS compared to the F14 cells in response to the Mn and hydrogen peroxide insults, however this protective effect was not as evident against the DMSO and xanthine oxidase insults, most likely due to these reagents producing a less potent insult.

5.4 Conclusions

The high conservation of the copper-binding octameric repeat region across all characterised mammalian species (Wopfner *et al.*, 1999), suggests that copper binding is fundamental to PrP^c function. Previous studies have found PrP^c protects neurones against copper toxicity (Brown *et al.*, 1998; Brown, 2004; Nishimura *et al.*, 2004), leading to the hypothesis that PrP^c is involved in cellular protection against metal ion fluctuations. Furthermore, PrP^c has been shown to have superoxide dismutase-like activity when copper is bound (Brown *et al.*, 1999; Wong *et al.*, 2000; Brown *et al.*, 2001), resulting in the development of the highly controversial theory that the function of PrP^c is as an anti-oxidant.

The data presented here clearly show that PrP^c protects against toxicity induced by copper and oxidative stress. The protective effect against copper is much more pronounced when copper is delivered to PrP^c via a carrier such as glycine. In biological systems copper is chelated by chaperones or amino acids to protect against its high toxicity, and so is rarely found in a free or unbound form, therefore these findings are consistent with a protection effect that would be physiologically relevant. However, the studies on PrP^c protection against free radicals on exposure to copper and copper-glycine showed that changes in free radical levels were only seen when free, unbound copper was applied to the cells. The copper-glycine did not induce oxidative stress in the null cells despite being significantly more toxic to the cells than the free copper. Therefore, protection against copper is not just against the oxidative stress that copper can produce by switching redox states, it is against the metal ion itself.

The cause of this non-oxidative toxicity of copper when presented as a chelate may be due to increased incorporation into incorrect cellular proteins. Copper is more efficiently delivered into PrP^c when presented as a chelate (Brown, 1999). It is likely that chelated copper ions are also more efficiently delivered into other copper-binding proteins than free ions, saturating cellular copper storage mechanisms and resulting in copper incorporation into proteins that would, under standard physiological conditions, bind other metal ions. Predki and Sarkar (1992) showed that copper could be substituted for zinc in zinc finger proteins and by doing so ablates their function. Chelation of copper is known to increase uptake by neurones (Hartter & Barnea, 1988), therefore it is likely that more copper is being transported inside the cells and so can bind to intracellular proteins. Other

mechanisms by which copper is suggested to cause toxicity included altering energy metabolism and glycolysis (Lai & Blass, 1984), and by formation of cupric salt crystals, which could damage cellular organelles (Johnson & Campbell, 1982).

The regions of PrP^c important for protection against the copper, DMSO and xanthine oxidase insults are illustrated figure 5.19. When the different insults are considered together, deletion of the same regions repeatedly reduces PrP^c activity. In agreement with previous studies (Brown *et al.*, 2001; Zeng *et al.*, 2003; Sakudo *et al.*, 2003), the octameric repeat domain is essential for the protective function of PrP^c. Since the protection against copper toxicity is impaired in the absence of the octameric repeat domain this region is evidently important for PrP^c function. The fifth copper-binding site, although still intact, is unable to compensate for this effect. This suggests that the PrP^c protective response against copper requires more than one copper molecule to be chelated in the N-terminal region. In addition, the anti-oxidant activity of PrP^c is diminished in the absence of Cu binding to the octameric repeat region (Brown *et al.*, 1999), therefore in the absence of the octameric repeats a lack of function would be expected. This was observed in these experiments. The observation that when just one repeat is present protective ability is restored is also indicative of the importance of this region for the function of the protein.

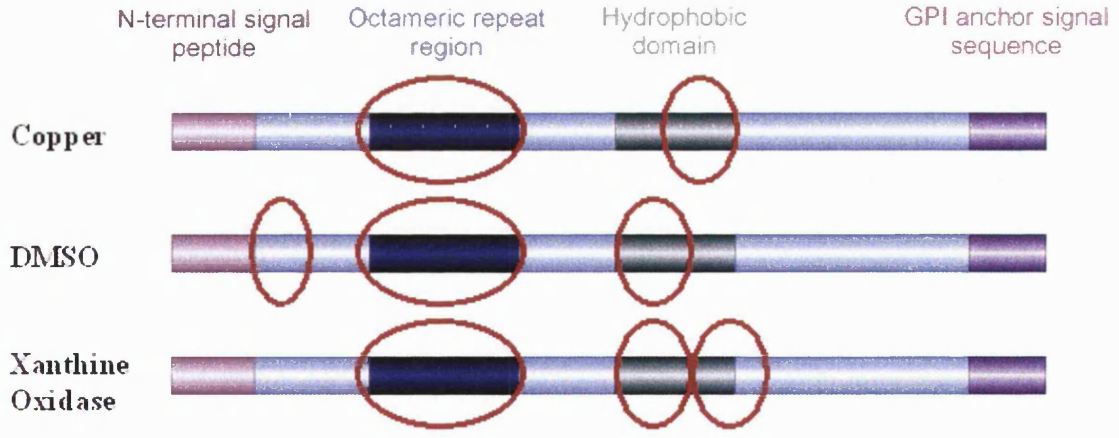

Figure 5.19 Domains of PrP^c important for protection against copper, DMSO, and xanthine oxidase insults.

Deleting the hydrophobic region or part of it impairs PrP^c function in response to Cu or oxidative stress. This region has previously been shown to be essential for PrP^c activity (Cui *et al.*, 2003). If the cellular protection shown by PrP^c is an enzymatic response the removal of the hydrophobic region, which is likely to be at the core of the protein, would

be likely to result in destabilisation of the tertiary structure (see chapter 4), so affecting the active site and preventing the protein from functioning properly. Alternatively this region may be a radical binding site for a chelation function, or may mediate binding to other cellular proteins to commence signal transduction cascades that might result in activation of cellular protection factors.

Deletion of amino acids 23-38 reduced PrP^c protection against DMSO, but not xanthine oxidase or copper. This region has been suggested to be involved in PrP^c internalisation (Sunyach *et al.*, 2003). DMSO is highly cell permeable, therefore it may penetrate the cell and cause damage. The Δ23-38 mutant may be unable to internalise quickly enough to protect the cell. This would not be the case for xanthine oxidase or copper where the insults could be mostly removed at the cell surface.

In conclusion, the data presented shows PrP^c is able to protect against cellular injury from copper, manganese and oxidative stress. Defence against copper is due to both protection against non-oxidative toxicity of the metal ion itself, and prevention of oxidative stress induced by redox changes that the metal ion can undergo. The protective ability of PrP^c against copper and oxidative stress requires the octameric repeat domain and the hydrophobic region. In addition, the N-terminus may play a role in defence against cellular insults possibly by controlling the position of PrP^c within the cell.

6 Discussion

There is a lack of knowledge on the regulatory control of PrP^c expression at the genetic level and, despite much investigation, no consensus concerning the function of PrP^c. This study aimed to reveal the mechanisms of gene control at the DNA level, and to further the knowledge of the metabolism and properties of PrP^c. Ultimately, this study endeavoured to provide clues as to the true function of PrP^c and offer potential pathways for therapeutic intervention in TSE pathogenesis.

6.1 *Prnp* and Tissue Specific PrP^c Expression and Regulation

The control of *prnp* is complex. It involves control elements in the pre-exon 1 promoter region, requires intron 1 for full activity, and responds to certain cellular stresses via heat shock elements found in the region of DNA preceding the promoter region (Baybutt & Manson, 1997; Inoue *et al.*, 1997; Shyu *et al.*, 2000; Shyu *et al.*, 2002; Premzel *et al.*, 2005). In addition, this study has shown that intron 1 may have its own promoter activity, sufficient to drive the production of PrP mRNA lacking exon 1. In bovine *prnp* this alternative transcription is possibly initiated by the presence of a TATA box, a motif that had not been found previously in the PrP gene of any characterised species (Basler *et al.*, 1986; Westaway *et al.*, 1994; Inoue *et al.*, 1996; Saeki *et al.*, 1996; O'Neill *et al.*, 2003). To determine the importance of the TATA motif in the production of an mRNA transcript, mutational studies to remove the important bases could be used to look for reduction or elimination of the transcript lacking exon 1. An additional finding of this study is that exon 1 may be involved in *prnp* regulation either at the gene or mRNA level. The precise nature of exon 1 in the control of PrP^c expression is an area of further study.

The construct containing the full-length *prnp* promoter plus non-coding region differed in expression levels in the different cell types studied. Intron control elements have been implicated in tissue specificity, implying that the importance of the intron 1 control region may lie in tissue specific expression of PrP^c. PrP^c is expressed at different levels in different tissues, with the highest expression found in tissues of the central nervous system.

This variation is involved in disease propagation and pathology (Brown *et al.*, 1994; Brandner *et al.*, 1996; Scott *et al.*, 1989; Fischer *et al.*, 1996). Differences in genetic regulation may account for tissue specific expression, however PrP^c half-life also differs across different tissues (Caughey *et al.*, 1989; Borchelt *et al.*, 1990; Parizek *et al.*, 2001; Li *et al.*, 2003), which may contribute to the different PrP^c levels. Consequently, not only the genetic regulation of *prnp,* but also protein metabolism of PrP^c is influenced by the underlying cell type. Expression level and turnover may be related to PrP^c function. In tissues where PrP^c is less required, it may persist for longer than in tissues where it is highly functionally active and requires rapid replacement.

The intron 1 control region may be involved in gene activation in response to various stresses. This study shows that wild type mouse neuroblastoma fusion cells, mouse myoblasts, and monkey kidney cells expressing the bovine complete non-coding region, and human neuroblastoma cells expressing just intron 1 and exon 2 of the non-coding region are up-regulated in response to copper, despite the full length construct showing no change in activity in any of these cells lines. Mouse PrP^c knock-out neuroblastoma fusion cells expressing either of the above constructs showed up-regulation to a DMSO insult, as did the mouse myoblast cells expressing intron 1 and exon 2 only. This suggests that this region could be important in stress associated *prnp* regulation in certain cell types. Activation of these control mechanisms may only happen on PrP^c depletion, when the cell becomes vulnerable to the insult and so activates transcription via up-regulation of stress associated transcription factors. Additionally, hamster *prnp* usually transcribes a two-exon splice variant, however the emergence of a three-exon splice variant has been found during infection (Li & Bolton, 1997). Therefore, the intron 1 region may have a role in splicing, with stress altering the splice variant produced. Further studies should aim to determine the specific regions of *prnp,* and the control elements contained within these regions, that are important for alteration in gene activity in response to stimuli.

From the data presented in these studies it is not possible to conclude if the different responses to stimuli seen across the cell lines are due to the transfection of bovine as opposed to murine *prnp.* Experiments are currently underway to establish if murine *prnp* constructs behave in the same way as the bovine constructs. This is especially important since four of the host cell lines are murine and the variation in genetic responses seen cannot be attributed to changes in *prnp* activity, but may instead be a confounding factor introduced by the underlying species difference.

6.2 *Prnp*, PrP^c and Copper

PrP^c is a copper binding protein, with up to five copper molecules coordinated within the unstructured N-terminal region. Four copper molecules may be bound by the octameric repeat domain and a further copper molecule is potentially bound by a fifth site located immediately C-terminal to the octameric repeat domain (Hornshaw *et al.*, 1995; Brown *et al.*, 1997; Jackson *et al.*, 2001). Previous studies have shown that copper regulates *prnp* (Toni *et al.*, 2005; Varela-Nallar *et al.*, 2005), however the two studies report opposing effects, with down-regulation seen by Toni *et al.* and up-regulation by Varela-Nallar *et al.* This study finds that cells deficient in PrP^c up-regulate *prnp* in response copper, but unlike the above previous studies, no effect of copper was found on any of the cell lines that endogenously expressed PrP^c. In this study, however, copper was applied as copper sulphate, unchelated, so it may not have been delivered into the cell as efficiently as when applied bound to a chelator. Evidence suggests that copper is more efficiently incorporated into PrP^c when it is delivered via a chelator (Brown, 1999; Ji & Zhang, 2004). In the study by Varela-Nallar *et al.* (2005), where an increase in promoter activity was observed in response to copper, the copper was applied as a glycine chelate and produced a reaction at lower concentrations than those that were used here, 50 μM as opposed to 100 μM. Therefore, to further these studies, copper applied with glycine should be studied. Up-regulation of *prnp* in response to copper-glycine in the Varela-Nallar *et al.* study may not directly involve copper incorporation into PrP^c, but rather may be due to the greater toxicity of the chelated copper as opposed to free copper to the cells. This is supported by the findings of the current study where only the null cells were seen to respond by up-regulation of *prnp* in response to copper. This may cause the cell to initiate a greater protective response than that required to deal with a free copper insult, including an increase in *prnp* promoter activity.

The importance of chelation for copper incorporation into PrP^c is seen in the copper induced internalisation reaction. Cell surface PrP^c is internalised much more rapidly when copper is applied as a glycine chelate. In addition, data from cellular viability assays comparing PrP^c null and wild type cells shows that PrP^c can efficiently protect against chelated copper, which is significantly more toxic to null cells than free copper.

When chelated with glycine, copper induced PrP^c internalisation is significant at concentrations as low as 5 μM $CuSO_4$. This is within normal extracellular copper

concentrations. At 20 μM this reaction is significant after just ten minutes exposure. Copper concentrations at the synapse are reportedly around 15 μM when the neurone is in its polarised resting state and can rise to over 100 μM on depolarisation (Vassallo & Herms, 2003). This suggests that PrP^c is quickly turned over or recycled at the synapse under resting conditions of the neurone, and on depolarisation would be internalised even more rapidly. The fate of internalised PrP^c is less clear. It is directed inside the cell, but may be trafficked to recycling, early or late endosomes, or to the golgi (Borchelt *et al.*, 1993; Shyng *et al.*, 1994; Magalhães *et al.*, 2002). The destination of PrP^c may be influenced by the concentration of exogenous copper. Under low copper conditions, internalisation may result in targeting of PrP^c to recycling endosomes where it can be stored for future use. Under high copper conditions, it may be internalised too rapidly to be directed to one specific site within the cell. This could result in cell surface PrP^c being sent back into the recycling pathway but also a significant quantity being diverted for destruction by lysosomes or the proteasome. If this were the case, it is likely that the promoter would be up-regulated in the event of sustained copper insult, as the cellular levels of PrP^c become depleted and cells are less able to cope with the insult.

Exogenous concentrations of metal ions are altered during the disease pathogenesis (Wong *et al.*, 2001b). Perturbations include decreased copper, iron, magnesium and calcium, and increased manganese. It is unclear if these variations are the result of or caused by disease pathogenesis. The metal ion perturbations seen during disease pathogenesis could alter *prnp* activity and might be considered for further investigation. Also, the effects of prolonged metal ion exposure on gene activity could be investigated in the future.

In contrast to previous studies that find the far N-terminal amino acids 23-38 of PrP^c are essential for internalisation (Shyng *et al.*, 1995; Nunziante *et al.*, 2003; Sunyach *et al.*, 2003), the data presented here show that the octarepeats and the palindromic region override requirement for the far N-terminus for PrP^c trafficking. The difference between the results presented here and those seen previously for the N-terminal trafficking may be due to inherent limitations of a GFP-fusion protein system. The inclusion of a large tag such as GFP within a protein may affect its structure, metabolism or processing. The GFP tag was inserted into the N-terminal, unstructured region of PrP^c to avoid the structural changes that might arise had it been inserted into the structured C-terminus. The C-terminal antibody (5C3, Li *et al.*, 2000) used to detect internalised GFP-PrP^c in the PrP^c trafficking studies is unable to detect synthetic peptides, and so is likely to be directed

against an epitope formed by correct folding of PrP^c. This indicates that the GFP tag is not interfering with the folding of the C-terminus. The GFP-PrP^c construct is correctly expressed at the cell surface so under normal conditions the processing of the protein is not affected, and GFP-PrP^c is internalised in response to copper as is seen for the untagged PrP^c, in agreement with the processing of PrP^c reported previously (Pauly & Harris, 1998; Brown & Harris, 2003). However it was still possible that the tag might alter processing related to the N-terminus. For this reason the immunofluorescent staining was carried out on the Δ23-38 mutant without the GFP tag. This showed that the GFP might be interfering with the processing of the mutant. The GFP tagged mutant was observed predominantly at the cell surface, whereas the untagged mutant was retained within the cell in a pattern that indicated it was in the membranes of organelles throughout the cell. This difference may be due to GFP in intracellular organelles fluorescing less intensely than cell surface GFP due to organelle acidity quenching the signal. The intracellular immunofluorescent staining pattern of the Δ23-38 mutant seen in this study also contradicts the previous studies on the role of the N-terminus in PrP^c trafficking. These previous studies reported that deletion of this region stopped PrP^c internalisation, but in the current study Δ23-38 PrP^c was retained within the cell. Therefore little could be concluded from its response to copper. The contrast seen may be due to experimental methods. The studies previously reporting the effect of N-terminal deletion on PrP^c trafficking may have used un-permeablised cells, preventing the anti-PrP^c antibody from staining mutant PrP^c retained within the cell, and instead only the fraction of mutant PrP^c that reaches the cell surface would be observed.

The mechanism of PrP^c internalisation may be altered by increased copper concentration. The importance of the palindromic cleavage site suggests that PrP^c may be internalised not in its complete form but, instead, after cleavage by proteases at the cell surface. The requirement for the palindromic region for PrP^c trafficking from the cell surface in response to copper seen in the present study has not been shown previously. This cleavage site is associated with normal, non-disease related cleavage of PrP^c. At the cell membrane PrP^c is localised to lipid rafts (Mahfoud *et al.*, 2002; Brügger *et al.*, 2003). The N-terminal amino acids may have a function directing PrP^c out of lipid rafts for internalisation via clathrin-coated vesicles (Taylor *et al.*, 2005). The C-terminus and GPI anchor may hold PrP^c in lipid rafts, while cleavage at the palindromic region could release the N-terminus. This would allow the N-terminus to move out of the lipid raft domain and be internalised by the clathrin-mediated pathway. The data presented in this study followed the path of N-

terminally-GFP tagged PrP^c, or untagged PrP^c with an N-terminally directed antibody. Therefore, from the current data, it is not possible to determine if the N-terminus alone is directed into the cell. The C-terminus may control the cellular position of the structured region of PrP^c (Kaneko *et al.*, 1997), causing it to be retained at the cell surface for a yet undetermined function. Alternatively, since the C-terminus is required for calveolae-mediated internalisation (Peters *et al.*, 2003), the two fragments of PrP^c may be internalised by different pathways, and potentially sent to different destinations. Disruption of lipid rafts and therefore caveolae-mediated internalisation could be used to determine the importance of this mode of internalisation. Caveolae-mediated internalisation may account for the differences observed for the N-terminal Δ23-38 mutant, as clathrin-mediated internalisation may have been blocked, and therefore the protein would be directed into other pathways for internalisation.

Although the above hypotheses explain some differences between the results presented here and those of other groups, they do not clarify the role of copper. Copper may increase cleavage of PrP^c, perhaps by inducing structural changes within the N-terminus allowing exposure of the palindromic cleavage site to proteases. This might increase the rate of internalisation of the N-terminus, thus directing more copper inside the cell. Clathrin mediated endocytosis usually occurs via the classical endocytic pathway, where PrP^c would be directed to acidic vesicles and so might release copper. From the acidic vesicles, copper could be directed back out of the cell by incorporation into cellular exocytotic vesicles, such as synaptic vesicles, and then released back into the surrounding environment. This is supported by a previous study by Brown (1999), who found that copper up-take and release at the synapse directly correlated with the expression of PrP^c. Following internalisation, the cleaved PrP^c would have served its function as a copper transporter and so would then be targeted for destruction. Degradation of PrP^c following cleavage is likely to require concomitant up-regulation of *prnp* to maintain cellular PrP^c levels. This is could explain copper mediated up-regulation of the promoter seen in this study and by Varela-Nallar *et al.* (2005). Alternatively, if the function of PrP^c were to be delivery of copper into cellular enzyme systems, it might respond to decreased copper concentrations by up-regulating gene activity and protein to allow the maximal collection of copper from the surrounding environment.

Copper may also mobilise PrP^c under conditions where cell surface PrP^c is depleted or unable to bind copper. The Δ51-89 mutant was seen to accumulate at the cell surface in

response to copper. To determine if copper alters trafficking to the cell surface as well as away from it, wild type cells could be pre-treated with phospholipase C or D to remove GPI anchored proteins from the cell membrane, and the appearance of PrP^c at the surface could then be monitored with and without increased exogenous copper.

The presence of PrP^c significantly protects the cells from copper. Cell viability assays showed that PrP^c significantly protected wild type cells against cell death induced by glycine chelated copper compared to PrP^c null cells. Glycine chelated copper treatment of PrP^c null cells did not produce the significant increase in ROS that free copper was able to induce. Therefore, protection against copper toxicity is not just against the oxidative stress that results from copper redox activity, but also against the metal ion itself. The protective effect may be due to the chelation of the copper ions within the octameric repeat region of PrP^c, or due to initiation of wider cellular protection mechanisms. For both copper induced internalisation and protection against the copper ion insult, the intact octameric repeat domain is required. This suggests that the binding of copper to this region is central to PrP^c function. Support for this is provided by previous studies, which have shown that disease associated mutation of the octameric repeat region has adverse effects on PrP^c copper induced internalisation (Perera & Hooper, 2001). Furthermore, PrP^c protective ability is diminished in the absence of the octameric repeat domain (Brown *et al.*, 2001; Sakudo *et al.*, 2003). Only one repeat is required to restore PrP^c trafficking and protection, albeit at a depleted level, emphasising the importance of this region.

The lack of activity when the octameric repeat region is missing suggests that the fifth copper-binding site is either not involved in this function or unable to coordinate copper correctly without some of the amino acids of an octarepeat. Brown *et al.* (2001) showed that at least two coppers ions need to be co-ordinated to the octameric repeat region for significant antioxidant activity, therefore one full repeat and the fifth site together may bind two copper molecules and restore PrP^c protective function and trafficking. A recent study suggests that in the absence of the octameric repeat domain, the fifth site has enhanced copper binding activity (Thompsett *et al.*, 2005). With just one repeat present, incorporation into the fifth site may be stronger than in the presence of the entire domain, allowing it to partially compensate for the lack of the remaining repeats. Mutational studies of the fifth site in the presence of a single octameric repeat would clarify this point.

The finding that the hydrophobic region of PrP^c is necessary for both its correct cellular processing and for function is not unexpected. Hydrophobic domains stabilise the structure of proteins by forming the core. In the absence of this region, the protein would not be expected to fold correctly and so would be redirected into cellular degradation pathways, such as ERAD, for destruction. Incorrectly folded protein is unlikely to retain structural features essential for function such as enzymatic active sites, and so would be expected to lack normal function. However, a study by Cui *et al.* (2003) has shown that these deletions do not significantly affect the secondary structure of PrP^c, with the mutant proteins expressing similar alpha helical content to the wild type. Therefore any effect that these mutations have on PrP^c structure would have to be at the tertiary level, which could still produce the same lack of function.

As previously stated, PrP^c protection against copper is directed against both oxidative stress caused by processes such as the Fenton reaction and also against the copper ion itself. These experiments are the first to show that PrP^c protects against non-oxidative toxicity. The protection provided by PrP^c against oxidative stress caused by free copper is rapid, in agreement with the internalisation studies that saw copper significantly internalise PrP^c within 10 minutes at concentrations of 20 μM or greater. Direct incorporation of copper into PrP^c may be part of PrP^c protective ability, but direct protection against free radicals may also be involved. This protection may be enzymatic, with PrP^c protecting by SOD like activity, or it may be a result of PrP^c having a high affinity for certain ROS and effectively mopping up the free radical insult before it can damage the cell. Further work would need to establish non-oxidative mechanisms by which chelated copper damages the cell, and thus determine how PrP^c is able to protect against these mechanisms. The requirement of the octameric repeat domain for the protection response strengthens the role of copper binding as the protective mechanism. However the hydrophobic domain, which causes relocation of PrP^c within the cell, also impairs the survival of copper treated cells. This may be a result of PrP^c not reaching the cell surface and so not being able to sequester copper before it can cause damage to the cell. Alternatively, it may be that the PrP^c hydrophobic core contains or stabilises an active site that is essential for its protective function.

The regions of PrP^c identified as important for metabolism and function are shown in figure 6.1.

The Cellular Processing and Function of PrP^c

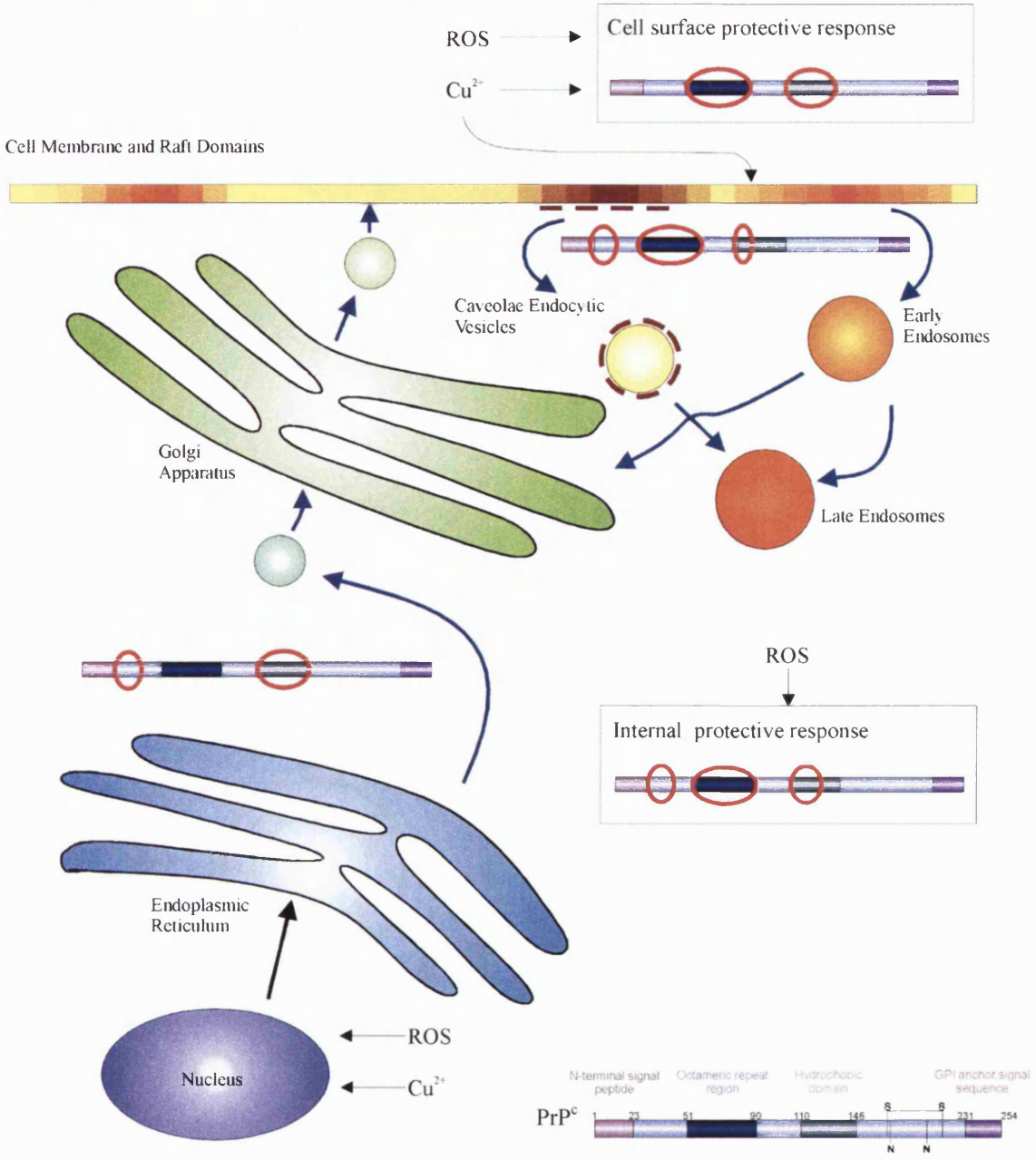

Figure 6.1 Cellular processing and function of PrP^c. The domains identified as important by the current study have been circled in red at the site where they are found to be relevant.

6.3 *Prnp*, PrP^c and Oxidative Stress

PrP^c has previously been suggested to have a role in the protection against cellular oxidative stress and PrP^c itself has been found to have superoxide dismutase like activity in the presence of bound copper (Brown *et al.*, 1999; Brown *et al.*, 2001). Data presented here show that PrP^c null cells have higher basal levels of ROS suggesting that PrP^c has a

role in modulating cellular antioxidant activity in unstressed cells. Oxidative stress induced by DMSO was found by this study to up-regulate the *prnp* promoter. Wild type PrP^c expressing cells showed increased survival in response to oxidative insults induced by DMSO and xanthine oxidase than PrP^c null cells. The increased survival is most likely to be due to the ability of PrP^c wild type cells to maintain lower intracellular levels of free radicals after insults from DMSO, xanthine oxidase and hydrogen peroxide compared to null cells. This data supports a role for PrP^c in dealing with cellular oxidative insults.

Deletion studies showed that the octameric repeat domain was essential for this protection. It is likely that the need for copper binding is the reason for the requirement of this domain. Similarly to the internalisation studies, function is restored in the presence of just one repeat. The hydrophobic domain is also required for this protection. However, in contrast to the internalisation studies, the deletion of the palindromic region alone does not abolish the protection against oxidative stress. This suggests that cleavage of this site may be less important for protection against oxidative stress insults.

A recent study by Watt *et al.* (2005) proposed that cleavage of cell surface PrP^c at the second cleavage site found at the end of the octameric repeat domain (amino acids 88-89 in mice) was the first step in the activation of a PrP^c mediated signal transduction cascade, which could result in the up-regulation of cellular stress proteins. This form of cleavage has previously been associated with disease due to increased cleavage products being found in infected brains (Chen *et al.*, 1995). In disease, the C-terminal fragment produced by this cleavage is protease resistant, however the fragment produced in response to oxidative stress is not (Watt *et al.*, 2005). Watt *et al.* find that mutation of the alanine residue at amino acid position 116 to valine (A116V) inhibits cleavage at the end of the octarepeat region in response to oxidative stress. This indicates that residues of the palindromic region may be required for the second cleavage and the authors suggest that the interaction of the alanine (116) with the copper bound octameric repeats is likely to initiate cleavage. This is in contrast to the results presented here, which do not find that the palindromic region is necessary for protection against oxidative stress. However, the octameric repeat domain is required. In its absence the loss of copper binding and removal of the cleavage site at the C-terminus of the repeats may prevent correct processing in response to oxidative stress, and thus prevent activation of any protective cascade. The N-terminus enhances the formation of proteinase K resistant PrP (PrP^{res}), as shown by Lawson *et al.* (2001), who find that N-terminally truncated PrP^c, whilst still able

to form PrP^{Sc}, does so at a much slower rate. The inability to undergo oxidative stress mediated cleavage during the pathogenesis of prion disease could result in impaired ability to respond to the insult directly. Alternatively activation of a signal transduction pathway could increase gene activity to produce more PrP^{c} to compensate for the insult, providing more full length PrP^{c} that might be converted into PrP^{res}. Specific mutation of this cleavage site could clarify the importance of processing in the PrP^{c} mediated oxidative stress response.

The requirement for the hydrophobic domain suggests that the structure of the C-terminus must be intact for its correct function. The high conservation of this structure across several species suggests that it is of considerable importance to the function of PrP^{c}. Therefore, if following cleavage the C-terminus was to remain on the cell surface, it would be likely to perform some function. Watt *et al.* (2005) suggest that the N-terminus may be a signalling molecule, translocated inside the cell in response to the cleavage stimuli, and that the C-terminus remains on the cell surface as a receptor. Pathological PrP^{c} mutations associated with some TSEs impair PrP^{c} trafficking through the cell, and are retained within the ER (Singh *et al.*, 1997; Ivanova *et al.,* 2001; Negro *et al.*, 2001). Likewise the mutants with deletions of the hydrophobic region used here were trapped within the ER. If PrP^{c} could not be correctly trafficked to the cell surface it would not be able to perform a signal transduction function that requires cell surface activation by cleavage. If it has an alternative cellular protection function at the cell surface, any mutation that alters trafficking to the cell surface or affects that rate of movement away from the membrane may impair the ability of PrP^{c} to exert a protective response.

Cleavage of PrP^{c} in response to stimuli may not result in separation of the N-terminal and C-terminal fragments. Instead, the two termini may be separate subunits of the complete protein, able to bind together and be activated by the cleavage event. In this situation, the complete uncleaved PrP^{c} protein could act as a proenzyme. If this were the case PrP^{c} would not be the only example of such a protein. Various caspases are synthesized as a single-chain zymogen, and activated by cleavage of the protein in a linker region between two subunits, in some cases releasing the short linker segment (for review see Stennicke & Salvesen, 2000; Shi, 2004). PrP^{c} has two cleavage sites in its putative linker region and so could undergo single or double cleavage events. The double cleavage of PrP^{c} in this region could potentially release a linker sequence. However this has been considered previously and no linker sequence has been found (Watt *et al.*, 2005). In support of an

interaction between two subunits, a study by Yao *et al.* (2003) found that the six most N-terminal amino acid residues in the mature protein (positions 23-28) interact with amino acids 143-146 just prior to the start of helix 1, indicating that the two parts of PrP^c could be bonded together. This reaction is dependant on the formation of the beta sheet. Epitope mapping has also suggested that the N-terminus is able to interact with the C-terminus, possibly through the threonine located on the exterior of helix 2 at position 189 of the murine protein (Li *et al.*, 2000). This interaction was suggested to be caused by ligand binding. These potential interactions and the destinations of the separate termini of cleaved PrP^c are both worthy of further investigation. Dual antibody labelling of PrP^c using antibodies directed against the N-terminus and the C-terminus could be used to follow the termini on internalisation. Disruption of specific internalisation pathways could be used to determine if one terminus will internalise without the other.

6.4 *Prnp*, Prion Disease, and Disease Management

The aim of determining the normal metabolism and function of PrP^c in health is to better understand cellular pathways or processes where therapeutic intervention can be used to manage disease pathogenesis. The differences in the expression of the murine constructs compared to the equivalent bovine constructs in the cell lines studied, and the variation in number and location of transcription factor binding sites, shows that, although the gene structure is conserved across the two species, the gene sequence shows considerable variation. Single nucleotide polymorphisms of the human pre-exon 1 promoter region have been associated with sporadic CJD (Mead *et al.*, 2001). Theoretically even point mutations of transcription factor binding sites that might allow more potent factors to bind the sites could result in higher PrP^c expression levels and increased susceptibility to prion disease. The lack of conservation of these regions across species may mean that some species are at greater risk of prion disease than others. In addition, the Mead *et al.* study found several polymorphic sites within intron 1. Since this region appears to be important in *prnp* regulation, polymorphisms may result in altered gene control and as a consequence lead to phenotypes that are more or less susceptible to disease. Studies to identify specific DNA motifs that might affect gene activity may clarify the importance of these polymorphisms in disease.

During the end stages of the disease, PrP^{c} (or PrP^{Sc}) may be regulating itself. Data presented here show that PrP^{c} can up-regulate *prnp* activity significantly in PrP^{c} null cells, indicating that regulation is indirect, possibly via interaction with other cell surface proteins. The lymphocyte signalling with which PrP^{c} has been associated is activated by the lattice of PrP^{c} formed in caps at the cell membrane (Li *et al.*, 2001; Bainbridge & Walker, 2005). Exogenous PrP^{c} might interact with the cell membrane to produce a similar effect. During the early stages of disease progression endogenous PrP^{c} levels may become depleted due to conversion to PrP^{Sc}. The loss of function associated with this change, as well as altered metal ion concentrations, may result in the cell up-regulating *prnp*. This may cause increased levels of PrP^{c}, increased substrate for the conversion reaction, and, by the overall increase in PrP, a further increase in promoter activity causing the disease to progress in an exponential fashion. Down-regulating the promoter and breaking the cycle could be a very important method of therapeutic intervention. Further investigation to determine the method by which PrP^{c} is able to regulate *prnp* would be valuable. It would also be of interest to repeat the current studies with PrP^{Sc} to determine if its presence in disease can up or down-regulate *prnp*.

Agents that might alter *prnp* regulatory pathways resulting in PrP^{c} protein down-regulation may have a role in disease management by providing less substrate for conversion into PrP^{Sc}. Copper modulates *prnp* activity, but this reaction is variable across different cell lines, so it is still unclear if copper modulation of *prnp* could be useful. Copper chelators would have limited application in disease management due to the importance of copper in various enzyme systems including SODs. In agreement with previous studies (Rybner *et al.*, 1992; Cabral *et al.*, 2002), this work shows that ATRA down-regulates *prnp* and PrP^{c} expression. It is likely to exert its effect by alteration of several transcription mechanisms, including modulation of transcription factors involved in cellular differentiation and alteration of chromatin structure. Unfortunately the potential side effects to the regulation of other genes may make this drug unsuitable for use in TSE patients. Serious side effects can be seen in those treated with ATRA for promyelocytic leukaemia, including retinoic acid syndrome which may lead to organ failure and death (for review see Larson & Tallman, 2003). Therefore it is beneficial to continue the search for a more benign treatment for TSE patients.

DMSO has previously been suggested as a potential therapeutic agent for TSE treatment due to findings that the accumulation of PrP^{Sc} and disease progression was delayed in

DMSO treated hamsters (Shaked *et al.*, 2003). This is in contrast to the data presented here, which show that *prnp* is up regulated in response to DMSO. An agent that up-regulates PrP^c expression would be expected to provide more substrate for conversion and therefore would be unsuitable for use in disease therapy. This highlights the difficulty in using a multifaceted agent such as DMSO. Agents with a more unambiguous mode of activity may be more suitable for trial.

Factors that could maintain low cellular levels of oxidative stress may down-regulate the activity of *prnp* and result in a decrease in the quantity of PrP^c protein produced by the cell. Antioxidant replacement could also counteract decreased activity of cellular SODs seen during disease pathogenesis due to aberrant metal metabolism. Mitochondrial SOD/SOD2 synthetic mimetics that can cross the blood brain barrier have been shown to protect SOD2 null mice against spongiform encephalopathy that results due to the null phenotype and may have a potential use in treatment of prion diseases (Melov *et al.*, 2001). Agents such as this should be further investigated for potential therapeutic uses.

6.5 Concluding Remarks

This study aimed to further understanding of the genetic regulation, metabolism, and function of PrP^c. *Prnp* was studied to consider regions of the gene important for activity, regulation of expression across different cell lines, and gene activity in response to stimuli. The internalisation and protection responses of PrP^c to copper, and the regions important for these responses were considered. Also, PrP^c protective response to oxidative stress was studied to provide insight into the putative function of PrP^c.

The importance of copper has been clearly demonstrated at the gene and at the protein level. Copper exerts significant effects on the regulation of PrP^c metabolism, and is essential for PrP^c protective function. PrP^c is internalised in response to physiological levels of copper complexed to glycine, and protects cells against copper induced death, both by protection against the metal ion itself and copper induced oxidative stress. PrP^c also protects against a direct oxidative stress insult. The octameric repeat domain is required for both the protective effect of PrP^c against copper and oxidative stress, and for the internalisation of PrP^c in response to copper. In both cases copper binding to at least one octameric repeat is essential for PrP^c response. The palindromic region and its

associated processing have been shown for the first time to have a role in copper induced internalisation of PrP^c. Also essential for both the correct cellular processing of PrP^c and its protective function is the hydrophobic core of the protein. The regulation of the gene is complex, involving interaction of the promoter with intron 1, with the gene showing additional activity initiated by intron 1 alone. Gene activity is tissue specific with basal expression varying across different cell lines, and separate regions of the gene important for regulating response to stimuli in various tissues.

Overall these results have provided significant insight into the genetic control of PrP^c expression, demonstrated the importance of PrP^c in copper and oxidative stress response, and confirmed that the octameric repeat domain and hydrophobic region are indispensable for PrP^c function. In addition, control elements within *prnp* may provide potential sites for therapeutic intervention by control of protein expression. This study presents a valuable contribution to the understanding of the physiological role of PrP^c and highlights new areas of relevance for future investigation into TSE pathogenesis.

Literature Cited

ACDP/SEAC Joint Working Group (2003). Transmissible spongiform encephalopathy agents: safe working and the prevention of infection. Infection control of CJD and related disorders in a healthcare setting – summary of revised advice.

Armendariz, AD, Gonzalez, M. Loguinov, AV. Vulpe, CD. (2004) Gene expression profiling in chronic copper overload reveals upregulation of Prnp and App. *Physiological Genomics* **20**(1), 45-54.

Aronoff-Spencer, E. Burns, CS. Avdievich, NI. Gerfen, GJ. Peisach, J. Antholine, WE. Ball, HL. Cohen, FE. Prusiner, SB. Millhauser, GL. (2000) Identification of the Cu^{2+} Binding Sites in the N-Terminal Domain of the Prion Protein by EPR and CD Spectroscopy. *Biochemistry* **39**, 13760-71.

Azarpazhooh, A. Leake, JL. (2006). Prions in Dentistry – What Are They, Should We Be Concerned, and What Can We Do? *Journal of the Canada Dental Association* **72**(1), 53-60.

Bainbridge, J. Walker, KB. (2005) The normal cellular form of prion protein modulates T cell responses. *Immunology Letters* **96**, 147-150.

Bastien, J. Rochette-Egly, C. (2004) Nuclear retinoid receptors and the transcription of retinoid-target genes. *Gene* **328**, 1-16.

Basler, K. Oesch, B. Scot, M. Westaway, D. Wäichli, M. Groth, DF. McKinley, MP. Prusiner, SB. Weissmann, C. (1986) Scrapie and Cellular PrP Isoforms Are Encoded by the Same Chromosomal Gene. *Cell* **46**, 417-28.

Baybutt, H. Manson, J. (1997) Characterisation of two promoters for prion protein (PrP) gene expression in neuronal cells. *Gene* **184**, 125-131.

Bertinato, J. L'Abbè, MR. (2004) Maintaining copper homeostasis: regulation of copper-trafficking protein in response to copper deficiency or overload. *Journal of Nutritional Biochemistry* **15**, 316-22.

Bramble, MG. Ironside, JW. (2002) Creutzfeldt-Jakob disease: implications for gastroenterology. *Gut* **50**, 888-90.

Brandner, S. Raeber, A. Sailer, A. Blättler, T. Fischer, M. Weissmann, C. Aguzzi, A. (1996) Normal host prion protein (PrP^c) is required for scrapie spread within the central nervous system. *Proceedings of the National Academy of Science USA* **93**, 13148-13151.

Brown, DR. Herms, J. Kretzschmar, HA. (1994) Mouse Cortical Cells lacking cellular PrP survive in culture with a neurotoxic PrP fragment. *Neuroreport* **5**(16), 2057-60.

Brown, DR. Schmidt, B. Kretzschmar, HA. (1997a) Effects of oxidative stress on prion protein expression in PC12 cells. *International Journal of Developmental Neuroscience* **15**(8), 961-72.

Brown, DR. Qin, K. Herms, JW. Madlung, A. Manson, J. Strome, R. Fraser, PE. Kruck, T. Bohlen, A. Schulz-Schaeffer, W. Giese, A. Westaway, D. Kretzschmar, H. (1997b) The cellular prion protein binds copper *in vivo*. *Nature* **390**, 684-687.

Brown, DR. Besinger, A. (1998) Prion protein expression and superoxide dismutase activity. *Biochemical Journal* **334**, 423-429.

Brown, DR. Schmidt, B. Kretzschmar, HA. (1998) Effects of Copper on Survival of Prion Protein Knockout Neurons and Glia. *Journal of Neurochemistry* **70**, 1686-93.

Brown, DR. (1999) Prion protein expression aids cellular uptake and veratridine-induced release of copper. *Journal of Neuroscience Research* **58**(5), 717-725.

Brown, DR. Wong, BS. Hafiz, F. Clive, C. Haswell, SJ. Jones, IM. (1999) Normal prion protein has an activity like that of superoxide dismutase. *Biochemical Journal* **344**, 1-5.

Brown, DR. Hafiz, F. Glasssmith, LL. Wong, BS. Jones, IM. Clive, C. Haswell, SJ. (2000) Consequences of manganese replacement of copper for prion protein function and proteinase resistance. *The EMBO Journal* **19**(6), 1180-1186.

Brown, DR. Clive, C. Haswell, SJ. (2001) Antioxidant activity related to copper binding of native prion protein. *Journal of Neurochemistry* **76**, 69-76.

Brown, DR. Nicholas, RSJ. Canevari, L. (2002) Lack of Prion Protein Expression Results in a Neuronal Phenotype Sensitive to Stress. *Journal of Neuroscience Research* **67**, 211-224.

Brown, DR. (2004) Role of the prion protein in copper turnover in astrocytes. *Neurobiology of Disease* **15**, 534-43.

Brown, LR. Harris, DA. (2003) Copper and zinc cause delivery of the prion protein from the plasma membrane to a subset of early endosomes and the golgi. *The Journal of Neurochemistry* **87**(2), 353-63.

Brown, P. Bradley, R. (1998) 1755 and all that: a historical primer of transmissible spongiform encephalopathy. *British Medical Journal* **317**, 1688-1692.

Bocharova, OV. Breydo, L. Salnikov, VV. Baskakov, IV. (2005) Copper(II) Inhibits in Vitro Conversion of Prion Protein into Amyloid Fibrils. *Biochemistry* **44**, 6776-87.

Borchelt, DR. Scott, M. Taraboulos, A. Stahl, N. Prusiner, SB. (1990) Scrapie and Cellular Prion Proteins Differ in Their Kinetics of Synthesis and Topology in Cultured Cells. *Journal of Cell Biology* **110**, 743-752.

Borchelt, DR. Rogers, M. Stahl, N. Telling, G. Prusiner, SB. (1993) Release of the cellular prion protein from cultured cells after loss of its GPI anchor. *Glycobiology* **3**(4), 319-329.

Brügger, B. Graham, C. Leibrecht, I. Mombelli, E. Jen, A. Wieland, F. Morris, R. (2004) The Membrane Domains Occupied by Glycolsylphosphatydlinositol-anchored Prion Protein and Thy-1 Differ in Lipid Composition. *Journal of Biological Chemistry* **279**(9), 7530-36.

Büeler, H. Fischer, M. Lang, Y. Bluethmann, H. Lipp, HP. DeArmond, S. Prusiner, SB. Aguet, M. Weissmann, C. (1992) Normal development and behaviour of mice lacking the neuronal cell-surface PrP protein. *Nature* **356**, 577-582.

Burns, CS. Aronoff-Spencer, E. Dunham, CM. Lario, P. Avdievich, NI. Antholine, WE. Olmstead, MM. Vrielink, A. Gerfen, GJ. Peisach, J. Scott, WG. Millhauser, GL. (2002) Molecular Features of the Copper Binding Sites in the Octarepeat Domain of the Prion Protein. *Biochemistry* **41**, 3991-4001.

Burns, CS. Aronoff-Spencer, E. Legname, G. Prusiner, SB. Antholine, WE. Gerfen, GJ. Peisach, J. Millhauser, GL. (2003) Copper Coordination in the Full-Length, Recombinant Prion Protein. *Biochemistry* **42**, 6794-6803.

Cabral, ALB. Lee, KS. Martins, VR. (2002) Regulation of the Cellular Prion Protein Gene Expression Depends on Chromatin Conformation. *The Journal of Biological Chemistry* **277**(7), 5675-5682.

Calzolai, L. Lysek, DA. Pérez, DR. Güntert, P. Wüthrich, K. (2005) Prion protein NMR structures of chickens, turtles and frogs. *Proceedings of the National Academy of Science, USA* **102**(3), 651-655.

Camakaris, J. Voskoboinik, I. Mercer, JF. (1999) Molecular Mechanisms of Copper Homeostasis. *Biochemical and Biophysical Research Communications* **261**, 225-232.

Cashman, NR. Loertscher, R. Nalbantoglu, J. Shaw, I. Kascsak, RJ. Bolton, DC. Bendheim, PE. (1990) Cellular isoform of the scrapie agent protein participates in lymphocyte activation. *Cell* **61**(1), 185-92.

Castilla, J. Saá, P. Soto, C. (2005) Detection of prions in blood. *Nature Medicine* **11**(9), 982-5.

Caughey, B. Race, R. Ernst, D. Buchmeier, MJ. Chesebro, B. (1989) Prion Protein Biosynthesis in Scrapie-Infected and Uninfected Neuroblastoma Cells. *Journal of Virology* **63**(1), 175-181.

Chamary, JV. Hurst, LD. (2004) Similar Rates but Different Modes of Sequence Evolution in Introns and at Exonic Silent Sites in Rodents: Evidence for Selectively Driven Codon Usage. *Molecular Biology and Evolution* **21**(6), 1014-23.

Chattopadhyay, M. Walter, ED. Newell, DJ. Jackson, PL. Aronoff-Spencer, E. Peisach, J. Gerfen, GJ. Bennett, B. Antholine, WE. Millhauser, GL. (2005) The Octarepeat Domain of the Prion Protein Binds Cu(II) with Three Distinct Coordination Modes at pH 7.4. *Journal of the American Chemistry Society.* **127**, 12647-56.

Chen, CS. Gee, KR (2000) Redox-dependent trafficking of 2,3,4,5,6-pentafluorodihydrotetramethylrosamine, a novel fluorogenic indicator of cellular oxidative activity. *Free Radical Biology & Medicine* **28**(8), 1266-78.

Chen, SG. Teplow, DB. Parchi, P. Teller, JK. Gambetti, P. Autilio-Gambetti, L. (1995) Truncated Forms of the Human Prion Protein in Normal Brain and in Prion Diseases. *Journal of Biological Chemistry* **270**(32), 19173-80.

Chiarini, LB. Freitas, ARO. Zanata, SM. Brentani, RR. Martins, VR. Linden, R. (2002) Cellular prion protein transduces neuroprotective signals. *EMBO Journal* **21**(13), 3317-3326.

Collee, JG. Bradley, R. (1997a). BSE: a decade on – part 1. *Lancet* **349**, 636-641.

Collee, JG. Bradley, R. (1997b). BSE: a decade on – part 2. *Lancet* **349**, 715-721.

Criado, JR. Sánchez-Alavez, M. Conti, B. Giacchino, JL. Wills, DN. Henriksen, SJ. Race, R. Manson, JC. Chesebro, B. Oldstone, MBA. (2005) Mice devoid of prion protein have cognitive defects that are rescued by reconstitution of PrP in neurons. *Neurobiology of Disease* **19**, 255-265.

Critchley, P. Kazlauskaite, J. Eason, R. Pinheiro, T. (2004) Binding of prion proteins to lipid membranes. *Biochemical and Biophysical Research Communications* **(313)**, 559-567.

Croes, EA. Roks, G. Jansen, GH. Nijssen, PCG. Van Duijn, CM. (2002) Creutzfeldt-Jakob disease 38 years after diagnostic use of human growth hormone. *Journal of Neurology Neurosurgery and Psychiatry* **72**, 792-793.

Cui, T. Daniels, M. Wong, BS. Li, R. Sy, MS. Sassoon, J. Brown, DR. (2003) Mapping the functional domain of the prion protein. *European Journal of Biochemistry* **270**, 3368-3376.

Dawson , RM. Elliott, DC. Elliott, WH. Jones, KM. (1994) Data for Biochemical Research (third edition). Oxford Scientific Publications.

Drisaldi, B. Stewart, RS. Adles, C. Stewart, LR. Quaglio, E. Biasini, E. Fioriti, L. Chiesa, R. Harris, DA. (2003) Mutant PrP is Delayed in its Exit from the Endoplasmic Reticulum, but Neither Wild-Type nor Mutant PrP Undergoes Retrotranslocation Prior to Proteasomal Degradation. *Journal of Biological Chemistry* **278**(24), 21732-21743.

Donne, DG. Viles, JH. Groth, D. Mehlhorn, I. James, TL. Cohen, FE. Prusiner, SB. Wright, PE. Dyson, HJ. (1997) Structure of the recombinant full-length hamster prion protein PrP(29-231): The N terminus is highly flexible. *Proceedings of the National Academy of Science USA* **94**, 13452-13457.

Esterbauer, H. Schaur, RJ. Zollner, H. (1991) Chemistry and biochemistry of 4-hydroxynonenal malonaldehyde and related aldehydes. *Free Radical Biology and Medicine* **11**(1), 81-128.

Fernaeus, S. Reis, K. Bedecs, K. Land, T. (2005) Increased susceptibility to oxidative stress in scrapie infected neuroblastoma cells is associated with intracellular iron status. *Neuroscience Letters IN Press.*

Fevrier, B. Vilette, D. Archer, F. Loew, D. Faigle, W. Vidal, M. Laude, H. Raposo, G. (2004) Cells release prions in association with exosomes. *Proceedings of the National Academy of Science USA* **101**(26), 9683-88.

Fischer, M. Rulicke, T. Raeber, A. Sailer, A. Moser, M. Oesch, B. Brandner, S. Aguzzi, A. Weissmann, C. (1996) *EMBO Journal* **15**(6), 1255-1264.

Food Standards Agency (2005). BSE and Beef New Controls Explained. Belmont Press.

Fournier, JG. Escaig-Haye, F. Billette de Villemeur, T. Robain, O. (1995) Ultrastructureal localisation of cellular prion protein (PrPc) in synaptic boutons of normal hamster hippocampus. *Comptes Rendus de l'Académie des Sciences – Series III.* **318**(3), 339-44.

Frosh, A. Joyce, R. Johnson, A. (2001) Iatrogenic vCJD from surgical instruments. *British Medical Journal* **322**, 1558-9.

Gabriela, GP. Permanne, B. Soto, C. (2001) Sensitive detection of pathological prion protein by cyclic amplification of protein misfolding. *Nature* **411**, 810-13.

Gagescu, R. Demaurex, N. Parton, RG. Hunziker, W. Huber, LA. Gruenberg, J. (2000) The Recycling Endosome of Madin-Darby Canine Kidney Cells is a Mildly Acidic Compartment Rich in Raft Components. *Molecular Biology of the Cell* **11**, 2775-91.

Gajdusek, CD. (1967) Slow-virus infection of the nervous system. *New England Journal of Medicine* **276**(7), 392-400.

Gale, P. Stanfield, G. (2001). Towards a quantitative risk assessment for BSE in sewage sludge. *Journal of Applied Microbiology* **91**, 563-569.

Gavier-Widen, D. Stack, MJ. Baron, T. Balachandran, A. Simmons, M. (2005) Diagnosis of transmissible spongiform encephalopathies in animals: a review. *Journal of Veterinary Diagnostic Investigation* **17**(6), 509-27.

Gilch, S. Nunziante, M. Ertmer, A. Wopfer, F. Laszlo, L. Schätzl, HM. (2004) Recognition of Lumenal Prion protein Aggregates by Post-ER Quality Control Mechanisms is Mediated by the Preoctarepeat Region of PrP. *Traffic* **5**, 300-313.

Glockshuber, R. Hornemann, S. Billeter, M. Riek, R. Woder, G. Wüthrich, K. (1998) Prion protein structural features indicate possible relations to signal peptidases. *FEBS Letters* **426**, 291-96.

Gohel, C. Grigoriev, V. Escaig-Haye, F. Lasmezas, CI. Deslys, JP. Langeveld, J. Akaabourne, M. Hantai, D. Fournier, JG. (1999) Ultrastructural localization of cellular prion protein (PrPc) at the neuromuscular junction. *Journal of Neuroscience Research.* **55**(2), 261-7.

Gordon, WS. (1946) Advances in Veterinary Research. *The Veterinary Record* **47**(58), 516-520.

Guentchev, M. Siedlak, SL. Jarius, C. Tagliavini, F. Castellani, RJ. Perry, G. Smith, MA. Budka, H. (2002) Oxidative Damage to Nucleic Acids in Human Prion Disease. *Neurobiology of Disease* **9**, 275-81.

Hachiya, NS. Watanabe, K. Yamada, M. Sakasegawa, Y. Kaneko, K. (2004) Anterograde and retrograde intracellular trafficking of fluorescent cellular prion protein. *Biochemical and Biophysical Research Communications* **315**, 802-807.

Hampton, RY. (2002) ER-associated degradation in protein quality control and cellular regulation. *Current Opinion in Cell Biology* **14**, 476-482.

Hartter, DE. Barnea, A. (1988) Brain tissue accumulates 67 copper by two ligand-dependant saturable processes. A high affinity, low capacity and a low affinity, high capacity process. *The Journal of Biological Chemistry* **263**(2), 799-805.

Hasnain, SS. Murphy, LM. Strange, RW. Grossmann, JG. Clarke, AR. Jackson, GS. Collinge, J. (2001) XAFS Study of the High-affinity Copper-binding Site of Human PrP^{91-231} and its Low-resolution Structure in Solution. *Journal of Molecular Biology* **311**, 467-73.

Herms, J. Tings, T. Gall, S. Madlung, A. Giese, A. Siebert, H. Schürmann, P. Windi, O. Brose, N. Kretzschmar, H. (1999) Evidence of Presynaptic Location and Function of the Prion Protein. *The Journal of Neuroscience* **19**(20), 8866-75.

Hills, D. Comincini, S. Schlaepfer, J. Dolf, G. Ferretti, L. Williams, JL. (2001) Complete genomic sequence of the bovine prion gene (PRNP) and polymorphism in its promoter region. *Animal Genetics* **32**, 231-233.

Hogan, RN. Cavanagh, HD. (1995) Transplantation of corneal tissue from donors with diseases of the central nervous system. *Cornea* **14**(6), 545-6.

Holme, A. Daniels, M. Sassoon, J. Brown, DR. A novel method of generating neuronal cell lines from gene-knockout mice to study prion protein membrane orientation. *European Journal of Neuroscience* **18**, 571-579.

Hölscher, C. Delius, H. Bürkle, A. (1998) Overexpression of Nonconvertible PrP^{c} Δ114-121 in Scrapie-Infected Mouse Neuroblastoma Cells Leads to trans-Dominant Inhibition of Wild-Type PrP^{Sc} Accumulation. *Journal of Virology* **72**(2), 1153-59.

Horiuchi, M. Yamazaki, N. Ikeda, T. Ishiguro, N. Shinagawa, M. (1995) A cellular form of prion protein (PrPC) exists in many non-neuronal tissues of sheep. *Journal of General Virology* **76**, 2583-87.

Hornshaw, MP. McDermott, JR. Candy, JM. (1995a) Copper binding to the N-terminal tandem repeat regions of mammalian and avian prion protein. *Biochemical and Biophysical Research Communications* **207**(2), 621-629.

Hornshaw, MP. McDermott, JR. Candy, JM. Lakey, JH. (1995b) Copper binding to the N-terminal tandem repeat region of mammalian and avian prion protein: Structural studies using synthetic peptides. *Biochemical and Biophysical Research Communications* **214**(3), 993-999.

Hural, JA. Kwan, M. Henkel, G. Hock, MB. Brown, MA. (2000) An Intron Transcriptional Enhancer Element Regulates IL-4 Gene Locus Accessibility in Mast Cells. *The Journal of Immunology* **165**, 3239-3249.

Hutter, G. Heppner, FL. Aguzzi, A. (2003) No superoxide dismutase activity of cellular prion protein in vivo. *Biological Chemistry* **384**(9), 1279-85.

Inoue, S. Tanaka, M. Horiuchi, M. Ishiguro, N. Shinagawa, M. (1997) Characterisation of the Bovine Prion protein Gene: The Expression Requires Interaction between the Promoter and Intron. *J. Vet. Med. Sci.* **59**(3), 175-183.

Ivanova, L. Barmada, S. Kummer, T. Harris, DA. (2001) Mutant Prion Proteins are Partially Retained in the Endoplasmic Reticulum. *Journal of Biological Chemistry.* **276**(45), 42409-42421.

Jackson, GS. Murray, I. Hosszu, LLP. Gibbs, N. Waltho, JP. Clarke, AR. Collinge, J. (2001) Location and properties of metal-binding sites on the human prion protein. *Proceedings of the National Academy of Science USA.* **98**(15), 8531-8535.

Ji, HF. Zhang, HY. (2004) A Theoretical Study on Cu(II) Binding Modes and Antioxidant Activity of Mammalian Normal Prion Protein. *Chem Res Toxicol* **17**, 471-5.

Jin, T. Gu, Y. Zanusso, G. Sy, MS. Kumar, A. Cohen, M. Gambetti, P. Singh, N. (2000) The Chaperone Protein BiP Binds to a Mutant Prion Protein and Mediates Its Degradation by the Proteasome. *Journal of Biological Chemistry.* **275**(49), 38699-704.

Johnson, RE. Campbell, RJ. (1982) Wilson's disease. Electron microscopic, X-ray energy spectroscopic studies of corneal copper deposition and distribution. *Laboratory Investigation* **46**(6), 564-9.

Jones, S. Batchelor, M. Bhelt, D. Clarke, AR. Collinge, J. Jackson, GS. (2005) Recombinant prion protein does not possess superoxide dismutase activity. *Biochemical Journal* **392**, 309-12.

Jonsson, JJ. Foresman, MD. Wilson, N. McIvor, RS. (1992) Intron requirement for expression of the human purine nucleoside phosphorylase gene. *Nucleic Acids Research* **20**(12) 3191-98.

Kaneko, K. Vey, M. Scott, M. Pilkuhn, S. Cohen, FE. Prusiner, SB. (1997) COOH-terminal sequence of the cellular prion protein directs subcellular trafficking and controls conversion in the scrapie isoform. *Proceedings of the Nation Academy of Science, USA* **94**, 2333-38

Kenward, N. Hope, J. Landon, M. Mayer, RJ. (1994) Expression of Polyubiquitin and Heat-Shock Protein 70 Genes Increases in the Later Stages of Disease Progression in Scrapie-Infected Mouse Brain. *Journal of Neurochemistry* **62**, 1870-77.

Kiachopoulos, S. Bracher, A. Winklhofer, KF. Tatzelt, J. (2004) Pathogenic mutations located in the hydrophobic core of the prion protein interfere with folding and attachment of the glycosylphosphatidylinositol anchor. *Journal of Biological Chemistry* **280**(10). 9320-9.

Kitamura, M. Ishikawa, Y. Moreno-Manzano, V. Xu, Q. Konta, T. Lucio-Cazana, J. Furusu, A. Nakayama, K. (2002) Intervention by retinoic acid in oxidative stress induced apoptosis. *Nephrology Dialysis Transplantation* **17**(9), 84-87.

Klamt, F. Dal-Pizzol, F. Conte Da Fronta Jr, ML. Walz, R. Andrades, ME. Da Silva, EG. Brentani, RR. Izquierdo, I. Moreira, JCF. (2001) Imbalance of antioxidant defence in mice lacking cellular prion protein. *Free Radical Biology and Medicine* **30**(10), 1137-44.

Kobayashi, Y. Hirata, K. Tanaka, H. Yamada, T. (2003) Quinacrine administration to a patient with Creutzfeldt-Jakob disease who received cadaveric dura mater graft--an EEG evaluation. *Clinical Neurology* **43**(7), 403-408.

Koch, TK. Berg, BO. DeArmond, SJ. Gravina, RF. (1985) Creutzfeldt-Jakob disease in a young adult with idiopathic hypopituitarism. Possible relation to the administration of cadaveric human growth hormone. *The New England Journal of Medicine* **313**(12), 731-33.

Kovacs, GG, Voigtlander, T. Gelpi, E. Budka, H. (2004) Rationale for diagnosing human prion disease. *World Journal of Biological Psychiatry* **5**(2), 83-91.

Kramer, ML. Kratzin, HD. Schmidt, B. Romer, A. Windl, O. Liemann, S. Hornemann, S. Kretzschmar, H. (2001) Prion Protein Binds Copper within the Physiological Concentration Range. *The Journal of Biological Chemistry* **276**(20), 16711-16719.

Lai, JCK. Blass, JP. (1984) Neurotoxic effects of copper. *Neurochemical Research* **9**, 1699-1711.

Laine, J. Marc, ME. Sy, MS. Axelrad, H. (2001) Cellular and subcellular morphological localisation of the normal prion protein in rodent cerebellum. *European Journal of Neuroscience* **14**, 47-56.

Larson, RS. Tallman, MS. (2003) Retinoic acid syndrome: manifestations, pathogenesis, and treatment. *Best Practise & Research Clinical Haematology* **16**(3), 453-61.

Lawson, VA. Priola, SA. Wehrly, K. Chesebro, B. (2001) N-terminal Truncation of Prion Protein Affects Both Formation and Conformation of Abnormal Protease-resistant Prion Protein Generated *in Vitro*. *The Journal of Biological Chemistry* **276**(38), 35265-71.

Lee, IY. Westaway, D. Smit, AFA. Wang, K. Seto, J. Chen, L. Acharya, C. Ankener, M. Baskin, D. Cooper, C. Yao, H. Prusiner, SB. Hood, LE. (1998) Complete Genomic Sequence and Analysis of the Prion Protein Gene Region from Three Mammalian Species. *Genome Research* **8**, 1022-1037.

Lee, KS. Magalhães, AC. Zanata, SM. Brentani, RR. Martins, VR. Prado, MA. (2001) Internalisation of mammalian fluorescent cellular prion protein and N-terminal deletion mutants in living cells. *Journal of Neurochemistry* **79**(1), 79-87.

Lee, Y. Lee, C. Yoon, J. (2004) Kinetics and mechanisms of DMSO (dimethylsulphoxide) degradation by UV/H_2O_2 process. *Water Research* **38**, 2579-88.

Lehmann, S. Harris, D.A. (1997). Blockade of Glycosylation Promotes Acquisition of Scrapie-like Properties by the Prion Protein in Cultured Cells. The *Journal of Biological Chemistry* **272**, 21479-21487.

Lewis, AM. Yu, M. DeArmond, SJ. Dillon, WP. Miller, BL. Geschwind, MD. (2006) Human growth hormone-related iatrogenic Creutzfeldt-Jakob disease with abnormal imaging. *Archives of Neurology* **63**(2), 288-90.

Li, G. Bolton, D. (1997) A novel hamster prion protein mRNA contains an extra exon: increased expression in scrapie. *Brain Research* **751**, 265-274.

Li, L. He, S. Sun, JM. Davie, JR. (2004) Gene regulation by SP1 and SP3. *Biochemical Cell Biology* **82**, 460-471.

Li, R. Liu, T. Wong, BS. Pan, T. Morillas, M. Swietnicki, W. O'Rourke, K. Gambetti, P. Surewicz, WK. Sy, MS. (2000) Identification of an Epitope in the C terminus of Normal Prion protein whose Expression is Modulated by Binding Events in the N terminus. *Journal of Molecular Biology* **301**, 567-73.

Li, R. Liu, D. Zanusso, G. Liu, T. Fayen, JD. Huang, JH. Petersen, RB. Gambetti, P. Sy, MS. (2001) The Expression and potential Function of Cellular Prion Protein in Human Lymphocytes. *Cellular Immunology* **207**, 49-58.

Li, R. Liu, T. Yoshihiro, F. Tary-Lehmann, M. Obrenovich, M. Kuekrek, H. Kang, SC. Pan, T. Wong, BS. Medof, ME. Sy, MS. (2003) On the same cell type GPI-anchored normal cellular prion and DAF protein exhibit different biological properties. *Biochemical and Biophysical Research Communications* **303**, 446-51.

Li, X. Zhao, X. Fang, Y. Jiang, X. Duong, T. Fan, C. Huang, CC. Kain, SR. (1998) Generation of Destabilised Green Fluorescent Protein as a Transcription Reporter. *Journal of Biological Chemistry.* **273**(52), 34970-75.

Lledo, PM. Tremblay, P. DeArmond, SJ. Prusiner, SB. Nicoll, RA. (1996) Mice deficient for prion protein exhibit normal neuronal excitability and synaptic transmission in the hippocampus. *Proceedings of the National Academy of Science USA* **93**, 2403-2407.

Llewelyn, CA. Hewitt, PE. Knight, RS. Amar, K. Cousens, S. Mackenzie, J. Will, RG. (2004) Possible transmission of variant Creutzfeldt-Jakob disease by blood transfusion. *Lancet* **363**(9407), 417-21.

Ma, J. Lindquist, S. (2002) Conversion of PrP to a Self-Perpetuating PrPsc-like Conformation in the Cytosol. *Science* **298**, 1785-1788.

Ma, J. Wollmann, R. Lindquist, S. (2002) Neurotoxicity and Neurodegeneration When PrP Accumulates in the Cytosol. *Science* **298**, 1781-1784.

Mahfoud, R. Garmy, N. Maresca, M. Yahi, N. Puigserver, A. Fantini, J. (2002) Identification of a Common Sphingolipid-binding Domain in Alzheimer, Prion and HIV-1 Proteins. *Journal of Biological Chemistry* **277**(13), 11292-96.

Magalhães, AC. Silva, JA. Lee, KS. Martins, VR. Prado, VF. Ferguson, SSG. Gomez, MV. Brentani, RR. Prodo, MAM. (2002) Endocytic Intermediates Involved with the

Intracellular Trafficking of a Fluorescent Cellular Prion Protein. *Journal of Biological Chemistry* **277**(36), 33311-18.

Mangé, A. Milhavet, O. Umlauf, D. Harris, D. Lehmann, S. (2002) PrP-dependent cell adhesion in N2a neuroblastoma cells. *FEBS Letters* **514**, 159-62.

Manson, J. West, JD. Thomson, V. McBride, P. Kaufman, MH. Hope, J. (1992) The prion protein gene: a role in mouse embryogenesis? *Development* **115**(1), 117-22.

Marella, M. Lehmann, S. Grassi, J. Chabry, J. (2002) Filipin Prevents Pathological Prion Protein Accumulation by Reducing Endocytosis and Inducing Cellular PrP Release. *Journal of Biological Chemistry* **277**(28), 25457-64.

Martin, BD. Schoenhard, JA. Sugden, KD. (1998) Hypervalent chromium mimics reactive oxygen species as measured by the oxidant-sensitive dyes 2',7'-dichlorofluorescin and dihydrorhodamine. *Chemical Research and Toxicology* **11**(12), 1402-10.

Martinez-Lage, JF. Poza, M. Sola, J. Tortosa, JG. Brown, P. Cervenakova, L. Esteban, JA. Mendoza, A. (1994) Accidental transmission of Creutzfeldt-Jakob disease by dural cadaveric grafts. *Journal of Neurology Neurosurgery and Psychiatry* **57**(9), 1091-94.

McLennan, NF. Brennan, PM. McNeill, A. Davies, I. Fotheringham, A. Rennison, KA. Ritchie, D. Brannan, F. Head, MW. Ironside, JW. Williams, A. Bell, JE. (2004) Prion Protein Accumulation and Neuroprotection in Hypoxic Brain Damage. *The American Journal of Pathology* **165**, 227-235.

Mead, S. Mahal, SP. Beck, J. Campbell, T. Farral, M. Fisher, E. Collinge, J. (2001) Sporadic-but Not Variant-Creutzveldt-Jakob Disease Is Associated with Polymorphisms Upstream of *PRNP* Exon 1. *American Journal of Human Genetics* **69**, 1225-35.

Melov, S. Doctrow, SR. Schneider, JA. Haberson, J. Patel, M. Coskun, PE. Huffman, K. Wallace, DC. Malfroy, B. (2001) Lifespan Extension and Rescue of Spongiform Encephalopathy in Superoxide Dismutase 2 Nullizygous Mice Treated with Superoxide Dismutase-Catalase Mimetics. *The Journal of Neuroscience* **21**(21), 8348-53.

Miele, G. Jeffrey, M. Turnbull, D. Manson, J. Clinton, M. (2002) Ablation of Cellular Prion protein Expression Affects Mitochondrial Numbers and Morphology. *Biochemical and Biophysical Research Communications* **291**, 372-77.

Miele, G. Alejo Blanco, AR. Baybutt, H. Horvat, S. Manson, J. Clinton, M. (2003) Embryonic activation and developmental expression of the murine prion protein gene. *Gene Expression* **11**(1), 1-12.

Milhavet, O. McMahon, HEM. Rachidi, W. Nishida, N. Katamine, S. Mange, A. Arlotto, M. Casanova, D. Riondel, J. Favier, A. Lehmann, S. (2000) Prion infection impairs the cellular response to oxidative stress. *Proceedings of the Nation Academy of Science, USA* **97**(25), 13937-42.

Miller, MW. Williams, ES. (2004) Chronic wasting disease of cervids. *Current Topics in Microbiological Immunology* **284**, 193-214.

Miller, MW. Williams, ES. Hobbs, NT. Wolfe, LL. (2004) Environmental Sources of Prion Transmission in Mule Deer. *Emerging Infectious Diseases* **10**(6), 1003-6.

Mišík, V. Riesz, P. (1996) Peroxyl radical formation in aqueous solutions of N,N-dimethylformamide, N-methylformamide, and dimethylsulphoxide by ultrasound: Implications for sonosensitized cell killing. *Free Radical Biology & Medicine* **20**(1), 129-138.

Miura, T. Hori-I, A. Takeuchi, H. (1996) Metal-dependent α-helix formation promoted by the glycine-rich octapeptide region of the prion protein. *FEBS Letters* **396**, 248-252.

Miura, T. Sasaki, S. Toyama, A. Takeuchi, H. (2005) Copper Reduction by the Octameric Repeat Region of Prion Protein: pH Dependence and Implications in Cellular Copper Uptake. *Biochemistry* **44**, 8712-20.

Mouillet-Richard, S. Ermonval, M. Chebassier, C. Laplanche, JL. Lehmann, S. Launay, JM. Kellermann, O. (2000) Signal transduction through prion protein. *Science* **289**(5486), 1925-8.

Mouillet-Richard, S. Pietri, M. Schneider, B. Vidal, C. Mutel, V. Launay, JM. Kellermann, O. (2005) Modulation of Serotonergic Receptor Signalling and Cross-talk by Prion Protein. *The Journal of Biological Chemistry* **280**(6), 4592-4601.

Nico, PBC. de-Paris, F. Vinade, ER. Amaral, OB. Rockenbach, I. Soares, BL. Guarnieri, R. Wichert-Ana, L. Calvo, F. Walz, R. Izquierdo, I. Sakamoto, AC. Brentani, R. Martins, VR. Bianchin, MM. (2005a) Altered behavioural response to acute stress in mice lacking cellular prion protein. *Behavioural Brain Research* **162**, 173-181.

Nico, PBC. Lobão-Soares, B. Landemberger, MC. Marques Jr, W. Tasca, CI. de Mello, F. Walz, R. Carlotti, CG. Brentani, R. Sakamoto, AC. Bianchin, MM. (2005b) Impaired exercise capacity, but unaltered mitochondrial respiration in skeletal or cardiac muscle of mice lacking cellular prion protein. *Neuroscience Letters* **388**(1), 21-6.

Nishida, N. Katamine, S. Shigematsu, K. Nakatani, A. Sakamoto, N. Hasegawa, S. Nakaoke, R. Atarashi, R. Kataoka, Y. Miyamoto, T. (1997) Prion Protein is Necessary for Latent Learning and Long-term Memory Retention. *Cellular and Molecular Neurobiology* **17**(5), 537-45.

Nishimura, T. Sakudo, A. Nakamura, I. Lee, D. Taniuchi, Y. Saeki, K. Matsumoto, Y. Ogawa, M. Sakaguchi, S. Itohara, S. Onodera, T. (2004) Cellular prion protein regulates intracellular hydrogen peroxide level and prevents copper-induced apoptosis. *Biochemical and Biophysical Research Communications* **323**, 218-22.

Negro, A. Ballarin, C. Bertoli, A. Massimino, ML. Sorgato, MC. (2001) The Metabolism and Imaging in Live Cells of the Bovine Prion Protein in its Native Form or Carrying Single Amino Acid Substitutions. *Molecular and Cellular Neuroscience* **17**, 521-38.

Norstrom, EM. Mastrianni, JA. (2005) The AGAAAAGA palindrome in PrP is required to generate a productive PrP^{Sc}-PrP^{c} complex that leads to prion propagation. *Journal of Biological Chemistry.* **280**(29), 27236-43.

Nunziante, M. Gilch, S. Schatzl, HM. (2003) Essential role of the prion protein N-terminus in subcellular trafficking and half-life of PrPc. *Journal of Biological Chemistry* **278**(6), 3726-3734.

O'Neill, GT. Donnelly, K. Marshall, E. Cairns, D. Goldmann, W. Hunter, N. (2003) Characterisation of ovine PrP gene promoter activity in N2a neuroblastoma and ovine foetal brain cell lines. *Journal of Animal Breeding and Genetics* **120**, 114-123.

Pan, KM. Baldwin, M. Nguyen, J. Gasset, M. Serban, A. Groth, D. Mehlorn, I. Huang, Z. Fletterick, RJ. Cohen, FE. Prusiner, SB. (1993) Conversion of α-helices into β-sheets features in the formation of the scrapie prion proteins. *Proceedings of the National Academy of Science USA* **90**, 10962-10966.

Parizek, P. Roeckl, C. Weber, J. Flechsig, E. Aguzzi, A. Raeber, AJ. (2001) Similar Turnover and Shedding of the Cellular Prion Protein in Primary Lymphoid and Neuronal Cells. *Journal of Biological Chemistry* **276**(48), 44627-32.

Parkin, ET. Watt, NT. Turner, AJ. Hooper, NM. (2004) Dual mechanisms for shedding of the cellular prion protein. *Journal of Biological Chemistry* **279**(12), 11170-8.

Pauly, PC. Harris, DA. (1998) Copper Stimulates Endocytosis of the Prion Protein. *The Journal of Biological Chemistry* **273**(50), 33107-33110.

Pattison, J. (1998) The emergence of bovine spongiform encephalopathy and related diseases. *Emerging Infectious Diseases* **4**(3), 390-4.

Peters, PJ. Mironov Jr, A. Peretz, D. van Donselaar, E. Leclerc, E. Erpel, S. DeArmond, SJ. Burton, DR. Williamson, RA. Vey, M. Prusiner, SB. (2003) Trafficking of prion proteins through a caveolae-mediated endosomal pathway. *Journal of Cell Biology* **162**(4), 703-717.

Perera, S. Hooper, NM. (2001) Ablation of the metal ion-induced endocytosis of the prion protein by disease associated mutation of the octarepeat region. *Current Biology* **11**, 519-523.

Périer, RC. Praz, V. Junier, T. Bonnard, C. Bucher, P. (2000) The Eukaryotic Promoter Database (EPD). *Nucleic Acids Research* **28**(1) 302-3.

Predki, PF. Sarkar, B. (1992) Effect of Replacement of "Zinc Finger" Zinc on Estrogen Receptor DNA Interactions. *The Journal of Biological Chemistry* **267**(9), 5842-46.

Premzl, M. Delbridge, M. Gready, JE. Wilson, P. Johnson, M. Davis, J. Kuczek, E. Marshall Graves, JA. (2005) The prion protein gene: Identifying regulatory signals using marsupial sequence. *Gene* **349**, 121-34.

Prestridge, DS. (1991) SIGNAL SCAN: A computer program that scans DNA sequences for eukaryotic transcription elements. *CABIOS* **7**, 203-206.

Prusiner, SB. (1982) Novel proteinaceous infectious particles cause scrapie. *Science* **216**(4542), 136-144.

Puckett, C. Concannon, P. Casey, C. Hood, L. (1991) Genomic structure of the human prion protein gene. *American Journal of Human Genetics* **49**(2), 320-329.

Quaglio, E. Chiesa, R. Harris, DA. (2001) Copper Converts the Cellular Prion Protein into a Protease-Resistant Species That Is Distinct from the Scrapie Isoform. *Journal of Biological Chemistry* **276**(14), 11432-38.

Riek, R. Hornemann, S. Wider, G. Billeter, M. Glockshuber, R. Wuthrich, K. (1996) NMR structure of the mouse prion protein domain PrP (121-231). *Nature* **382**(6587), 180-182.

Riek, R. Hornemann, S. Wider, G. Glockshuber, R. Wüthrich, K. (1997) NMR characterization of the full-length recombinant murine prion protein, *m*PrP(23-231). *FEBS Letters* **413**, 282-288.

Robakis, NK. Sawh, P. Wolfe, GC. Rubenstein, R. Carp, RI. Innis, MA. (1986) Isolation of a cDNA clone encoding the leader peptide of prion protein and expression of the homologous gene in various tissues. *Proceedings of the National Academy of Science, USA* **83**, 6377-81.

Rohrer, J. Conley, ME. (1998) Transcriptional Regulatory Elements Within the First Intron of Bruton's Tyrosine Kinase. *Blood* **91**(1), 214-21.

Rybner, C. Hilion, J. Sahraoui, T. Lanotte, M. Botti, J. (2002) All-*trans* retinoic acid down-regulates prion protein expression independently of granulocyte maturation. *Leukaemia* **16**, 940-948.

Saeki, K. Matsumoto, Y. Matsumoto, Y. Onodera, T. (1996) Identification of a Promoter Region in the Rat Prion Gene. *Biochemical and Biophysical Research Communications* **219**, 47-52.

Sakudo, A. Lee, DC. Saeki, K. Nakamura, Y. Inoue, K. Matsumoto, Y. Itohara, S. Onodera, T. (2003) Impairment of superoxide dismutase activation by N-terminally truncated prion protein (PrP) in PrP-deficient neuronal cell line. *Biochemical and Biophysical Research Communications* **308**, 660-667.

Sakudo, A. Lee, DC. Nishimura, T. Li, S. Tsuji, S. Nakamura, Y. Matsumoto, Y. Saeki, K. Itohara, S. Ikuta, K. Onodera, T. (2005) Octapeptide repeat region and N-terminal half of the hydrophobic region of prion protein (PrP) mediate PrP-dependent activation of superoxide dismutase. *Biochemical and Biophysical Research Communications* **326**, 600-6.

Sander, P. Hamann, H. Drögemüller, C. Kashkevich, K. Schiebel, K. Leeb, T. (2005) Bovine prion protein gene (*PRNP*) promoter polymorphism modulate *PRNP* expression and may be responsible for differences in BSE susceptibility. *Journal of Biological Chemistry.* **280**(45), 37408-14.

Santos, NC. Figueira-Coelho, J. Martins-Silva, J. Saldanha, C. (2003) Multidisciplinary utilisation of dimethyl sulphoxide: pharmacological, cellular, and molecular aspects. *Biochemical Pharmacology* **65**, 1035-41.

Schmitt-Ulms, G. Legname, G. Baldwin, MA. Ball, HL. Bradon, N. Bosque, PJ. Crossin, KL. Edelman, GM. DeArmond, SJ. Cohen, FE. Prusiner, SB. (2001) Binding of neural cell adhesion molecules (N-CAMs) to the cellular prion protein. *Journal of Molecular Biology* **314**(5), 1209-25.

Schneider, B. Mutel, V. Pietri, M. Ermonval, M. Mouillet-Richard, S. Kellermann, O. (2003) NADPH oxidase and extracellular regulated kinases 1/2 are targets of prion protein signalling in neuronal and non neuronal cells. *Proceedings of the National Academy of Science, USA* **100**(23), 13326-31.

Schug, J. Overton, GC. (1997) TESS: Transcription Element Search Software on the www. Technical Report CBIL-TR-1997-1001-v0.0. Computational Biology and Informatics Laboratory. School of Medicine, University of Pennsylvania.

Scott, M. Foster, D. Mirenda, C. Serban, D. Coufal, F. Walchli, M. Torchia, M. Groth, D. Carlson, G. DeArmond, SJ. *et al.* (1989) Transgenic mice expressing hamster prion protein produce species-specific scrapie infectivity and amyloid plaques. *Cell* **59**(5), 847-857.

Senthilkumar, R. Viswanathan, P. Nalini, N. (2003) Effect of glycine on oxidative stress in rats with alcoholic induced liver injury. *Pharmazie* **59**, 55-60.

Shaked, GM. Engelstein, R. Avraham, I. Kahana, E. Gabizon, R. (2003) Dimethyl sulfoxide delays PrP^{sc} accumulation and disease symptoms in prion-infected hamsters. *Brain Research* **983**, 137-143.

Sharma, P. Sabharanjak, S. Mayor, S. (2002) Endocytosis of lipid rafts: an identity crisis. *Cell and Developmental Biology* **13**, 205-214.
Shi, Y. (2004) Caspase Activation: Revisiting the Induced proximity Model. *Cell* **117**, 855-58.

Shyng, SL. Heuser, JE. Harris, DA. (1994) A glycolipid-anchored prion protein is endocytosed via clathrin coated pits. *Journal of Cell Biology* **125**(6), 1239-50.

Shyng, SL. Moulder, KL. Lesko, A. Harris, DA. (1995) The N-terminal domain of a glycolipid-anchored prion protein is essential for its endocytosis via clathrin coated pits. *Journal of Biological Chemistry* **270**(24), 14793-800.

Shyu, WC. Kao, MC. Chou, WY. Hsu, YD. Soong, BW. (2000) Heat shock modulates prion protein expression in human NT-2 cells. *Molecular Neuroscience* **11**(4), 771-774.

Shyu, WC. Harn, HJ. Saeki, K. Kubosaki, A. Matsumoto, Y. Onodera, T. Chen, CJ. Hsu, YD. Chiang, YH. (2002) Molecular Modulation of Expression of Prion Protein by Heat Shock. *Molecular Neurobiology* **26**, 1-12.

Shyu, WC. Lin, SZ. Saeki, K. Kubosaki, A. Matsumoto, Y. Onodera,T. Chiang, MF. Thajeb, P. Li, H. (2004) Hyperbaric Oxygen Enhances the Expression of Prion Protein and Heat Shock Protein 70 in a Mouse Neuroblastoma Cell Line. *Cellular and Molecular Neurobiology* **24**(2), 257-268.

Shyu, WC. Chen, CP. Saeki, K. Kubosaki, A. Matsumoto, Y. Onodera, T. Ding, DC. Chiang, MF. Lee, YJ. Lin, SZ. Li, H. (2005a) Hypoglycaemia enhances the expression

of prion protein and heat-shock protein 70 in a mouse neuroblastoma cell line. *Journal of Neuroscience Research.* **80**(6), 887-94.

Shyu, WC. Lin, SZ. Chiang, MF. Ding, DC. Li, DC. Chen, SF. Yang, HI. Li, H. (2005b) Overexpression of PrP^c by Adenovirus-Mediated Gene Targeting Reduces Ischemic Injury in a Stroke Rat Model. *The Journal of Neuroscience* **25**(39), 8967-8977.

Singh, N. Zanusso, G. Chen, SG. Fujioka, H. Richardson, S. Gambetti, P. Petersen, RB. (1997) Prion Protein Aggregation Reverted by Low Temperature in Transfected Cells Carrying a Prion Protein Gene Mutation. *Journal of Biological Chemistry* **272**(45), 28461-70.

Sipos, L. Gyurkovics, H. (2005) Long-distance interactions between enhancers and promoters. *FEBS Journal* **272**, 3253-3259.

Spielhaupter, C. Schätzl, HM. (2001) PrP^c Directly Interacts with Proteins Involved in Signalling Pathways. *Journal of Biological Chemistry* **276**(48), 44604-12.

Stahl, N. Borchelt, DR. Hsiao, K. Prusiner, SB. (1987) Scrapie prion protein contains a phosphatidylinositol glycolipid. *Cell* **51**(2), 229-240.

Stennicke, HR. Salvesen, GS. (2000) Caspases – controlling intracellular signals by protease zymogen activation. *Biochimica et Biophisica Acta* **1477**, 299-306.

Stewart, RS. Drisaldi, B. Harris, DA. (2001) A Transmembrane Form of the Prion Protein Contains an Uncleaved Signal Peptide and is Retained in the Endoplasmic Reticulum. *Molecular Biology of the Cell* **12**, 881-889.

Stöckel, J. Sarfar, J. Wallace, AC. Cohen, FE. Prusiner, SB. (1998) Prion Protein Selectively Binds Copper (II) Ions. *Biochemistry* **37**, 7185-7193.

Strumbo, B. Ronchi, S. Bolis, LC. Simonic, T. (2001) Molecular cloning of the cDNA coding for *Xenopus laevis* prion protein. *FEBS Letters* **508**, 170-4.

Stuermer, CA. Langhorst, MF. Wiechers, MF. Legler, DF. Von Hanwehr, SH. Guse, AH. Plattner, H. (2004) PrPc capping in T cells promotes its association with the lipid raft proteins reggie-1 and reggie-2 and leads to signal transduction. *FASEB Journal* **18**(14), 1731-3.

Sumbayev, VV. Yasinska, IM. (2005) Regulation of MAP kinase-dependent apoptotic pathway: implication of reactive oxygen and nitrogen species. *Archives of Biochemistry and Biophysics* **436**, 406-12.

Sunyach, C. Jen, A. Deng, J. Fitzgerald, KT. Frobert, Y. Grassi, J. McCaffrey, MW. Morris, R. (2003) The mechanism of internalisation of glycosylphosphatidylinositol-anchored prion protein. *The EMBO Journal* **22**(14), 3591-3601.

Tabrizi, S.J. Elliott, C.L. Weissmann, C. (2003). Ethical issues in human prion diseases. *British Medical Bulletin* **66**, 305-316.

Taylor, DR. Watt, NT. Perera, WSS. Hooper, NM. (2005) Assigning functions to distinct regions of the N-terminus of the prion protein that are involved in its copper-stimulated, clathrin-dependant endocytosis. *Journal of Cell Science* **118**, 5141-53.

Thackray, AM. Knight, R. Haswell, SJ. Bujdoso, R. Brown, DR. (2002) Metal imbalance and compromised anti-oxidant function are early changes in prion disease. *Biochemical Journal* **362**, 253-258.

Thadani, V. Penar, PL. Partington, J. Kalb, R. Janssen, R. Schonberger, LB. Rabkin, CS. Prichard, JW. (1988) Creutzfeldt-Jakob disease probably acquired from a cadaveric dura mater graft. Case report. *Journal of Neurosurgery* **69**(5), 766-69.

The vCJD Working Party of the Standard Advisory Committee on Transfusion Transmitted Infections (2005) Joint UKBTS/NIBSC Professional Advisory Committee – Position Statement.

Thompsett, AR. Abdelraheim, SR. Daniels, M. Brown, DR. (2005) High affinity binding between copper and full length prion protein identified by two different techniques. *Journal of Biological Chemistry.* [Epub ahead of print].

Tobler, I. Gaus, SE. Deboer, T. Achermann, P. Fischer, M. Rulicke, T. Moser, M. Oesch, B. McBride, PA. Manson, JC. (1996) Altered circadian activity rhythms and sleep in mice devoid of prion protein. *Nature* **380**, 639-42.

Tobler, I. Deboer, T. Fischer, M. (1997) Sleep and Sleep Regulation in Normal and Prion-Deficient Mice. *The Journal of Neuroscience* **17**(5) 1869-79.

Todd, NV. Morrow, J. Doh-ura, K. Dealler, S. O'Hare, S. Farling, P. Duddy, M. Rainov, NG. (2005) Cerebroventricular infusion of pentosan polysulphate in human variant Creutzfeldt-Jakob disease. *Journal of Infection* **50**, 394-6.

Toni, M. Massimino, ML. Griffoni, C. Salvato, B. Tomasi, V. Spisni, E. (2005) Extracellular copper ion regulate cellular prion protein (PrP^c) expression and metabolism in neuronal cells. *FEBS Letters* **579**, 741-44.

Torii, S. Nakayama, K. Yamamoto, T. Nishida, E. (2004) Regulatory mechanisms and function of ERK MAP kinases. *Journal of Biochemistry (Tokyo)* **136**(5), 557-61.

UK Blood Transfusion Services (2005) Guidelines for the Blood Transfusion Services in the United Kingdom, 7th edition. TSO.

van Driel, R. Fransz, PF. Verschure, PJ. (2003) The eukaryotic genome: a system regulated at different hierarchical levels. *Journal of Cell Science* **116**(20), 4067-75.

Varela-Nallar, L. Toledo, EM. Larrondo, LF. Cabral, ALB, Martins, VR. Inestrosa, NC. (2005) Induction of cellular prion protein (PrP^c) gene expression by copper in neurones. *American Journal of Cell Physiology*, [Epub ahead of print].

Vassallo, N. Herms, J. (2003) Cellular prion protein function in copper homeostasis and redox signalling at the synapse. *Journal of Neurochemistry* **86**, 538-44.

Vincent, B. Paitel, E. Saftig, P. Frobert, Y. Hartmann, D. De Strooper, B. Grassi, J. Lopez-Perez, E. Checler, F. (2001) The Disintegrins ADAM10 and TACE Contribute to the Constitutive and Phorbol Ester-regulated Normal Cleavage of the Cellular Prion Protein. *Journal of Biological Chemistry* **276**(41), 37743-46.

Walmsley, AR. Zeng, F. Hooper, NM. (2001) Membrane topology influences N-glycosylation of the prion protein. *The EMBO Journal* **20**(4), 703-712.

Wang, V. Chuang, TC. Hsu, YD. Chou, WY. Kao, MC. (2005) Nitric oxide induces prion protein via MEK and p38 MAPK signalling. *Biochemical and Biophysical Research Communications* **333**, 95-100.

Watt, NT. Taylor, DR. Gillott, A. Thomas, DA. Perera, WSS. Hooper, NM. (2005) Reactive Oxygen Species-mediated β-Cleavage of the Prion Protein in the Cellular Response to Oxidative Stress. *The Journal of Biological Chemistry* **280**(43), 35914-21.

Weissmann, C. Büeler, H. Fischer, M. Sailer, A. Aguzzi, A. Aguet, M. (1994) PrP-deficient mice are resistant to scrapie. *Annals of the New York Academy of Science* **724**, 235-40.

Westaway, D. Cooper, C. Turner, S. Costa, MD. Carlson, GA. Prusiner, SB. (1994) Structure and polymorphism of the mouse prion protein gene. *Proceedings of the National Academy of Science USA* **91**, 6418-6422.

Wilesmith, JW. Ryan, JB. Hueston, WD. Hoinville, LJ. (1992) Bovine spongiform encephalopathy: epidemiological features 1985 to 1990. *Veterinary Records* **130**(5), 90-4.

Will, RG. Ward, HJ. (2004) Clinical Features of variant Creutzfeldt-Jakob disease. *Current Topics in Microbiological Immunology*. **284**, 121-32.

Wingender, E. Chen, X. Hehl, R. Karas, H. Liebich, I. Matys, V. Meinhardt, T. Prüß, M. Reuter, I. Schacherer, F. (2000) TRANSFAC: an integrated system for gene expression regulation. *Nucleic Acids Research* **28**(1), 316-19.

Winklhofer, KF. Heske, J. Heller, U. Reintjes, A. Muranyi, W. Moarefi, I. Tatzelt, J. (2003) Determinants of the *in vivo* folding of the prion protein: a bipartate function of helix 1 in folding and aggregation. *Journal of Biological Chemistry* **278**(17), 14961-14970.

Wong, BS. Pan, T. Liu, T. Li, R. Gambetti, P. Sy, MS. (2000) Differential Contribution of Superoxide Dismutase Activity by Prion Protein *in Vivo*. *Biochemical and Biophysical Research Communications* **273**, 136-139.

Wong, BS. Chen, SG. Colucci, M. Xie, Z. Pan, T. Liu, T. Li, R. Gambetti, P. Sy, MS. Brown, DR. (2001a) Aberrant metal binding by prion protein in human prion disease. *Journal of Neurochemistry* **78**, 1400-1408.

Wong, BS. Brown, DR. Pan, T. Whitemann, M. Liu, T. Bu, X. Li, R. Gambetti, P. Olesik, J. Rubenstein, R. Sy, MS. (2001b) Oxidative impairment in scrapie-infected mice is associated with brain metal perturbations and altered anti-oxidant activities. *Journal of Neurochemistry* **79**, 689-698.

Wopfner, F. Weidenhöfer, G. Schneider, R. von Brunn, A. Gilch, S. Schwarz, T.F. Werner, T. Schätzl, H.M. (1999). Analysis of 27 Mammalian and 9 Avian PrPs Reveals High Conservation of Flexible Regions of the Prion Protein. *Journal of Molecular Biology* **289**, 1163-1178.

World Health Organisation (2003). WHO infection control guidelines for the Transmissible Spongiform Encephalopathies. Report of a WHO consultation, Geneva, Switzerland, 23-26 March 1999. Annex C Decontamination and Waste Disposal.

Yadavalli, R. Guttmann, RP. Seward, T. Centers, AP. Williamson, RA. Telling, GC. (2004) Calpain-dependent Endoproteolytic Cleavage of PrPsc Modulates Scrapie Prion Propagation. *Journal of Biological Chemistry* **279**(21), 21948-56.

Yanai, A. Meiner, Z. Gahali, I. Gabizon, R. Taraboulos, A. (1999) Subcellular trafficking abnormalities of a prion protein with a disrupted disulphide loop. *FEBS Letters* **460**, 11-16.

Yao, Y. Ren, J. Jones, IM. (2003) Amino terminal interaction in the prion protein identified using fusion to green fluorescent protein. *Journal of Neurochemistry* **87**, 1057-65.

Yedidia, Y. Horonchik, L. Tzaban, S. Yanai, A. Taraboulos, A. (2001) Proteasome and ubiquitin are involved in the turnover of the wild type prion protein. *The EBMO Journal* **20**(19) 5383-5391.

Zelko, IN. Folz, RJ. (2003) Myeloid zinc finger (MZF)-like, kruppel-like and Ets families of transcription factors determine the cell-specific expression of mouse extracellular superoxide dismutase. *Biochemical Journal* **369**, 375-386.

Zeng, F. Watt, NT. Walmsley, AR. Hooper, NM. (2003) Tethering the N-terminus of the prion protein compromises the cellular response to oxidative stress. *Journal of Neurochemistry* **84**, 480-90.

Appendix A – Plasmid Maps

Shown below are the plasmid maps for vectors used to clone the test constructs.

pcDNA3.1 Vectors

Map of pcDNA3.1(+) and pcDNA3.1(-)

The figure below summarizes the features of the pcDNA3.1(+) and pcDNA3.1(-) vectors. **The complete sequences for pcDNA3.1(+) and pcDNA3.1(-) are available for downloading from our World Wide Web site (www.invitrogen.com) or from Technical Service (see page 13).** Details of the multiple cloning sites are shown on page 3 for pcDNA3.1(+) and page 4 for pcDNA3.1(-).

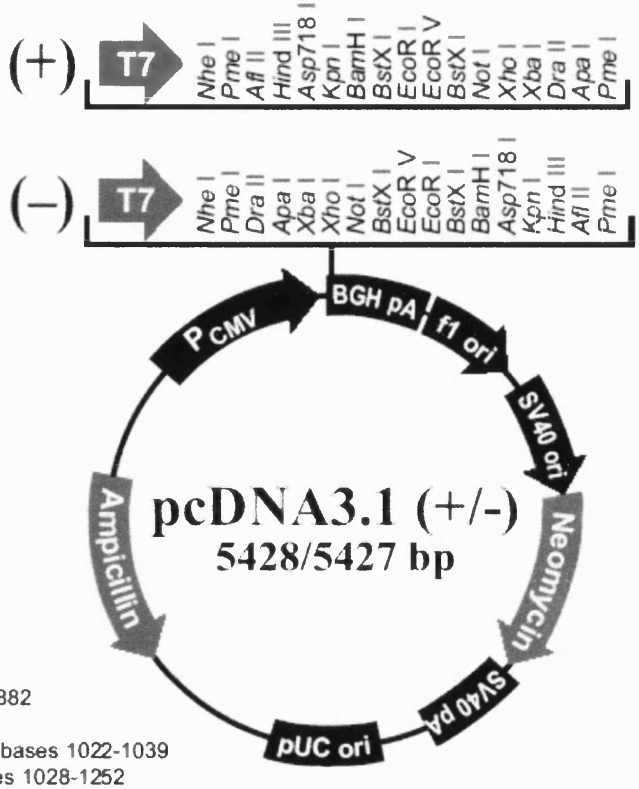

Comments for pcDNA3.1 (+)
5428 nucleotides

CMV promoter: bases 232-819
T7 promoter/priming site: bases 863-882
Multiple cloning site: bases 895-1010
pcDNA3.1/BGH reverse priming site: bases 1022-1039
BGH polyadenylation sequence: bases 1028-1252
f1 origin: bases 1298-1726
SV40 early promoter and origin: bases 1731-2074
Neomycin resistance gene (ORF): bases 2136-2930
SV40 early polyadenylation signal: bases 3104-3234
pUC origin: bases 3617-4287 (complementary strand)
Ampicillin resistance gene (*bla*): bases 4432-5428 (complementary strand)
ORF: bases 4432-5292 (complementary strand)
Ribosome binding site: bases 5300-5304 (complementary strand)
bla promoter (P3): bases 5327-5333 (complementary strand)

pd2EGFP-1† Vector Information PT3205-5

Catalog #6008-1

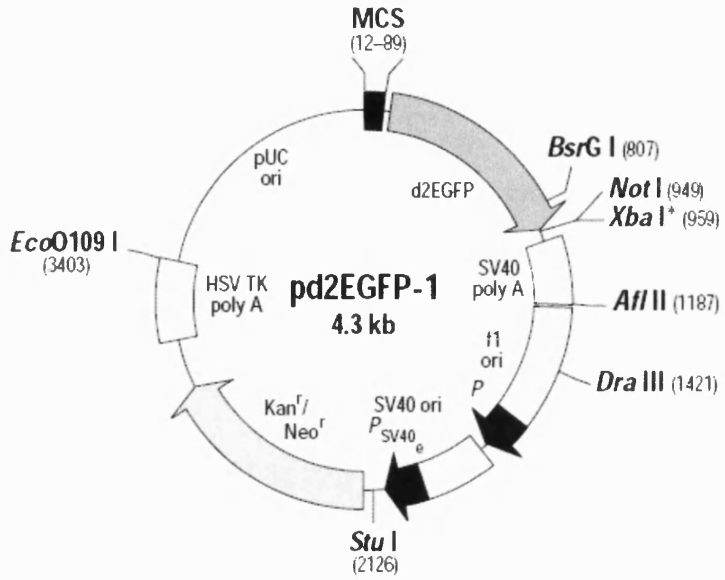

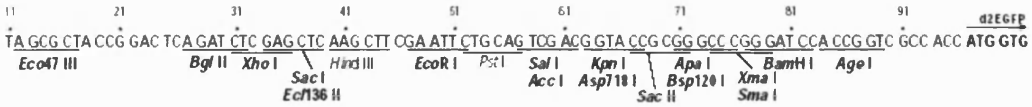

Restriction Map and Multiple Cloning Site (MCS) of pd2EGFP-1. Unique restriction sites are in bold. The *Not*I site follows the d2EGFP stop codon. The *Xba* I site is methylated in the DNA provided by BD Biosciences Clontech. If you wish to digest the vector with this enzyme, you will need to transform the vector into a *dam*⁻ host and make fresh DNA.

Location of features:

- MCS: 12–89
- Destabilized enhanced green fluorescent protein (d2EGFP) gene
  Start codon (ATG): 97–99; stop codon: 940–942
  Insertion of Val at position 2: 100–102
  GFPmut1 chromophore mutations (Phe-64 to Leu; Ser-65 to Thr): 286–291
  His-231 to Leu mutation (A→T): 789
  Mouse ornithine decarboxylase PEST sequence: 820–942
- SV40 early mRNA polyadenylation signal
  Polyadenylation signals: 1099–1104 & 1128–1133
  mRNA 3' ends: 1137 & 1149
- f1 single-strand DNA origin: 1196–1651 (packages noncoding strand of d2EGFP)
- Bacterial promoter for expression of Kan^r gene
  –35 region: 1713–1718; –10 region: 1736–1740
  Transcription start point: 1748
- SV40 origin of replication: 1992–2127
- SV40 early promoter
  Enhancer (72-bp tandem repeats): 1823–1986 & 1897–1968
  21-bp repeats: 1972–1992, 1993–2013 & 2015–2035
  Early promoter element: 2048–2054
  Major transcription start points: 2044, 2082, 2088 & 2093
- Kanamycin/neomycin resistance gene
  Neomycin phosphotransferase coding sequences:
  Start codon (ATG): 2176–2178; stop codon: 2968–2970
  G→A mutation to remove Pst I site: 2358
  C→A (Arg→Ser) mutation to remove BssH II site: 2704
- Herpes simplex virus (HSV) thymidine kinase (TK) polyadenylation signal
  Polyadenylation signals: 3206–3211 & 3219–3224
- pUC plasmid replication origin: 3555–4201

pd2EGFP-N1[†] Vector Information PT3206-5

Catalog #6009-1

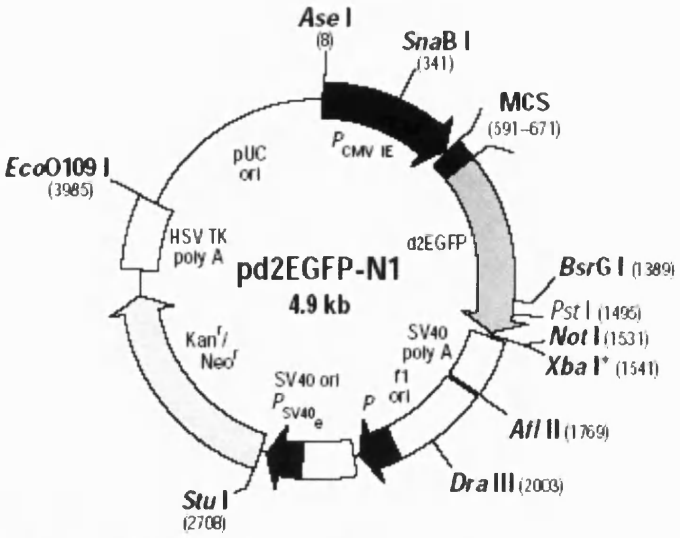

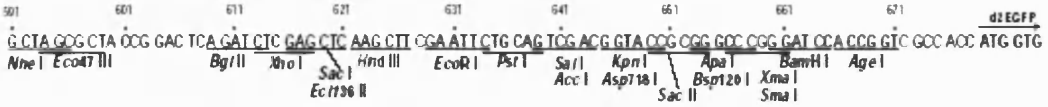

Restriction Map and Multiple Cloning Site (MCS) of pd2EGFP-N1 Vector. Unique restriction sites are in bold. The *Not* I site follows the d2EGFP stop codon. The *Xba* I site is methylated in the DNA provided by BD Biosciences Clontech. If you wish to digest the vector with this enzyme, you will need to transform the vector into a *dam*[-] strain and make fresh DNA.

Location of features:

- Human cytomegalovirus (CMV) immediate early promoter: 1–589
  - Enhancer region:59–465; TATA box: 554–560
  - Transcription start point: 583
  - C→G mutation to remove *Sac* I site: 569
- MCS: 591–671
- Destabilized enhanced green fluorescent protein (d2EGFP) gene
  - Start codon (ATG): 679–681; stop codon: 1522–1524
  - Insertion of Val at position 2: 682–684
  - GFPmut1 chromophore mutations (Phe-64 to Leu; Ser-65 to Thr): 871–876
  - His-231 to Leu mutation (A→T): 1373
  - Mouse ornithine decarboxylase PEST sequence: 1402–1524
- SV40 early mRNA polyadenylation signal
  - Polyadenylation signals: 1681–1685 & 1710–1714; mRNA 3' ends: 1719 & 1742
- f1 single-strand DNA origin: 1778–2233 (packages the noncoding strand of d2EGFP.)
- Bacterial promoter for expression of Kan[r] gene:
  - –35 region: 2295–2300; –10 region: 2318–2322
  - Transcription start point: 2330
- SV40 origin of replication: 2574–2709
- SV40 early promoter
  - Enhancer (72-bp tandem repeats): 2407–2479 & 2480–2550
  - 21-bp repeats: 2554–2574, 2575–2595, & 2598–2618
  - Early promoter element: 2630–2636
  - Major transcription start points: 2626, 2664, 2670, & 2675
- Kanamycin/neomycin resistance gene
  - Neomycin phosphotransferase coding sequences: start codon (ATG): 2758–2760, stop codon:3550–3552
  - G→A mutation to remove *Pst* I site: 2940
  - C→A (Arg to Ser) mutation to remove *Bss*H II site: 3286
- Herpes simplex virus (HSV) thymidine kinase (TK) polyadenylation signal
  - Polyadenylation signals: 3788–3793 & 3801–3806
- pUC plasmid replication origin: 4137–4780

pDsRed2-ER Vector Information PT3642-5

Catalog #6982-1

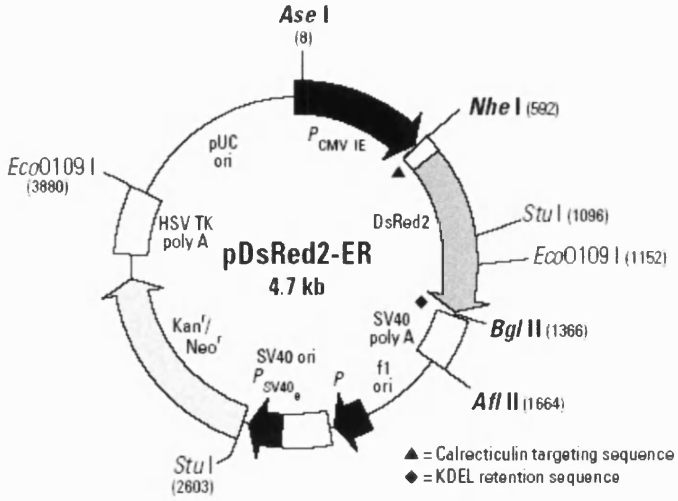

Plasmid Map of pDsRed2-ER. Unique restriction sites are shown in bold.

Location of features

- Human cytomegalovirus (CMV) immediate early promoter: 1–589
  Enhancer region: 59–465; TATA box: 554–560
  Transcription start point: 583
- Calreticulin signal sequence: 597–647
- *Discosoma sp.* red fluorescent protein (DsRed2) gene: 663–1337
  KDEL coding sequence (in frame with DsRed2): 1350–1361
  Stop codon: 1362–1364
- SV40 early mRNA polyadenylation signal
  Polyadenylation signals: 1576–1581 & 1605–1610; mRNA 3' ends: 1614 & 1626
- f1 single-strand DNA origin: 1673–2128 (packages the noncoding strand of DsRed2-ER)
- Bacterial promoter for expression of Kan^r gene
  –35 region: 2190–2195; –10 region: 2213–2218
  Transcription start point: 2225
- SV40 origin of replication: 2469–2604
- SV40 early promoter
  Enhancer (72-bp tandem repeats): 2302–2373 & 2374–2445
  21-bp repeats: 2449–2469, 2470–2490 & 2492–2512
  Early promoter element: 2525–2531
  Major transcription start points: 2521, 2559, 2565 & 2570
- Kanamycin/neomycin resistance gene
  Neomycin phosphotransferase coding sequences:
  Start codon (ATG): 2653–2655; stop codon: 3445–3447
- Herpes simplex virus (HSV) thymidine kinase (TK) polyadenylation signal
  Polyadenylation signals: 3683–3688 & 3696–3701
- pUC plasmid replication origin: 4032–4675

pEGFP-C1 Vector Information PT3028-5

GenBank Accession # U55763 Catalog #6084-1

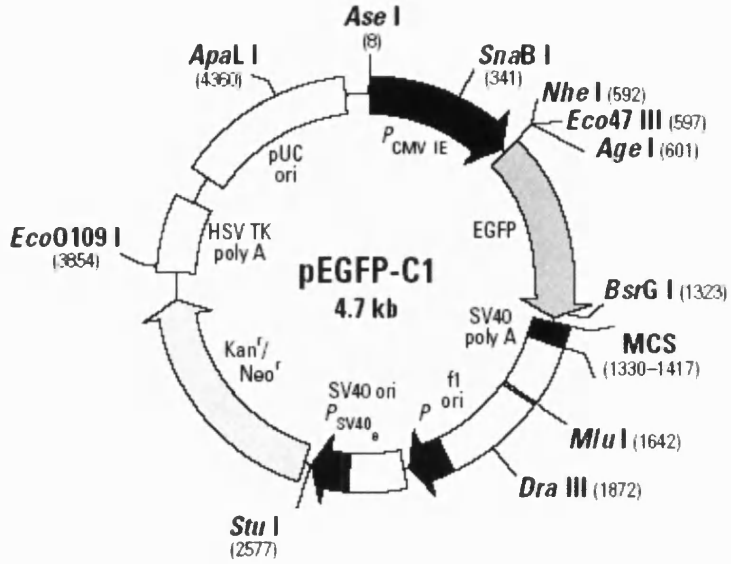

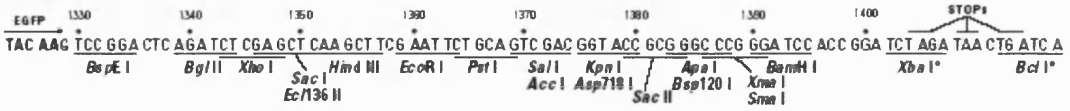

Restriction Map and Multiple Cloning Site (MCS) of pEGFP-C1. All restriction sites shown are unique. The *Xba* I and *Bcl* I sites (*) are methylated in the DNA provided by BD Biosciences Clontech. If you wish to digest the vector with these enzymes, you will need to transform the vector into a *dam*- host and make fresh DNA.

Location of features

- Human cytomegalovirus (CMV) immediate early promoter: 1–589
  Enhancer region: 59–465; TATA box: 554–560
  Transcription start point: 583
  C→G mutation to remove *Sac* I site: 569
- Enhanced green fluorescent protein gene
  Kozak consensus translation initiation site: 606–616
  Start codon (ATG): 613–615; Stop codon: 1408–1410
  Insertion of Val at position 2: 616–618
  GFPmut1 chromophore mutations (Phe-64 to Leu; Ser-65 to Thr): 805–810
  His-231 to Leu mutation (A→T): 1307
  Last amino acid in wild-type GFP: 1327–1329
- MCS: 1330–1417
- SV40 early mRNA polyadenylation signal
  Polyadenylation signals: 1550–1555 & 1579–1584; mRNA 3' ends: 1588 & 1600
- f1 single-strand DNA origin: 1647–2102 (Packages the noncoding strand of EGFP.)
- Bacterial promoter for expression of Kan^r gene
  –35 region: 2164–2169; –10 region: 2187–2192
  Transcription start point: 2199
- SV40 origin of replication: 2443–2578
- SV40 early promoter
  Enhancer (72-bp tandem repeats): 2276–2347 & 2348–2419
  21-bp repeats: 2423–2443, 2444–2464, & 2466–2486
  Early promoter element: 2499–2505
  Major transcription start points: 2495, 2533, 2539 & 2544
- Kanamycin/neomycin resistance gene
  Neomycin phosphotransferase coding sequences:
  Start codon (ATG): 2627–2629, stop codon: 3419–3421
  G→A mutation to remove *Pst* I site: 2809
  C→A (Arg to Ser) mutation to remove *Bss*H II site: 3155
- Herpes simplex virus (HSV) thymidine kinase (TK) polyadenylation signal
  Polyadenylation signals: 3657–3662 & 3670–3675
- pUC plasmid replication origin: 4006–4649

Appendix B – CMV Blots

Shown below are examples of phosphorimager readings for the CMV control in response to A) copper, B) DMSO and C) ATRA treatments.

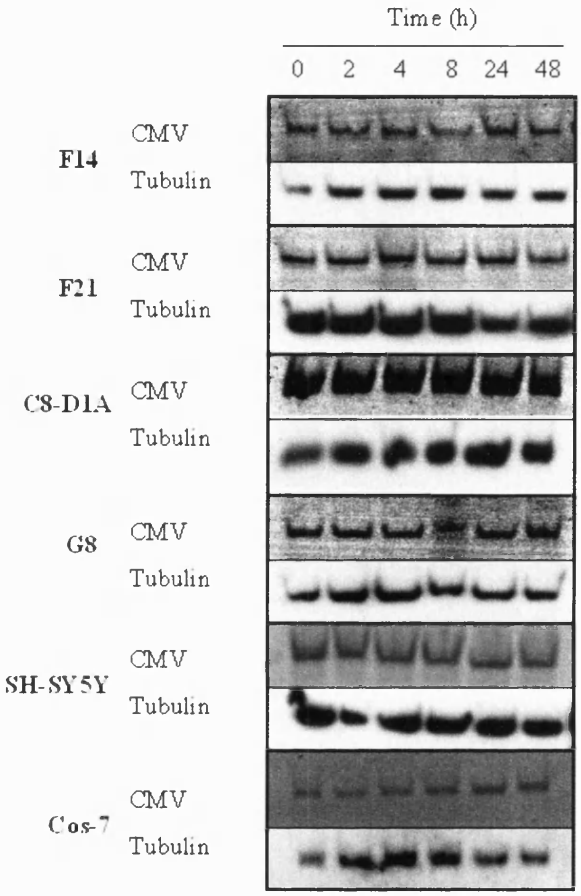

A) Copper.

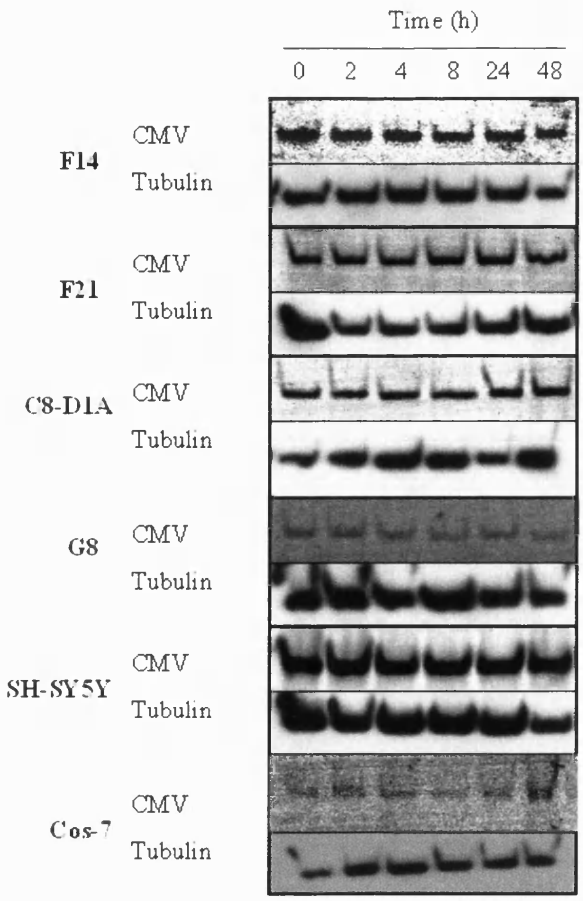
Time (h)
0 2 4 8 24 48
F14
CMV
Tubulin
F21
CMV
Tubulin
C8-D1A
CMV
Tubulin
G8
CMV
Tubulin
SH-SY5Y
CMV
Tubulin
Cos-7
CMV
Tubulin

B) DMSO.

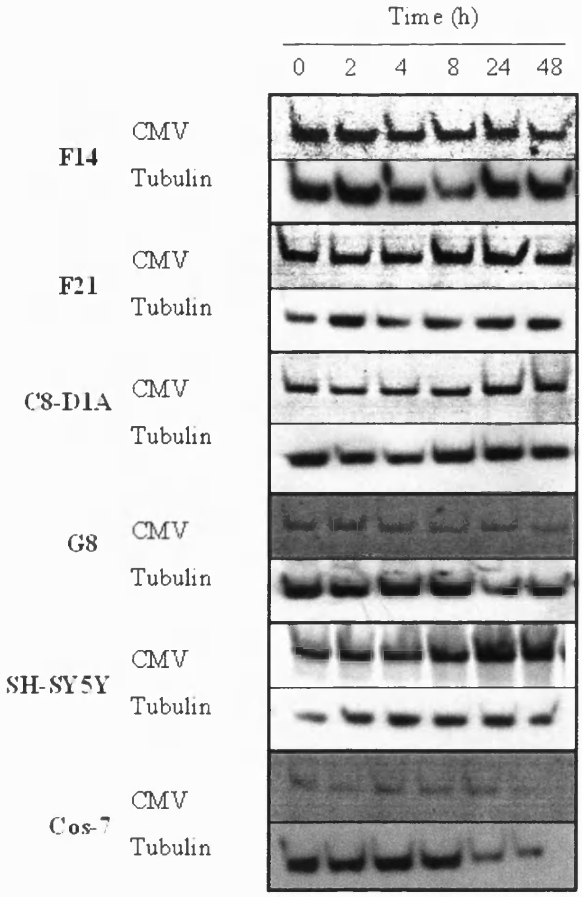
Time (h)
0 2 4 8 24 48
F14
CMV
Tubulin
F21
CMV
Tubulin
C8-D1A
CMV
Tubulin
G8
CMV
Tubulin
SH-SY5Y
CMV
Tubulin
Cos-7
CMV
Tubulin

C) ATRA.

Appendix C – Trafficking Controls

Examples of the A) untreated and B) glycine only treated trafficking controls for the cell lines not shown in the main text.

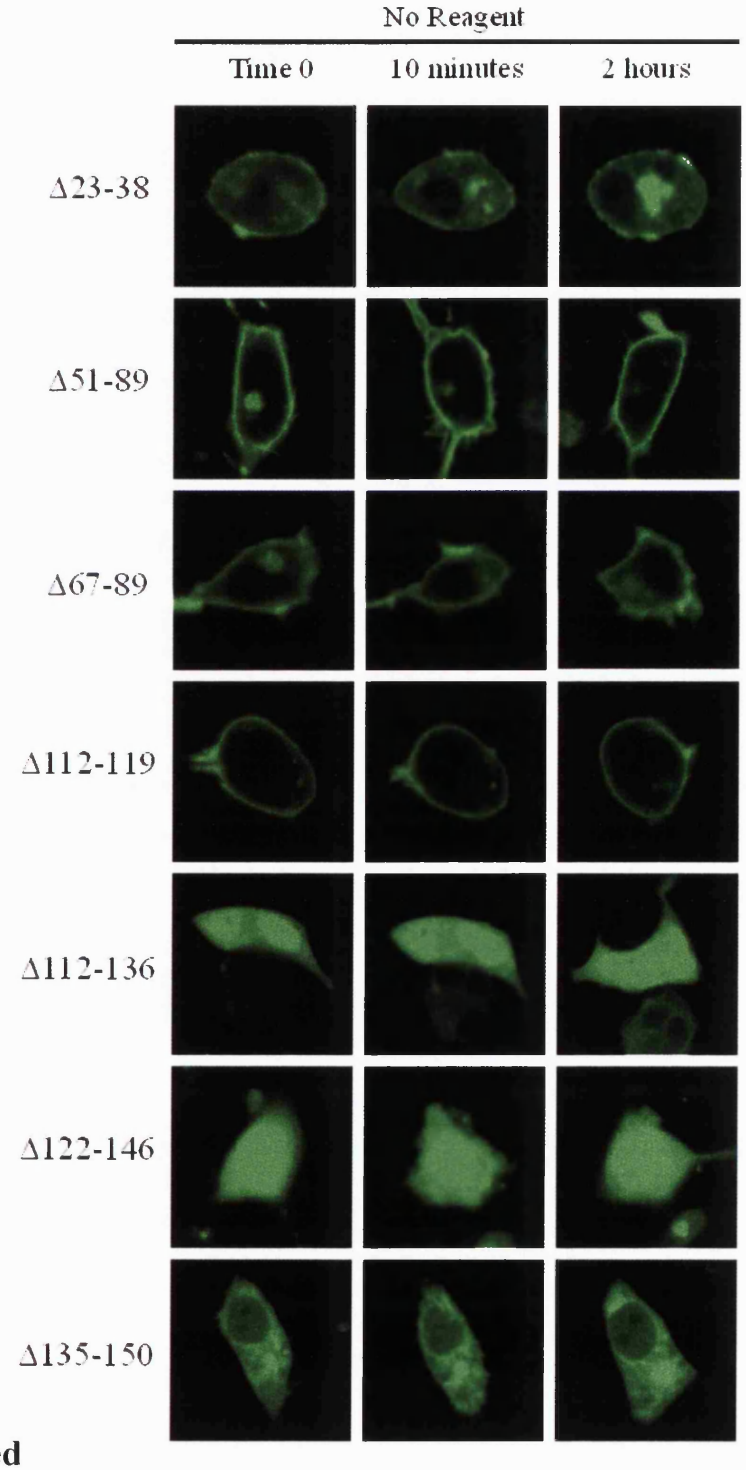

A) Untreated

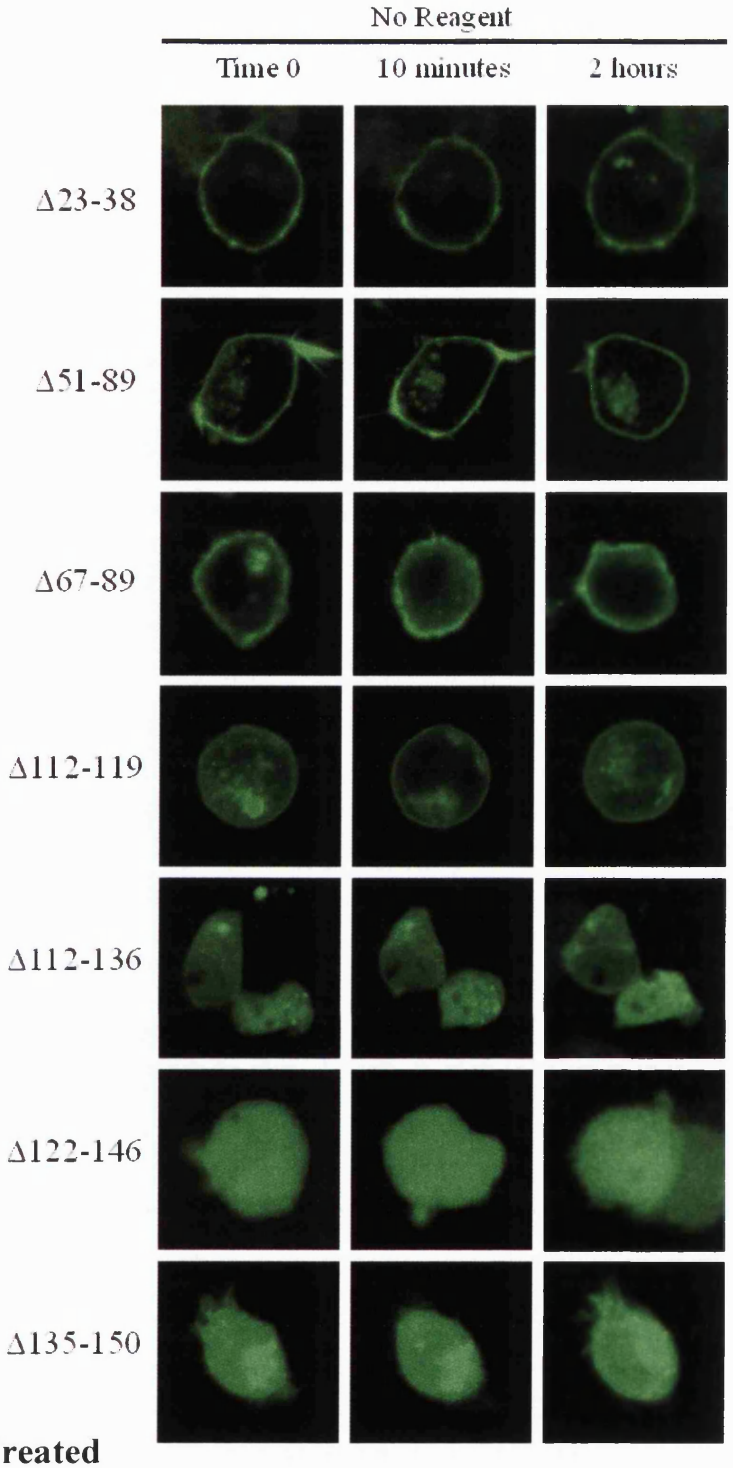

B) Glycine Treated